

A WAVY WALL ANALYTICAL MODEL OF MUCO-CILIARY PUMPING

ROSS, STEPHEN MARK

ProQuest Dissertations and Theses; 1971; ProQuest Dissertations & Theses Global

71-29,158

ROSS, Stephen Mark, 1945-
A WAVY WALL ANALYTICAL MODEL OF MUCO-CILIARY
PUMPING.

The Johns Hopkins University, Ph.D., 1971
Engineering, biomedical

University Microfilms, A XEROX Company, Ann Arbor, Michigan

(C) 1971

Stephen Mark Ross

ALL RIGHTS RESERVED

THIS DISSERTATION HAS BEEN MICROFILMED EXACTLY AS RECEIVED

**A WAVY WALL ANALYTICAL MODEL OF MUCO-CILIARY
PUMPING**

by

Stephen M. Ross

**A dissertation submitted to The Johns Hopkins University
in conformity with the requirements for the degree of
Doctor of Philosophy.**

**Baltimore, Maryland
1971**

ABSTRACT

It is proposed the metachronal waves of the ciliary carpet in muco-ciliary pumping can be analytically modeled as a continuous impermeable wall with a travelling geometric wave on it. This model has been solved for "normal" conditions in mammalian trachea, and for cases in which the mucus departs from its normal state. A "pathological" flow and a purely Newtonian case are also considered.

A two-fluid system with a visco-elastic upper layer and a Newtonian sublayer models the mucous-serous fluid layers in the mammalian system. A wall material point (possibly, but not necessarily corresponding to a cilium tip) moves in a closed ellipse. The wall is extensible, but is at rest on the average. The mucous layer is bounded above by a gas at constant pressure, so there is a free surface and consequently no "squeezing" effects as in peristaltic pumping.

Inertial and gravitational forces are found to be negligible relative to viscous forces in normal muco-ciliary flow. Surface tension (which may be important) is neglected for simplicity. A pathological case with a deep, "watery" mucus in which gravity affects the flow is considered.

The system of equations is solved by expanding all unknown functions asymptotically in small parameters. Functions are assumed to be periodic in distance and time, so that each order solution can be expanded in Fourier series. Solutions are found correct to $O(\epsilon^3)$ where ϵ is the ratio of wall amplitude to total depth of fluid. The particle trajectories and cyclic drift of mucus and serous fluid are found. The average speed (i.e. "mucous flow rate") is then determined. Values for normal flow agree roughly with physiological data.

Near the normal state, the mucous layer moves nearly like an elastic slab, in a direction opposite to the travelling geometric wave of the wall. Changes in mucous viscosity do not affect the drift. For a given ciliary motion, however, the drift increases if the serous viscosity decreases, the modulus of rigidity (i.e. elastic modulus) of the mucus increases, or the ciliary beating frequency increases (at fixed wave speed). The drift decreases if the depth of the serous layer (above the waving wall) decreases, or if the cilia change the form of their beat so that, for example, the ellipticity of a wall point path decreases.

ACKNOWLEDGMENTS

I would like to express my sincere appreciation to my principal adviser, Professor Stanley Corrsin, who made many helpful suggestions and whose door was always open for professional and friendly conversations, and to my second adviser, Professor Stephen Davis, whose valuable comments were a great help.

I am also indebted to Professor Donald Proctor and Mrs. Betsy Bang of the Johns Hopkins School of Hygiene for pointing out the usefulness of this work and for introducing me to actual biological systems.

Thanks are also due to my wife and fellow doctoral graduate, Elizabeth, and to my friend, Gary Odell who made many useful suggestions on my work.

Lastly, I am grateful to Mrs. Jean McFeely and Mrs. Jane Zee for typing the manuscript and to Mrs. Virginia Pradick for drawing the figures.

This work was supported by a National Institutes of Health Predoctoral Fellowship and by the Office of Naval Research under contract number N000-14-67A-0163-0005.

TABLE OF CONTENTS

ABSTRACT

ACKNOWLEDGEMENTS

I. INTRODUCTION	1-13
A. Basic Information about Cilia	
B. Analytical and Mechanical Research	
II. MECHANICAL PHYSIOLOGY OF THE MUCO-CILIARY SYSTEM	14-29
A. The Individual Cilium	
B. Ciliated Epithelium	
C. The Muco-ciliary System	
D. The Nature of Mucus	
E. The Effect of Gravity on Normal Mucous Transport	
III. MODEL OF THE MUCO-CILIARY SYSTEM	30-33
IV. BASIC NOTATION AND SYMBOLS	34-41
A.1. Scalar, Vector and Tensor Fields	
A.2. Others	
B. Dimensional Constants	
C. Dimensionless Constants	
V. CONSTITUTIVE EQUATIONS	42-54
A. Constitutive Equations in General	
B. Principle of Material Indifference	
C. Classical Visco-elasticity	
D. Special Time Rates Satisfying Material Indifference	
E. Constitutive Equation for Mucus	
F. Constitutive Equation of the Serous Fluid	

TABLE OF CONTENTS (con't)

VI. BOUNDARY CONDITIONS	55-81
A. Model Diagram	
B. Condition at the Free Surface and Interface	
C. Wall Boundary Condition	
1. Wall particle trajectory	
2. Lagrangian velocity	
3. Eulerian wall velocity	
4. Constraint on $\alpha \beta \epsilon$	
5. Wall curve	
6. Extensibility of the wall	
7. Effect of long and short regions	
D. Condition on α and t	
VII. "EXACT" SET OF EQUATIONS AND BOUNDARY CONDITIONS	82-86
A. Set of Equations	
B. Determinacy of the System	
VIII. NON-DIMENSIONALIZATION	87-99
A. Dimensionless Groups and Dimensional Constants	
B. Non-dimensionalization of the Unknown Functions	
C. Dimensionless Equations	
D. Values of Dimensional Constants	
IX. ASYMPTOTIC EXPANSION	100-120
A. Asymptotic Expansion and Mixed Equations	
B. Double Expansion	
1. Neglecting gravity (normal flow)	
2. Effect of surface tension	
C. Method	
D. The (1,0) System (ϵ)	
E. The (2,0) System (ϵ^2)	
F. The (0,1) System (B)	

TABLE OF CONTENTS (con't)

X. GENERAL METHOD OF SOLUTION OF THE (p,q) SYSTEM	121-130
A. Equations	
B. Fourier Series and Coefficient Equations	
C. Homogeneous and Particular Solutions	
D. Homogeneous Solution	
E. Neglect of Inertia Terms	
XI. SOLUTION OF THE (1,0) SYSTEM	131-149
A. Pressure-independent Equations	
B. Fourier Series and Coefficient Equations	
C. Form of the Solution	
D. Neglect of the Inertia Terms	
E. Zero Order Solution	
F. Free Surface and Interface	
G. Pressures and Total Stress	
H. Entire (1,0) Solution	
XII. SOLUTION OF THE (2,0) SYSTEM	150-171
A. Pressure-independent Equations	
B. Fourier Series and Coefficient Equations	
C. Product Formula and Non-trivial Modes	
D. Equations Neglecting Inertia	
E. Particular solution and Form of Homogeneous Solution	
F. Zero Mode Solution	
G. Free Surface and Interface	
H. Pressures and Total Stress	
I. Entire (2,0) Solution	
XIII. SOLUTION OF THE (0,1) SYSTEM	172-182
A. Pressure-independent equations	
B. Fourier Series and Coefficient Equations	
C. Solution	
D. Free Surface and Interface	
E. Hypothetical Pathological Case	

TABLE OF CONTENTS (con't)

XIV. PARTICLE TRAJECTORIES AND CYCLIC DRIFT	183-193
A. General Theory	
B. The (1,0) calculation	
C. The (2,0) calculation	
D. The (0,1) calculation	
E. Trajectory	
F. Cyclic Drift, Volume Flux and Average Speed	
XV. WORK RATE AND ENERGY DISSIPATION	194-206
A. Work Rate due to Boundary Forces	
B. Dissipation of Kinetic Energy	
XVI. GRAPHS AND DISCUSSION OF RESULTS	207-244
A. General Discussion	
B. Normal Flow	
C. Departures from the Normal State	
D. The Newtonian Case	
APPENDIX	
A. Fourier Coefficients γ_i , b_i , Ψ_i , b_{3i} , b_{4i}	
B. Proof of $g(z,y)=0$	
C. Calculation of I_i and $F_i^{(2,0)}$	
D. Experiment with Wire Brush	

BIBLIOGRAPHY

VITA

FIGURES

- I. A Paramecium Opinala
- II. A Ciliary Cycle
- II. B Longitudinal Section of Tracheal Epithelium
- II. C Sketch of Ciliated Epithelium
- III. Model of Muco-Ciliary System
- VI. A Model Diagram
- VI. C. 1. a,b Wall Points
- VI. C. 5 Wall Curve
- VI. C. 7.a,b Wall Curves ($\rho = \pm 1$)
- VII. Model Sketch
- VIII. D. 4 Sketch Showing Serous-Mucous Depths
- XVI. C. 7.a Drift vs. K_T
- XVI. C. 7.b Drift vs. h
- XVI. C. 7.c Drift vs. ρ
- XVI. C. 7.d Drift vs. ω
- Normal Muco-Ciliary Flow: $\alpha_N = 1$, $\rho_N = 1.5$, $\epsilon_N = .2$, $K_N = .67(10^{-4})$,
 $T_N = 1.5(10^3)$, $h_N = .8$
- XVI. B.1 Drift
- XVI. B.2 Free Surface, Interface and Wall
- XVI. B.3 Trajectories at Three Heights and Drift

FIGURES (con't)

Perturbations from the Normal State:

- XVI. C. 1. a** Drift for Different Serous Viscosities
- XVI. C. 1. b** Trajectories for Different Serous Viscosities
- XVI. C. 2. a** Drift for Different Moduli of Rigidity ("elasticity") or for Different Beating Frequencies at Constant Wavelength.
- XVI. C. 2. b** Trajectories for Different Moduli of Rigidity or Frequencies.
- XVI. C. 3** Drift for Different Frequencies at Constant Wave Speed.
- XVI. C. 5** Drift for Different Depths of the Mucous Layer Relative to the Serous Layer.
- XVI. C. 6** Drift for Different Axis Ratios of the Wall Particle Motion.

Newtonian and Nearly-Newtonian Flow:

- XVI. D. 1. a** Trajectories at Three Heights and Drift for Circular Clockwise Wall Particle Motion (Single Newtonian Fluid). $\alpha = 1$, $\beta = 1$, $\epsilon = .2$, $K = .95$, $T = 0$
- XVI. D. 1. b** Trajectories at Three Heights and Drift for Circular Counter-clockwise Wall Motion (Single Newtonian Fluid).
- XVI. D. 1. c** Trajectories for Different Axis Ratios of the Wall Particle Motion (Single Newtonian Fluid).
- XVI. D. 1. d** Trajectories for Different Axis Ratios (Single Newtonian Fluid).

FIGURES (con't)

- XVI. D. 1.e** Free Surface for Different Axis Ratios (Single Newtonian Fluid).
- XVI. D. 2.a** Drift for Different Relaxation Times.
- XVI. D. 2.b** Trajectories for Different Relaxation Times.
- XVI. D. 2.c** Free Surface and Wall for a Visco-elastic Upper Fluid.
- XVI. D. 3.a** Drift for Different Viscosity Ratios (Two Newtonian Fluids).
- XVI. D. 3.b** Trajectories for Different Viscosity Ratios.
- XVI. D. 3.c** Free Surface and Wall for Different Viscosity Ratios.
- XVI. D. 4** Free Surface and Wall (Single Newtonian Fluid).
- XVI. D. 5** Horizontal Velocity Profiles (Single Newtonian Fluid).

Appendix:

- D. 1-3** Flat Plate Experiment
- D. 4-7** Brush Experiment
- D. 7** Brush

TABLES

Table II. A	Data on Individual Cilia
Table II. B	Data on Metachronal Waves
Table II. C. 1	Data on Ciliated Epithelia
Table II. C. 2	Data on Mucous Transport
Table II. D	Rheological Properties of Mucus
Table VIII. D. 9	Dimensionless Constants in Normal Flow
Table XVI. C. 8. a	Drifting Tendencies
Table XVI. C. 8. b	Power at the Wall
Table XVII. D. 1, 2	Experiment with Plate and Brush

I. INTRODUCTION

This dissertation is an attempt to further the understanding of the flow of mucus over ciliated epithelium from the viewpoint of fluid mechanics. Basic information about cilia and flagella and the functions cilia perform shall form the substance of this section along with a review of some important mechanical and rheological results in the literature.

I. A. Basic Information about Cilia and Ciliary Systems

Cilia are vibratile or non-vibratile cell organelles having a high degree of molecular organization. In recent years they have been more specifically defined by electron microscopists according to their ultrastructure. The terms flagella and cilia are now often used interchangeably since their structures appear to be the same under close electron microscopic examination. However, it is conventional to call those organelles that move fluid nearly parallel to their long axes flagella, an example being spermatozoa "tails." Those moving fluid nearly perpendicular to their long axes may be called cilia (Sleigh, 1962). This paper will delve neither into the

structural details of the cilia nor the chemical and biological factors that influence their behavior. Interested readers are referred to a book by Sleigh for an excellent account of the above.

The bending motion of these organelles resulting in the flow of fluid relative to the organelle itself is due to "active contractile elements" distributed along their length (Sleigh, 1962; Gray, 1928; Afzelius, 1966 and others). Thus in this analysis, the cilia drive the fluid, albeit in a special way; the fluid does not drive the cilia.

Cilia are found in large numbers covering many of the epithelial (i.e. surface) cells of all the major animal groups except the Nematoda and Anthropoda (Gray). They appear to form a dense covering and have qualitatively been described as looking like "pile of a carpet" (Proetz, 1941) and a "waving field of grain" (Tremble, 1948). Detailed electron microscopic studies of the ciliated epithelia of rats were undertaken by Dalhamn and Rhodin (1956), but no study of the motion of the cilia was made.

Although cilia on a given surface beat at the same frequency, each is slightly out of phase with its neighbor in one direction and in phase with its neighbor in a direction perpendicular to the previous

one. Thus travelling geometric wave fronts called "metachronal waves" are formed by the envelope of the uppermost portion of the cilia (Sleigh). Of the four different classifications of metachronism, the type denoted as anti-plectic* is found most often in ciliated epithelia which are required to move a layer of mucus.

Figure I. A is a picture of the metachronal waves of the paramecium Opinala clearly illustrating moving wave fronts (Horridge and Tamm, 1969). A critical drying point technique was used to study the geometry of the ciliary pattern at a fixed instant of time. Note that this is a specific metachronal wave pattern and that it should not be assumed that the ciliated epithelium involved with mucous transport will look the same. It does suffice, however, to give us some insight into the problem with which we are concerned.

*

Each cilium is out of phase with its neighbor in the direction of the beat and in phase with its neighbor in a direction perpendicular to the beat, and the wave geometry moves opposite in direction to the gross fluid transport.

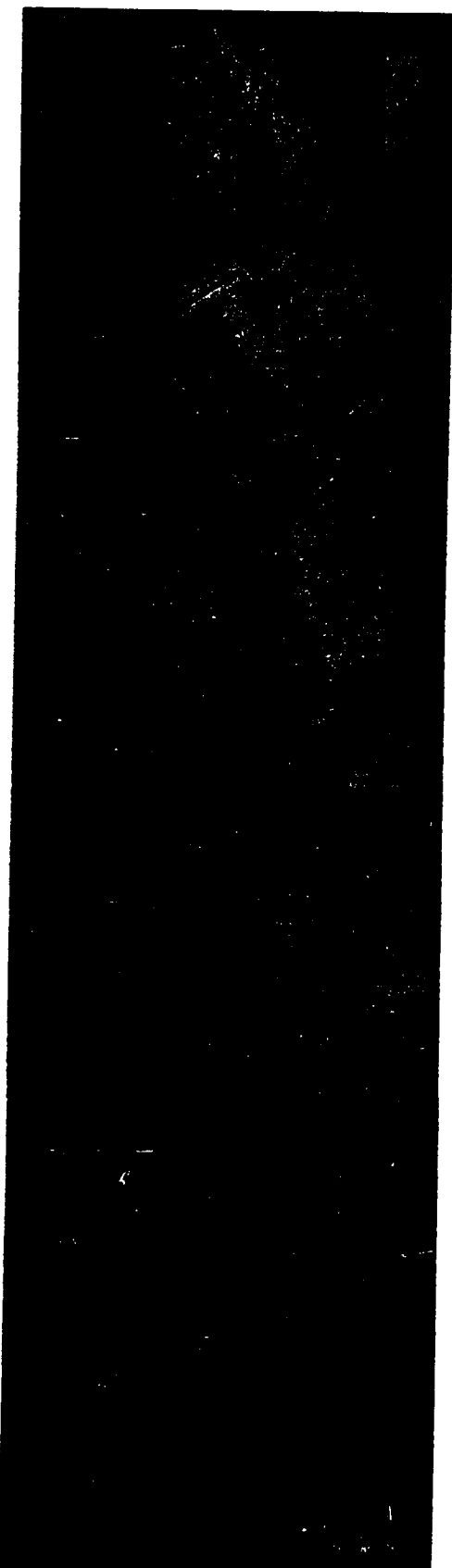


Fig. I.A

Ciliated epithelia cause a fluid motion relative to the solid surface. This motion performs a variety of functions in animals, prominently including locomotion, feeding and cleansing. Table I. A shows some of the types of ciliated organs and their functions (Rivera, 1962).

Type of tissue	Typical example	Ciliary function
Epidermis	(a) Most invertebrate larvae Ctenophores (b) Turbellaria	Locomotion
Digestive system	(a) Frog's esophagus (b) Intestine and liver of molluscs	Maintains superficial current Propulsion of fluid through narrow tubes, the walls of which are ciliated
Excretory system	Nephrostomes and nephridia of most invertebrates	Propulsion of fluid through narrow tubules
Reproductive system	(a) Vasa efferentia in vertebrates (b) Fallopian tubes and uterus in mammals	Propulsion of fluid through narrow tubules Moves ova into uterus and conducts sperm into tubes
External appendages	(a) Disc of rotifers (b) Tentacles of Polychaets, Polyzoa, etc.	Locomotion and nutrition Maintains superficial nutritive current
Central nervous system: 1. Sensory 2. Motor or sensory	(a) Ciliated tracts of ctenophores (b) Eyes of molluscs, otocysts of Pteropods (a) Ventricles of the brain in mammals	? Conduction of stimulus ? Sensory receptors Cerebrospinal fluid circulation
Respiratory tract	(a) Nose and accessory sinuses in mammals (b) Entire extent of bronchial tree in mammals	Cleansing of mucous surfaces and removal of foreign bodies To keep air passages open
Endocrine	Thyroid gland	? Follicular secretion

Table I. A

In this thesis, we are concerned with the flow of mucus induced by the beating of cilia in the respiratory tract of mammals. In humans, a layer of mucus and serous fluid covers the ciliated epithelium of the whole respiratory tract including the nose, trachea, sinuses, and the proximal bronchioles. This system is believed to perform the cleansing function of removing foreign matter (e.g. bacteria) by creating a continual flow of particle-laden mucus to the laryngeal pharynx where it is either swallowed or expectorated. A multitude of diseases caused by malfunctions of the mucociliary system exist and include upper respiratory infections such as rhinitis, sinusitis, pharyngitis, laryngitis; serious conditions such as pneumonia, asthma, pneumononiosis, bronchiectosis and others (Rivera).

According to Hilding (1943), impairment of normal ciliary function in some diseases of the lower respiratory tract such as tracheo-bronchitis, influenzal pneumonia, and bronchopneumonia results in part from a change of many ciliated cells to mucous-secreting goblet cells. Thus, in many of these pathological conditions, the mucus is not removed so that death from asphyxiation may result. Also studied by Hilding (1956) were the effects of cigarette smoke on ciliary activity and in bronchial

carcinoma. Ciliary beating stopped after only a few minutes exposure to the smoke and there appeared to be a correlation between squamous-cell carcinoma in the respiratory tract and ciliary streaming.

I. B. Analytical and Mechanical Research on Muco-Ciliary Flow

Although research on muco-ciliary flow occupies a sizeable place in medical physiology, mechanical investigations, both experimental and theoretical, are few and far between. This has probably been due to the unawareness of this flow problem relative to more obvious ones such as blood flow, uretal flow and other large scale phenomena. Few quantitative physiological data are available to guide mechanical study. Furthermore, the facts that mucus is not Newtonian, that the kinematics of the ciliary boundary conditions are not well established, and that there may be two fluids, may have discouraged attempts at mathematical modeling of the muco-ciliary system. Also, the amount of sample of normal mucus that can be obtained is small, which makes rheological testing of the material difficult. Only within the past few years have physical scientists

begun to consider muco-ciliary flow in detail.

Apparently, the only published analytical approach to muco-ciliary flow up to now is that of Barton and Raynor (1967). In their model, the ciliated wall is replaced by a known average shear stress and average velocity acting parallel to the wall which induces an average flow in a Newtonian fluid of variable viscosity.

More specifically, a single cilium is regarded as a rigid cylinder of variable length composed of infinitesimally short cylindrical sections undergoing simple harmonic (thus effective and recovery strokes are of equal duration) translatory oscillations. A drag force for two-dimensional flow of a Newtonian fluid past a circular cylinder at small Reynolds numbers is calculated for each cylindrical segment and averaged over one period and over the entire length of the cilium by integration. Thus it is implicitly assumed that each infinitesimal cylindrical segment does not exert any influence on a neighboring segment and that the two-dimensional solutions can be superposed to obtain a flow valid in three dimensions.

An area average about each cilium assuming that the flow near a particular cilium is unaffected by other cilia near it, yields an

overall average velocity and shear stress acting on the mucus parallel to the wall. Thus, metachronal waving is neglected and the ciliated wall is replaced by an average stress and velocity.

The velocity throughout a layer of Newtonian fluid is then obtained with the condition that the viscosity varies linearly with depth necessary to satisfy the physical constraints.

Although the computed results are close to experimental values of mucous flow rate (i.e. average drift speed), the assumptions that the mucus is Newtonian, that the viscosity varies in a specific way, and that the metachronal waves of the cilia can be ignored may be serious deficiencies in their model. Furthermore, the analysis involves several steps (e.g. superposing two-dimensional solutions) that seem to need clarification.

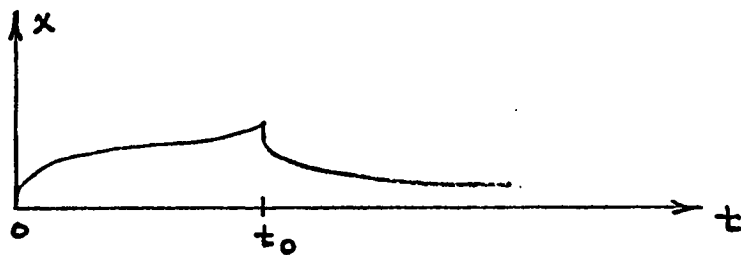
Experimental attempts to understand the hydrodynamic nature of the muco-ciliary flow system have been undertaken principally by C. E. Miller (1965, 1966, 1968). He constructed a mechanical model of ciliary flow in which fluid particle trajectories, dye streak patterns, velocities and so forth caused by oscillating mechanical

cilia "ribbons" were observed as a function of metachronal and synchronous phasing of the cilia. Both Newtonian and non-Newtonian fluids were used. According to Miller, experimental results showed close qualitative parallels with his own physiological observations and with other physiological reports. Among these phenomena are the following: a wave-like motion near the tips of the "cilia", which moves in a direction opposite to that of the movement of fluid material particles, and an indication that the "motion of particles is initiated only if the visco-elastic material is a small portion of the total fluid or if it occupies the region above the tips of the vibrating ribbons. If the region surrounding the ribbons is visco-elastic, little or no progressive motion is observed." Also stated are that "...the flow of fluid in the ciliary fluid system is kinematically initiated primarily by the metachronal phasing of the cilia." And that "...the asymmetric period of oscillation of the cilia (i.e. duration of effective and recovery strokes) is of minor importance in sustaining the motion of particulate matter in Newtonian liquids" (Miller, 1968). The expression in parentheses has been added.

The rheological properties of mucus have been considered in

* Nuogel-in-Varsol

depth by S. H. Hwang and M. Litt (1967, 1969, 1970). Their experiments involved placing a nickel sphere in a small homogeneous volume of a mucus sample, subjecting it to a steady magnetic field at $t = 0$, and turning the field off at some time, $t = t_0$, later on. Curves of displacement vs. time were obtained, e.g.:



The sphere jumped at $t = 0$ and then moved until current was turned off, allowing an immediate "elastic recoil."

The data in the time domain were Fourier transformed to the frequency domain, and interpreted as a classical linear visco-elastic model (Maxwell fluid). Data in this form were then interpreted to give estimates of a "principle" relaxation time* and dynamic viscosity

* Relaxation time is defined in Section V.C.

for the various samples of mucus tested. These values scatter over a wide range, but orders of magnitude of 1000 poise and 100 seconds were reported for normal cervical* mucus (Denton, et al., 1967; Hwang et al., 1969). Since the frequency of the ciliary beat is about 15 cycles per second, the ratio of relaxation time to period is very large; in ciliary pumping, mucus must be regarded as a visco-elastic rather than purely viscous fluid.

These experimental results seem to be the most relevant ones now available on mucus rheology. They should, however, be regarded as "tentative" (Hwang et al., 1969) for several reasons. The samples were taken from human subjects and were quick-frozen, stored for long periods of time, and then thawed out before testing. This may have degraded the polymer and changed its properties; it may have caused loss of the normal water content of the mucus. In addition, the method of collection (performed by physicians) of the mucus is important since it is sensitive to any stresses placed upon it. In addition, the gross samples of mucus were so heterogeneous that small homogeneous subfractions had to be isolated for testing. It is

*

Values for normal tracheal mucus (in dogs) are discussed in Section VIII. D. 5.

not clear which were "normal" or whether, in fact, the heterogeneous condition itself is normal. Finally, the calculation of the drag force on the sphere made in interpreting the data ignores wall effects which may have influenced the results. Also, since the stress and strain-rate field around any finite body (even in an infinite fluid) is inhomogeneous, its gross behavior (like drag) is not an absolute measure of rheological properties.

II. MECHANICAL PHYSIOLOGY OF THE MUCO-CILIARY SYSTEM

This section describes the local mechanics of some typical muco-ciliary systems. The references dealt with an assortment of mammals (e.g. cats, rats, dogs, humans), so pieces and bits of information apply to different animals. This procedure is necessitated by the scarcity of information on muco-ciliary systems. In fact, the close similarity of these systems in most mammals is remarkable.

For the present hydrodynamic analysis, it is required to know the depth of mucus, its rheological properties, the direction, wavelength, frequency and amplitude of the metachronal wave, the motion of the cilia, preferably all under "normal" circumstances. Pathological data will be considered as a special case. The data are tabulated at the end of each subsection.

II. A. The Individual Cilium

In general, a cilium has the appearance of a long slender rod of fairly constant cross section. Cilia beat in a regular cyclic fashion in which bending waves pass from the basal body to the tip. This beat of a cilium is usually considered to take place in one plane (Sleigh, Proetz)

although there is some disagreement (Horridge and Tamm, 1969).

The form of the beat varies according to the function of the cilia; those found on the epithelium of paramecia and protozoa do not usually wave in the same way as those in the mammalian mucociliary system with which we are concerned. The motion of a cilium has been described as consisting of two phases: an "effective" stroke during which the rod is extended and fairly rigid, and a "recovery" stroke in which the rod is bent, perhaps, but not necessarily limp, and is returning to its former position (Sleigh). These phases are not totally distinct but are overlapping; in addition, they do not occupy the same time fraction of the period; the effective stroke is shorter in duration by a factor of three to five (Proetz).

Figure II. A is a sketch of a possible beat of a typical cilium showing the position of the tip of the cilium at equal intervals of time. The "effective" stroke which is more rapid, may be regarded as occupying the upper portion of the path and the "recovery" stroke occupies the lower portion. In this figure, the trajectory of the tip has been idealized as almost elliptical. This is probably only approximately true in an actual ciliary motion.*

* Another drawing of a ciliary beating cycle can be found in Proetz, p. 193. Cilia in other types of organelles not involved with mucociliary pumping, may have a different beating form (Sleigh).

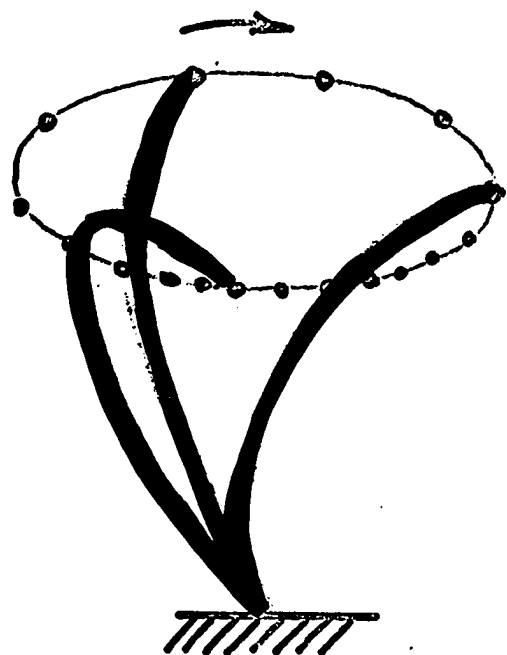


Fig. II. A

Table of data on individual cilia

	Miller 1968	Proetz 1941	Ewert 1965
mammal	general	human	general
length (microns)	5	7	8
diameter (microns)	.25	.3	.3
frequency (cps)	15-20	8-12	17

Table II. A

II. B. Ciliated Epithelium

In mammals, cilia are found in large numbers lining the pseudo-stratified and columnar epithelium of "the entire respiratory tract, the eustachian tubes, the paranasal sinuses except in the alveoli and respiratory bronchioles, over the vocal cords, the epiglottis and oropharynx, in the crypts of lymphoid masses, between the anterior ends of the nasal turbinates and the nostrils, and over the olfactory area" (Proctor).

Their function of transporting a mucous covering is thought to be accomplished by the organized pattern of beating (metachronism) that exists throughout (Miller, 1968). These geometric waves are usually of constant speed and direction and are such that they progress opposite to the effective stroke, thus falling into the class termed anti-plectic*. The wave fronts appear to be much longer than the wavelengths (under direct microscopic observation), so that the flow phenomenon can be considered two dimensional. This agrees with the pictures of ciliary streaming from Hilding (1959).

Figure II. B shows the densely packed ciliated surface along a longitudinal section of a normal rat tracheal epithelium (Dalhamn, 1956).

* See Section I. A.



Fig. II. B

Table of data on metachronal waves in muco-ciliary systems

	Miller 1968	Dalhamn 1956	Proetz 1941	Sleigh 1962
mammal	cat	rat	human	general
wavelength (microns)	41	20		
direction of metachronal wave relative to "effective" stroke	opposite		opposite	opposite (anti-plectic)

Table II. B

II. C. Muco-ciliary System

Electron microscopic studies of ciliated epithelium involved with muco-ciliary pumping have been undertaken by Dalhamn and Rhodin (1956). They found that the types of epithelial cells in a normal rat trachea can be classified into four types: ciliated, goblet, basal and brush. The mucous-secreting goblet cells are interspersed randomly throughout the epithelium and are only about one-fourth as abundant as the ciliated cells. This is true in most normal mammalian muco-ciliary systems, although in some diseases (e.g. asthma) the number of goblet cells increases to such an extent that the cilia are not abundant enough to move the mucus and clogging of the bronchial tubes may result causing asphyxiation (Rivera, 1962).

The fluid lying "above" the cilia is believed to consist of two layers; an upper visco-elastic or gel-like layer of mucinous fluid and a lower "watery" or sol-like layer of serous fluid in which the cilia beat (Lucas and Douglas, 1934). According to them, the facts that water and mucus are not readily miscible and have different specific gravities may explain the separation into two distinct layers at the surface of the epithelium. This two fluid system also helps to explain,

in part, some experimental data in which dyed particles in the sublayer drifted along even though the mucus did not, and it stresses the importance of the relative depth of the two fluids (Bang and Bang, 1961). Several researchers, however, favor the idea that there exists only one fluid with properties varying with height; i.e. an abundance of long chain mucin at the top making it more visco-elastic than the parts near the cilia (Keiser-Nielsen, 1953). The two layer system can be considered to be a model of this.

The mucus continuously enters the system through the goblet cells, but the origin of the sublayer is unknown. One possibility is that it consists of intercellular fluid that has "oozed" to the surface of the epithelium (Lucas and Douglas). Another possibility may be that the sublayer is a sol-like substance produced in the alveoli and respiratory bronchioles (Litt, 1970).

In this paper, we shall usually refer to the upper layer as the mucous layer and the sublayer as the serous layer.

Figure II. C is a simplified diagram, based on those of Miller and Goldfarb (1965) and of Lucas & Douglas, of one wavelength of the mammalian respiratory muco-ciliary system, showing the metachronal wave, the cilia in their positions throughout the cycle, and the possibly double-layer nature of the fluids being transported.

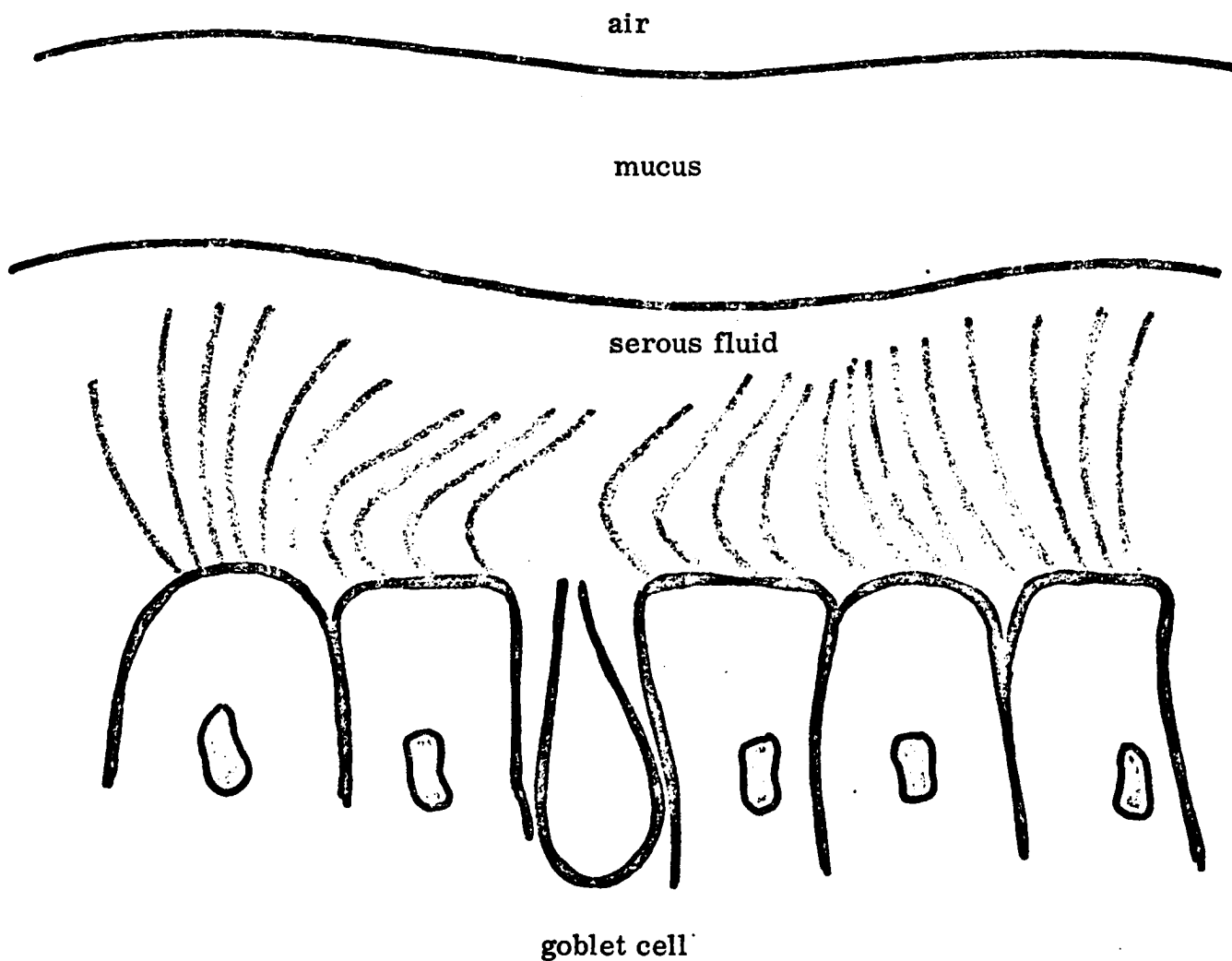


Fig. II. C

Note that the actual photograph [Figure II. B] of the normal ciliated epithelium shows that the cilia are much closer together than the drawing above indicates.

Table of data on ciliated epithelia.

These values were taken from the electron microscopic studies of Dalhn and Rhodin (1956).

mammal	rat
organ	trachea
cells	
type	ciliated, goblet, basal and brush
width	7 microns
area	33 sq. microns
ciliated cells	
distribution	most abundant, four times more than goblet cells
density of cilia	8.4/sq. micron or 270/cell
distance of cilia from center to center	.3 - .4 microns
individual cilia	
length	5 microns
diameter	.24 microns

Table II. C. 1

Table of data on mucous transport

	Dalhamn 1956	Miller 1968	Proetz 1941	Tremble 1948
total depth of fluids (microns)	5-normal 20-25 ab-normal	15		
*average speed of mucus (mm/min) (mucous flow rate)	5-14	15	2.5-7.5	4-6
mammal	rat	cat	human	human

Table II. C. 2

* most of these values refer to particulate matter on the mucous surface.

II. D. The Nature of Mucus

The study of the properties of mucus has been limited in the past due to the difficulties in obtaining a sufficient sample with which to experiment. Thus physiologists described mucus in qualitative terms such as "....thin, slippery, adhesive, tenacious" (Proetz). The chemical and molecular properties of mucus are discussed in papers by Breuninger (1964) and Keiser-Nielsen (1953). It will suffice for us to know that mucus is an aqueous solution of mucin which is a gluco-protein containing a complex polysaccharide combined with a protein. The percentage of mucin in normal nasal mucus is 2.5-3%, and water 95-97%, and the viscosity varies "greatly"^{*} with slight changes in mucin content (Proetz, 1941). The detailed morphology of the mucin structure is not really pertinent to this paper; however, it is of interest to note that: "....according to this hypothesis (on the morphology), mucin in the native state, consists of strongly hydrated, but continuously connected, molecular complexes, which occur in a more or less rolled or folded state. During stretching,

*

Proetz doesn't give any quantitative estimates.

they occur as long chains of molecules, but on account of the state of tension thus produced, they will immediately try to roll up again" (Keiser-Nielsen). From a mechanical viewpoint, this indicates that mucus is a material having quasi-solid as well as fluid properties, so that it falls into the category denoted by the term "visco-elastic". The investigations of Litt, Hwang, and others provide some of the necessary information with which to formulate a constitutive equation for mucus that takes its springiness into account. A complete description is given in section V.

II. E. The Effect of Gravity on Normal Mucous Transport

Since the cilia drive the mucus so that there is a net transport of fluid parallel to the epithelium, we may suspect that gravity may influence the flow in cases where it also acts parallel to the epithelium. In fact, in the upright human trachea, where the epithelial wall is vertical, the gravitational forces would appear to act directly counter to the upward flow of mucus.

It is generally agreed, however, that gravity does not appreciably affect the movement of mucus under "normal" circumstances.

Statements to that effect can be found in articles by Proctor, Ewert and Proetz. To quote Ewert, "The influence of gravity was tested in a small group by comparing the speed of flow with the septum in the vertical and horizontal positions without finding any differences. This is in good agreement with earlier investigations (Hilding, 1931b; Negus, 1958, van Ree & van Dishoeck, 1962) where gravity was shown to be of no importance in animal and human in vitro and in vivo* studies. The effect of gravity under pathological conditions when there is an excess of secretions... or where the viscosity is too low must not, however, be disregarded." A detailed discussion of the effect of gravity will be considered in section XIII.

*

In vitro here denotes a removed section of ciliated epithelium in which the cilia are still beating.

Table of some rheological properties of mucus based on a simple classical Maxwell fluid.*

Relaxation time (sec)	278	80
Dynamic viscosity at zero frequency (poise)	21,800	1,450
Spring constant (dyne/sq. cm.)	78.4	18.1
Area & type of sample	lung abnormal	cervix normal
Mammal	human	human

Table II. D

*

These data can be found in S. H. Hwang's Ph. D. dissertation and in the published paper by Denton et al (1968).

III. MODEL OF MUCO-CILIARY SYSTEM

The actual muco-ciliary system is modelled here as a two-fluid system with a visco-elastic "mucus" above a Newtonian "serous fluid." The depths of the layers are chosen arbitrarily for the initial analysis.

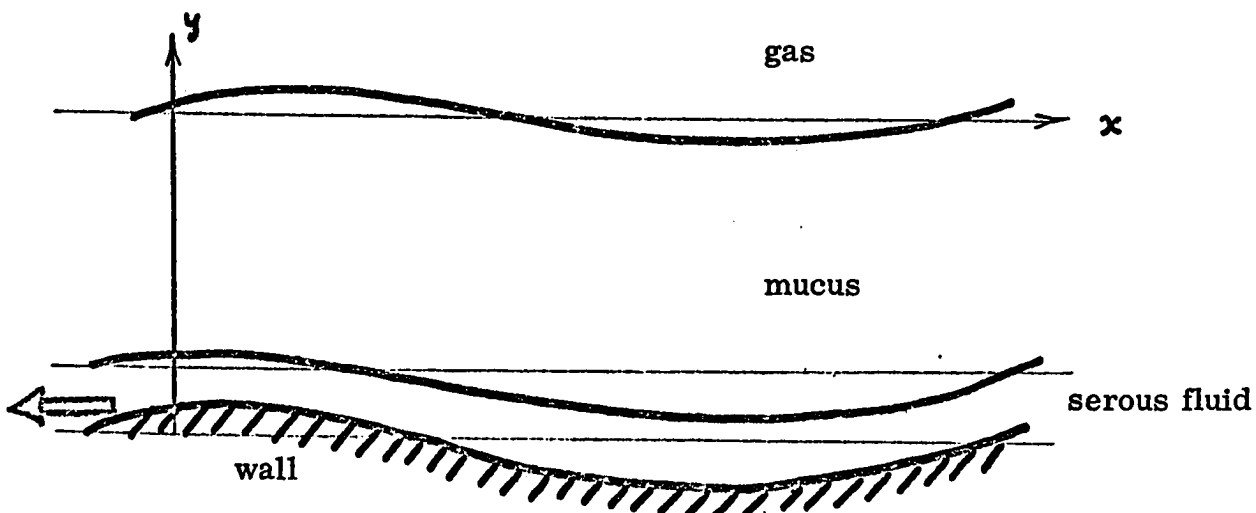


Fig. III

This fluid system is bounded by a non-porous continuous wall that is assumed to approximate the envelope of the uppermost portions of the cilia.* In the "laboratory frame" of reference, the wall geometry

*

It would be interesting to consider the effect of a porous wall in future work.

appears to be a travelling wave moving to the left at a constant speed. The material particles of the wall, however, move in closed ellipses in the same frame, so they have no net motion. (If the tips of the individual cilia are indeed roughly equivalent to the wall material, then one can imagine a cilium tip moving in an ellipse in one cycle as in Fig. II. A). In the real physiological case, it is not altogether clear that the tips alone do form the envelope (see section VI. C.); however, that is a detail which seems unlikely to influence the success or failure of the wavy wall model.

The conjecture that the envelope of the discrete cilia can be replaced by a continuous wall may seem unusual, so it must be justified to some extent.* A relevant experiment is described in Appendix D. Small Reynolds number "Stokes" flows induced by a moving wire brush and by a smooth wall were compared. The fluid particle parallel displacement distribution profiles were nearly the same, measuring the distance from the brush wire tips in one case

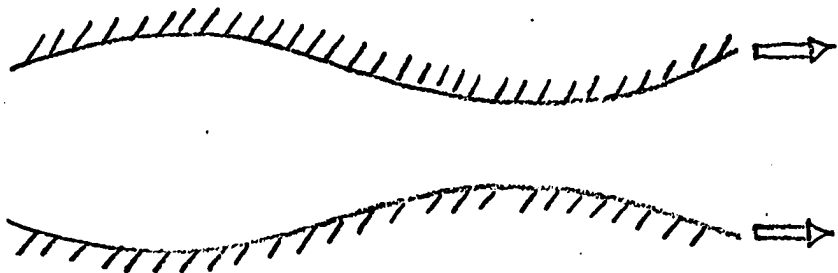
*

In a recent paper by Blake (J. Fluid Mech., 1971, 46, 199-208) ciliary propulsion of microscopic organisms has been modelled by an "envelope" covering the ends of the cilia.

and from the flat wall in the other.

The goal of the analysis is to discover whether such a wavy wall can actually "drive" the fluid, i. e. give it a non-zero average ("drift") velocity and, if so, whether it pumps in the observed direction. We shall find that it can indeed drive the fluid; then we shall explore how closely the qualitative and (then) the quantitative performance of this "pump" approximates that observed for living epithelium.

The type of pumping described above is not related to the closed tube "peristaltic" action studied (among others) by Shapiro et al (1968). In peristaltic pumping the fluid is "squeezed" between two symmetrically moving wavy wall geometries.



The solution for small Reynolds number in the case where there is no external pressure gradient influencing the flow, indicates that the "time-mean flow" (related to the fluid material drift) is a first

order quantity in the amplitude ratio, in cases where this ratio is small. However, in the muco-ciliary pumping considered here, there is no squeezing effect since there is only one wall geometry and a free surface. This wall is both extensible and finite in wavelength. The resulting fluid material drift turns out to be second order in a (small) amplitude ratio.

IV. BASIC NOTATION AND SYMBOLS

Vectors will usually be denoted by lower case Latin letters with a squiggle below, or by a subscript identifying its component:

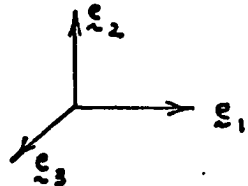
$$\underline{f} \text{ with components } f_i$$

Tensor components will generally be denoted by lower case Latin letters with subscripts. All tensors will be Cartesian.

The tensor itself has two squiggles $\underline{\underline{f}}$.

The unit (Cartesian) direction vectors will be denoted by

$$\underline{\epsilon}_1, \underline{\epsilon}_2, \underline{\epsilon}_3$$



Partial differentiation of a field with respect to space will often be denoted by a comma-index subscript:

$$\frac{\partial A}{\partial x_j} \equiv A_{,j}$$

$$\frac{\partial f_{ij}}{\partial x_k} \equiv f_{ij,k}$$

x and y will be often used interchangeably with x_1 and x_2 respectively, and the corresponding spatial derivative may be written as follows:

$$\frac{\partial f}{\partial y} \equiv f_{,y} \equiv f_{,2}$$

$$\frac{\partial f}{\partial x} \equiv f_{,x} \equiv f_{,1}$$

The partial derivative with respect to time may be written as $f_{,t}$.

A prime will often denote the total derivative of a function of y with respect to y . Repeated indices are understood to be summed:

$$f_{ij} h_j \equiv \sum_{j=1}^z f_{ij} h_j$$

The "material" (or "Stokes") derivative of a field in the Eulerian (spatial) frame will be denoted by $\frac{d}{dt}$, and is defined to be

$$\frac{d}{dt} f_{ij} \equiv f_{ij,t} + u_k f_{ij,k}$$

where u is the velocity field.

Barred symbols will represent fields in the serous sublayer; those applicable to the (upper) mucous layer are unbarred:

\bar{f} : serous layer

f : mucous layer

All fields are understood to be functions of x, t and the parameters of the system.

An asterisk denotes either a dimensionless quantity or a complex

conjugate; its meaning is given where applied.

Quantities not in the list of symbols are those with only limited usage, and they will be defined where used.

IV.A.1. Scalar, Vector and Tensor Fields

s_{ij} , \bar{s}_{ij}	total stress tensors	$\left. \begin{array}{l} s_{ij} = -P\delta_{ij} + t_{ij} \\ \bar{s}_{ij} = -\bar{P}\delta_{ij} + \bar{t}_{ij} \end{array} \right\}$
t_{ij} , \bar{t}_{ij}	"extra" stress tensors	
P , \bar{P}	pressure	
d_{ij} , \dot{d}_{ij}	rate of deformation or stretch tensors	
	$d_{ij} \equiv \frac{1}{2} \{ u_{i,j} + u_{j,i} \}$	
	$\dot{d}_{ij} \equiv \frac{1}{2} \{ \bar{u}_{i,j} + \bar{u}_{j,i} \}$	
ω_{ij}	vorticity tensor	$\omega_{ij} \equiv \frac{1}{2} \{ u_{i,j} - u_{j,i} \}$
u_i , \bar{u}_i	velocity vectors	
γ	free surface measured from $y=0$	
$\bar{\gamma}$	interface measured from $y= -h$	
n_i	outward (upper) normal to free surface	

\bar{n}_i upper normal to interface (outward relative
to the serous fluid)

c_i, g_{ij}, P, A_{ij} }
 $\bar{c}_i, \bar{g}_{ij}, \bar{P}, \bar{A}_{ij}$ } Fourier coefficients

x_i Eulerian frame space points

X_i initial coordinate identifying a fluid particle
(i.e. material or Lagrangian frame coordinates)

IV. A. 2. Others

P_0 static pressure of air above upper layer

$s_{0,j}$ total stress in air = $-P_0 \delta_{ij}$

ξ_i unit directions

y_w wall curve with undisturbed position $y = -1.$

z Lagrangian point identifying a cilium tip

$u_L(z, t)$ Lagrangian form of the velocity at the wall

$u_w(x, t)$	Eulerian form of wall velocity
$x_t(z, t)$	equations of a wall particle path
R_u	upper layer region
R_L	lower layer region
R	entire region bounded by ∂R ; $R = R_u + R_L$
δ	energy dissipation $\equiv \int_R S_{ij} u_{i,j} da$
\dot{W}	work rate due to boundary tractions $\equiv \int_{\partial R} u_i S_i da$
c_h	Fourier coefficient of "homogeneous" system
c_p	Fourier coefficient of "particular" system
X_{ij}	8 by 8 matrix of the boundary condition equations
ξ_i	unknown solution vector component for a Fourier coefficient of the velocity field
s_i	vector of inhomogeneous part of boundary conditions

$F_i, \bar{F}_i, G_{ij}, B_{ij}$, } product terms of second order systems
 $C_i, B_{3i}, B_{4i}, D, \bar{D}$

$\gamma_{ij}, b_{3i}, b_{4i}, b_i, \psi_i$ Fourier coefficients of the product terms

IV. B. Dimensional Constants

μ	viscosity of mucus]	$\tau_r \equiv \frac{\mu}{G}$
G	spring constant of mucus		
τ_r	relaxation time of mucus		
$\bar{\mu}$	viscosity of sublayer		
ρ	density of mucus		
$\bar{\rho}$	density of sublayer		
d	total depth of the two layers with all boundaries plane		
h	relative depth of the mucus		
g	gravitational constant		
g_i	components of gravity vector		

ω, f frequencies of the beat of the cilia, $\omega = 2\pi f$

θ wall amplitude or amplitude of a wall particle in the y direction

λ wavelength of the wall wave, $\lambda = \frac{2\pi}{k}$

k wave number

c speed of wall travelling wave geometry, $c = \frac{\omega}{k}$

IV.C. Dimensionless Constants

ϵ amplitude $\equiv \frac{\theta}{d}$

α wave number $\equiv \frac{2\pi d}{\lambda}$

β x to y axis ratio of elliptical wall particle trajectory

γ ratio of sublayer to mucous density $\equiv \frac{\rho_s}{\rho_m}$

κ ratio of sublayer to mucous viscosity $\equiv \frac{\mu_s}{\mu_m}$

A ratio of inertial to viscous forces $\equiv \frac{\rho \omega d^2}{\mu}$

B ratio of gravitational to viscous forces $\equiv \frac{\rho g d}{\mu \omega}$

T

ratio of relaxation time to period $\equiv \omega \tau_R$

$$Q \equiv \frac{2}{1 + i n T} \quad n=1,2$$

$$N \equiv n\alpha$$

$$n=1,2$$

$$\phi \equiv \alpha x + t$$

$$\Phi \equiv \alpha X + t$$

$$\Phi' \equiv \alpha X + t'$$

V. CONSTITUTIVE EQUATIONS

The analysis of the flow of mucus is, among other things, complicated by the fact that the main fluid involved has been recognized as visco-elastic. The fact that mucous secretions can flow as a fluid yet demonstrate a clear springiness should be familiar to most of us (Hwang et al, 1969). Thus in this section, we shall touch upon some relevant ideas in continuum mechanics in order to clarify the equations used in this model.

V.A. Constitutive Equations in General

A constitutive equation, for our purposes, will be a relation between the stress and the motion that defines an ideal material. This is actually a mathematical model which approximates some real materials as closely as possible, or perhaps as closely as is convenient for analysis. An example is the "incompressible Newtonian fluid," having the constitutive equation for "extra" stress:

$$\tau_{ij} = 2\mu d_{ij} \quad ; \quad S_{ij} = -P\delta_{ij} + \tau_{ij}$$

A constitutive equation is "good" if it describes the flow

behavior of the material under a wide variety of motions. Restrictions on the quantities which may be used in the formulation of constitutive equations are prescribed by a set of physical principles that must be imposed on them in order for them to be valid.

V. B. The Principle of Material Indifference (or Material Objectivity)

The "principle of material indifference", considered as one of the most important by Truesdell and Toupin (1960), states that the response of the material should be independent of the observer. In other words, the stress field associated with a given motion is the same no matter from what reference frame one looks at it.

There are several ways to approach the formulation of constitutive equations such that the principle of material indifference holds. One way is to require that the form of the constitutive relations be invariant under the most general transformations of space and time such that the distance and angle between any two points is preserved. This can be shown to reduce to changes of frame of the following type (Eringen, 1962):

$$x'_i = Q_{ij} x_j + a_i \quad (\text{V. B. 1})$$

where $Q_{ij} = Q_{ij}(t)$ is an arbitrary non-singular orthogonal tensor function of time and a_i is an arbitrary vector function of time.

As an example, one immediate result of this requirement is that constitutive equations cannot depend on the vorticity tensor.

Another approach to the formulation of some types of constitutive equations (especially those involving time rates of stress and deformation) is to write the relation in an "intrinsic" coordinate frame attached to the material in some way. This frame need not be an inertial frame, nor is it fixed in space. Supposedly, the principle of material indifference is automatically satisfied since we are in an "intrinsic" frame. The difficulty with this approach, however, is that boundary value problems are best dealt with relative to a fixed frame in which the laws of motion and boundary conditions are formulated. Thus, the constitutive equation formulated in this "intrinsic" frame must be transformed to a fixed frame (Oldroyd, 1950). We shall consider this in more detail in section

V. D.

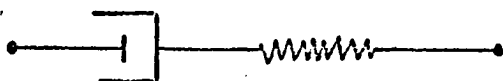
V. C. Classical Visco-elasticity

Combining the linear theories of a Hookean solid with a Newtonian fluid, Maxwell, Voigt and others obtained constitutive equations that could be called visco-elastic in that they exhibit both solid and fluid properties. In particular, the "Maxwell fluid" of classical linear visco-elasticity is defined relative to a fixed coordinate system by the following equation for "extra" stress (Eirich, 1956, I):

$$\frac{\partial t_{ij}}{\partial t} = -\frac{1}{\tau_R} t_{ij} + 2G \dot{\gamma}_j \quad (\text{V.C.1})$$

where $G \equiv \frac{\mu}{\tau_R}$ is the modulus of rigidity or shear modulus of the fluid and τ_R is the relaxation time.*

The above was originally derived in its one-dimensional form by imagining small fluid elements to behave like a spring and dashpot :



These ideas were later extended by including time derivate of higher order to get a more general linear theory:

*

This describes a homogeneous fluid since all material elements have the same constitutive equation.

$$\sum_{k=0}^N A_k \frac{\partial^k}{\partial t^k} t_{ij} = \sum_{k=0}^M B_k \frac{\partial^k}{\partial t^k} d_{ij} \quad (\text{V.C.2})$$

A major criticism of the above equations is that they can be shown to satisfy the principle of material indifference only for special motions in which the displacement of a material particle is small. This is due to the fact that the time derivatives of stress and deformation are not "objective" quantities (Oldroyd).

V.D. Special Time Rates Satisfying the Principle of Material Indifference

Not all time rates of change of quantities that are themselves materially "objective" (i.e. satisfy material indifference) are also objective. For example, the stress tensor, t_{ij} , is materially objective by definition; it transforms as a normal tensor under the most general frame changes that preserve distance and angle. However, the partial derivative, $\frac{\partial}{\partial t} t_{ij}$, and the material derivative, $\frac{d}{dt} t_{ij} = t_{ij,t} + u_k t_{ij,k}$, do not transform as tensors under general changes of frame and so they cannot be used in the formulation of constitutive equations. In other words, constitutive equations using partial time derivatives or material derivatives

do not (in general) satisfy the principle of material indifference; they are not independent of the observer.

Fortunately, this difficulty can be remedied by using specially defined time rates that do satisfy the principle of material indifference. Recent interest in the development of such a time flux was initiated by Oldroyd (1950). The basic idea involved in his method, is that the response of a material particle is independent of an observer if the constitutive equations defining the material are formulated in a coordinate system in which tensors "...have a significance for the material element independent of its motion as a whole in space". A particular frame automatically satisfying this condition is one convected with the material (i. e. the coordinate surfaces are material surfaces and they translate, rotate and deform locally with the material). Time derivatives of tensors expressed in this convected frame must then be transformed to a fixed frame so that boundary value problems can be solved. If the convected coordinates ξ and the fixed coordinates ξ are related by $\xi = \xi(\xi, t)$, then the following tensor transformations must hold:

$$\beta_{ij}(\tilde{x}, t) = \frac{\partial x^m}{\partial \tilde{x}^i} \frac{\partial x^p}{\partial \tilde{x}^j} b_{mp}(x, t)$$

$$\left. \frac{\partial}{\partial t} \right|_{\tilde{x}} \beta_{ij} = \frac{\partial x^m}{\partial \tilde{x}^i} \frac{\partial x^p}{\partial \tilde{x}^j} \left\{ \frac{dc}{dt} b_{mp}(x, t) \right\}$$

Thus a convected derivative, $\frac{dc}{dt}$, relative to a fixed frame can be determined.

Although constitutive equations using the convected derivative satisfy the principle of material indifference, there is a physical inconsistency in the fact that the same constitutive equation when expressed in covariant and contravariant form does not define the same material. That is, the covariant and contravariant character of the tensors has an effect on the intrinsic response of the material and there is no reason why this should happen physically. For example, the following two equations can be shown to define two different fluids (Oldroyd):

$$(1 + \lambda \frac{dc}{dt}) t_{ij} = 2\mu (1 + \gamma \frac{dc}{dt}) d_{ij}$$

$$(1 + \lambda \frac{dc}{dt}) t^{ij} = 2\mu (1 + \gamma \frac{dc}{dt}) d^{ij}$$

The difficulty discussed above can be removed by considering

the co-rotational (also called "Jaumann") derivative, discussed by Prager (1961), Fredrickson (1964) and more formally by Truesdell and Toupin (1960). In this case, a time derivative is considered in a rigid frame that translates and rotates instantaneously with each material particle (but it does not deform as does Oldroyd's convected coordinate system). Constitutive equations formulated with respect to this frame (which participates in the instantaneous rotation of the material) are automatically independent of an observer. Transformation to a fixed frame with coordinates \tilde{x} gives the co-rotational derivative, $\frac{d}{dt}^*$. Relative to a fixed frame, the co-rotational (Jaumann) derivative is

$$\hat{\frac{d}{dt}} t_{ij} \equiv \frac{d}{dt} t_{ij} + t_{ik} \omega_{kj} - t_{kj} \omega_{ik} \quad (\text{V. D. I})$$

where $\frac{d}{dt} t_{ij} = t_{ij,t} + u_k t_{ij,k}$ and ω_{ij} is the vorticity tensor.

The two time rates we have discussed so far are not the only ones that can be shown to satisfy material indifference. Eringen (1962) lists a total of five different "stress fluxes" and Truesdell and Toupin (1960) consider three. According to Prager (1961),

and Truesdell and Toupin, of the several different possible choices of time rates, the best one to use in the formulation of constitutive equations is the co-rotational derivative defined above. The reasons for this choice are that it is the simplest in form because it involves the vorticity tensor alone, whereas the others depend also on the rate of deformation, and because it defines the same material whether covariant or contravariant tensors are used in the relation.

V. E. Constitutive Equation for a Linearly Visco-elastic Fluid Mucus

For simplicity, we shall choose the simplest visco-elastic fluid constitutive equation, i. e. one which is linear and which has only a single relaxation time. In a co-rotational frame (with co-ordinates ξ) translating and rotating instantaneously with each fluid particle, the constitutive equation for an element of mucus is taken to be that of a Maxwell fluid, defined by the equation:

$$\frac{\partial}{\partial t} \left| \begin{matrix} \mathcal{T}_{ij}(\xi, t) = -\frac{1}{\tau_R} \mathcal{T}_{ij}(\xi, t) + 2G \Delta_{ij}(\xi, t) \end{matrix} \right. \quad (\text{V. E. 1})$$

where \mathfrak{T}_{ij} and Δ_{ij} are, respectively, the "extra" stress and rate of deformation tensors relative to the co-rotational frame.

Transforming the above equation to a fixed, inertial frame with coordinates, ξ , gives a usable constitutive equation for mucus of the form:

$$\hat{\frac{d}{dt}} t_{ij} = -\frac{1}{\tau_R} t_{ij} + 2G d_{ij} \quad (\text{V.E. 2})$$

where the total stress, $S_{ij} = -P\delta_{ij} + t_{ij}$, the extra stress, $t_{ij} = t_{ij}(\xi, t)$, and rate of deformation, $d_{ij} = d_{ij}(\xi, t)$, are relative to fixed axes. $\hat{\frac{d}{dt}}$ is the co-rotational derivative defined by (V.D.1).

Writing out each term of the constitutive equation gives the following:

$$\frac{\partial}{\partial t} t_{ij} + u_k t_{ij,k} + t_{ik} \omega_{kj} - t_{kj} \omega_{ik} = -\frac{1}{\tau_R} t_{ij} + 2G d_{ij}$$

(V.E. 3)

where ω_{ij} is the vorticity tensor, u_k is the velocity vector, τ_R is the relaxation time, and G is the modulus of rigidity.

This equation describes a linearly visco-elastic, stress-relaxing fluid for any general motion. The form of the constitutive equation with respect to fixed coordinates differs from the classical

Maxwell fluid (also relative to fixed axes) by the addition of the product terms $\omega_k t_{ij,k} + t_{ik} \omega_{kj} - t_{kj} \omega_{ik}$ to the left side of the equation. It is these terms that are necessary to satisfy the principle of material indifference for all motions; they can be neglected only when the velocity and velocity gradients are "small". Thus the classical Maxwell fluid is a valid constitutive equation only for special motions in which the product terms can be omitted, and the intuitive notion of a fluid element behaving like a spring and dashpot is not exactly applicable (in a fixed frame).

Fredrickson (1962) has discussed constitutive equations of stress-relaxing solids similar to the (fluid) one considered above and has found that they predict normal stress effects but not a non-Newtonian viscosity (probably due to its linearity).

A Maxwell model of mucus has been used by Hwang (1967) and Denton et al (1968) in experiments determining its rheological constants. According to him, an equation of this form would exhibit what he considers as one of the most pronounced non-Newtonian aspects of mucus: its "...large amount of initial elastic deformation and subsequent recoil". Some of the experimental results of Hwang and Litt are also found in published form in the paper by

Denton et al (1968). In another paper (Litt, 1970), a Maxwell model is used as a basis for a discussion of the visco-elasticity of mucus.

It is by no means claimed here that our constitutive equation will describe all or even most of the rheological behavior of mucus; it does describe an ideal fluid material which possesses memory and satisfies the principle of material indifference. Real mucus exhibits not only elastic recoil and stress relaxation, but it is heterogeneous and extremely shear sensitive and may have plasticity and thread-forming properties (Hwang et al, 1969). Furthermore, under more testing, it may also turn out to be a non-linear visco-elastic fluid with the fairly common polymeric property of a normal stress effect.

V. F. Constitutive Equation of Serous Fluid

The serous fluid lying under the mucous blanket has been described as a watery fluid which does not exhibit the marked visco-elasticity of mucus. As previously stated, it is not clearly agreed upon that two distinct layers of fluid exist. Nevertheless, the majority of physiologists believe that the fluid in which the cilia beat

is not visco-elastic but is in fact quite "watery".* However, no quantitative results appear to have been published on the mechanical properties of this fluid.

We shall simply assume that the serous fluid is an incompressible Newtonian fluid, i.e.

$$\dot{\epsilon}_{ij} = 2\bar{\mu} \ddot{\sigma}_{ij} \quad (\text{V. F. I})$$

*

For example see papers by Lucas and Douglas (1934) and Litt (1970).

VI. BOUNDARY CONDITIONS

VI. A. Model Diagram

A sketch of the theoretical model is drawn below. The most radical aspect is the replacement of the ciliary envelope by a continuous, impermeable wavy wall. A layer of linearly visco-elastic mucus is bounded above by still air at constant pressure and below by a Newtonian serous fluid. The stress tensors are shown in their respective regions of application.

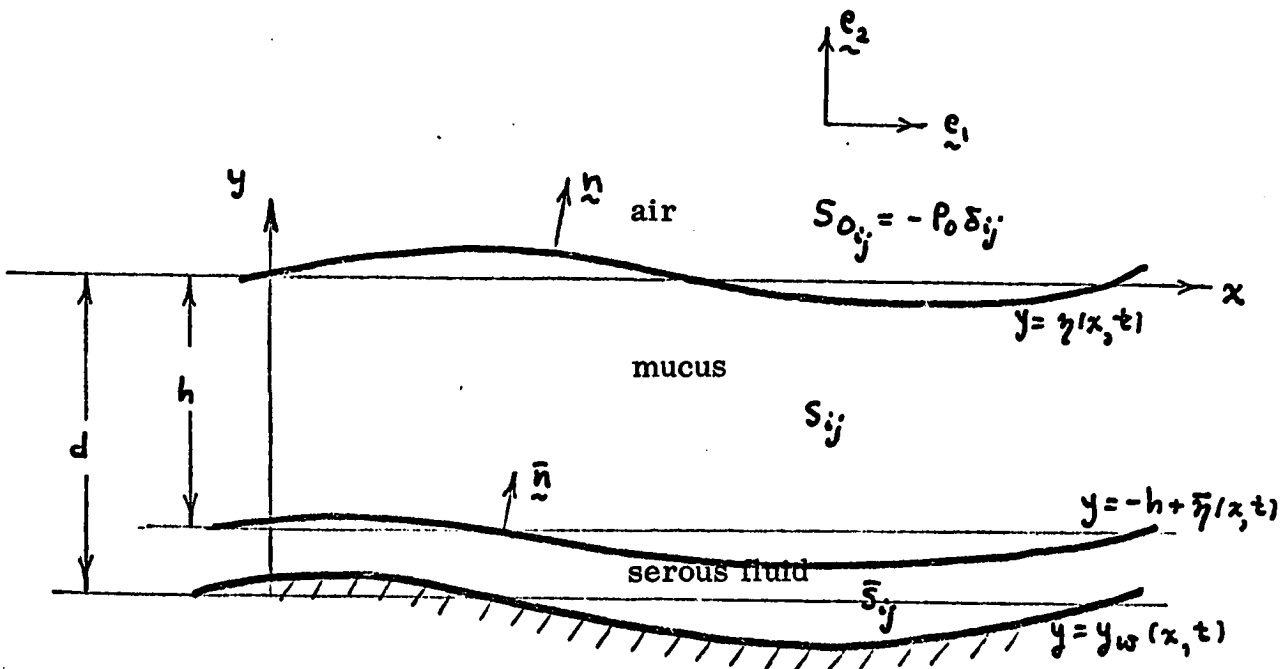


Fig. VI. A

The horizontal lines $y = 0$ and $y = -h$ are the undisturbed positions of the free surface and interface respectively and $y = -l$ is the wall in the case of no motion of a wall material particle.

VI. B. Boundary Conditions at the Free Surface and Interface

Conditions at the free surface and the two-fluid interface are (I, II) that the stress tractions and velocities are continuous and (III) that the surfaces are material curves. The last condition may be regarded as an equation for the unknown surface or interface rather than a boundary condition. In that case, the field equations can be solved for the velocity field with boundary conditions I and II, and III is used to find the region in which the field is defined (see the first order system of equations of section IX. C.). In the above sense, we may consider equations for the free surface and interface (i. e. boundary condition number III) as "uncoupled" from the other field equations.

The statement that the stress tractions are continuous implicitly neglects surface tension forces between the gas-mucus "free" surface and the mucus-serum (immiscible) interface. The importance

of surface tension is discussed in section IX. B. 2.

The boundary conditions are listed as follows:

1. at the free surface, $y \equiv \gamma(x, t)$

$$\text{I. } S_{ij} n_j = S_{0ij} n_j \quad (\text{VI. B. 1})$$

$$\text{III. } u_z = \frac{d}{dt} \gamma \quad (\text{VI. B. 2})$$

2. at the interface, $y \equiv -h + \bar{\gamma}(x, t)$

$$\text{I. } \bar{S}_{ij} \bar{n}_j = S_{ij} \bar{n}_j \quad (\text{VI. B. 3})$$

$$\text{II. } u_i = \bar{u}_i \quad (\text{VI. B. 4})$$

$$\text{III. } \bar{u}_z = \frac{d}{dt} \bar{\gamma} \quad (\text{VI. B. 5})$$

One difficulty in applying the above conditions is that the curves γ and $\bar{\gamma}$ are unknown. This will be surmounted by expanding in powers of small parameters about their undisturbed positions.

VI. C. Wall Boundary Condition

The waving wall presumably corresponds to the envelope of

the tips of the cilia as shown in Figs. II. C and VI. C. 1. b. Our model takes this boundary to be a continuous, impermeable wall although the actual ciliary "carpet" is porous and so it is not obvious that the no-slip condition is valid there. However, at these very small Reynolds numbers based on representative dimensions and velocities of the ciliary wall, where*

$$R = \frac{d_{cilia} \times (u_w)_{max} \times \rho_{serous}}{\bar{\mu}_{serous}} = O(10^5)$$

the porosity and slip may be negligible. This seems to be the case for experiments in which a wire file brush was dragged through a viscous fluid in small Reynolds number ("Stokes") flow. Comparison between a flat wall and the wire brush showed little difference. **

Two conditions are required to express the two components of

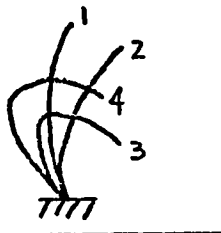
* $d_{cilia} = .2 \text{ mic}$, $(u_w)_{max} = \omega \theta = 200 \text{ mic/sec.}$,
 $\bar{\mu}_{serous} = .1 \text{ poise}$, $\rho_{serous} = 1 \text{ gm/cm}^3$

**

For a more detailed discussion of this experiment, see Appendix D.

velocity at the wall. In this analysis, it is convenient to specify the trajectory of any wall material point (or equivalently, "particle") rather than the shape of the wall plus an extensibility condition. The trajectory itself is of basic importance in the problem, and if it could be identified as that of a cilium tip, a good basis for this boundary condition would exist. If one were to choose a travelling sine curve for the wall geometry and require that the wall material be inextensible, for example, then the wall point trajectory would be like a "figure eight" to second order in wall amplitude.* This would be a poor model of cilium tip motion and, as we shall see, would not give a suitable pumping effect.

In cases where the cilia bend so much that the tip is not the highest point during part of the cycle, e.g.:



*

An inextensible sine curve was used to model a sperm tail in a paper by G. I. Taylor (1951). He doesn't mention that the wall point trajectory is a "figure eight", however,

the continuum model in which a wall material point models a cilium tip might be valid, if the high part of the cilium is covered by the tips of neighboring cilia. It is conceivable, however, that a different detailed boundary behavior and interpretation may be required in such cases.

VI.C.1. With the non-dimensional quantities considered in section VIII, the trajectory of the wall material particle [identified by x -component material ("Lagrangian") coordinate \bar{z}] is given by

$$x = x_T(\bar{z}, t) = \bar{z} - \epsilon \beta \cos(\alpha \bar{z} + t)$$

(VI. C. 1.a, b)

$$y = y_T(\bar{z}, t) = -1 + \epsilon \sin(\alpha \bar{z} + t)$$

where ϵ is an amplitude parameter (taken to be small), α is dimensionless wave number, and β is used to determine the direction of the orbit (clockwise or counter-clockwise) as well as its ellipticity. The continuum set of points $(\bar{z}, -1)$ identify the material particles of the wall. For each \bar{z} located on the axis, the position of a wall material point is given by equations (VI. C. 1. a and b).

At $t = 0$, the position of the wall point is

$$X = \bar{z} - \epsilon \beta \cos(\alpha \bar{z})$$

(VI. C. 1. c)

$$Y = -1 + \epsilon \sin(\alpha \bar{z})$$

where (X, Y) represent initial position in this case. Thus, the initial coordinates also identify a wall point from (VI.C.1.c). We use the Lagrangian representation \bar{z} because the Lagrangian y coordinate is fixed at -1 and the transformation from Lagrangian to Eulerian ("laboratory") coordinates is easier.

Sketched below are the wall points corresponding to some evenly spaced Lagrangian points ($\bar{z}_1, \bar{z}_2, \bar{z}_3, \dots$) for $\alpha = \beta = 1$ at $t = 0$.

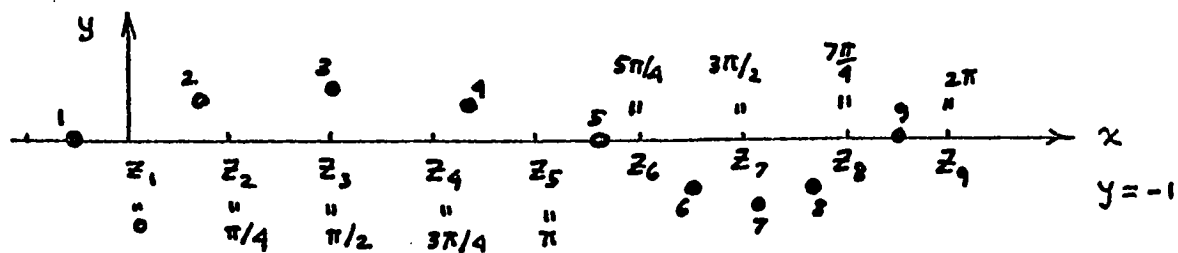


Fig. VI.C.1.a

Number	\bar{z}	x	y
1	0	$-\epsilon$	0
2	$\pi/4$	$\pi/4 - .71\epsilon$	$.71\epsilon$
3	$\pi/2$	$\pi/2$	ϵ
4	$3\pi/4$	$3\pi/4 + .71\epsilon$	$.71\epsilon$
5	π	$\pi + \epsilon$	0
6	$5\pi/4$	$5\pi/4 + .71\epsilon$	$-.71\epsilon$
7	$3\pi/2$	$3\pi/2$	$-\epsilon$
8	$7\pi/4$	$7\pi/4 - .71\epsilon$	$-.71\epsilon$
9	2π	$2\pi - \epsilon$	0

The points (x, y) in Figure (VI.C.1.a) are locations of the wall material points; a line drawn through a continuum set of points (z) will give the wall curve. * A possible configuration of the cilia (where the wall points are cilia tips) is drawn below. (Only 9 points are shown; there is actually a continuum).

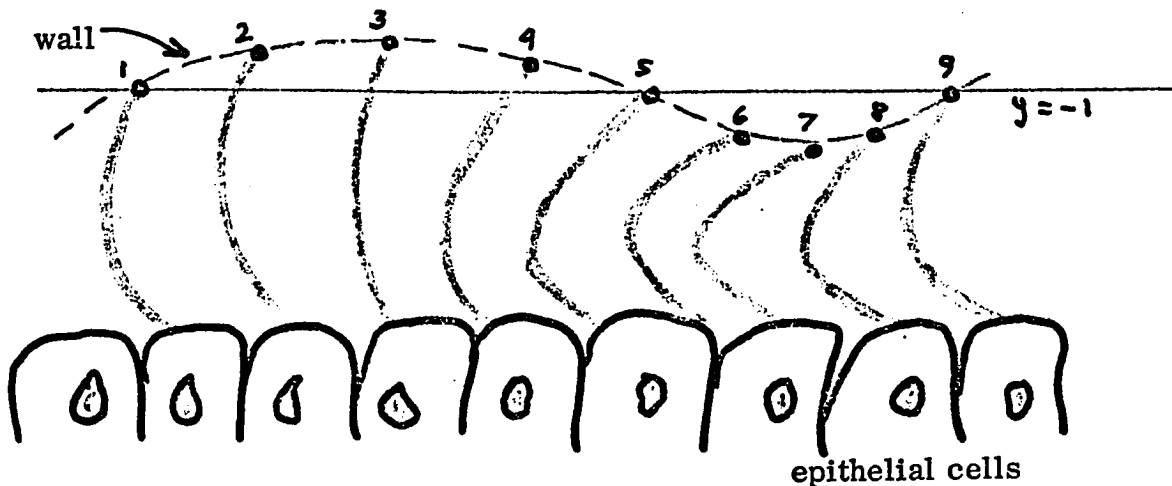


Fig. VI. C.1. b

If time is eliminated between the two equations (VI.C.1.a,b), the locus of points (i.e. the trajectory of a wall material particle) is found to be an ellipse of vertical (y) axis 2ϵ and horizontal

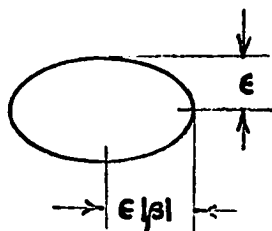
*

The equation of the wall curve is considered in detail in section VI.C.4.

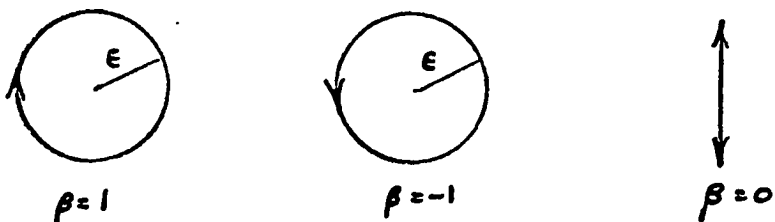
(x) axis $z \in |\beta|$:

$$\left(\frac{x-z}{\beta} \right)^2 + (y+1)^2 = \epsilon^2 \quad (\text{VI. C. 1. d})$$

This ellipse is drawn below (see Fig. II. A. 1).



The sign of β determines the direction taken by the wall particle, and the absolute value of β determines the axis length, e.g.



VI. C. 2. The Lagrangian (or "material" frame) form of the wall particle velocity is, by definition,

$$u_L(z, t) \equiv \frac{\partial}{\partial t} x_T(z, t)$$

where all quantities are dimensionless and \bar{z} identifies the material wall point. The velocity components are thus

$$u_{L_1}(\bar{z}, t) = \epsilon \beta \sin(\alpha \bar{z} + t)$$

$$u_{L_2}(\bar{z}, t) = \epsilon \cos(\alpha \bar{z} + t)$$

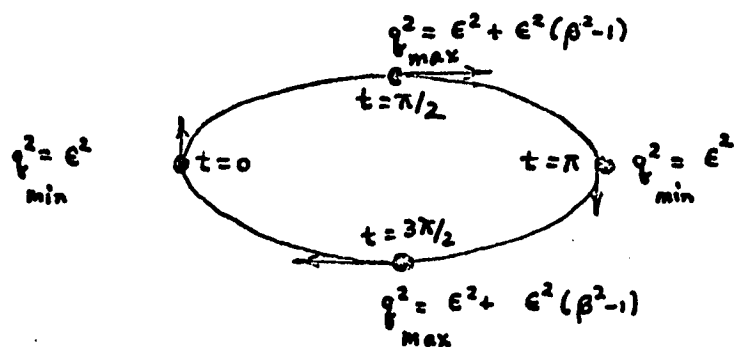
(VI. C. 2. a, b)

The squared speed of a wall point is

$$q^2 = u_{L_1}^2 + u_{L_2}^2 = \epsilon^2 \{ 1 + (\beta^2 - 1) \sin^2(\alpha \bar{z} + t) \}$$

(VI. C. 2. c)

This indicates that the speed of a wall particle as it travels on its elliptical path is not constant in time except for the case of a purely circular motion ($\beta = \pm 1$). For example, if $\beta > 1$ and $\bar{z} = 0$, then the squared speed varies as follows:



However, the time average "squared" speed over any half period $(t, t+\pi)$ is constant; that is

$$\int_{t}^{t+\pi} q^2(z, t') dt' = \epsilon^2 \left\{ t' + (\beta^2 - 1) \left[t'/2 - \frac{1}{4} \sin 2(x^2 + t') \right] \right\} \Big|_{t'=t}$$

(VI. C. 2. d)

= constant

Thus our model does not incorporate the observed difference in average velocities of the actual cilium tip in the "effective" and "recovery" parts of its cycle (section II. A.). This may not be critical, at least for Newtonian fluids, since experimental results on mechanical ciliary systems indicate that the "...asymmetric period of the beat of the cilia is of minor importance in sustaining the motion of particulate matter in Newtonian liquids" (Miller, 1968).

VI. C.3. The Eulerian frame expression for the wall velocity is found by inverting the x trajectory equation (VI. C.1. a). The equation giving the y coordinate of the wall particle (VI. C.1. b) is not explicitly needed because the Lagrangian coordinates are located at $(z, -1)$ so that this representation is already referred to the undisturbed wall position, $y = -1$. This simplification is one major reason for our choice of the z Lagrangian representation

over others (e.g. initial coordinates).

Recall that (VI.C.1.a):

$$x = z - \epsilon \beta \cos(\alpha z + t)$$

and (VI.C.2.a,b):

$$u_{L_1} = \epsilon \beta \sin(\alpha z + t)$$

$$u_{L_2} = \epsilon \cos(\alpha z + t)$$

The Eulerian frame expression can be found by inverting (VI.C.1.a) as follows:

$$\underline{u}_L(z, t) \xrightarrow{z(x, t)} \underline{u}_w(x, t)$$

where \underline{u}_w is the velocity along the wall referred to $y = -1$.

Now, for simplicity, write

$$f = f(z, t) \equiv \beta \cos(\alpha z + t) \quad (\text{VI.C.3.a})$$

so that (VI.C.1.a) becomes

$$x = z - \epsilon f(z, t) \quad (\text{VI.C.3.b})$$

$$z = x + \epsilon f(z, t) \quad \text{and} \quad |f| \leq |\beta| \leq O(1)$$

Expand f in a Taylor series in x about $\epsilon=0$ (i.e. about $z=x$):

$$f(z, t) = f(x, t) + (z - x) \left. \frac{\partial f}{\partial z} \right|_{z=x} + \frac{1}{2} (z - x)^2 \left. \frac{\partial^2 f}{\partial z^2} \right|_{z=x} + \dots$$

$$= f(x, t) + \epsilon f(z, t) \left. \frac{\partial f}{\partial z} \right|_{z=x} + O(\epsilon^2)$$

$$f(x, t) + \epsilon f(z, t) \left. \frac{\partial f}{\partial z} \right|_{z=x} + O(\epsilon^2)$$

$$= f(x, t) + \epsilon f(x, t) \left. \frac{\partial f}{\partial z} (z, t) \right|_{z=x} + O(\epsilon^2)$$

$$= \beta \cos \phi - (\alpha \beta^2 \sin \phi \cos \phi) \epsilon + O(\epsilon^2)$$

(VI. C. 3. c)

where

$$\Phi = \alpha x + t$$

Similarly, the Lagrangian velocities (VI. C. 2. a, b) are expanded in Taylor series about $\epsilon=0$ using (VI. C. 3. b).

$$\dot{x}_L(z, t) = \dot{x}_L(x, t) + \epsilon f(z, t) \left. \frac{\partial \dot{x}_L}{\partial z} \right|_{z=x} + \frac{1}{2} \epsilon^2 f^2(z, t) \left. \frac{\partial^2 \dot{x}_L}{\partial z^2} \right|_{z=x} +$$

(VI. C. 3. d)

$$+ O(\epsilon^3 f^3 \left. \frac{\partial^3 \dot{x}_L}{\partial z^3} \right|_{z=x})$$

Using (VI.C.3.c) for $f(z, t)$, and the necessary partial derivatives of u_L , we get the Eulerian form of the wall material velocity components (i.e. the right side of (VI.C.3.d)):

$$u_{w_1}(x, t) = \epsilon \beta \sin \phi + \epsilon^2 \alpha \beta^2 \cos^2 \phi + \epsilon^3 \left\{ -\frac{3}{2} \alpha^2 \beta^3 \sin \phi \cos^2 \phi \right\} + O(\epsilon^4 \alpha^3 \beta^4)$$

$$u_{w_2}(x, t) = \epsilon \cos \phi + \epsilon^2 \left\{ -\alpha \beta \cos \phi \sin \phi \right\} + \epsilon^3 \left\{ \alpha^2 \beta^2 \cos \phi \sin^2 \phi - \frac{1}{2} \alpha^2 \beta^3 \cos^3 \phi \right\} + O(\epsilon^4 \alpha^3 \beta^3)$$

These equations give the velocity along the undisturbed ($y = -1$) wall in the "laboratory" frame. If the wall velocity is regarded as an expansion in amplitude, ϵ , then

$$u_{w_i} = u_{w_i}(x, t) = \sum_{k=1}^{\infty} \epsilon^k u_{w_i}^{(k)}$$

where $u_{w_i}^{(k)} = u_{w_i}^{(k)}(x, t)$ and:

$$u_{w_1}^{(1)} = \beta \sin \phi$$

$$u_{w_1}^{(2)} = \frac{1}{2} \alpha \beta^2 (1 + \cos 2\phi)$$

$$u_{w_2}^{(1)} = \cos \phi$$

$$u_{w_2}^{(2)} = -\frac{1}{2} \alpha \beta \sin 2\phi$$

$$u_{w_1}^{(3)} = O(\alpha^2 \beta^3)$$

$$u_{w_1}^{(4)} = O(\alpha^3 \beta^4) \quad (\text{VI.C.3.e})$$

$$u_{w_2}^{(3)} = O(\alpha^2 \beta^2)$$

$$u_{w_2}^{(4)} = O(\alpha^3 \beta^3)$$

Thus, the boundary condition for the velocity field,

$$\underline{u} = \sum_k \sum_m \epsilon^k B^m \underline{u}^{(k,m)}, \quad \text{is}$$

$$\epsilon: \quad \left. \underline{u}^{(1,0)} \right|_{y=-1} = \underline{u}_w^{(1)}$$

$$\epsilon^2: \quad \left. \underline{u}^{(2,0)} \right|_{y=-1} = \underline{u}_w^{(2)}$$

$$B: \quad \left. \underline{u}^{(0,1)} \right|_{y=-1} = 0$$

VI.C.4. From the orders of magnitude of the wall velocity emerges a restriction on the values allowed for α and β . Consider the asymptotic expansion for any function $\tilde{z}(x, t, \epsilon)$:

$$\tilde{z} = \epsilon f^{(1)} + \epsilon^2 f^{(2)} + \epsilon^3 f^{(3)} + \dots + \epsilon^k f^{(k)} + \dots$$

(VI.C.4.a)

$$\text{where } f^{(k)} = f^{(k)}(x, t)$$

This expansion converges asymptotically as $\epsilon \rightarrow 0$ because the remainder after k terms approaches zero faster than the k^{th} term. That is

$$\lim_{\epsilon \rightarrow 0} \left| \frac{f^{(k+1)} \epsilon^{k+1} + f^{(k+2)} \epsilon^{k+2} + \dots}{f^{(k)} \epsilon^k} \right| = 0$$

The accuracy of the expansion for a given "small" ϵ depends on the magnitudes of the $f^{(k)}$. If the $f^{(k)}$ are $O(1)$, then an expansion to 2nd order ($\tilde{z} \sim \epsilon f^{(1)} + \epsilon^2 f^{(2)}$) would be a "good" approximation to the actual function if $\epsilon^2 \ll 1$.

Since the expansion for u_{w_1} is (equation (VI.C.3.e))

$$\begin{aligned} u_{w_1} &= \epsilon u_{w_1}^{(1)} + \epsilon^2 u_{w_1}^{(2)} + \epsilon^3 u_{w_1}^{(3)} + \dots \\ &= \beta \epsilon \{ U^{(1)} + (\alpha \beta \epsilon) U^{(2)} + (\alpha \beta \epsilon)^2 U^{(3)} + \dots \} \end{aligned}$$

where $U^{(k)} = O(1)$

then the requirement is

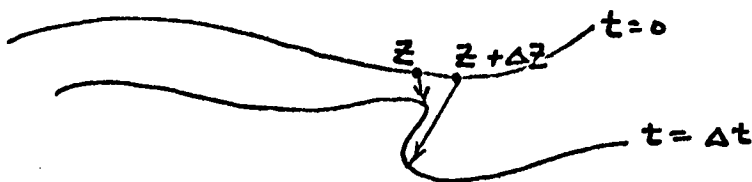
$$(\alpha \beta \epsilon)^2 \ll 1$$

(VI. C. 4. b)

The expansion for u_{w_2} yields the same result. This same criterion (VI. C. 4. b) also emerges from the kinematic constraint on a "well-behaved" continuous wall that no material point can overtake its neighbor. For a single-valued continuous material curve at any instant of time, t , consider two particles separated by the (Lagrangian) distance Δz (z and $z + \Delta z$ identify two wall particles):



The displacement Δx must be of the same sign as Δz for all future times. This is not true for Δy nor for a curve that is not single-valued, e.g.:



The requirement that the material cannot overtake its neighbor can be expressed mathematically as

$$\frac{\partial x}{\partial z} \Big|_t > 0$$

so that $\Delta x > 0$ when $\Delta z > 0$. Since the equation for the x component of the wall particle trajectory (VI. C. 1. a) is $x = z - \epsilon \beta \cos(\alpha z + t)$, then

$$\frac{\partial x}{\partial z} = 1 + \alpha \beta \epsilon \sin(\alpha z + t) \quad (\text{VI. C. 4. b})$$

and the constraint is satisfied since $|\alpha \beta \epsilon| < 1$ according to (VI. C. 4. b).

VI. C. 5. The equation of the wall curve in an Eulerian frame is found by inverting the x trajectory equation (VI. C. 1. a) and expanding in a Taylor series about $\epsilon = 0$ in much the same way that the Eulerian form of the velocity is obtained from the Lagrangian in section VI. C. 3.

The y trajectory equation (VI. C. 1. b) is

$$y = y(z, t) = -1 + \epsilon \sin(\alpha z + t)$$

and (VI. C. 3. b) is the inverted x equation:

$$z = x + \epsilon f(z, t)$$

where $f(z, t) \equiv \beta \cos(\alpha z + t)$

The equation of the wall curve, $y_w(x, t)$, is obtained as follows.

$$\begin{array}{ccc} y(z, t) & \xrightarrow{\text{(VI. C. 3. b)}} & y_w(x, t) \quad (\text{VI. C. 5. a}) \\ \downarrow & & \\ \text{(VI. C. 1. b)} & & \end{array}$$

$$\sin(\alpha z + t) = \sin(\alpha x + t) + \epsilon f(z, t) \stackrel{\frac{\partial}{\partial z}}{=} \sin(\alpha z + t) \Big|_{z=x} + O(\epsilon^2 f^2)$$

Using (VI. C. 3. c) which gives the Taylor series expansion for $f(z, t)$

we get

$$\sin(\alpha z + t) = \sin \phi + (\alpha \beta \cos^2 \phi) \epsilon + O(\epsilon^2 \beta^2)$$

Therefore,

$$y_w = y_w(x, t) = -1 + \epsilon \sin(\alpha x + t) + \epsilon^2 \alpha \beta \cos^2(\alpha x + t) + O(\epsilon^3) \quad (\text{VI. C. 5. b})$$

Regarding the wall curve as an expansion in amplitude, we have:

$$y_w = y_w(x, t) = -1 + \epsilon y_w^{(1)} + \epsilon^2 y_w^{(2)} + O(\epsilon^3)$$

(VI. C. 5. c)

$$y_w^{(1)} = y_w^{(1)}(x, t) \equiv \sin \phi$$

(VI. C. 5. d)

$$y_w^{(2)} = y_w^{(2)}(x, t) \equiv \frac{1}{2} \alpha \beta (1 + \cos 2\phi)$$

(VI. C. 5. e)

$$\phi \equiv \alpha x + t$$

The wall is a sine curve only to first order and its geometry moves to the left ($-\xi$) at a constant speed ($\frac{1}{\alpha}$ in these dimensionless variables). The departure from a purely sinusoidal shape is of order $\alpha \beta \epsilon^2$.

The curve $y_w(x, t)$ is most easily drawn from the actual trajectory equations regarding them as parametric in ξ . For a positive β and at $t = 0$, the curve can be drawn:

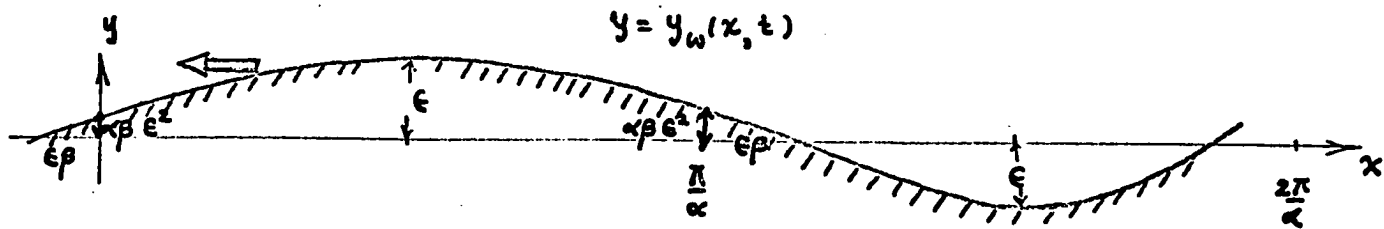
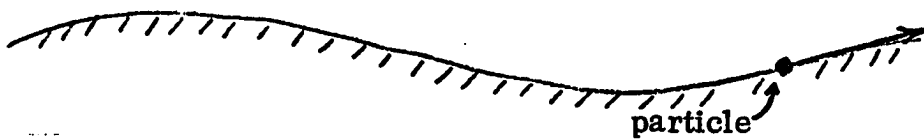


Fig. VI. C. 5

VI. C. 6. The wall can be shown to be an extensible curve by demonstrating that the speed, $q = \{\hat{u}_{w_1}^2 + \hat{u}_{w_2}^2\}^{1/2}$, of the wall material particle in a "wave frame" translating with the wall geometry is not a constant, but is a function of position along the curve. In this wave frame, the wall material point moves along the wall curve at speed q .



wall geometry is fixed in the "wave frame"



$$\alpha \hat{x} = \alpha x + t$$

$$\hat{y} = y$$

$$\alpha \hat{u}_{w_1} = \alpha u_{w_1} + 1 \quad \text{Galilean transformation}$$

$$\hat{u}_{w_2} = u_{w_2}$$

$$\alpha^2 q^2 = (\alpha u_{w_1} + 1)^2 + (\alpha u_{w_2})^2$$

$$\therefore q^2 = \frac{1}{\alpha^2} \left\{ 1 + 2\epsilon \alpha \beta \sin \alpha \hat{x} + \epsilon^2 (\alpha^2 \beta^2 \sin^2 \alpha \hat{x} + \alpha^2 \cos^2 \alpha \hat{x}) + O(\epsilon^3) \right\}$$

(VI. C. 6)

Clearly, the speed is a function of \hat{x} to the first order in ϵ so the wall is an extensible curve. The above result also reveals that the case of a purely vertical wall particle motion ($\beta = 0$) corresponds to an inextensible curve to $O(\epsilon)$ but not to $O(\epsilon^2)$ since the speed of a particle is constant to $O(\epsilon)$ when $\beta = 0$. Thus all material wall particles move at the same speed and there can be no stretching or contracting of the wall curve ($\beta = 0$).

VI. C. 7. It would be informative to separate the effects on the flow of the directions of the wall geometry travel and of the wall material point orbit. This cannot be done because a change in one

involves a corresponding change in the other, according to the

trajectory equations $\dot{x}_T(z, t)$ (IV.C.1.a and b).

For example, if t is replaced by $-t$ in $\dot{x}_T(z, t)$, the wall geometry travels in the \underline{e}_1 direction, but now positive values of β result in a counter-clockwise trajectory.

Fortunately, some insight can be gained if the wall shape and particle velocities are examined qualitatively. The fact that the wall curve is not a sine curve to second order leads to some interesting phenomena. For general values of the parameters α , β and ϵ , the lengths of crests and troughs are unequal, and one suspects that the longer will exert a stronger influence on the mucous flow. Consider two special cases sketched below, in which $\beta = \pm 1$. Note that the directions of the wall velocities in the longer regions tend toward the \underline{e}_1 direction in both cases even though the particle trajectories are opposite in direction.

(i) case of clockwise circular wall particle trajectory. The wall geometry is moving to the left .

$\beta = 1$ C

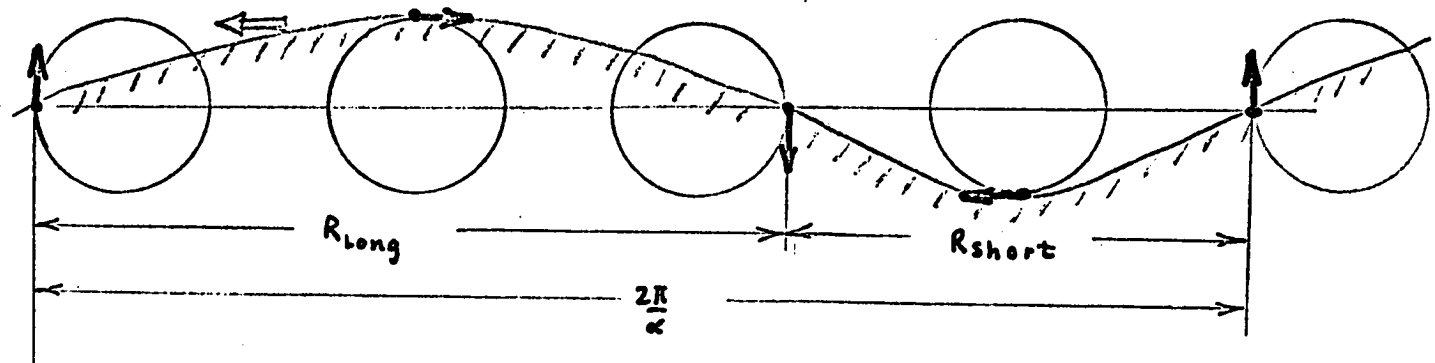


Fig. VI. C. 7.a

(ii) case of counter-clockwise circular wall particle trajectory.

The wall geometry moves to the left.

$\beta = -1$ C

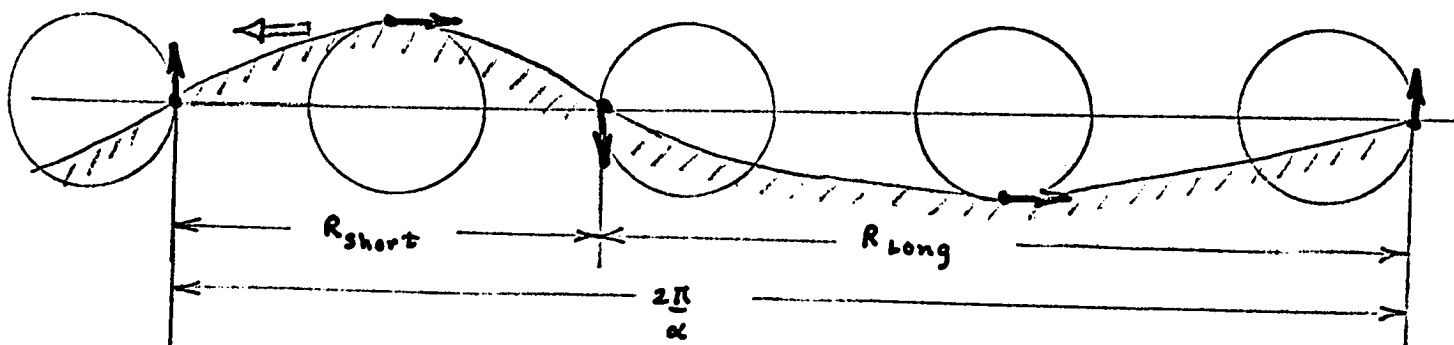


Fig. VI. C. 7.b

The longer and shorter regions have the lengths (to order ϵ):

$$R_{\text{Long}} = \frac{\pi}{\alpha} + 2\epsilon|\beta|$$

$$R_{\text{Short}} = \frac{\pi}{\alpha} - 2\epsilon|\beta| \quad \alpha > 0$$

From the drawings, it appears plausible that the material drift (section XIV) of fluid particles may be in the ξ_1 direction in both cases, because this is the wall material velocity direction in the longer regions. This indeed turns out to be true for both clockwise and counter-clockwise cases when the ratio of long regions to short regions is sufficiently large (see section XVI. D.1.).

$$r \equiv \frac{R_{\text{Long}}}{R_{\text{Short}}} = \frac{\pi + 2\epsilon\alpha|\beta|}{\pi - 2\epsilon\alpha|\beta|} \quad (\text{VI. C. 7})$$

The minimum value of r is 1.0, which occurs when $\alpha\beta = 0$.

For small ϵ , the bound on the product $\alpha\beta\epsilon$ limits the maximum value of r to $O(\frac{\pi+2\epsilon}{\pi-2\epsilon})$ because if $\epsilon^2 \ll 1$,

$|\alpha\beta| \leq 1$ and $\alpha \neq 0$

$$1 \leq r \leq O\left(\frac{\pi+2\epsilon}{\pi-2\epsilon}\right)$$

We may therefore expect the following phenomena to occur at

the two limits:

(a) when $| \alpha \beta | \rightarrow 1$ the ratio of long to short regions is appreciably greater than 1.0. Then the fluid material drift may tend to be in the $+ \xi$, direction regardless of whether the wall particle has a clockwise or counter-clockwise trajectory, and hence regardless of whether the cilium tip is moving in the $+ \xi$, or $- \xi$, direction at the "top" of its stroke.

(b) when $| \alpha \beta | \rightarrow 0$ the ratio of long to short regions approaches unity so that the crests probably exert more influence than the troughs. Since the direction of the wall particle trajectory (sign of β) determines the direction of the wall velocity in the crests, it is important in this limit.

VI. D. Conditions on x and t Dependence

In this analysis, boundary conditions in the x direction and initial conditions are replaced by the assumption that the solution is periodic in x and t with the same fundamental wavelength and frequency as the wall curve. This is equivalent to assuming that there exists a "wave frame" translating with the wall geometry, in which the

solution is independent of time and periodic in x . For the function f :

$$f(x, y, t) = f(x + 2\frac{\pi}{\alpha}, y, t + 2\pi)$$

Thus f may be expanded in a Fourier series of the form

$$f(x, t) = \sum_{n=0}^{\infty} R_n \{ b(n, y) e^{in(\alpha x + t)} \} \quad (\text{VI. D})$$

where b is complex.

VII. "EXACT" SET OF EQUATIONS AND BOUNDARY CONDITIONS

The boundary value problem is completely stated in the present section. Approximations will be made afterward. The only exception will be the wall material velocity \dot{u}_w , which will be approximated by a truncated expansion in the small parameter ϵ . The symbols used are defined in section IV.

The flow system is sketched as follows:

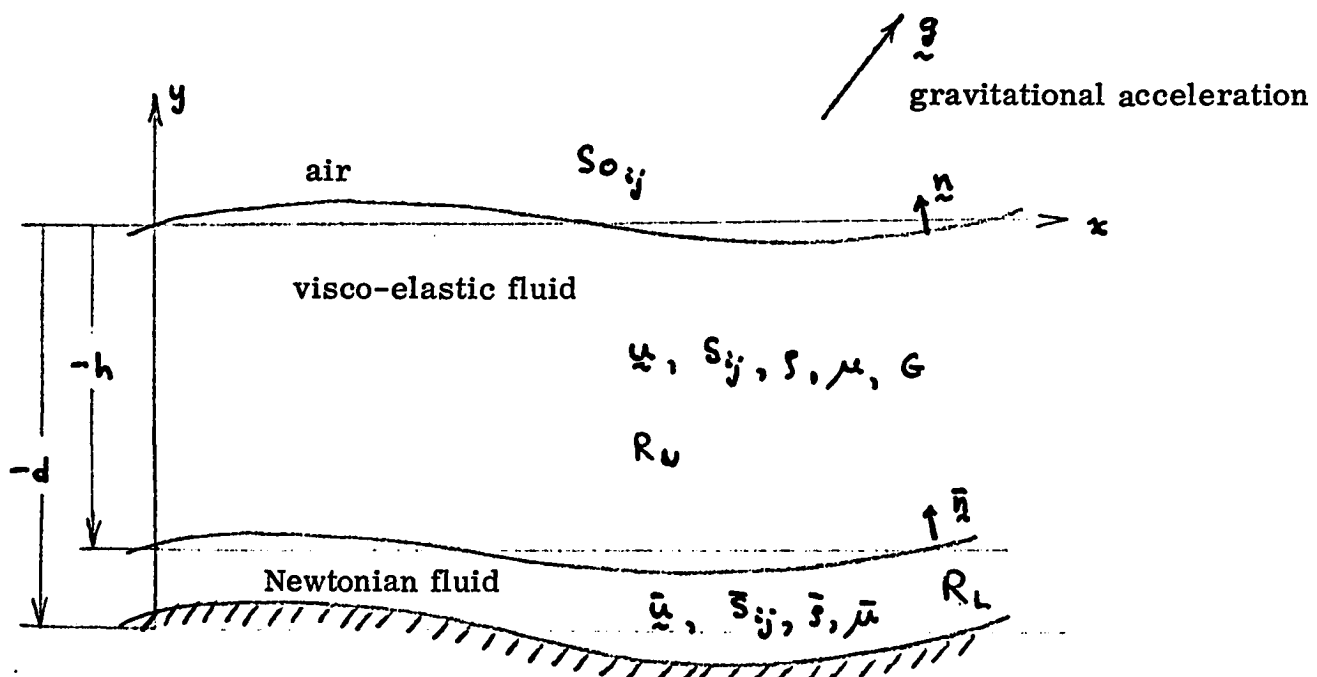


Fig. VII

The momentum equations are

$$\text{mucus: } \oint \frac{d u_i}{dt} = S_{ij,j} + \oint g_i \quad y \in R_U$$

$$\text{serous fluid: } \bar{\int} \frac{d \bar{u}_i}{dt} = \bar{S}_{ij,j} + \bar{\int} g_i \quad y \in R_L$$

where $\frac{d}{dt} \equiv \frac{\partial}{\partial t} + u_k \frac{\partial}{\partial x_k}$ is the material or Stokes derivative.

The continuity equations for constant density fluids are

$$\text{mucus: } u_{k,k} = 0 \quad y \in R_U$$

$$\text{serous fluid: } \bar{u}_{k,k} = 0 \quad y \in R_L$$

The constitutive equations are

$$\text{air: } S_{0,ij} = -P_0 \delta_{ij}$$

$$\text{mucus: } \begin{aligned} S_{ij} &= -P \delta_{ij} + t_{ij} \\ \frac{d}{dt} t_{ij} &= -\frac{1}{J_R} t_{ij} + 2G d_{ij} \end{aligned} \quad y \in R_U$$

serous fluid:

$$\bar{S}_{ij} = -\bar{P} \delta_{ij} + \bar{E}_{ij} \quad y \in R_L$$

$$\bar{E}_{ij} = 2\bar{\mu} \dot{d}_{ij}$$

where $\hat{\frac{d}{dt}}$ is the co-rotational or Jaumann derivative,

$$\hat{\frac{d}{dt}} t_{ij} \equiv \frac{d}{dt} t_{ij} + t_{ik} \omega_{kj} - t_{kj} \omega_{ik}$$

VII. A. Equations and Boundary Conditions

Collected, these are (regions of application are taken to be understood)

$$g \frac{du_i}{dt} = S_{jj,i} + gg_i$$

$$\bar{g} \frac{d\bar{u}_i}{dt} = \bar{S}_{jj,j} + \bar{g} g_i$$

$$u_{k,k} = \bar{u}_{k,k} = 0$$

$$S_{0ij} = -P_0 \delta_{ij}$$

$$S_{ij} = -P \delta_{ij} + t_{ij} ; \quad \hat{\frac{d}{dt}} t_{ij} = -\frac{1}{2} \gamma_R t_{ij} + 2G d_{ij}$$

$$\left(\hat{\frac{d}{dt}} t_{ij} \equiv \frac{d}{dt} t_{ij} + t_{ik} \omega_{kj} - t_{kj} \omega_{ik} \right)$$

$$\bar{S}_{ij} = -\bar{P} \delta_{ij} + \bar{t}_{ij} ; \quad \bar{t}_{ij} = 2\bar{\mu} \dot{d}_{ij}$$

(VII. A. 1)

and the boundary conditions are

$$\begin{array}{ll} S_{ij} n_j = S_{0ij} n_j & \text{at } y = \gamma \\ u_2 = \frac{d}{dt} \gamma & " \\ S_{ij} \bar{n}_j = \bar{S}_{ij} \bar{n}_j & \text{at } y = -h + \bar{\eta} \\ u_i = \bar{u}_i & " \\ \bar{u}_2 = \frac{d}{dt} \bar{\eta} & " \\ \bar{u}_i = u_{\omega i} & \text{at } y = \gamma_{\omega} \end{array}$$

(VII. A. 2)

VII. B. Determinacy of the System

The system is determinate according to the rule of thumb that the number of equations should equal the number of unknowns.* If the stresses are regarded as known in terms of the velocity gradients through the constitutive equations, and the boundary conditions (VI. B. 3 and 6) are regarded as equations for the free surface and interface**,

* This is not always true as can be shown by counter example (Truesdell, 1965)

** See section VI. B.

the number of equations left can be broken down as follows:

momentum 4

continuity 2

kinematic B.C. 2

at γ and $\bar{\gamma}$ ————— 8 equations

The boundary conditions, excluding the ones counted as equations above, are:

dynamic B.C. at γ and $\bar{\gamma}$ 4

kinematic no-slip at $\bar{\gamma}$ and q_w 4

————— 8 boundary conditions

Thus there are 8 equations and 8 boundary conditions available to solve for the 8 unknowns $\{u_1, u_2, \bar{u}_1, \bar{u}_2, \gamma, \bar{\gamma}, p, \bar{p}\}$.

VIII. NON-DIMENSIONALIZATION

VIII. A. Dimensionless Groups and Dimensional Constants

In this problem, there are twelve independent dimensional constants, viz.

- ρ density of mucus
- $\bar{\rho}$ density of serous fluid
- μ viscosity of mucus
- $\bar{\mu}$ viscosity of serous fluid
- τ_R relaxation time of mucus
- ω frequency of beat of the cilia
- d total depth of the two fluids
- h thickness of the upper layer
- λ wavelength of the wall
- ϵ y amplitude of the wall particle trajectory
- $\beta \theta$ x amplitude of the wall particle trajectory
- g gravitational acceleration

Since there are three basic dimensions (mass, length and time) the Vashy-Buckingham theorem on dimensionless groups dictates

that there are $12-3 = 9$ independent such groups. They are listed in the table below.

wave number; depth to wavelength ratio	$\alpha \equiv \kappa d = 2\pi \frac{d}{\lambda}$
ratio of relaxation time to frequency time	$T \equiv \omega T_R$
ratio of amplitude to depth	$\epsilon \equiv \frac{\Theta}{d}$
ratio of inertial to viscous forces (Reynolds no.)	$A \equiv \frac{\rho \omega d^2}{\mu}$
ratio of gravitational to viscous forces	$B \equiv \frac{\rho g d}{\mu \omega}$
ratio of sublayer to mucous viscosity	$k \equiv \frac{\mu}{\mu_s}$
ratio of sublayer to mucous density	$\gamma \equiv \frac{\rho_s}{\rho}$
ratio of mucous layer thickness to total depth	$h^* \equiv \frac{h}{d}$
ellipticity of wall particle trajectory	$\beta \equiv \frac{\beta \Theta}{\Theta}$

We shall show in the next section that **A** is a Reynolds number and **B** is the ratio of Reynolds number to the square of the Froude number. The ratio of surface tension force to viscous force is discussed in section IX, B. 2.

VIII. B. Non-Dimensionalization of the Unknown Functions

First, consider the wall particle trajectory equations corresponding to (VI. C. 1. a and b):

$$\left. \begin{aligned} x &= z - \theta \beta \cos(\kappa z + \omega t) \\ y &= -d + \theta \sin(\kappa z + \omega t) \end{aligned} \right] \quad (\text{VIII. B. 1})$$

where \mathbf{z} identifies the wall material particle. The Lagrangian form of y -component velocity is

$$u_{L_2} \equiv \frac{\partial y(z, t)}{\partial t} = \theta \omega \cos(\kappa z + \omega t),$$

of order $\theta \omega$. However, $\omega = \kappa c$, where κ is wave number and c is wave speed. The product $\theta \omega$ can be written:

$$\theta \omega = \theta \kappa c = \frac{\theta}{d} (\kappa d) c = \epsilon \alpha c$$

The wall velocity is of order $\epsilon \alpha c$. We make the velocity dimensionless with αc (or equivalently, $d \omega$) so that the dimensionless velocity \tilde{u}^* is $O(\epsilon)$. The asymptotic expansion for \tilde{u}^* is found in section IX. B. Denoting dimensionless quantities by an asterisk:

$$\begin{aligned}
 \tilde{x} &= d \tilde{x}^* \\
 t &= \frac{1}{\omega} t^* \\
 \tilde{u} &= \alpha c \tilde{u}^* = d \omega \tilde{u}^* \\
 S_{ij} &= \mu \omega S_{ij}^* \\
 \bar{S}_{ij} &= \mu \omega \bar{S}_{ij}^* \\
 \tilde{g} &= \tilde{g} \tilde{g}^*
 \end{aligned}$$

(VIII. B. 2)

where \tilde{g}^* is a unit vector in the direction of the gravitational acceleration. Note that both Newtonian and non-Newtonian stresses are non-dimensionalized the same way and that dimensionless quantities are not necessarily of $O(1)$.

In this flow, if the inertia force is $O(\frac{\rho U^2}{d})$ and the viscous force is $O(\frac{\mu U}{d^2})$, the Reynolds number is

$$Re \equiv \frac{\rho U d}{\mu} = \frac{\rho \omega d^2}{\mu} = A$$

If the Reynolds number is based on serous viscosity, then

$$Re = \frac{\rho U d}{\mu} = \frac{A}{k}$$

The gravity force is $\rho(gg)$ so that the ratio of gravitational to viscous forces is

$$\frac{\rho g d^2}{\mu U} = \frac{\rho g d}{\mu \omega} \equiv B$$

If a Froude number squared is denoted by $F^2 \equiv \frac{U^2}{g d}$, then

$$B = \left(\frac{g d}{U^2} \right) \left(\frac{\rho U d}{\mu} \right) = \frac{A}{F^2} \quad (\text{VIII. B. 3})$$

Numerical values of A and B for "normal" muco-ciliary flow are given in section VIII. D. 9.

VIII. C. Dimensionless Equations and Boundary Conditions

Using the equations of part B, the dimensional equations are made dimensionless in the standard straightforward manner. The asterisks are dropped from now on for convenience; unless otherwise stated, the functions are to be assumed dimensionless in all future work.

momentum $A \frac{du_i}{dt} = -p_{,i} + t_{ij,j} + B g_i \quad y \in R_u$

$$rA \frac{du_i}{dt} = -\bar{p}_{,i} + \bar{t}_{ij,j} + \bar{B} g_i \quad y \in R_L$$

constitutive $T \frac{d}{dt} t_{ij} = -t_{ij} + 2 d_{ij} \quad y \in R_u$

$$\bar{t}_{ij} = 2 k \sigma_{ij} \quad y \in R_L$$

continuity $u_{k,k} = \bar{u}_{k,k} = 0 \quad (VIII. C. 1)$

dynamic boundary condition $s_{ij} n_j = s_{0j} n_j \quad \text{at } y = \eta$

$$\bar{s}_{ij} \bar{n}_j = \bar{s}_{0j} \bar{n}_j \quad \text{at } y = \bar{\eta} - h$$

kinematic boundary condition $u_2 = \frac{d}{dt} \eta \quad \text{at } y = \eta$

$$\bar{u}_2 = \frac{d}{dt} \bar{\eta} \quad \text{at } y = -h + \bar{\eta}$$

$$u_i = \bar{u}_i \quad "$$

$$\bar{u}_i = u_{wi} \quad \text{at } y = -l$$

VIII. D. Values of the Dimensionless Constants

Values of the dimensionless constants for normal muco-ciliary flow are found subject to the fact that there are meager and insufficient data available. As stated previously, the sources are not limited to the human system but are necessarily concerned with a variety of mammals. Thus the viscosity taken may be that of the human cervix, the depth of the layers may refer to a rat, and etc. There is no alternative but to follow the above procedure. Its plausibility lies in the fact that the muco-ciliary systems of different animal species are similar.

Mucus is a complex material with rheological properties varying considerably in testing. For example, according to Litt* any value of relaxation time between 1 and 100 seconds would be a "reasonable" one and viscosity values may be widely different. At best, the results (on rheological properties of mucus) obtained by experiments should be considered as "tentative" (Hwang et al, 1969). In addition, the mechanical properties of the sublayer are not known

*

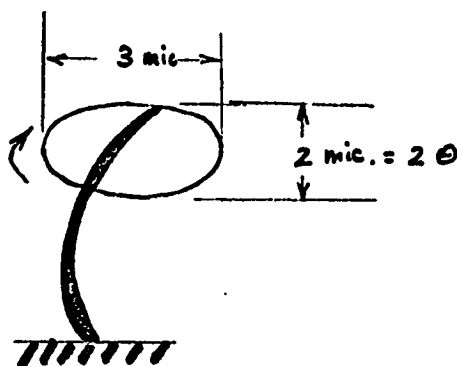
Private communication

and must be guessed.

From the assortment of data values, we shall define a "normal" muco-ciliary flow as one in which the values are those listed in the following pages. Hopefully, this flow will be "realistic" in the sense that the values taken approximate those in the respiratory systems of some normal mammals.

The symbol \approx denotes "approximate" (within about 5%) equality.

VIII. D. 1. The motion of the wall particle models that of a cilium tip. This ciliary path has been idealized as an ellipse with x to y axis ratio (ellipticity) β . We shall suppose that a typical cilium of length 6 microns (Table II.A.2) has a path in which the y amplitude is about 2 microns, the ellipticity is 1.5, and the motion is clockwise. Thus, the wall particle motion is sketched below:



and the values of the constants describing the wall particle motion

are:

$$\Theta = 1 \text{ micron}$$

$$\beta = 1.5$$

VIII. D. 2. The wavelength of the wall corresponds to the metachronal wave of the cilia. It is taken to be about 30 microns in accordance with the data of Table II. B. 2.

$$\lambda = 30 \text{ microns}$$

VIII. D. 3. The frequency of the ciliary beat is about 15 cyc/sec in normal mammals (Table II. A. 2). In radians/second this frequency is

$$\omega = 2\pi f \doteq 100 \text{ rad/sec}$$

VIII. D. 4. According to Dalhamn (Table II.C. 3), the depth of the mucoserous layers is about 5 microns in normal rat tracheas. This value was found by quick-freezing a fresh section of tissue which was then imbedded in plastic and sectioned. Miller's estimate of the depth is 15 microns (cats), but he does not indicate how these values were

obtained, nor whether the cat was healthy. We shall suppose that an accurate measure of total depth of the two fluids lying above the undisturbed ciliary tips (i.e. the wall) is about 5 microns.

Unfortunately, there are no available data on which to base a definitive choice of the amount of serous fluid lying above the cilia tips relative to the total amount of the two fluids. We shall, therefore, arbitrarily estimate that the serous layer above the cilia tips occupies only about 1/5 of the total depth. That is, if the wall were undisturbed, and the total depth of mucus and serous fluid were equal to α (5 microns), then the depth of the serous fluid layer would be 1 micron. Therefore, $h = .8$. Below is a sketch of the field:

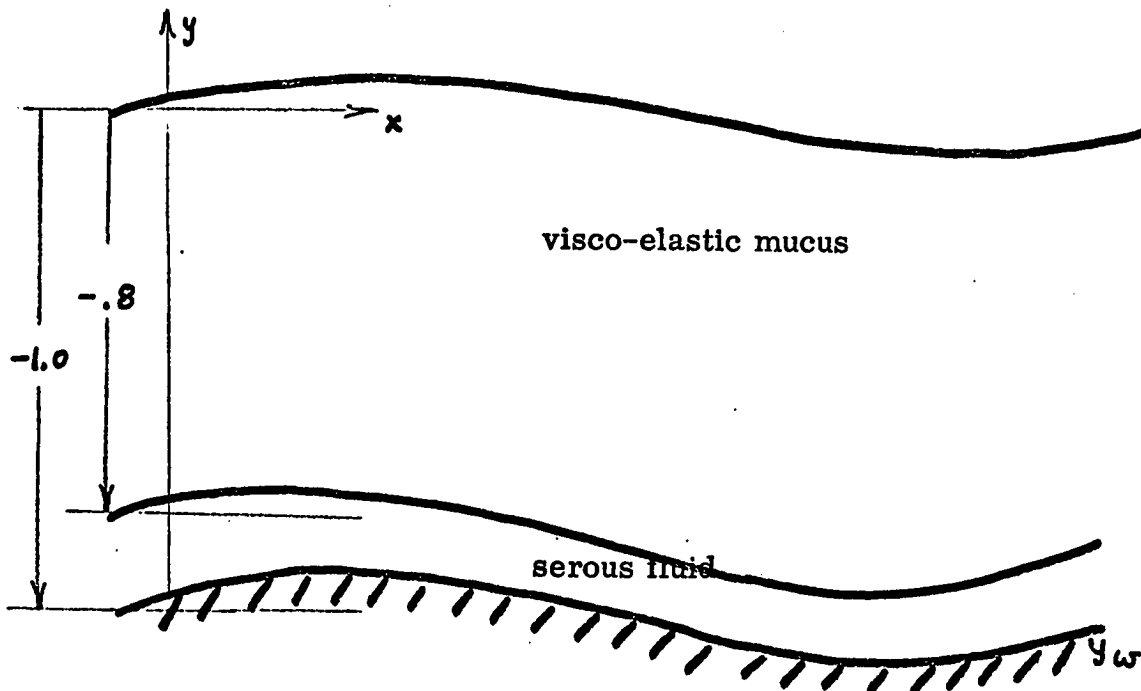


Fig. VIII. D. 4

VIII. D.5. The value of the dynamic viscosity of normal mucus (human) is roughly 1500 poise according to Hwang and Litt (Table II. D. 1), and we shall use that value. They reported the relaxation time of normal cervical mucus to be about 80 seconds.* In a recent personal communication, Litt indicated that relaxation times of tracheal mucus between 1 and 100 seconds have been obtained on fresh samples from laboratory dogs. We shall assume a relaxation time for normal mucous flow to be 15 seconds.

VIII. D.6. Quantitative values of the viscosity of the serous fluid (Newtonian) are unavailable in the literature. This layer may consist of a watery solution with molecules of mucin at a much lower concentration than that of the upper (mucous) layer. In fact, since mucus enters the system through the goblet cells in the epithelial surface (see Fig. II.C.2), it is likely that there is always a quantity of mucin floating around in the serous layer. In this case, the viscosity of the serous fluid will be larger than that of pure water.

*

These values should only be regarded as "tentative" according to Litt and Hwang. They were based on stored frozen and then defrosted samples of mucus that may have degraded biologically. Section I. B. contains a detailed discussion of the experiment and the results.

Values of other solutions (e.g. blood plasma) may not be applicable to this system, but have been chosen as a guide. According to Whitmore (1968), the viscosity of plasma is about twice that of water. If the fact that mucin consists of long-chain, cross-linked polymers (Keiser-Nielsen) is taken into account, then the viscosity of the serous layer may be even greater than that of plasma. We shall suppose, therefore, a serous viscosity about 10 times that of water:^{*}

$$\bar{\mu} \doteq .1 \text{ poise}$$

VIII. D. 7. The density of mucus is about $.9 \text{ gm/cm}^3$ according to Miller (1968). We shall suppose that the densities of serous fluid and of mucus are nearly equal; i.e. both are about the same as water, 1 gm/cm^3 .

VIII. D. 8. Dimensional values in normal flow, summary:

$$\omega = 100 \text{ rad/sec}, \theta = 1 \text{ micron}, \beta = 1.5$$

$$\lambda = 30 \text{ microns}, \mu = 1500 \text{ poise}, \bar{\mu} = .1 \text{ poise}$$

$$d = 5 \text{ microns}, T_R = 15 \text{ sec}, \rho = 1 \text{ gm/cm}^3$$

$$h = .8, \bar{\rho} = 1 \text{ gm/cm}^3$$

* The viscosity of pure water at 20°C is about 1 centipoise.

VIII. D. 9. Dimensionless constants in normal flow.

$$\alpha \equiv \frac{2\pi d}{\lambda} \doteq 1.$$

$$\beta = 1.5$$

$$\epsilon = \frac{\theta}{d} = .2$$

$$\gamma = \frac{s}{g} \doteq 1.$$

$$k \equiv \frac{\bar{\mu}}{\mu} = \frac{1}{1500} = .67(10^{-4})$$

$$T \equiv \omega \tau_R \doteq 100(15) = 1.5(10^3)$$

$$A \equiv \frac{\rho \omega d^2}{\mu} = 1.67(10^{-8})$$

$$B \equiv \frac{\tau g d}{\mu \omega} = 3.3(10^{-6})$$

Table VIII. D. 9

The subscript N will sometimes be used to denote "normal" values of the constants in cases where confusion may arise.

IX. ASYMPTOTIC EXPANSION

IX. A. Asymptotic Expansion and "Mixed Equations"

In the normal muco-ciliary flow problem, there are three small parameters (Table VIII. D. 9): A , B and ϵ .^{*} Since all unknown functions are assumed periodic in time, no small parameters multiply the highest order derivatives so that the system does not result in a singular perturbation. A regular asymptotic expansion in the three parameters, however, obscures an important condition on the product of the small number, A , and the large number, T , required for validity. This arises from the fact that the constitutive equation and the momentum equation have not yet been combined. Consider a simplified set of equations analogous to the system of equations (section VIII.C).

$$A \frac{\partial u}{\partial t} = \frac{\partial t_u}{\partial x} + B g$$

$$T \frac{\partial}{\partial t} t_u = -t_{uu} + \frac{\partial u}{\partial x}$$

*

t_u is also small, but we shall not use it as an expansion parameter. We can then consider more general flows where $t_u \neq 1$.

where $A \ll 1$, $T \gg 1$.

Elimination of stress t_{11} yields

$$A \frac{\partial u}{\partial t} + AT \frac{\partial^2 u}{\partial t^2} = \frac{\partial^2 u}{\partial x^2} + Bg$$

If both $A \ll 1$ and $AT \ll 1$ then the approximate equation is *

$$0 = \frac{\partial^2 u}{\partial x^2} + Bg$$

Now suppose that we had neglected the $\frac{du}{dt}$ term before eliminating the stress:

$$0 = \frac{\partial t_{11}}{\partial x} + Bg$$

$$T \frac{\partial t_{11}}{\partial t} = -t_{11} + \frac{\partial u}{\partial x}$$

$$\begin{aligned} T \frac{\partial^2 t_{11}}{\partial x \partial t} &= -\frac{\partial t_{11}}{\partial x} + \frac{\partial^2 u}{\partial x^2} \\ \downarrow &\quad \downarrow \\ 0 &= Bg + \frac{\partial^2 u}{\partial x^2} \end{aligned}$$

The resulting equation is the same as the previous one, but the

*

This equation looks singular near $t = 0$ but isn't since we seek a periodic solution.

condition that $A T \ll 1$ was obscured. Thus we shall not expand in A (i.e. neglect inertia) until the set of equations has been manipulated so that the actual approximation condition is clearer.

IX. B. The Double Asymptotic Expansion of any Unknown Function f in ϵ and B

$$f(x, t; \epsilon, B) = \sum_{k=1}^{\infty} \sum_{m=1}^{\infty} \epsilon^k B^m f^{(k, m)}(x, t)$$

where $f^{(k, m)}$ is also dependent upon all the other parameters of the system; $A, \alpha, \beta, T, k, h$. Take the following for each particular unknown function:

$u_i = \epsilon u_i^{(1,0)} + \epsilon^2 u_i^{(2,0)} + B u_i^{(0,1)} + O(\epsilon B, B^2, \epsilon^3)$	
$\bar{u}_i = \epsilon \bar{u}_i^{(1,0)} + \epsilon^2 \bar{u}_i^{(2,0)} + B \bar{u}_i^{(0,1)} + \dots$	
$t_{ij} = \epsilon t_{ij}^{(1,0)} + \epsilon^2 t_{ij}^{(2,0)} + B t_{ij}^{(0,1)} + \dots$	
$\bar{t}_{ij} = \epsilon \bar{t}_{ij}^{(1,0)} + \epsilon^2 \bar{t}_{ij}^{(2,0)} + B \bar{t}_{ij}^{(0,1)} + \dots$	(IX. B. 1)
$P = P_0 + \epsilon P^{(1,0)} + \epsilon^2 P^{(2,0)} + B P^{(0,1)} + \dots$	
$\bar{P} = \bar{P}_0 + \epsilon \bar{P}^{(1,0)} + \epsilon^2 \bar{P}^{(2,0)} + B \bar{P}^{(0,1)} + \dots$	
$\eta = \epsilon \eta^{(1,0)} + \epsilon^2 \eta^{(2,0)} + B \eta^{(0,1)} + \dots$	
$\bar{\eta} = \epsilon \bar{\eta}^{(1,0)} + \epsilon^2 \bar{\eta}^{(2,0)} + B \bar{\eta}^{(0,1)} + \dots$	

The zeroth order terms are absent except in the pressure, because it is obvious that for zero wall trajectory amplitude ($\epsilon = 0$) and no gravity ($B=0$), there is nothing driving the motion and all functions are zero except pressure which is equal to P_0 . The functions $f^{(k,m)}$ are not necessarily $O(\epsilon)$.

The solution of equations (VII.A.1) and boundary conditions (VII.A.2) will be found to order ϵ^2 and B . That is, each unknown function, f , will be determined correct to

$$f = \epsilon f^{(1,0)} + \epsilon^2 f^{(2,0)} + B f^{(0,1)}$$

where terms of order ϵ^3 , ϵB , B^2 and higher are neglected.

This is a valid expansion for normal muco-ciliary flow because we can show a posteriori that B terms can be neglected relative to ϵ^2 (section IX.B.1). In other words, it turns out that we actually need only ϵ and ϵ^2 terms for normal flow* (i.e. that gravitational effects are small compared to ϵ^2 effects). However, this is known only after the solution in which B terms are retained has

*

In a pathological flow where gravity is important (i.e. $O(\epsilon^2)$) the drift of a particle on the free surface could be retarded by the B term. However, terms of order ϵ^3 , ϵB , B^2 can still be neglected in this approximation, even though the B terms must be included.

been found.

IX.B.1. For the normal muco-ciliary flow we have defined, the small parameters are (section VIII.D.9): $\epsilon = .2$ and $B = 3.3 (10^{-6})$ so that $B \ll \epsilon^2 \ll 1$. This does not mean that gravitational terms can always be neglected; the dimensionless functions in the expansions are not necessarily $O(1)$. For example, if the constitutive equation (VIII.C.4) is put into the equation of motion (VIII.C.2), then

$$\frac{\gamma A}{K} \frac{d\bar{u}_i}{dt} = -\frac{1}{K} \bar{P}_{,i} + 2 \dot{d}_{ij,j} + \frac{\gamma B}{K} g_i$$

where g_i is the unit vector for gravity. For normal values,

$$\frac{\gamma A}{K} = \frac{1.67 (10^{-8})}{.67 (10^{-4})} \doteq O(10^4)$$

and $\frac{\gamma B}{K} = \frac{3.3 (10^{-6})}{.67 (10^{-4})} \doteq .05$

Since $\epsilon = .2$, $\epsilon^2 = .04$, and gravitational terms may be important (i.e. $\frac{\gamma B}{K} \sim \epsilon^2$) unless $O(\{|\dot{d}_{ij,j}|^2\}) \gg 1$.

However, it happens that the velocity gradients (\dot{d}_{ij}) can be "large"

in the (thin) sublayer for normal flow*, implying that gravitational (G) terms may be neglected. This result can be shown a posteriori by considering the solution of the problem in which terms of order ϵ^2 and B are retained in the expansions.

The equation of the fluid material drift (XIII. E. 1) turns out to be

$$\text{drift} = 2\pi \left\{ A^{(2,0)} \epsilon^2 + A^{(0,1)} B \right\}$$

where equation (XIII. E. 2): $A^{(0,1)} \equiv -\frac{g_1}{2} \left\{ y^2 + \frac{1}{K} [h^2(1-K)-1] \right\}$

and $A^{(2,0)}$ is the coefficient of drift due to the wall (cilia). The component of the unit gravity vector parallel to the x axis is g_1 .

From the computed results** (XVI. B. 2), we find that

$$2\pi A^{(2,0)} \epsilon^2 \doteq .33$$

for a fluid particle at $y=0$. Calculating the contribution to drift

*

A balance of stresses along with the condition $KT \gg K$ gives $\sigma_{ij} \doteq \frac{1}{K} d_{ij}$ at the interface. Hence the velocity gradients in the serous fluid are an order of magnitude larger than those in the mucus. For more detail, see section XVI. B. 1.

**

Drift neglecting gravity.

due to gravity (where $g_1=1$, $y=0$, $h=.8$, and $\kappa=.67(10^{-4})$):

$$|z\pi A^{(0,1)} B| \doteq .055$$

Thus, the effect of gravity is of higher order than the ϵ^2 effects and so gravity can be neglected in normal muco-ciliary flow to within the accuracy of our expansion (i.e. the actual effect of gravity is approximately equal to ϵ^3).

Under some circumstances (e.g. a "watery" mucus of larger than normal thickness) gravity may be important. For example, consider a hypothetical pathological state in which the mucous-serous fluids become one Newtonian layer of thickness 10 microns (twice normal) and of viscosity 1 poise (100 times greater than water but 1000 times less than normal mucous). Then, for a fluid particle at $y=0$:

$$|A^{(0,1)} B| \doteq \frac{1}{\kappa} B = \frac{\gamma g d}{\bar{\mu} \omega} \doteq .01$$

where γ, g, ω are normal valued (VIII.D.9.), $\bar{\mu} = 1$ poise, and depth $d = 10$ microns. The contribution to the drift due to the cilia is $O(\epsilon^2) \doteq .01$ which is the same order as the B terms.*

*

Order ϵB , B^2 and ϵ^3 terms can still be neglected to within our approximation.

Therefore, gravitational effects may be important in certain diseased muco-ciliary flows. We shall discuss pathological flow in more detail in section XIII. E.

IX. B. 2. (Surface Tension Effects). The stress boundary condition between two different fluids can be expressed in two dimensions by the equation*

$$S_{ij} n_j - S_{0ij} n_j = \sigma \left\{ \frac{\gamma_{xx}}{\left[1 + \frac{\gamma^2}{\gamma_{xx}} \right]^{3/2}} \right\} n_i \quad (\text{IX. B. 2. a})$$

where n is the outward normal to the surface $\gamma(x, t)$, S_{ij} and S_{0ij} are the stress tensors of the inner and outer fluids respectively, and σ is the surface tension:



The influence of surface tension may be compared to the visco-elastic stress forces by comparing the left and right sides of (IX. B. 2. a). The fluid velocity, u , is $O(\theta\omega)$ according to equation (VIII. B. 2). θ is the wall amplitude. The characteristic

*

This is a generalization of boundary conditions (VI. B. 2 & 3).

depth* of fluid is λ and so the stress is

$$s_{ij} = O\left(\frac{\mu u}{\lambda}\right) = O\left(\frac{\mu \omega \omega}{\lambda}\right) \quad (\text{IX. B. 2. b})$$

For small slopes, the right side of (IX. B. 2. a) is

$$\sigma_{\eta,xx} = O\left(\frac{\sigma \theta}{\lambda^2}\right) \quad (\text{IX. B. 2. c})$$

where the surface $\eta = \theta \sin(\kappa x + \omega t)$ and κ is the wave number.

The ratio, C , of surface tension forces to viscous forces is thus

$$C = O\left\{ \frac{\left(\frac{\sigma \theta}{\lambda^2}\right)}{\left(\frac{\mu \omega \theta}{\lambda}\right)} \right\} = O\left(\frac{\sigma \lambda}{\lambda^2 \mu \omega}\right) \quad (\text{IX. B. 2. d})$$

For the values of $\lambda = 1$ micron (depth of serous layer)

$$\sigma = 10 \text{ dyne/cm} = 10 \text{ erg/cm}^{**}$$

$$\lambda = 30 \text{ micron}$$

$$\omega = 100 \text{ rad/sec}$$

$$\mu = .1 \text{ poise (serous viscosity)}$$

*

The serous depth will be used for λ .

**This is an arbitrary choice of σ .

we obtain $C = O(10)$

*

Thus, surface tension forces may be important in muco-ciliary flow. However, due to the mathematical complexity of the analysis, we have elected to neglect surface tension effects for the present.

IX.C. Method of Finding ϵ , ϵ^2 , B Equations

The equations for the ϵ , ϵ^2 and B systems can be found by putting the expansions into the exact equations (VIII.C.1) and then setting the coefficients separately equal to zero. For example, consider the momentum equation (VIII.C.1.a):

$$A \{ u_{i,t} + u_k u_{i,k} \} = -P_{,i} + t_{;j,j} + B g_i$$

Using the expansions (IX.B.1):

$$u_i = \epsilon u_i^{(1,0)} + \epsilon^2 u_i^{(2,0)} + B u_i^{(0,1)} + O(\epsilon^3, \epsilon B, B)$$

$$P = P_0 + \epsilon P^{(1,0)} + \epsilon^2 P^{(2,0)} + B P^{(0,1)} + \dots$$

$$t_{;j} = \epsilon t_{;j}^{(1,0)} + \epsilon^2 t_{;j}^{(2,0)} + B t_{;j}^{(0,1)} + \dots$$

*

If the mucous viscosity were used, then $C \ll 1$.

we get

$$\begin{aligned}
 A \{ \epsilon u_{i,t}^{(1,0)} + \epsilon^2 [u_{i,t}^{(2,0)} + u_k^{(1,0)} u_{i,k}^{(1,0)}] + Bu_{i,t}^{(0,1)} + O(\epsilon B, \epsilon^3 B^2) \} \\
 = \epsilon \{ -P_{i,i}^{(1,0)} + t_{j,j}^{(1,0)} \} + \epsilon^2 \{ -P_{i,i}^{(2,0)} + t_{j,j}^{(2,0)} \} + \\
 + B \{ -P_{i,i}^{(0,1)} + t_{j,j}^{(0,1)} + g_i \} + O(\epsilon B, \epsilon^3 B^2)
 \end{aligned}$$

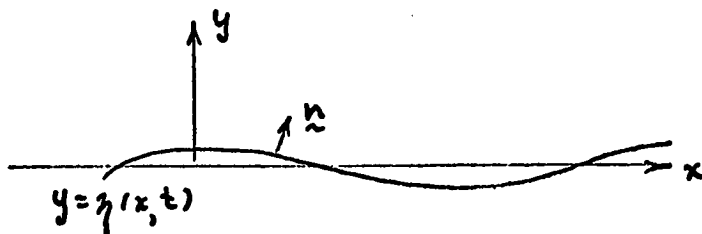
Setting the coefficients of the ϵ , ϵ^2 and B terms separately equal to zero gives

$$\epsilon: A u_{i,t}^{(1,0)} = -P_{i,i}^{(1,0)} + t_{j,j}^{(1,0)}$$

$$\epsilon^2: A \{ u_{i,t}^{(2,0)} + u_k^{(1,0)} u_{i,k}^{(1,0)} \} = -P_{i,i}^{(2,0)} + t_{j,j}^{(2,0)}$$

$$B: A u_{i,t}^{(0,1)} = -P_{i,i}^{(0,1)} + t_{j,j}^{(0,1)} + g_i$$

This procedure is followed in all equations (VIII.C.1). However, the boundary conditions are more involved because they are applied at unknown surfaces. This necessitates expanding the boundary condition in a Taylor series about the undisturbed surface. For example, consider a typical boundary condition modelling any one in (VIII.C.1) at the surface, γ .



From the method outlined above, a boundary condition would be of the form (neglecting $O(\epsilon B, \epsilon^3, B^2)$) :

$$f(x, y, t) \Big|_{y=\eta} = \epsilon f^{(1,0)}(x, \eta, t) + \epsilon^2 f^{(2,0)}(x, \eta, t) + B f^{(0,1)}(x, \eta, t) + \dots$$

where

$$\eta = \epsilon \eta^{(1,0)}(x, t) + \epsilon^2 \eta^{(2,0)}(x, t) + B \eta^{(0,1)}(x, t) + \dots$$

In order to use this boundary condition, then, we must find it at the undisturbed surface (i.e. $y=0$ in this case). This is accomplished by a Taylor series as follows:

$$f \Big|_{y=\eta} = f(x, 0, t) + \eta f_{,y}(x, 0, t) + \frac{1}{2} \eta^2 f_{,yy}(x, 0, t) + \dots \quad (\text{IX. C. 1})$$

$$\eta f_{,y}(x, 0, t) = \epsilon^2 \eta^{(1,0)} f_{,y}^{(1,0)} + O(\epsilon^3, \epsilon B, B^2)$$

$$\eta^2 f_{,yy}(x, 0, t) = O(\epsilon^3, \epsilon^2 B, \epsilon B^2)$$

Hence

(IX. C. 2)

$$f \Big|_{y=\eta} = \epsilon f^{(1,0)} + \epsilon^2 \{ f^{(2,0)} + \eta^{(1,0)} f_{,y}^{(1,0)} \} + B f^{(0,1)} + O(\epsilon^3, \epsilon B, B^2)$$

$\text{at } y=0$

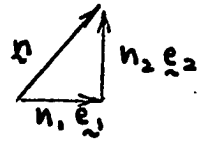
Other boundary conditions in (VIII.C.1) such as the stress continuity equations involve the normal at the surface in the form:

$$f_{ij} n_j \quad \text{at } y = \eta.$$

The function f_{ij} can be expressed directly using equation (IX.C.2) and the normal in terms of η as follows:

$$n_1 = -\eta_{,x} \{ 1 + \eta_{,x}^2 \}^{-\frac{1}{2}}$$

$$n_2 = \{ 1 + \eta_{,x}^2 \}^{-\frac{1}{2}}$$



which when expanded becomes:

$$n_i = \sum_{k=0}^l \sum_{m=0}^k \epsilon^k B^m n_i^{(k,m)}$$

where

$$n_1^{(0,0)} = 0$$

$$n_2^{(0,0)} = 1$$

(IX.C.3)

$$n_1^{(1,0)} = -\eta_{,x}^{(1,0)}$$

$$n_2^{(1,0)} = 0$$

$$n_1^{(0,1)} = -\eta_{,x}^{(0,1)}$$

$$n_2^{(0,1)} = 0$$

$$n_1^{(2,0)} = -\eta_{,x}^{(2,0)}$$

$$n_2^{(2,0)} = -\frac{1}{2} \eta_{,x}^{(2,0)}$$

The boundary condition at $y = \gamma$ is thus of the form

$$f_{ij} n_j \Big|_{y=\gamma} = \epsilon a_i^{(1,0)} + \epsilon^2 a_i^{(2,0)} + B a_i^{(0,1)} + O(\epsilon^3, \epsilon B, B^2)$$

(IX. C. 4)

where

$$a_i^{(1,0)} \equiv f_{ij}^{(1,0)} n_j^{(0,0)} \quad \text{at } y=0$$

$$a_i^{(2,0)} \equiv f_{ij}^{(2,0)} n_j^{(0,0)} + f_{ij}^{(1,0)} n_j^{(1,0)} + \gamma f_{ij,y}^{(1,0)} n_j^{(0,0)} \quad \text{at } y=0$$

$$a_i^{(0,1)} \equiv f_{ij}^{(0,1)} n_j^{(0,0)} \quad \text{at } y=0$$

The complete sets of equations can now be written down for the

ϵ , ϵ^2 and B systems.

IX. D. The (1,0) or ϵ System of Equations

$$\begin{aligned} A u_{i,t}^{(1,0)} &= -P_{,i}^{(1,0)} + t_{ij,j}^{(1,0)} \\ A \bar{u}_{i,t}^{(1,0)} &= -\bar{P}_{,i}^{(1,0)} + \bar{t}_{ij,j}^{(1,0)} \\ T t_{ij,t}^{(1,0)} &= -t_{ij}^{(1,0)} + 2 d_{ij}^{(1,0)} \\ \bar{t}_{ij}^{(1,0)} &= 2 \kappa \bar{\sigma}_{ij}^{(1,0)} \\ u_{k,k}^{(1,0)} &= \bar{u}_{k,k}^{(1,0)} = 0 \end{aligned}$$

(IX. D. 1)

$$\begin{aligned} t_{12}^{(1,0)} &= 0 & \text{at } y=0 \quad \forall x,t \\ t_{22}^{(1,0)} &= P^{(1,0)} & " \\ \Delta t_{12}^{(1,0)} &= 0 & \text{at } y=-h \quad \forall x,t \\ \Delta t_{22}^{(1,0)} &= \Delta P^{(1,0)} & " \\ u_i^{(1,0)} &= \bar{u}_i^{(1,0)} & " \\ u_i^{(1,0)} &= u_{w_i}^{(1)} & \text{at } y=-l \quad \forall x,t \end{aligned}$$

(IX. D. 2)

where $\Delta f \equiv f - \bar{f}$ and $u_{w_i}^{(1)}$ is found
from (VI. C. 3. e).

The kinematic conditions that the surfaces are material curves are uncoupled from the previous set, and are used to find $\gamma^{(1,0)}$ and $\tilde{\gamma}^{(1,0)}$.

$$\boxed{u_z^{(1,0)} = \gamma_{,x}^{(1,0)} \quad \text{at } y=0 \quad \forall x, t}$$
$$\bar{u}_z^{(1,0)} = \tilde{\gamma}_{,x}^{(1,0)} \quad \text{at } y=-h \quad \forall x, t$$

(IX. D. 3)

The wall velocity is (from VI. C. 3. e):

$$u_{w_1}^{(1)} = \beta \sin \phi$$

$$u_{w_2}^{(1)} = \cos \phi$$

$$\phi \equiv \alpha x + t$$

(IX. D. 4)

IX.E. The $(2,0)$ or ϵ^2 System of Equations

$$A \{ u_{i,t}^{(2,0)} + F_i \} = - P_{,t}^{(2,0)} + t_{ij,j}^{(2,0)}$$

$$A \{ \bar{u}_{i,t}^{(2,0)} + \bar{F}_i \} = - \bar{P}_{,t}^{(2,0)} + \bar{t}_{ij,j}^{(2,0)}$$

$$T \{ t_{ij,t}^{(2,0)} + G_{ij} \} = - t_{ij}^{(2,0)} + z d_{ij}^{(2,0)}$$

$$\bar{t}_{ij}^{(2,0)} = z k d_{ij}^{(2,0)}$$

$$u_{k,k}^{(2,0)} = \bar{u}_{k,k}^{(2,0)} = 0$$

(IX.E.1)

$$t_{12}^{(2,0)} = B_1 \quad \text{at } y=0 \quad \forall x, t$$

$$t_{22}^{(2,0)} = P^{(2,0)} + C_1 \quad "$$

$$\Delta t_{12}^{(2,0)} = B_2 \quad \text{at } y=-h \quad \forall x, t$$

(IX.E.2)

$$\Delta t_{22}^{(2,0)} = \Delta P^{(2,0)} + C_2 \quad "$$

$$u_i^{(2,0)} - \bar{u}_i^{(2,0)} = B_{3i} \quad "$$

$$\bar{u}_i^{(2,0)} = B_{4i} \quad \text{at } y=-l \quad \forall x, t$$

where $\Delta f \equiv f - \bar{f}$ so that $\Delta t_{12}^{(2,0)} = t_{12}^{(2,0)} - \bar{t}_{12}^{(2,0)}$, etc.

The inhomogeneities in the above equations can be regarded as due to the products of order ϵ solutions.

Uncoupled equations for $\gamma^{(2,0)}$ and $\bar{\gamma}^{(2,0)}$ are

$$u_2^{(2,0)} + D = \gamma_{,t}^{(2,0)} \quad \text{at } y=0 \quad \forall x,t \quad (\text{IX. E. 3})$$

$$\bar{u}_2^{(2,0)} + \bar{D} = \bar{\gamma}_{,t}^{(2,0)} \quad \text{at } y=-h \quad \forall x,t$$

The product terms of the (1,0) system are defined below:

$$F_i \equiv u_k^{(1,0)} u_{i,k}^{(1,0)}$$

$$\bar{F}_i \equiv \bar{u}_k^{(1,0)} \bar{u}_{i,k}^{(1,0)} \quad (\text{IX. E. 4})$$

$$G_{ij} \equiv u_k^{(1,0)} t_{ij,k}^{(1,0)} + t_{ik}^{(1,0)} \omega_{kj}^{(1,0)} - t_{kj}^{(1,0)} \omega_{ik}^{(1,0)}$$

$$B_1 \equiv \gamma_{,x}^{(1,0)} \{ t_{11}^{(1,0)} - P^{(1,0)} \} - \gamma_{,y}^{(1,0)} t_{12,y}^{(1,0)} \quad \text{at } y=0$$

$$C_1 \equiv \gamma_{,x}^{(1,0)} \{ P_{,y}^{(1,0)} - t_{22,y}^{(1,0)} \} + \gamma_{,x}^{(1,0)} t_{12}^{(1,0)} \quad "$$

$$B_2 \equiv \bar{\gamma}_{,x}^{(1,0)} \{ \Delta t_{11}^{(1,0)} - \Delta P^{(1,0)} \} - \bar{\gamma}_{,y}^{(1,0)} \Delta t_{12,y}^{(1,0)} \quad \text{at } y=-h$$

$$C_2 \equiv \bar{\gamma}_{,x}^{(1,0)} \{ \Delta P_{,y}^{(1,0)} - \Delta t_{22,y}^{(1,0)} \} + \bar{\gamma}_{,x}^{(1,0)} \Delta t_{12}^{(1,0)} \quad "$$

$$\begin{aligned}
 B_{3i} &\equiv \bar{\gamma}^{(1,0)} \left\{ \bar{u}_{i,y}^{(1,0)} - u_{i,y}^{(1,0)} \right\} && \text{at } y = -h \\
 B_{4i} &\equiv u_{w_i}^{(2)} - \sin \phi \bar{u}_{i,y}^{(1,0)} && \text{at } y = -l \\
 D &\equiv \bar{\gamma}^{(1,0)} u_{z,y}^{(1,0)} - u_1^{(1,0)} \bar{\gamma}_{,x}^{(1,0)} && \text{at } y = 0 \\
 \bar{D} &\equiv \bar{\gamma}^{(1,0)} \bar{u}_{z,y}^{(1,0)} - \bar{u}_1^{(1,0)} \bar{\gamma}_{,x}^{(1,0)} && \text{at } y = -h
 \end{aligned}$$

$$\begin{aligned}
 u_{w_1}^{(2)} &= \frac{1}{2} \alpha \beta^2 (1 + \cos 2\phi) \\
 u_{w_2}^{(2)} &= -\frac{1}{2} \alpha \beta \sin 2\phi
 \end{aligned}
 \quad] \quad (\text{IX. E. 5})$$

$$\phi \equiv \alpha z + t$$

IX. F. The (0, 1) or B System of Equations

$$\begin{aligned} A u_{i,t}^{(0,1)} &= -P_{,i}^{(0,1)} + t_{ij,j}^{(0,1)} + g_i \\ A \bar{u}_{i,t}^{(0,1)} &= -\bar{P}_{,i}^{(0,1)} + \bar{t}_{ij,j}^{(0,1)} + \bar{g}_i \\ T t_{ij,t}^{(0,1)} &= -t_{ij}^{(0,1)} + 2d_{ij}^{(0,1)} \\ \bar{t}_{ij}^{(0,1)} &= 2K d_{ij}^{(0,1)} \\ u_{k,k}^{(0,1)} &= \bar{u}_{k,k}^{(0,1)} = 0 \end{aligned}$$

(IX. F. 1)

$$\begin{aligned} t_{12}^{(0,1)} &= 0 & \text{at } y=0 \quad \forall x, t \\ t_{22}^{(0,1)} &= P^{(0,1)} & " \\ \Delta t_{12}^{(0,1)} &= 0 & \text{at } y=-h \quad \forall x, t \\ \Delta t_{22}^{(0,1)} &= \Delta P^{(0,1)} & " \\ u_i^{(0,1)} &= \bar{u}_i^{(0,1)} & " \\ \bar{u}_i^{(0,1)} &= 0 & \text{at } y=-l \quad \forall x, t \end{aligned}$$

(IX. F. 2)

where $\Delta f \equiv f - \bar{f}$.

Note the presence of the gravity term g_i in the momentum equations and that the wall velocity is zero.

Uncoupled equations for $u_z^{(0,1)}$ and $\tilde{\eta}^{(0,1)}$ are

$$u_z^{(0,1)} = \eta_{,t}^{(0,1)} \quad \text{at } y=0$$

$$\tilde{u}_z^{(0,1)} = \tilde{\eta}_{,t}^{(0,1)} \quad \text{at } y=-h$$

(IX. F. 3)

X. GENERAL METHOD OF SOLUTION OF THE (p, q) SYSTEM

As is the case of all regular perturbation problems, the sets of equations for each system are similar, making it possible to discuss the method of solution in some generality. The basis steps will be shown in this section.

X.A. If the pressures are eliminated by cross differentiation (giving the vorticity equation) and the constitutive equation for the Newtonian stress is used, the resulting equations have the form

$$\boxed{\begin{aligned} A \{ u_{1,y,t}^{(p,q)} - u_{2,x,t}^{(p,q)} - \bar{z}^{(p,q)} \} &= t_{ij,jy}^{(p,q)} - t_{2j,jx}^{(p,q)} \\ B \{ \bar{u}_{1,y,t}^{(p,q)} - \bar{u}_{2,x,t}^{(p,q)} - \bar{z}^{(p,q)} \} &= \nabla^2 \{ \bar{u}_{1,y}^{(p,q)} - \bar{u}_{2,x}^{(p,q)} \} \\ T \{ t_{ij,z,t}^{(p,q)} + G_{ij}^{(p,q)} \} &= -t_{ij}^{(p,q)} + u_{ij}^{(p,q)} + u_{ji}^{(p,q)} \\ u_{k,k}^{(p,q)} &= 0 \\ \bar{u}_{k,k}^{(p,q)} &= 0 \end{aligned}} \quad (\text{X. A. 1})$$

$$\begin{aligned}
 t_{12}^{(p,q)} &= B_1 & \text{at } y=0 \\
 t_{22,x}^{(p,q)} &= t_{1j,j}^{(p,q)} - A \{ u_{1,t}^{(p,q)} + F_1^{(p,q)} \} + C_{1,z}^{(p,q)} & \text{at } y=0 \\
 t_{12}^{(p,q)} &= K \{ \bar{u}_{1,y}^{(p,q)} + \bar{u}_{2,x}^{(p,q)} \} + B_2^{(p,q)} & \text{at } y=-h \\
 t_{22,x}^{(p,q)} &= t_{1j,j}^{(p,q)} + A \{ \bar{u}_{1,t}^{(p,q)} + \bar{F}_1^{(p,q)} - u_{1,t}^{(p,q)} - F_1^{(p,q)} \} - \\
 &\quad - K \nabla^2 \bar{u}_1^{(p,q)} + 2K \bar{u}_{2,xy}^{(p,q)} + C_{2,z}^{(p,q)} & \text{at } y=-h \\
 u_i^{(p,q)} - \bar{u}_i^{(p,q)} &= B_{3i}^{(p,q)} & \text{at } y=-h \\
 \bar{u}_i^{(p,q)} &= B_{4i}^{(p,q)} & \text{at } y=-1
 \end{aligned}
 \tag{X. A. 2}$$

The functions $\tilde{x}^{(p,q)}$, $\tilde{\gamma}^{(p,q)}$, $G_{ij}^{(p,q)}$, $B_i^{(p,q)}$, $F_i^{(p,q)}$, ... etc.
may be regarded as known inhomogeneous terms. Specifically for

the (1,0) system, we would have ($p=1, q=0$)

$$\tilde{x}^{(1,0)} = \tilde{\gamma}^{(1,0)} = G_{ij}^{(1,0)} = B_1^{(1,0)} = F_1^{(1,0)} = 0 \quad \text{and so forth.}$$

For the (2,0) system, they result from product terms of the (1,0) system, so that they are not necessarily zero.

X. B. The unknown functions are expanded in Fourier series of the form

$$f^{(p,q)} = f^{(p,q)}(x, t; \alpha, \beta, K, A, T, h)$$

$$= \sum_{n=0}^{\infty} \operatorname{Re} \{ \alpha^{(p,q)}(n, y; \alpha, \beta, K, A, T, h) e^{in\phi} \}$$

where $\phi \equiv \alpha x + t$ and $\alpha^{(p,q)}$ is complex. In particular,

$$u_j^{(p,q)} = \sum_{n=0}^{\infty} \operatorname{Re} \{ c_j^{(p,q)} e^{in\phi} \}$$

$$\bar{u}_j^{(p,q)} = \sum_{n=0}^{\infty} \operatorname{Re} \{ \bar{c}_j^{(p,q)} e^{in\phi} \}$$

$$t_{ij}^{(p,q)} = \sum_{n=0}^{\infty} \operatorname{Re} \{ g_{ij}^{(p,q)} e^{in\phi} \} \quad \boxed{(X.B.1)}$$

In addition, all of the inhomogeneous terms are similarly expanded in Fourier series, whose coefficients are known. The resulting linear ordinary differential equations in $g_{ij}^{(p,q)}$, $c_j^{(p,q)}$ and $\bar{c}_j^{(p,q)}$ for each mode n are manipulated to obtain two linear, fourth order ordinary differential equations in $c_2^{(p,q)}$ and $\bar{c}_2^{(p,q)}$, along with eight boundary conditions. We drop superscripts (p,q) and the subscript 2 for ease of writing:

$$c''' - 2 \left[N^2 + i n \frac{A}{Q} \right] c'' + N^2 \left[N^2 + 2 i n \frac{A}{Q} \right] c = \frac{A}{Q} f + l \quad]$$

$$\bar{c}''' - 2 \left[N^2 + i n \frac{A}{2\kappa} \right] \bar{c}'' + N^2 \left[N^2 + i n \frac{A}{\kappa} \right] \bar{c} = \frac{A}{\kappa} \bar{f} \quad] \quad (X. B. 2)$$

$$c'' + N^2 c = z_1 \quad \text{at } y=0$$

$$c''' - \left[3N^2 + 2 A i n \frac{A}{Q} \right] c' = z_2 + \frac{A}{Q} f_2 \quad "$$

$$c'' + N^2 c - 2 \frac{\kappa}{Q} [\bar{c}'' + N^2 \bar{c}] = z_3 \quad \text{at } y=-h$$

$$c''' - \left[3N^2 + 2 A i n \frac{A}{Q} \right] c' - 2 \frac{\kappa}{Q} [\bar{c}''' - (3N^2 + A i n \frac{A}{\kappa}) \bar{c}'] \\ = z_4 + \frac{A}{Q} f_4 \quad \text{at } y=-h$$

$$c' - \bar{c}' = z_5 \quad \text{at } y=-h$$

$$c - \bar{c} = z_6 \quad "$$

$$\bar{c}' = z_7 \quad \text{at } y=-1$$

$$\bar{c} = z_8 \quad "$$

where $f, l, \bar{f}, z_1, z_2, \dots$ are known and

$Q = Q(n, T) \equiv \frac{2}{1 + i n T}$ and $N = n\omega$. Note that Q is a function of n .

The above sets of equations may be compactly written as

$$L \{ c \} = d$$

$$\bar{L} \{ \bar{c} \} = \bar{d}$$

$$B \{ c, \bar{c} \} = r \quad \text{at specified points of } y ,$$

where $c = c(y)$, $d = d(y)$, $r = \text{constant}$, $\bar{c} = \bar{c}(y)$.

X.C. Since the systems are linear, the solutions can be split into "homogeneous" and "particular" parts, viz.,

$$c = c_h + c_p$$

$$\bar{c} = \bar{c}_h + \bar{c}_p$$

The equations $L \{ c_p \} = d$ and $\bar{L} \{ \bar{c}_p \} = \bar{d}$ will give "particular" solutions c_p and \bar{c}_p which, when put into the boundary conditions, yield $B \{ c_p, \bar{c}_p \} = e$. The remaining homogeneous sets of equations are (for each n)

$$L\{c_h\} = \bar{L}\{\bar{c}_h\} = 0$$

$$B\{c_h, \bar{c}_h\} = r - e$$

$$\therefore L\{c\} = L\{c_p + c_h\} = d$$

$$L\{\bar{c}\} = L\{\bar{c}_p + \bar{c}_h\} = \bar{d}$$

$$B\{c, \bar{c}\} = B\{c_h + c_p, \bar{c}_h + \bar{c}_p\} = r$$

X.D. The solutions of the homogeneous systems defined above are of the form

$$c_h = \sum_{k=1}^4 \{a_k e^{A_k y}\}$$

$$\bar{c}_h = \sum_{k=1}^4 \{\bar{a}_k e^{A_k y}\}$$

involving eight unknown constants, which can be written as a vector,

$$\mathbf{z}_i \equiv (a_1, a_2, a_3, a_4, \bar{a}_1, \bar{a}_2, \bar{a}_3, \bar{a}_4)$$

The eight boundary conditions $B\{c_h, \bar{c}_h\} = r - e$ result in a matrix equation

$$\sum_i c_{ij} z_j = b_i \quad i = 1, 2, \dots, 8$$

where \mathfrak{X}_{ij} and \mathfrak{Y}_i are known functions of the parameters of the system and n . Inversion of the above yields the solution vector \mathfrak{Z}_i , which gives us c_h and \bar{c}_h directly.

Common to the three systems with which we are concerned, are the facts

$$\det \mathfrak{X}_{ij} \neq 0 \quad \text{for } n = 0, 1, 2, \dots$$

$$\mathfrak{Y}_i = 0 \quad \text{for } n = 3, 4, 5, \dots$$

thereby implying that $\mathfrak{Z}_i = 0$ for $n = 3, 4, 5, \dots$. Thus the Fourier modes $n = 3, 4, 5, \dots$ yield trivial homogeneous solutions

$$c_h = \bar{c}_h = 0 \quad \text{for } n = 3, 4, 5, \dots$$

Furthermore, the inhomogeneous terms are also zero-valued for modes $n = 3, 4, 5, \dots$, so that we have

$$c_p = \bar{c}_p = 0 \quad \text{for } n = 3, 4, 5, \dots$$

The net result is that for each (p, q) system,
the only non-trivial modes are for $n < 3$ and

$$c_i^{(p,q)} = \bar{c}_i^{(p,q)} = g_{ij}^{(p,q)} = 0 \quad \text{for } n = 3, 4, 5$$

X.E. The fact that non-zero solutions exist only for $n < 3$ allows the functions c and \bar{c} to be expanded asymptotically (because n and Q are bounded) in the small parameters

$$\frac{A}{Q} = \frac{A}{2} (1 + i n T) \quad \text{and} \quad \frac{A}{2k}$$

where

$$\left| \frac{A}{Q} \right| = O(AT) = O(\tilde{\omega}^4) \ll 1$$

$$\left| \frac{A}{2k} \right| = O(\tilde{\omega}^3) \ll 1$$

Thus we can neglect inertia terms relative to viscous terms; the system is mixed visco-elastic and Newtonian "Stokes" flow. Note that if inertia had been neglected from the start, the above conditions would have been obscured.

The resulting equations for $c_2^{(P,t)}$ and $\bar{c}_2^{(T,t)}$ are

$$\begin{aligned} c'' - 2N^2 c''' + N^4 c &= \lambda & -h \leq y \leq 0 \\ \bar{c}'' - 2N^2 \bar{c}''' + N^4 \bar{c} &= 0 & -1 \leq y \leq -h \end{aligned} \quad] \quad (\text{X.E.1})$$

$$\begin{aligned}
 c'' + N^2 c &= \gamma_1 & \text{at } y=0 \\
 c''' - 3N^2 c' &= \gamma_2 & " \\
 c'' + N^2 c - 2\frac{k}{Q} [\bar{c}'' + N^2 \bar{c}] &= \gamma_3 & \text{at } y=-h \\
 c''' - 3N^2 c' - 2\frac{k}{Q} [\bar{c}''' - 3N^2 \bar{c}'] &= \gamma_4 & " \\
 c' - \bar{c}' &= \gamma_5 & \text{at } y=-h \\
 c - \bar{c} &= \gamma_6 & " \\
 \bar{c}' &= \gamma_7 & \text{at } y=-1 \\
 \bar{c} &= \gamma_8 & "
 \end{aligned}
 \tag{X. E. 2)
 }$$

The forms of the solution to the fourth order ordinary differential equations above (with double roots) are

$$\begin{aligned}
 c &= \sum_{k=1}^2 \{a_k + b_k y\} e^{s_k y} \\
 \bar{c} &= \sum_{k=1}^2 \{\bar{a}_k + \bar{b}_k y\} e^{s_k y}
 \end{aligned}$$

$$s_{1,2} = \pm N$$

The matrix equation arising from the eight boundary conditions is

$$\mathcal{K}_{ij} \xi_j = \beta_i \quad *$$

The unknown vector $\xi \equiv (a_1, a_2, b_1, b_2, \bar{a}_1, \bar{a}_2, \bar{b}_1, \bar{b}_2)$

is found by inverting. Thus the homogeneous solutions are obtained for each non-trivial mode $n=0, 1, 2$.

In our specific problem, there are two additional relevant facts:

(i) Some (but not all) of the inhomogeneous terms are zero.

In particular $\lambda \equiv 0$, so that there is no distinct "particular" solution for $n=0, 1, 2$.

(ii) The mode $n=0$ deserves special treatment because once c_2 and \bar{c}_2 are found, we cannot obtain c_1 and \bar{c}_1 from the relation $iN c_1 + c_2' = 0$. Thus the zero mode will be considered separately.

*

\mathcal{K}_{ij} and β_i are now different from the previous similar equation.

XI. SOLUTION OF THE $(1,0)$ SYSTEM

Following the basic outline of the previous section, the solution of the $O(\epsilon)$ system will now be obtained. The set of equations found in section IX.D. is repeated here for convenience:

$$A u_{i,t}^{(1,0)} = - p_{,i}^{(1,0)} + t_{j,j}^{(1,0)}$$

$$A \bar{u}_{i,t}^{(1,0)} = - \bar{p}_{,i}^{(1,0)} + \bar{t}_{j,j}^{(1,0)}$$

$$T t_{j,j,t}^{(1,0)} = - t_{j,j}^{(1,0)} + 2 d_{j,j}^{(1,0)}$$

$$\bar{t}_{j,j}^{(1,0)} = 2 \kappa \bar{d}_{j,j}^{(1,0)}$$

$$u_{k,k}^{(1,0)} = \bar{u}_{k,k}^{(1,0)} = 0$$

$$t_{12}^{(1,0)} = 0 \quad \text{at } y=0$$

$$t_{22}^{(1,0)} = p_{,2}^{(1,0)} \quad "$$

$$\Delta t_{12}^{(1,0)} = 0 \quad \text{at } y=-h, \Delta f \equiv f - \bar{f}$$

$$\Delta t_{22}^{(1,0)} = \Delta p_{,2}^{(1,0)} \quad "$$

$$u_i^{(1,0)} = \bar{u}_i^{(1,0)} \quad "$$

$$\bar{u}_i^{(1,0)} = u_{w_i}^{(1)} \quad \text{at } y=-l$$

XI.A. The above are "homogeneous" except for the wall boundary condition, so that the pressure-independent equations are (see section X.A.).*

$$A \{ u_{1,t}^{(1,0)} - u_{2,x,t}^{(1,0)} \} = t_{1j,jy}^{(1,0)} - t_{2j,jx}^{(1,0)}$$

$$A \{ \bar{u}_{1,y,t}^{(1,0)} - \bar{u}_{2,x,t}^{(1,0)} \} = \nabla^2 \{ \bar{u}_{1,y}^{(1,0)} - \bar{u}_{2,x}^{(1,0)} \}$$

$$T t_{ij,t}^{(1,0)} = -t_{ij}^{(1,0)} + \{ u_{i,j}^{(1,0)} + u_{j,i}^{(1,0)} \}$$

$$u_{k,k}^{(1,0)} = \bar{u}_{k,k}^{(1,0)} = 0$$

$$t_{1z}^{(1,0)} = 0 \quad \text{at } y=0$$

$$t_{2z,x}^{(1,0)} = t_{1j,j}^{(1,0)} - A u_{1,t}^{(1,0)} \quad "$$

$$t_{1z}^{(1,0)} = k \{ \bar{u}_{1,y}^{(1,0)} + \bar{u}_{2,x}^{(1,0)} \} \quad \text{at } y=-h$$

$$t_{2z,x}^{(1,0)} = t_{1j,j}^{(1,0)} + A \{ \bar{u}_{1,t}^{(1,0)} - u_{1,t}^{(1,0)} \} - k \nabla^2 \bar{u}_{1,y}^{(1,0)} + 2k \bar{u}_{2,xy}^{(1,0)} \quad \text{at } y=-h$$

$$u_i^{(1,0)} = \bar{u}_i^{(1,0)} \quad \text{at } y=-h$$

$$\bar{u}_i^{(1,0)} = (\beta \sin \phi, \cos \phi) \quad \text{at } y=-l$$

*

Regions of application of the equations are to be taken as understood.

XI.B. Fourier series expansions of $u_i^{(1,0)}$, $\bar{u}_i^{(1,0)}$ and $t_{ij}^{(1,0)}$ give expressions of the form

$$\sum_{n=0}^{\infty} \operatorname{Re} \{ a(n,y) e^{in\phi} \} = \sum_{n=0}^{\infty} \operatorname{Re} \{ b(n,y) e^{in\phi} \} \quad (\text{XI.B.})$$

where a and b are linear functions of the complex-valued Fourier coefficients $c_i^{(1,0)}$, $\bar{c}_i^{(1,0)}$, $g_{ij}^{(1,0)}$. If $a = a_r + i a_i$ and $b = b_r + i b_i$ (a_r, a_i, b_r, b_i all real), we can write equation (XI.B.) as

$$\sum_{n=0}^{\infty} \{ (a_r - b_r) \cos n\phi - (a_i - b_i) \sin n\phi \} = 0$$

This must be valid for all n and ϕ so that

$$a = b \quad \text{for } n = 0, 1, 2, \dots$$

These equations are listed as follows [dropping superscripts (1,0) except when necessary]

(XI.B.1)

$$\text{momentum } A(i n c_1' + n N c_2) = i N (g_{11}' - g_{22}') + g_{12}'' + N^2 g_{12} \quad]$$

$$\text{momentum } \frac{A}{k} (i n \bar{c}_1' + n N \bar{c}_2) = \bar{c}_1''' - N^2 \bar{c}_1' + i N (N^2 \bar{c}_2 - \bar{c}_2'') \quad]$$

$$\text{continuity } i N c_1 + c_2' = 0 = i N \bar{c}_1 + \bar{c}_2' \quad]$$

(XI.B.2)

$$\text{constitutive } g_{11} = - g_{22} = - Q c_2' \quad]$$

$$g_{12} = \frac{Q}{2} (c_1' + i N c_2) = \frac{Q}{2N} (c_2'' + N^2 c_2) \quad]$$

boundary conditions

$$q_{12} = 0 \quad \text{at } y=0$$

$$A \ln c_1 = 2iN q_{11} + q'_{12} \quad " \quad (\text{XI.B.3})$$

$$q_{12} = k(\bar{c}'_1 + iN\bar{c}_2) \quad \text{at } y=-h$$

$$A \ln c_1 + 2iN q_{22} - q'_{12} = A \ln \bar{c}_1 - k(\bar{c}''_1 - N^2 \bar{c}_1) + 2k iN \bar{c}'_2 \quad \text{at } y=-h$$

$$c_i = \bar{c}_i \quad \text{at } y=-h$$

$$\bar{c}_1 = \begin{cases} -i\beta & \text{for } n=1 \\ 0 & \text{for } n=0, 2, 3, 4, \dots \end{cases} \quad \text{at } y=-h$$

$$\bar{c}_2 = \begin{cases} 1 & \text{for } n=1 \\ 0 & \text{for } n=0, 2, 3, 4, \dots \end{cases} \quad \text{at } y=-h$$

$$N \equiv n\omega, \quad Q \equiv \frac{2}{1+i\pi T}$$

From equations (XI.B.2), the resulting ordinary differential equations and boundary conditions are derived in a straightforward manner.

$$\left. \begin{aligned} c_2'' - 2(N^2 + i\ln \frac{A}{Q}) c_2'' + N^2 (N^2 + 2i\ln \frac{A}{Q}) c_2 = 0 \\ \bar{c}_2'' - 2(N^2 + i\ln \frac{A}{2K}) \bar{c}_2'' + N^2 (N^2 + i\ln \frac{A}{K}) \bar{c}_2 = 0 \end{aligned} \right] \quad (XI.B.4)$$

$$\left. \begin{aligned} c_2'' + N^2 c_2 = 0 & \quad \text{at } y=0 \\ c_2''' - (3N^2 + 2i\ln \frac{A}{Q}) c_2' = 0 & \quad " \\ c_2'' + N^2 c_2 - 2\frac{K}{Q} (\bar{c}_2'' + N^2 \bar{c}_2) = 0 & \quad \text{at } y=-h \\ c_2''' - (3N^2 + 2i\ln \frac{A}{Q}) c_2' - 2\frac{K}{Q} [\bar{c}_2''' - (3N^2 + i\frac{A_n}{K}) \bar{c}_2'] = 0 & \quad " \\ c_2' = \bar{c}_2' & \quad \text{at } y=-h \\ c_2 = \bar{c}_2 & \quad " \end{aligned} \right] \quad (XI.B.5)$$

$$\bar{c}_2' = \begin{cases} -\beta N & \text{for } n=1 \\ 0 & \text{for } n \neq 1 \end{cases} \quad \text{at } y=-1$$

$$\bar{c}_2 = \begin{cases} 1 & \text{for } n=1 \\ 0 & \text{for } n \neq 1 \end{cases} \quad \text{at } y=-1$$

$$N = n\alpha, \quad Q = \frac{2}{1+i\pi T}$$

XI.C. The solutions of the above fourth order linear ordinary differential equations (XI.B.4) are of the form

$$c_2 = \sum_{k=1}^4 \{ a_k e^{\lambda_k y} \} \quad (XIC.1)$$

$$\bar{c}_2 = \sum_{k=1}^4 \{ \bar{a}_k e^{\lambda_k y} \}$$

Substituted into the eight boundary conditions (XI.B.5), these give the matrix equation

$$K_{ij} \xi_j = \xi_i \quad (XIC.2)$$

where the unknown vector $\xi \equiv (a_1, a_2, a_3, a_4, \bar{a}_1, \bar{a}_2, \bar{a}_3, \bar{a}_4)$ and the vector ξ_i is known from the wall velocity.

$$\xi_i = 0 \quad \text{when } n \neq 1 \quad (n = 0, 2, 3, 4, \dots)$$

$$\xi_i \neq 0 \quad \text{when } n = 1$$

The 8×8 matrix K_{ij} is a function of $n, \alpha, \beta, h, k, Q, A$ having components given later (after inertia is neglected) in section XI.D.

Since the determinant of K_{ij} is not zero, and since $\xi_i = 0$ for $n \neq 1$, the following statement holds:

$$\xi_j = 0 \quad \text{for } n \neq 1$$

$$\xi_j \neq 0 \quad \text{for } n = 1$$

Therefore,

the only non-trivial $c_2^{(1,0)}$ and $\bar{c}_2^{(1,0)}$ solutions
are for the mode $n=1$; $c_2^{(1,0)} = \bar{c}_2^{(1,0)} = 0$ for $n \neq 1$

XI.D. From the foregoing discussion, it is clear that n is never greater than unity so that inertia terms can be neglected by expanding the Fourier coefficients c_2 and \bar{c}_2 in the small parameters $\frac{A}{Q}$ and $\frac{A}{k}$ where

$$O\left\{\left|\frac{A}{Q}\right|\right\} \ll 1$$

$$O\left\{\left|\frac{A}{k}\right|\right\} \ll 1$$

For example, if we have an analogous equation

$$\frac{d^2 f}{dx^2} + 6n \frac{df}{dx} = 0 \quad \epsilon \ll 1, \quad f = f(n, x)$$

we cannot neglect $\frac{df}{dx}$ if n happens to be very large.

In our case, however, n is bounded ($n=1$) so the term can indeed be neglected. The resulting approximate c_2 and \bar{c}_2 equations neglecting inertia terms are

$$\begin{aligned} c_2'' - 2N^2 c_2''' + N^4 c_2 &= 0 \\ \bar{c}_2'' - 2N^2 \bar{c}_2''' + N^4 \bar{c}_2 &= 0 \end{aligned} \quad] \quad (\text{XI.D.1})$$

and the boundary conditions are

$$\begin{aligned}
 c''_2 + N^2 c_2 &= 0 & \text{at } y = 0 \\
 c'''_2 - 3N^2 c'_2 &= 0 & " \\
 c'''_2 - 3N^2 c'_2 - \frac{2K}{Q} (\bar{c}'''_2 - 3N^2 \bar{c}'_2) &= 0 & \text{at } y = -h \\
 c''_2 + N^2 c_2 - \frac{2K}{Q} (\bar{c}''_2 + N^2 \bar{c}_2) &= 0 & " \\
 c'_2 = \bar{c}'_2, \quad c_2 = \bar{c}_2 & & " \\
 \bar{c}'_2 = -\beta N, \quad \bar{c}_2 = 1 & & \text{at } y = -l
 \end{aligned}
 \tag{XI.D.2}$$

where $n=1$, $N=\alpha$

Since the inertia-free linear ordinary differential equations have double roots, the solutions are of the form:

$$c_2 = c_2^{(1,0)} = \sum_{k=1}^{2j} (a_k^{(1,0)} + b_k^{(1,0)} y) e^{s_k y} \tag{XI.D.3}$$

$$\bar{c}_2 = \bar{c}_2^{(1,0)} = \sum_{k=1}^{2j} (\bar{a}_k^{(1,0)} + \bar{b}_k^{(1,0)} y) e^{s_k y}; \quad s_{1,2} = \pm N$$

The new matrix equation resulting from substituting (XI.D.3) into the boundary conditions (XI.D.2) is

$$\mathcal{K}_{ij} \mathfrak{S}_j^{(1,0)} = \mathfrak{S}_i^{(1,0)} \quad i=1,2,\dots,8 \quad (\text{XI. D. 4})$$

where the "unknown" vector is $\mathfrak{S}_j^{(1,0)} = (a_1, a_2, b_1, b_2, \bar{a}_1, \bar{a}_2, \bar{b}_1, \bar{b}_2)^T$

and

$$\mathfrak{S}_i^{(1,0)} = \begin{cases} 0 & \text{for } i=1,2,\dots,6 \\ -\beta N & \text{for } i=7 \\ 1 & \text{for } i=8 \end{cases} \quad (\text{XI. D. 5})$$

The elements of the matrix \mathcal{K}_{ij} are

$$\mathcal{K}_{11} = N$$

$$\mathcal{K}_{12} = N$$

$$\mathcal{K}_{13} = 1$$

$$\mathcal{K}_{14} = -1$$

$$\mathcal{K}_{15} = 0$$

:

:

:

$$\mathcal{K}_{18} = 0$$

$$\left. \begin{array}{l} \mathcal{K}_{31} = N e^{-Nh} \\ \mathcal{K}_{32} = N e^{Nh} \\ \mathcal{K}_{33} = (1-Nh) e^{-Nh} \\ \mathcal{K}_{34} = -(1+Nh) e^{Nh} \\ \mathcal{K}_{35} = - \odot \mathcal{K}_{31} \\ \mathcal{K}_{36} = - \odot \mathcal{K}_{32} \\ \mathcal{K}_{37} = - \odot \mathcal{K}_{33} \\ \mathcal{K}_{38} = - \odot \mathcal{K}_{34} \end{array} \right]$$

$$\mathcal{K}_{21} = 1$$

$$\mathcal{K}_{22} = -1$$

$$\mathcal{K}_{23} = 0$$

:

:

:

:

$$\mathcal{K}_{28} = 0$$

$$\left. \begin{array}{l} \mathcal{K}_{41} = e^{-Nh} \\ \mathcal{K}_{42} = -e^{Nh} \\ \mathcal{K}_{43} = -he^{-Nh} \\ \mathcal{K}_{44} = he^{Nh} \\ \mathcal{K}_{45} = - \odot \mathcal{K}_{41} \\ \mathcal{K}_{46} = - \odot \mathcal{K}_{42} \\ \mathcal{K}_{47} = - \odot \mathcal{K}_{43} \\ \mathcal{K}_{48} = - \odot \mathcal{K}_{44} \end{array} \right|$$

$$\begin{aligned}
 x_{51} &= Ne^{-Nh} \\
 x_{52} &= -Ne^{Nh} \\
 x_{53} &= (1-Nh)e^{-Nh} \\
 x_{54} &= (1+Nh)e^{Nh} \\
 x_{55} &= -x_{51} \\
 x_{56} &= -x_{52} \\
 x_{57} &= -x_{53} \\
 x_{58} &= -x_{54}
 \end{aligned}$$

$$\begin{aligned}
 x_{71} &= 0 \\
 &\vdots \\
 &\vdots \\
 x_{75} &= Ne^N \\
 x_{76} &= -Ne^N \\
 x_{77} &= (1-N)e^{-N} \\
 x_{78} &= (1+N)e^N
 \end{aligned}$$

$$\begin{aligned}
 x_{61} &= e^{-Nh} \\
 x_{62} &= e^{Nh} \\
 x_{63} &= -he^{-Nh} \\
 x_{64} &= -he^{Nh} \\
 x_{65} &= -x_{61} \\
 x_{66} &= -x_{62} \\
 x_{67} &= -x_{63} \\
 x_{68} &= -x_{64}
 \end{aligned}$$

$$\begin{aligned}
 x_{81} &= 0 \\
 &\vdots \\
 &\vdots \\
 x_{85} &= e^{-N} \\
 x_{86} &= e^N \\
 x_{87} &= -e^{-N} \\
 x_{88} &= -e^N
 \end{aligned}$$

(XI. D. 6)

$$\Theta = k(1+i\tau) \approx \frac{2k}{Q} \Big|_{n=1}, \quad N \gtrless n \alpha$$

XI.E. Inversion of the matrix equation (XI.D.4) gives $\mathbf{g}_j^{(1,0)}$,

which in turn yields $c_2^{(1,0)}$ and $\bar{c}_2^{(1,0)}$ (for $n=1$) directly.

Since $c_2^{(1,0)} = \bar{c}_2^{(1,0)} = 0$ for $n \neq 1$, equations (XI.B.2) imply that

$$c_1^{(1,0)} = \bar{c}_1^{(1,0)} = g_{ij}^{(1,0)} = 0 \quad \text{for } n=2,3,4,\dots$$

The Fourier series is no longer an infinite summation. However, it is not obvious that $c_1^{(1,0)} = \bar{c}_1^{(1,0)} = g_{ij}^{(1,0)} = 0$ when $n=0$, because equations (XI.B.2) are not applicable. Instead, we are forced to consider the actual system of x, t independent equations (all unknowns are functions of y alone). From the equations in section XI.A. neglecting inertia,

constitutive $T(0) = -t_{ij} + u_{i,j} + u_{j,i}$

$t_{11} = t_{22} = 0$, $t_{12} = \omega_i'$

momentum $0 = t_{12}'' = \omega_i''$, $0 = \bar{\omega}_i''$

boundary conditions

$u_i'(0) = 0$, $u_i''(0) = 0$

$u_i'(-h) = k \bar{u}_i'(-h)$, $u_i''(-h) = k \bar{u}_i''(-h)$

$u_i(-h) = \bar{u}_i(-h)$, $\bar{u}_i(-1) = 0$

There are six boundary conditions for the two third order equations having solutions of the form

$$u_1 = ay^2 + by + c, \quad \bar{u}_1 = \bar{a}y^2 + \bar{b}y + \bar{c}.$$

It can be shown after some calculation that

$$a = b = c = \bar{a} = \bar{b} = \bar{c} = 0$$

$$u_1 \equiv \bar{u}_1 \equiv t_{12} \equiv 0$$

Thus

$$c_i^{(1,0)} = \bar{c}_i^{(1,0)} = g_{ij}^{(1,0)} = 0 \quad \text{for } n=0$$

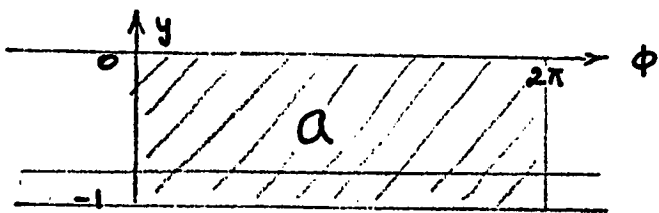
XI.F. The shapes of the free surface and interface can be calculated from equations (IX.D.3):

$$u_2^{(1,0)} = \gamma_{,t}^{(1,0)} \quad \text{at } y=0$$

$$\bar{u}_2^{(1,0)} = \bar{\gamma}_{,t}^{(1,0)} \quad \text{at } y=-h$$

In order to evaluate the constants of integration, we must consider the area* α of the fluid in one wavelength ($0 \leq \phi \leq 2\pi$).

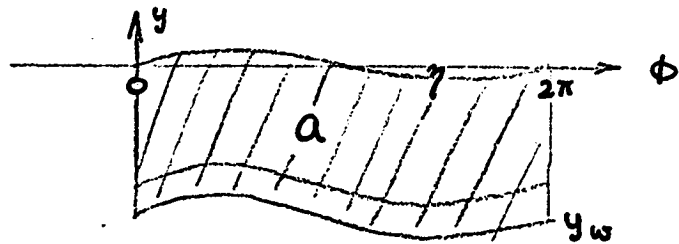
In an undisturbed state, ($\epsilon = 0$), the wall is flat:



*

Actually it is the volume considering unit depth in ϵ_3 .

Since the densities of both mucus and serous fluid are constant, the area(or volume) of fluid in one wavelength must be the same as the undisturbed area at any time t later on (after the transient flow has stopped and functions are periodic in time, as in our problem):



These statements can be expressed mathematically as

$$\int_0^{2\pi} \{ \eta - y_w \} d\phi = A = 2\pi$$

where

$$\begin{aligned} \eta - y_w &= 1 + \epsilon \{ \eta^{(1,0)} - y_w^{(1)} \} + \epsilon^2 \{ \eta^{(2,0)} - y_w^{(2)} \} + \\ &\quad + B \eta^{(0,1)} + O(\epsilon^3, \epsilon B, B^2) \\ \therefore 2\pi + \epsilon \int_0^{2\pi} \{ \eta^{(1,0)} - y_w^{(1)} \} d\phi + \epsilon^2 \int_0^{2\pi} \{ \eta^{(2,0)} - y_w^{(2)} \} d\phi + \\ &\quad + B \int_0^{2\pi} \eta^{(0,1)} d\phi + \dots = 2\pi \end{aligned}$$

Thus, $\int_0^{2\pi} \gamma^{(1,0)} d\phi = \int_0^{2\pi} y_w^{(1)} d\phi$. From equation (VI.C.5.d), we find

$$\int_0^{2\pi} \gamma^{(1,0)} d\phi = \int_0^{2\pi} \sin \phi d\phi = 0$$

and from (VI.C.5.e):

$$\int_0^{2\pi} \gamma^{(2,0)} d\phi = \int_0^{2\pi} \frac{1}{2} \alpha \beta (1 + \cos 2\phi) d\phi = \alpha \beta \pi$$

The three conditions used to evaluate the constants of integration are:

$$\int_0^{2\pi} \gamma^{(1,0)} d\phi = 0 \quad (\text{XI. F. 1})$$

$$\int_0^{2\pi} \gamma^{(2,0)} d\phi = \alpha \beta \pi \quad (\text{XI. F. 2})$$

$$\int_0^{2\pi} \gamma^{(0,1)} d\phi = 0 \quad (\text{XI. F. 3})$$

These same conditions also hold for the interface $\bar{\gamma}$.

For the $O(\epsilon)$ case, the constants are zero so that direct integration gives

$$\gamma^{(1,0)} = -\operatorname{Re} \left\{ i c_2^{(1,0)} e^{i\phi} \right\} \quad \text{at } y=0 \quad (\text{XI. F. 4})$$

$$\bar{\gamma}^{(1,0)} = -\operatorname{Re} \left\{ i \bar{c}_2^{(1,0)} e^{i\phi} \right\} \quad \text{at } y=-h \quad (\text{XI. F. 5})$$

XI.G. The pressures and total stresses can be found from equations (IX.D.1). Neglecting inertia,

$$\sigma = -P_{,i} + t_{,j;j}$$

$$\sigma = -\bar{P}_{,i} + \kappa \nabla^2 \bar{u}_i$$

The only non-zero solutions are for the mode $n=1$, so that

$$P^{(1,0)} = Re \{ p^{(1,0)} e^{i\phi} \}$$

$$\bar{P}^{(1,0)} = Re \{ \bar{p}^{(1,0)} e^{i\phi} \}$$

In the direction of \hat{e}_1 :

$$\sigma = -P_{,x} + t_{,y;y}$$

$$\sigma = Re \{ (-i\omega p + i\omega g_{11} + g'_{12}) e^{i\phi} \}$$

$$\therefore p = g_{11} - \frac{i}{\omega} g'_{12}$$

In terms of c_2 the pressure Fourier coefficient is

$$p = \frac{\Omega}{2\alpha^2} \{ c''_2 - \alpha^2 c'_2 \}$$

The Newtonian pressure can be similarly obtained, and the two are:

$$P^{(1,0)} = g_{11}^{(1,0)} - \frac{i}{\alpha} g_{12}^{(1,0)} = \frac{Q}{2\alpha^2} \left\{ c_2^{(1,0)} - \alpha^2 c_2'^{(1,0)} \right\}$$

$$\bar{P}^{(1,0)} = \bar{g}_{11}^{(1,0)} - \frac{i}{\alpha} \bar{g}_{12}^{(1,0)} = \frac{K_1}{\alpha^2} \left\{ \bar{c}_2^{(1,0)} - \alpha^2 \bar{c}_2'^{(1,0)} \right\}$$

(XI. G. 1)

$$Q = \frac{2}{1+i\tau}$$

The total stresses are $S_{ij}^{(1,0)} = -P^{(1,0)} \delta_{ij} + T^{(1,0)}_{ij}$ so that

$$A_{ij}^{(1,0)} = -P^{(1,0)} \delta_{ij} + g_{ij}^{(1,0)}$$

$$\bar{A}_{ij}^{(1,0)} = -\bar{P}^{(1,0)} \delta_{ij} + \bar{g}_{ij}^{(1,0)}$$

which give

$$A_{11}^{(1,0)} = \frac{i}{\alpha} g_{12}^{(1,0)}$$

$$A_{12}^{(1,0)} = g_{12}^{(1,0)}$$

$$A_{22}^{(1,0)} = -2 g_{11}^{(1,0)} + \frac{i}{\alpha} g_{12}^{(1,0)}$$

$$\bar{A}_{11}^{(1,0)} = \frac{i}{\alpha} \bar{g}_{12}^{(1,0)}$$

$$\bar{A}_{12}^{(1,0)} = \bar{g}_{12}^{(1,0)}$$

$$\bar{A}_{22}^{(1,0)} = -2 \bar{g}_{11}^{(1,0)} + \frac{i}{\alpha} \bar{g}_{12}^{(1,0)}$$

(XI. G. 2)

XI.H. The entire $(1,0)$ solution can now be written. The unknown functions are

$$u_i^{(1,0)} = \operatorname{Re} \{ c_i^{(1,0)} e^{i\phi} \}$$

$$\bar{u}_i^{(1,0)} = \operatorname{Re} \{ \bar{c}_i^{(1,0)} e^{i\phi} \}$$

$$t_{ij}^{(1,0)} = \operatorname{Re} \{ g_{ij}^{(1,0)} e^{i\phi} \}$$

$$\bar{t}_{ij}^{(1,0)} = \operatorname{Re} \{ \bar{g}_{ij}^{(1,0)} e^{i\phi} \}$$

$$p^{(1,0)} = \operatorname{Re} \{ \gamma p^{(1,0)} e^{i\phi} \}$$

$$\bar{p}^{(1,0)} = \operatorname{Re} \{ \bar{\gamma} \bar{p}^{(1,0)} e^{i\phi} \}$$

$$s_{ij}^{(1,0)} = \operatorname{Re} \{ A_{ij}^{(1,0)} e^{i\phi} \}$$

$$\bar{s}_{ij}^{(1,0)} = \operatorname{Re} \{ \bar{A}_{ij}^{(1,0)} e^{i\phi} \}$$

The Fourier coefficients $c_2^{(1,0)}$ and $\bar{c}_2^{(1,0)}$ are known from the matrix equation

$$X_j \bar{x}_j^{(1,0)} = \bar{x}_i^{(1,0)} \quad i = 1, 2, \dots, 8$$

where

$$\bar{x}_j^{(1,0)} = (a_1^{(1,0)}, a_2^{(1,0)}, b_1^{(1,0)}, b_2^{(1,0)}, \bar{a}_1^{(1,0)}, \bar{a}_2^{(1,0)}, \bar{b}_1^{(1,0)}, \bar{b}_2^{(1,0)})$$

$$\bar{x}_i = \begin{cases} 0 & i = 1, 2, \dots, 6 \\ -\alpha\beta & i = 7 \\ 1 & i = 8 \end{cases}$$

\mathcal{X}_{ij} is found in section XI.D.

and

$$c_2^{(1,0)} = \sum_{k=1}^2 (a_k^{(1,0)} + b_k^{(1,0)} y) e^{s_k y}$$

$$\bar{c}_2^{(1,0)} = \sum_{k=1}^2 (\bar{a}_k^{(1,0)} + \bar{b}_k^{(1,0)} y) e^{s_k y} ; s_{1,2} = \pm \alpha$$

The Fourier coefficients of the other unknown functions
are given in terms of $c_2^{(1,0)}$ and $\bar{c}_2^{(1,0)}$ as follows

$$c_1^{(1,0)} = \frac{i}{\alpha} c_2^{(1,0)}$$

$$g_{11}^{(1,0)} = -g_{22}^{(1,0)} = -Q c_2^{(1,0)}$$

$$g_{12}^{(1,0)} = \frac{Qi}{2\alpha} \{ c_2^{(1,0)} + \alpha^2 c_2^{(1,0)} \}$$

$$T^{(1,0)} = g_{11}^{(1,0)} - \frac{i}{\alpha} g_{12}^{(1,0)}$$

$$A_{11}^{(1,0)} = \frac{i}{\alpha} g_{12}^{(1,0)}$$

$$A_{12}^{(1,0)} = g_{12}^{(1,0)}$$

$$A_{22}^{(1,0)} = -2g_{11}^{(1,0)} + \frac{i}{\alpha} g_{12}^{(1,0)}$$

$$Q = \frac{1}{1+iT}$$

$$\bar{c}_1^{(1,0)} = \frac{i}{\alpha} \bar{c}_2'^{(1,0)}$$

$$\bar{g}_{11}^{(1,0)} = -\bar{g}_{22}^{(1,0)} = -2\lambda^2 \bar{c}_2'^{(1,0)}$$

$$\bar{g}_{12}^{(1,0)} = \frac{i\lambda^2}{\alpha^2} \left\{ \bar{c}_2''^{(1,0)} + \alpha^2 \bar{c}_2^{(1,0)} \right\}$$

$$\bar{p}^{(1,0)} = \bar{g}_{11}^{(1,0)} - \frac{i}{\alpha} \bar{g}_{12}^{(1,0)}$$

$$\bar{A}_{11}^{(1,0)} = \frac{i}{\alpha} \bar{g}_{12}^{(1,0)}$$

$$\bar{A}_{12}^{(1,0)} = \bar{g}_{12}^{(1,0)}$$

$$\bar{A}_{22}^{(1,0)} = -2\bar{g}_{11}^{(1,0)} + \frac{i}{\alpha} \bar{g}_{12}^{(1,0)}$$

The free surface and interface are

$$\eta^{(1,0)} = -Re \left\{ i \bar{c}_2^{(1,0)} e^{i\phi} \right\} \quad \text{at } y=0$$

$$\bar{\eta}^{(1,0)} = -Re \left\{ i \bar{c}_2'^{(1,0)} e^{i\phi} \right\} \quad \text{at } y=-h$$

For convenience the following function is defined:

$$w^{(1,0)} \equiv \frac{i}{2\alpha} \left\{ \bar{c}_2''^{(1,0)} - \alpha^2 \bar{c}_2^{(1,0)} \right\}$$

It will be used in the (2,0) solution.

XII. SOLUTION OF THE (2, 0) SYSTEM

This set of equations is more difficult to solve than the previous one because of the inhomogeneous terms resulting mainly from product terms of the (1, 0) system. The solution, however, follows the basic outline of section X, with some exceptions. The (2, 0) equations are (section IX. E.):

$$A \{ u_{i,t}^{(2,0)} + F_i \} = - P_{,i}^{(2,0)} + t_{ij,j}^{(2,0)}$$

$$A \{ \bar{u}_{i,t}^{(2,0)} + \bar{F}_i \} = - \bar{P}_{,i}^{(2,0)} + \bar{t}_{ij,j}^{(2,0)}$$

$$T \{ t_{ij,t}^{(2,0)} + G_{,j} \} = - t_{ij,j}^{(2,0)} + d_{ij}^{(2,0)}$$

$$\bar{t}_{ij}^{(2,0)} = 2 \nabla d_{ij}^{(2,0)}$$

$$u_{k,k}^{(2,0)} = \bar{u}_{k,k}^{(2,0)} = 0$$

$$t_{12}^{(2,0)} = B_1, \quad t_{22}^{(2,0)} = P^{(2,0)} + C_1, \quad \text{at } y=0$$

$$\Delta t_{12}^{(2,0)} = B_2, \quad \Delta t_{22}^{(2,0)} = \Delta P^{(2,0)} + C_2, \quad \text{at } y=-h$$

$$u_i^{(2,0)} - \bar{u}_i^{(2,0)} = B_{3,i}, \quad \text{at } y=-h$$

$$\tilde{u}_i^{(2,0)} = B_{4,i}, \quad \text{at } y=-l$$

$$\Delta f \equiv f - \tilde{f}$$

$$F_i \equiv u_k^{(1,0)} u_{i,k}^{(1,0)}$$

$$\bar{F}_i \equiv \bar{u}_k^{(1,0)} \bar{u}_{i,k}^{(1,0)}$$

$$G_{ij} \equiv u_k^{(1,0)} t_{ij,k}^{(1,0)} + t_{ik}^{(1,0)} \omega_{kj}^{(1,0)} - t_{kj}^{(1,0)} \omega_{ik}^{(1,0)}$$

$$B_1 \equiv \gamma_{,x}^{(1,0)} (t_{11}^{(1,0)} - p^{(1,0)}) - \gamma_{,x}^{(1,0)} t_{12,y}^{(1,0)} \quad \text{at } y=0$$

$$C_1 \equiv \gamma_{,x}^{(1,0)} (p_{,y}^{(1,0)} - t_{22,y}^{(1,0)}) + \gamma_{,x}^{(1,0)} t_{12}^{(1,0)} \quad "$$

$$B_2 \equiv \bar{\gamma}_{,x}^{(1,0)} (\Delta t_{11}^{(1,0)} - \Delta p_{,y}^{(1,0)}) - \gamma_{,x}^{(1,0)} \Delta t_{12,y}^{(1,0)} \quad \text{at } y=-h$$

$$C_2 \equiv \bar{\gamma}_{,x}^{(1,0)} (\Delta p_{,y}^{(1,0)} - \Delta t_{22,y}^{(1,0)}) + \bar{\gamma}_{,x}^{(1,0)} \Delta t_{12}^{(1,0)} \quad "$$

$$B_{3i} \equiv \bar{\gamma}^{(1,0)} (\bar{u}_{i,y}^{(1,0)} - u_{i,y}^{(1,0)}) \quad "$$

$$B_{4i} \equiv u_{\omega_i}^{(2)} - \sin \phi \bar{u}_{i,y}^{(1,0)} \quad \text{at } y=-l$$

$$u_{\omega_1}^{(2)} = \frac{1}{2} \alpha \beta^2 (1 + \cos 2\phi)$$

$$u_{\omega_2}^{(2)} = -\frac{1}{2} \alpha \beta \sin 2\phi$$

XII. A. The pressure-independent (vorticity) equations obtained by cross differentiation of equations (IV. E. 1, 2) are:

$$A \{ u_{1,y,t}^{(2,0)} - u_{2,x,t}^{(2,0)} - \tilde{\gamma}^{(2,0)} \} = t_{1j,jy}^{(2,0)} - t_{2j,jx}^{(2,0)}$$

$$\frac{A}{K} \{ \bar{u}_{1,y,t}^{(2,0)} - \bar{u}_{2,x,t}^{(2,0)} - \tilde{\gamma}^{(2,0)} \} = \nabla^2 \{ \bar{u}_{1,y}^{(2,0)} - \bar{u}_{2,x}^{(2,0)} \}$$

$$T \{ t_{ij,t}^{(2,0)} + G_{ij}^{(2,0)} \} = -t_{ij}^{(2,0)} + u_{i,j}^{(2,0)} + u_{j,i}^{(2,0)}$$

$$u_{k,j,k}^{(2,0)} = \bar{u}_{k,k}^{(2,0)} = 0$$

$$t_{1z}^{(2,0)} = B_1 \quad \text{at } y=0$$

$$t_{2z,x}^{(2,0)} = t_{y,j}^{(2,0)} - A \{ u_{1,t}^{(2,0)} + F_1^{(2,0)} \} + C_{1,x} \quad \text{at } y=0$$

$$t_{1z}^{(2,0)} = K \{ \bar{u}_{1,y}^{(2,0)} + \bar{u}_{2,x}^{(2,0)} \} + B_2 \quad \text{at } y=-h$$

$$t_{2z,x}^{(2,0)} = t_{y,j}^{(2,0)} + A \{ \bar{u}_{1,t}^{(2,0)} + \bar{F}_1^{(2,0)} - u_{1,t}^{(2,0)} - F_1^{(2,0)} \} - K \nabla^2 \bar{u}_{1,y}^{(2,0)} + \\ + 2K \bar{u}_{2,xy}^{(2,0)} + C_{2,x} \quad \text{at } y=-h$$

$$u_i^{(2,0)} - \bar{u}_i^{(2,0)} = B_{3,i} \quad \text{at } y=-h$$

$$\bar{u}_i^{(2,0)} = B_{4,i} \quad \text{at } y=-1$$

$$\tilde{\gamma}^{(2,0)} = F_{2,x}^{(2,0)} - F_{1,y}^{(2,0)}, \quad \tilde{\gamma}^{(2,0)} = \bar{F}_{2,x}^{(2,0)} - \bar{F}_{1,y}^{(2,0)}$$

The constitutive equation of the Newtonian fluid has been used above.

XII. B. All functions are expanded in Fourier series as follows:

the unknown functions are

$$\left. \begin{aligned} u_i^{(2,0)} &= \sum_{n=0}^{\infty} \operatorname{Re} \{ c_i^{(2,0)}(n,y) e^{in\phi} \} \\ \bar{u}_i^{(2,0)} &= \sum_{n=0}^{\infty} \operatorname{Re} \{ \bar{c}_i^{(2,0)}(n,y) e^{in\phi} \} \\ t_{ij}^{(2,0)} &= \sum_{n=0}^{\infty} \operatorname{Re} \{ g_{ij}^{(2,0)}(n,y) e^{in\phi} \} \end{aligned} \right] \quad (\text{XII. B. 1})$$

the known functions are

$$\left. \begin{aligned} f^{(2,0)} &= \sum_{n=0}^{\infty} \operatorname{Re} \{ f(n,y) e^{in\phi} \} & B_{4i}^{(2,0)} &= \sum_{n=0}^{\infty} \operatorname{Re} \{ b_{4i}(n) e^{in\phi} \} \\ \bar{f}^{(2,0)} &= \sum_{n=0}^{\infty} \operatorname{Re} \{ \bar{f}(n,y) e^{in\phi} \} & C_1 &= \sum_{n=0}^{\infty} \operatorname{Re} \{ \psi_1(n) e^{in\phi} \} \\ G_{ij}^{(2,0)} &= \sum_{n=0}^{\infty} \operatorname{Re} \{ \gamma_{ij}(n,y) e^{in\phi} \} & C_2 &= \sum_{n=0}^{\infty} \operatorname{Re} \{ \psi_2(n) e^{in\phi} \} \\ B_1 &= \sum_{n=0}^{\infty} \operatorname{Re} \{ b_1(n) e^{in\phi} \} & F_i^{(2,0)} &= \sum_{n=0}^{\infty} \operatorname{Re} \{ f_i(n) e^{in\phi} \} \\ B_2 &= \sum_{n=0}^{\infty} \operatorname{Re} \{ b_2(n) e^{in\phi} \} & \bar{F}_i^{(2,0)} &= \sum_{n=0}^{\infty} \operatorname{Re} \{ \bar{f}_i(n) e^{in\phi} \} \\ B_{3i} &= \sum_{n=0}^{\infty} \operatorname{Re} \{ b_{3i}(n) e^{in\phi} \} \end{aligned} \right] \quad (\text{XII. B. 2})$$

The equations and boundary conditions (section XII. A.) give the following relations between Fourier coefficients (dropping superscripts):

(XII. B. 3)

$$\text{momentum } A \{ i n c'_1 + n N c_2 - f \} = i N (g''_{11} - g'_{12}) + g''_{12} + N^2 g_{12}]$$

$$A \{ i n \bar{c}'_1 + n N \bar{c}_2 - \bar{f} \} = \bar{c}'''_1 - N^2 \bar{c}'_1 + i N (N^2 \bar{c}_2 - \bar{c}''_2)]$$

continuity (gives c_1, \bar{c}_1 and g_{ij} in terms of c_2, \bar{c}_2 for $n \neq 0$)

$$i N c_1 + c'_1 = 0, \quad i N \bar{c}_1 + \bar{c}'_1 = 0 \quad (\text{XII. B. 4})$$

constitutive

$$g_{11} = - g_{22} = - \frac{Q}{2} \{ 2 c'_2 + T \gamma_{11} \}]$$

$$g_{12} = \frac{Q}{2} \{ c'_1 + i N c_2 - T \gamma_{12} \}] \quad (\text{XII. B. 5})$$

boundary conditions

$$g_{12} = b_1 \quad \text{at } y=0 \quad (\text{XII. B. 6})$$

$$A i n c_1 = 2 i N g_{11} + g'_{12} - A f_1 + i N \Psi_1 \quad \text{at } y=0$$

$$g_{12} = k \{ \bar{c}'_1 + i N \bar{c}_2 \} + b_2 \quad \text{at } y=-h$$

$$A i n c_1 - 2 i N g_{11} - g'_{12} = A i n \bar{c}_1 - k (\bar{c}'''_1 - N^2 \bar{c}'_1) + 2 i k N \bar{c}'_2 +$$

$$+ i N \Psi_2 + A (\bar{f}_1 - f_1) \quad \text{at } y=-h$$

$$c_i - \bar{c}_i = b_{3i} \quad \text{at } y=-h$$

$$\bar{c}_i = b_{4i} \quad \text{at } y=-1$$

$$Q = \frac{2}{1+i n T} \rightarrow N = n \infty$$

Using the relations between c_1, \bar{c}_1, g_{ij} and c_2, \bar{c}_2 [equations (XII. B. 4, 5)] equations (XII. B. 3, 6) can be put in terms of c_2 and \bar{c}_2 alone, giving, after considerable (but elementary) algebraic manipulation:

(XII. B. 7)

$$\begin{aligned} c_2''' - 2[N^2 + i\pi \frac{A}{Q}] c_2'' + N^2 [N^2 + 2i\pi \frac{A}{Q}] c_2 &= \frac{2A}{Q} iNf + g(n, y) \\ \bar{c}_2''' - 2[N^2 + i\pi \frac{A}{2K}] \bar{c}_2'' + N^2 [N^2 + i\pi \frac{A}{K}] \bar{c}_2 &= A \frac{iN}{K} \bar{f} \\ c_2'' + N^2 c_2 = -2i\pi \frac{N}{Q} b_1 - iNT \gamma_{12} &\quad \text{at } y=0 \\ c_2''' - [3N^2 + 2A \frac{i\pi}{Q}] c_2' &= 2N^2 T \gamma_{11} - iNT \gamma_{12}' - \frac{2}{Q} [iNAf_1 + N^2 \psi_1] \\ &\quad \text{at } y=0 \\ c_2'' + N^2 c_2 - \frac{2K}{Q} [\bar{c}_2'' + N^2 \bar{c}_2] &= -iNT \gamma_{12} - 2i\pi \frac{N}{Q} b_2 \quad \text{at } y=-h \\ c_2''' - [3N^2 + 2A \frac{i\pi}{Q}] c_2' - \frac{2K}{Q} \{\bar{c}_2''' - [3N^2 + A \frac{i\pi}{K}] \bar{c}_2'\} &= \frac{2}{Q} [-N^2 \psi_2 + \\ &+ iNA(\bar{f} - f)] - iNT \gamma_{12}' + 2N^2 T \gamma_{11} \quad \text{at } y=-h \end{aligned}$$

$$c_2' - \bar{c}_2' = -iN b_{31} \quad \text{at } y=-h$$

(XII. B. 8)

$$c_2 - \bar{c}_2 = b_{32} \quad //$$

$$\bar{c}_2' = -iN b_{41} \quad \text{at } y=-1$$

$$\bar{c}_2 = b_{42} \quad //$$

$$g(n, y) \equiv 2N^2 T \gamma_{11}' - iNT (\gamma_{12}'' + N^2 \gamma_{12})$$

XII.C. The Fourier series for each inhomogeneous function (including the wall velocity) involves only the modes $n=0$ and $n=2$. This important fact is due to the $(1,0)$ solution, for which the only non-trivial mode has been shown to be $n=1$. Suppose that the inhomogeneous term is a product of the two real functions a and b :

$$a = \operatorname{Re} \{ A e^{i\phi} \}, \quad b = \operatorname{Re} \{ B e^{i\phi} \}$$

and

$$A = A_r + iA_i, \quad B = B_r + iB_i \quad (\text{complex-valued})$$

Then we can show that the product is (* denotes complex conjugate)

$$ab = \frac{1}{2} \operatorname{Re} \{ AB^* \} + \frac{1}{2} \operatorname{Re} \{ AB e^{2i\phi} \} \quad (\text{XII.C.1})$$

$$\frac{1}{2} \operatorname{Re} \{ A^* B \}$$

Written as a Fourier series,

$$ab = \sum_{n=0}^{\infty} \operatorname{Re} \{ \delta(n,y) e^{in\phi} \} \quad (\text{XII.C.2})$$

$$\delta(0,y) = \frac{1}{2} AB^* = \frac{1}{2} A^* B, \quad \delta(2,y) = \frac{1}{2} AB$$

$$\delta(n,y) = 0 \quad \text{for } n = 1, 3, 4, 5, \dots$$

The fourth order ordinary differential equations have homogeneous solutions of the form (section X.D.):

$$c_{2h} = \sum_{k=1}^4 a_k e^{A_k y}, \quad \bar{c}_{2h} = \sum_{k=1}^4 \bar{a}_k e^{A_k y}$$

which give the matrix equation $\mathbf{A}_{ij} \mathbf{s}_j = \mathbf{s}_i \quad i=1,2,\dots,8$

where \mathbf{s}_j is a vector of the constants a_k, \bar{a}_k . The absence of modes $n=1,3,4,5,\dots$ in the expansions for the inhomogeneous terms means

$$s_i = 0 \quad \text{for } n=1,3,4,5,\dots$$

Since the determinant of $\mathbf{A}_{ij} \neq 0 \forall n$, the solution vector $\mathbf{s}_j = 0$ for $n=1,3,4,5,\dots$ so that the only non-trivial homogeneous $c_{2h}^{(2,0)}$ and $\bar{c}_{2h}^{(2,0)}$ solutions may exist for the modes $n=0$ and $n=2$;
 $c_{2h} = \bar{c}_{2h} = 0 \quad \text{for } n \neq 0,2$.

In addition, the Fourier coefficients s_{ij} , f and \bar{f} are zero for $n \neq 0,2$ since they also result from product terms of the first order system so that $g(n,y) = 0$ for these same modes.

Therefore, the only non-trivial particular solutions $c_{2p}^{(2,0)}$ and $\bar{c}_{2p}^{(2,0)}$ correspond to the modes $n=0$ and $n=2$; $c_{2p} = \bar{c}_{2p} = 0$ for $n=1,3,4,5,\dots$. In fact, we shall show (section XII.E.) that the particular solution is zero for all modes (including $n=2$).

XII. D. As in the previous discussion for the first order system, the inertia terms may be neglected because the coefficients can be expanded asymptotically in $\frac{A}{Q}$ and $\frac{A}{K}$, now that n is bounded. The equations neglecting inertia terms are

$$c''_2 - 2N^2 c'_2 + N^4 c_2 = g(n, y) \quad] \quad (\text{XII. D. 1})$$

$$\bar{c}''_2 - 2N^2 \bar{c}'_2 + N^4 \bar{c}_2 = 0 \quad]$$

$$c''_2 + N^2 c_2 = \gamma_1 \quad \text{at } y=0$$

$$c''_2 - 3N^2 c'_2 = \gamma_2 \quad "$$

$$c''_2 + N^2 c_2 - \frac{2K}{Q} [\bar{c}''_2 + N^2 \bar{c}_2] = \gamma_3 \quad \text{at } y=-h$$

$$c''_2 - 3N^2 c'_2 - \frac{2K}{Q} [\bar{c}'''_2 - 3N^2 \bar{c}'_2] = \gamma_4 \quad "$$

$$c'_2 - \bar{c}'_2 = \gamma_5 \quad \text{at } y=-h$$

$$c_2 - \bar{c}_2 = \gamma_6 \quad "$$

$$\bar{c}'_2 = \gamma_7 \quad \text{at } y=-1$$

$$\bar{c}_2 = \gamma_8 \quad "$$

$$g(n, y) = 2N^2 T y''_{12} - iNT (y''_{12} + N^2 y'_{12}) \quad]$$

$$y_1 = -\frac{2i}{Q} Nb_1 - iNT y_{12} \quad \text{at } y=0 \quad]$$

$$\gamma_2 = 2N^2 T \gamma_{11} - iNT \gamma'_{12} - 2\frac{N^2}{Q} \psi_1 \quad \text{at } y=0$$

$$\gamma_3 = -\frac{iN}{Q} b_2 - iNT \gamma_{12} \quad \text{at } y=-h$$

(XII. D. 3)

$$\gamma_4 = 2N^2 T \gamma_{11} - iNT \gamma'_{12} - 2\frac{N^2}{Q} \psi_2 \quad "$$

$$\gamma_5 = -iNb_{31}, \quad \gamma_6 = b_{32} \quad "$$

$$\gamma_7 = -iNb_{41}, \quad \gamma_8 = b_{42} \quad \text{at } y=-1$$

$$G_{ij} = \sum_{n=0}^{\infty} \operatorname{Re} \{ \gamma_{ij} e^{in\phi} \} = u_{ik}^{(1,0)} t_{ij,k}^{(1,0)} + t_{ik}^{(1,0)} \omega_{kj}^{(1,0)} - t_{kj}^{(1,0)} \omega_{ik}^{(1,0)}$$

$$B_1 = \sum_{n=0}^{\infty} \operatorname{Re} \{ b_1 e^{in\phi} \} = \bar{\gamma}_{jz}^{(1,0)} (t_{11}^{(1,0)} - p^{(1,0)}) - \bar{\gamma}_{12}^{(1,0)} t_{12,y}^{(1,0)} \quad \text{at } y=0$$

$$B_2 = \sum_{n=0}^{\infty} \operatorname{Re} \{ b_2 e^{in\phi} \} = \bar{\gamma}_{jz}^{(1,0)} \Delta (t_{11}^{(1,0)} - p^{(1,0)}) - \bar{\gamma}_{12}^{(1,0)} \Delta t_{12,y}^{(1,0)} \quad \text{at } y=-h$$

$$B_{3i} = \sum_{n=0}^{\infty} \operatorname{Re} \{ b_{3i} e^{in\phi} \} = \bar{\gamma}_{iz}^{(1,0)} (\bar{u}_{iz,y}^{(1,0)} - u_{iz,y}^{(1,0)}) \quad "$$

$$B_{4i} = \sum_{n=0}^{\infty} \operatorname{Re} \{ b_{4i} e^{in\phi} \} = u_{w_i}^{(2)} - \sin \phi \bar{u}_{z,y}^{(1,0)} \quad \text{at } y=-1$$

$$C_1 = \sum_{n=0}^{\infty} \operatorname{Re} \{ \psi_1 e^{in\phi} \} = \bar{\gamma}_{1y}^{(1,0)} (p_{1y}^{(1,0)} - t_{22,y}^{(1,0)}) + \bar{\gamma}_{1x}^{(1,0)} t_{12}^{(1,0)} \quad \text{at } y=0$$

$$C_2 = \sum_{n=0}^{\infty} \operatorname{Re} \{ \psi_2 e^{in\phi} \} = \bar{\gamma}_{1y}^{(1,0)} \Delta (p_{1y}^{(1,0)} - t_{22,y}^{(1,0)}) + \bar{\gamma}_{1x}^{(1,0)} \Delta t_{12}^{(1,0)} \quad \text{at } y=-h$$

The known Fourier coefficients $\gamma_{ij}, b_i, b_{3i}, b_{4i}, \psi_i$ are

calculated in the Appendix A. They are listed in section XII. I. 2 of this chapter.

XII. E. The vector \underline{y} and the function $g(n, y)$ can be obtained in terms of the first order Fourier coefficients $c_2^{(1,0)}$, $\bar{c}_2^{(1,0)}$. The algebra involved is lengthy and is given in Appendix B.

One of the major results of the above calculation is that the inhomogeneous term of the differential equation (XII. D. 1) is zero for the $n = 2$ mode:

$$g(n, y) \equiv 0 \quad \text{for } n = 2$$

Thus, the particular solution $c_{2,p}^{(2,0)}$ for $n = 1, 2, 3, 4, \dots$ and the non-trivial homogeneous solutions $c_{2,h}^{(2,0)}, \bar{c}_{2,h}^{(2,0)}$ exist only for modes $n = 0$ and $n = 2$.

In all the following work, the subscript h will be dropped from $c_{2,h}^{(2,0)}, \bar{c}_{2,h}^{(2,0)}$ and it will be called merely the solution and will be denoted as c_2 or $c_2^{(2,0)}$.

The linear ordinary differential equations (XII. D. 1) have double roots so that the solution is of the form (see section XI. D.):

$$c_2 = c_2^{(2,0)} = \sum_{k=1}^2 (a_k^{(2,0)} + b_k^{(2,0)} y) e^{s_k y}$$

$$\bar{c}_2 = \bar{c}_2^{(2,0)} = \sum_{k=1}^2 (\bar{a}_k^{(2,0)} + \bar{b}_k^{(2,0)} y) e^{s_k y}$$

$$s_1 = N, s_2 = -N$$

The matrix equation resulting from the boundary conditions is

$$\mathbf{X}_{ij} \mathbf{Y}_j^{(2,0)} = \mathbf{Z}_i^{(2,0)}$$

where the unknown vector $\mathbf{Y}_j \equiv (a_1^{(2,0)}, a_2^{(2,0)}, b_1^{(2,0)}, b_2^{(2,0)}, \bar{a}_1^{(2,0)}, \bar{a}_2^{(2,0)}, \bar{b}_1^{(2,0)}, \bar{b}_2^{(2,0)})$
 $\mathbf{Z}_i^{(2,0)} = \mathbf{g}_i^{(2,0)}$ and \mathbf{X}_{ij} is the same as for the (1,0) case [equation (XI.D.6)] except that $n=2$.

XII.F. Inversion of the matrix equation gives $\mathbf{Y}_j^{(2,0)}$ which yields $c_2^{(2,0)}$ and $\bar{c}_2^{(2,0)}$ directly. For $n=2$, equations (XII.B.4,5) give $c_1^{(2,0)}, \bar{c}_1^{(2,0)}, g_{ij}^{(2,0)}$ immediately. Since $c_2^{(2,0)} = \bar{c}_2^{(2,0)} = 0$ for $n=1, 3, 4, 5, \dots$, these relations imply that $c_1^{(2,0)} = \bar{c}_1^{(2,0)} = g_{ij}^{(2,0)} = 0$ for $n=1, 3, 4, 5, \dots$.

The zero mode, however, must be considered separately because equations (XII.B.4) are not applicable when $n=0$. The pressure-independent (2,0) system (section XII.B.) with no terms dependent on x and t gives (neglecting inertia terms): ($n=0$)

$$0 = g_{12}'' , \quad 0 = \bar{c}_1'''$$

$$c_2' = 0 , \quad \bar{c}_2' = 0$$

$$g_{12} + T \gamma_{12} = c_1' , \quad g_{11} + g_{22} = -T(\gamma_{11} + \gamma_{22})$$

$$g_{11} = -T \gamma_{11} , \quad g_{22} = -g_{11}$$

$$g_{12} = b_1 , \quad g_{12}' = 0 \quad \text{at } y=0$$

$$g_{12} = k \bar{c}_1' + b_2 , \quad g_{12}' = k \bar{c}_1'' \quad \text{at } y=-h$$

$$c_1 - \bar{c}_1 = b_{3_1}, \quad c_2 - \bar{c}_2 = b_{3_2} \quad \text{at } y = -h$$

$$\bar{c}_1 = b_{4_1}, \quad \bar{c}_2 = b_{4_2} \quad \text{at } y = -1$$

Solving the above yields the zero mode solution:

$$c_1^{(2,0)}(o, y) = T \int_{-h}^y \gamma_{12}(o, y) dy + [b_{3_1} + b_{4_1}]_{n=0}$$

$$c_2^{(2,0)}(o, y) = \bar{c}_2^{(2,0)}(o, y) = 0 \quad (\text{XII. F. 1})$$

$$\bar{c}_1^{(2,0)}(o, y) = \frac{1}{2\alpha} \left\{ \alpha^2 \rho^2 + \bar{c}_2^{(1,0)} \right\}_{y=-1} = \text{constant}$$

$$\{b_{3_1} + b_{4_1}\}_{n=0} = \frac{1}{2\alpha} \left\{ \alpha^2 \rho^2 + \bar{c}_2^{(1,0)} \right\}_{y=-1} + \bar{c}_2^{(1,0)} \left(\bar{c}_2^{(1,0)} - c_2^{(1,0)} \right)_{y=-h}$$

The stress Fourier coefficients are:

$$\begin{aligned} g_{12}^{(2,0)}(o, y) &= \bar{g}_{ij}^{(2,0)}(o, y) = 0 \\ g_{11}^{(2,0)}(o, y) &= -T \gamma_{11} \\ g_{22}^{(2,0)}(o, y) &= -g_{11}^{(2,0)}(o, y) \end{aligned} \quad (\text{XII. F. 2})$$

XII. G. The second order free surface and interface shapes can be found from equations (IX. E. 3):

$$u_2^{(2,0)} + \gamma^{(1,0)} u_{z,y}^{(1,0)} = \gamma_{,t}^{(2,0)} + u_1^{(1,0)} \gamma_{,x}^{(1,0)} \quad \text{at } y=0$$

$$\bar{u}_2^{(2,0)} + \bar{\gamma}^{(1,0)} \bar{u}_{z,y}^{(1,0)} = \bar{\gamma}_{,t}^{(2,0)} + \bar{u}_1^{(1,0)} \bar{\gamma}_{,x}^{(1,0)} \quad \text{at } y=-h$$

For $\gamma^{(2,0)}$, the constant of integration is found from the equation

(XI. F. 2).

$$\int_0^{2\pi} \gamma^{(2,0)} d\phi = \alpha \beta \pi$$

At $y=0$ we have

$$\begin{aligned} \gamma_{,t}^{(2,0)} &= u_2^{(2,0)} + \gamma^{(1,0)} u_{z,y}^{(1,0)} - u_1^{(1,0)} \gamma_{,x}^{(1,0)} \\ &= \operatorname{Re} \{ c_2^{(2,0)} e^{2i\phi} \} + \operatorname{Re} \{ -i c_2^{(1,0)} e^{i\phi} \} \operatorname{Re} \{ c_2^{(1,0)} e^{i\phi} \} + \\ &\quad + \operatorname{Re} \{ c_1^{(1,0)} e^{i\phi} \} \operatorname{Re} \{ -\alpha c_2^{(1,0)} e^{i\phi} \} \end{aligned}$$

Using the product formula (XII. C. 1) $ab = \frac{1}{2} \operatorname{Re} \{ AB^* \} + \frac{1}{2} \operatorname{Re} \{ AB e^{2i\phi} \}$

we find

$$\gamma_{,t}^{(2,0)} = \operatorname{Re} \{ (c_2^{(2,0)} - i c_2^{(1,0)} c_2^{(1,0)}) e^{2i\phi} \} \quad \text{at } y=0$$

Note that the $n=0$ modes have cancelled out so that only the $n=2$ mode appears above.

Integration and the use of condition (XI. F. 2) gives

$$\eta^{(2,0)} = \operatorname{Re} \left\{ \frac{1}{2i} \left(c_2^{(2,0)} - i c_2^{(1,0)} c_2^{(1,0)} \right) e^{2i\phi} \right\} + \frac{\alpha\beta}{2} \quad \text{at } y=0$$

Similarly,

$$\bar{\eta}^{(2,0)} = \operatorname{Re} \left\{ \frac{1}{2i} \left(\bar{c}_2^{(2,0)} - i \bar{c}_2^{(1,0)} \bar{c}_2^{(1,0)} \right) e^{2i\phi} \right\} + \frac{\alpha\beta}{2} \quad \text{at } y=-h$$

XII. H. The pressures and total stresses can be obtained from the original equations containing the pressure terms, i.e. equations

(IX. E.1). Consider the $n=0$ and $n=2$ cases separately:

$$P^{(2,0)} = \sum_{n=0}^{\infty} \operatorname{Re} \left\{ \gamma^{(2,0)} c_n(y) e^{in\phi} \right\}$$

The inertia-free momentum equation for the visco-elastic fluid is

$$0 = -P_{,i}^{(2,0)} + T_{,j,j}^{(2,0)}$$

$$C_1: 0 = -iN P^{(2,0)} + iN q_{11}^{(2,0)} + q_{12}^{(2,0)}$$

$$C_2: 0 = -P^{(2,0)} + iN q_{12}^{(2,0)} + q_{22}^{(2,0)}$$

$$n=0 : \quad \gamma^{(2,0)} = q_{22}^{(2,0)}$$

$$\gamma^{(2,0)}(0,y) = q_{22}^{(2,0)}(0,y) + \text{const}$$

$$n=2: \quad \tau^{(2,0)}(r_2, y) = g_{11}^{(2,0)}(r_2, y) + \frac{1}{N} g_{12}^{(2,0)}(r_2, y)$$

The constant can be determined from the boundary condition at $y=0$

[see equation (IX.E.2)]:

$$\begin{aligned} t_{22}^{(2,0)} &= p^{(2,0)} + C, \quad , \quad g_{22}^{(2,0)}(0, y) = -p^{(2,0)}(0, y) + \Psi_1(0) \\ \therefore \text{const} &= -\Psi_1(0) \end{aligned}$$

Recall that $\Psi_1(0) = 0$ (Appendix A) so that $\text{const} = 0$ and

$$\begin{aligned} p^{(2,0)}(0, y) &= g_{22}^{(2,0)}(0, y). \quad \text{The total stress is } S_{ij}^{(2,0)} = -p^{(2,0)} \delta_{ij} + t_{ij}^{(2,0)} \\ \text{where } S_{ij}^{(2,0)} &= \sum_{n=0}^{\infty} \operatorname{Re} \{ A_{ij}^{(n)} e^{in\phi} \}. \quad \text{The coefficients are:} \end{aligned}$$

$$\begin{aligned} A_{12}^{(2,0)} &= g_{12}^{(2,0)}, \quad A_{11}^{(2,0)} = -p^{(2,0)} + g_{11}^{(2,0)} \\ A_{22}^{(2,0)} &= -p^{(2,0)} + g_{22}^{(2,0)} \end{aligned}$$

$$\begin{aligned} n=0: \quad A_{12}^{(2,0)} &= g_{12}^{(2,0)} = 0 \\ A_{11}^{(2,0)} &= -g_{22}^{(2,0)} + g_{11}^{(2,0)} = 2g_{11}^{(2,0)}(0, y) \\ A_{22}^{(2,0)} &= -g_{22}^{(2,0)} + g_{22}^{(2,0)} = 0 \end{aligned}$$

$$n_{22} : A_{12}^{(2,0)} = g_{12}^{(2,0)}$$

$$A_{11}^{(2,0)} = -g_{11}^{(2,0)} - \frac{1}{iN} g_{12}^{(2,0)} + g_{11}^{(2,0)} = -\frac{1}{iN} g_{12}^{(2,0)}$$

$$A_{22}^{(2,0)} = -g_{11}^{(2,0)} - \frac{1}{iN} g_{12}^{(2,0)} + g_{22}^{(2,0)} = -2g_{11}^{(2,0)} - \frac{1}{iN} g_{12}^{(2,0)}$$

$$\therefore P^{(2,0)} = \operatorname{Re} \{ \tau^{(2,0)}(0, y) + \tau^{(2,0)}(z, y) e^{2iz\phi} \}$$

$$S_{ij}^{(2,0)} = \operatorname{Re} \{ A_{ij}^{(2,0)}(0, y) + A_{ij}^{(2,0)}(z, y) e^{2iz\phi} \}$$

$$\tau^{(2,0)}(0, y) = g_{22}^{(2,0)}(0, y)$$

$$\tau^{(2,0)}(z, y) = g_{11}^{(2,0)}(z, y) + \frac{1}{iN} g_{12}^{(2,0)}(z, y)$$

$$A_{12}^{(2,0)}(0, y) = A_{22}^{(2,0)}(0, y) = 0, \quad A_{11}^{(2,0)}(0, y) = z g_{11}^{(2,0)}(0, y)$$

$$A_{12}^{(2,0)}(z, y) = g_{12}^{(2,0)}(z, y), \quad A_{11}^{(2,0)}(z, y) = -\frac{1}{iN} g_{12}^{(2,0)}(z, y)$$

$$A_{22}^{(2,0)}(z, y) = -2g_{11}^{(2,0)}(z, y) - \frac{1}{iN} g_{12}^{(2,0)}(z, y)$$

The same types of relations hold for the Newtonian fluid sublayer, where the extra stress Fourier coefficients $\bar{g}_{ij}^{(2,0)}$ are known in terms of $\bar{c}_2^{(2,0)}$.

XII. I. The entire (2, 0) solution can now be written. The unknown functions are:

$$u_i^{(2,0)} = \operatorname{Re} \{ c_i^{(2,0)} r_0(y) + c_i^{(2,0)}(2,y) e^{2i\phi} \}$$

$$t_{ij}^{(2,0)} = \operatorname{Re} \{ g_{ij}^{(2,0)} r_0(y) + g_{ij}^{(2,0)}(2,y) e^{2i\phi} \}$$

$$P^{(2,0)} = \operatorname{Re} \{ \gamma^{(2,0)} r_0(y) + \gamma^{(2,0)}(2,y) e^{2i\phi} \}$$

$$S_{ij}^{(2,0)} = \operatorname{Re} \{ \lambda_{ij}^{(2,0)} r_0(y) + \lambda_{ij}^{(2,0)}(2,y) e^{2i\phi} \}$$

The same forms hold for the barred (sublayer) functions.

The $n=0$ and $n=2$ modes are considered separately.

XII. I. 1. The $n=0$ mode. (* denotes complex conjugate)

$$c_1^{(2,0)}(r_0, y) = T \int_{-h}^y \gamma_{12}(0, y) dy + \{ b_{31} + b_{41} \}_{n=0}$$

$$\bar{c}_1^{(2,0)}(r_0, y) = \frac{1}{2} \alpha \left\{ \omega^2 \beta^2 + \left. \bar{c}_2^{(1,0)} \right|_y \right\}_{y=-1}$$

$$c_2^{(2,0)}(r_0, y) = \bar{c}_2^{(2,0)}(r_0, y) = 0$$

$$\{b_{31} + b_{41}\}_{n=0} = \frac{1}{2\alpha} \left\{ \alpha^2 \beta^2 + \bar{c}_2^{(1,0)} \Big|_{y=-1} + \bar{c}_2^{(1,0)} \left(\bar{c}_2^{(1,0)*} - c_2^{(1,0)*} \right) \Big|_{y=-h} \right\}$$

$$g_{12}^{(2,0)}(0,y) = \bar{g}_{12}^{(2,0)}(0,y) = 0$$

$$g_{11}^{(2,0)}(0,y) = - g_{22}^{(2,0)}(0,y) = -T \gamma_{11} \Big|_{n=0}$$

$$\gamma_{11} \Big|_{n=0} = \frac{1}{2} \left\{ c_2^{(1,0)*} g_{11}^{(1,0)} + c_2^{(1,0)*} g_{11}^{(1,0)} - 2 g_{12}^{(1,0)*} w^{(1,0)} \right\}$$

$$p^{(2,0)}(0,y) = g_{22}^{(2,0)}(0,y)$$

$$\mu_{12}^{(2,0)}(0,y) = \mu_{22}^{(2,0)}(0,y) = 0$$

$$\mu_{11}^{(2,0)}(0,y) = 2 g_{11}^{(2,0)}(0,y)$$

XII. I. 2. The $n=2$ mode

The Fourier coefficients $c_2^{(2,0)}$ and $\bar{c}_2^{(2,0)}$ are found from the solution of the matrix equation (see section XII. E.):

$$\partial C_{ij} \sum_j S_j^{(2,0)} = Y_i^{(2,0)} \quad i = 1, 2, \dots 8$$

where $Y_i^{(2,0)} = y_i$, $S_j^{(2,0)} \equiv (a_1^{(2,0)}, a_2^{(2,0)}, b_1^{(2,0)}, b_2^{(2,0)}, \bar{a}_1^{(2,0)}, \bar{a}_2^{(2,0)}, \bar{b}_1^{(2,0)}, \bar{b}_2^{(2,0)})$

$$y_1 = -\frac{2i}{Q} N b_1 - i N T \delta_{12} \quad \text{at } y=0, \quad y_5 = -i N b_{31}, \quad y_6 = b_{32} \quad \text{at } y=-h$$

$$y_2 = 2N^2 T \gamma_{11} - i N T \gamma'_{12} - \frac{2N^2}{Q} \psi_i \quad " \quad , \quad y_7 = -i N b_{41}, \quad y_8 = b_{42} \quad \text{at } y=-l$$

$$y_3 = -\frac{2iN}{Q} b_2 - i N T \gamma_{12} \quad \text{at } y=-h, \quad Q = \frac{1}{1+2iT}$$

$$y_4 = 2N^2 T \gamma_{11} - i N T \gamma'_{12} - \frac{2N^2}{Q} \psi_i \quad " \quad , \quad N = 2\alpha$$

$$\gamma_{11} \Big|_{n=2} = \frac{1}{2} \left\{ -c_2^{(1,0)} q_{11}^{(1,0)} + c_2^{(1,0)} q_{11}^{(1,0)} - 2 q_{12}^{(1,0)} w^{(1,0)} \right\}$$

$$\gamma_{12} \Big|_{n=2} = \frac{1}{2} \left\{ -c_2^{(1,0)} q_{12}^{(1,0)} + c_2^{(1,0)} q_{12}^{(1,0)} + 2 q_{11}^{(1,0)} w^{(1,0)} \right\}$$

$$b_1 \Big|_{n=2} = i c_2^{(1,0)} q_{12}^{(1,0)} \quad \text{at } y=0$$

$$b_2 \Big|_{n=2} = i \bar{c}_2^{(1,0)} (q_{12}^{(1,0)} - \bar{q}_{12}^{(1,0)}) \quad \text{at } y=-h$$

$$b_{31} \Big|_{n=2} = \frac{1}{2\alpha} \bar{c}_2^{(1,0)} (\bar{c}_2^{(1,0)} - c_2^{(1,0)}) \quad "$$

$$b_{32} \Big|_{n=2} = b_{42} \Big|_{n=2} = \psi_i \Big|_{n=2} = 0$$

$$b_{41} = \frac{1}{2\alpha} (\alpha^2 \rho^2 - \bar{c}_2^{(1,0)}) \quad \text{at } y=-l$$

The matrix \mathbf{X}_{ij} is found in section XI.D. where $n=2$.

The form of the solution is (section XII.E.) $S_{1,2} = \pm 2\alpha$

$$c_2^{(2,0)}(z, y) = \sum_{k=1}^2 (a_k^{(2,0)} + b_k^{(2,0)}y) e^{s_k y}, \quad \bar{c}_2^{(2,0)}(z, y) = \sum_{k=1}^2 (\bar{a}_k^{(2,0)} + \bar{b}_k^{(2,0)}y) e^{s_k y}$$

The Fourier coefficients for the other unknowns are given in terms of $c_2^{(2,0)}$, $\bar{c}_2^{(2,0)}$ and γ_{ij} as follows:

$$c_1^{(2,0)}(z, y) = \frac{i}{N} c_2^{(2,0)}(z, y)$$

$$\gamma_{11}^{(2,0)}(z, y) = -\gamma_{22}^{(2,0)}(z, y) = -\frac{Q}{2} \left\{ z \bar{c}_2^{(2,0)}(z, y) + T \gamma_{11} \right\}_{n=2}$$

$$\gamma_{12}^{(2,0)}(z, y) = \frac{Q}{2} \left\{ \frac{i}{N} \bar{c}_2^{(2,0)}(z, y) + iN c_2^{(2,0)}(z, y) - T \gamma_{12} \right\}_{n=2}$$

$$\gamma^{(2,0)}(z, y) = \gamma_{11}^{(2,0)}(z, y) + \frac{1}{iN} \gamma_{12}^{(2,0)}(z, y)$$

$$a_{12}^{(2,0)}(z, y) = \gamma_{12}^{(2,0)}(z, y)$$

$$a_{11}^{(2,0)}(z, y) = -\frac{1}{iN} \gamma_{12}^{(2,0)}(z, y)$$

$$a_{22}^{(2,0)}(z, y) = -2\gamma_{11}^{(2,0)}(z, y) - \frac{1}{iN} \gamma_{12}^{(2,0)}(z, y)$$

$$Q = \frac{1}{1+2iT}$$

$$N = 2\alpha$$

$$\begin{aligned}\bar{c}_1^{(2,0)}(z,y) &= \frac{i}{N} \bar{c}_2'(2,0)(z,y) \\ \bar{g}_{11}^{(2,0)}(z,y) &= -\bar{g}_{22}^{(2,0)}(z,y) = -2k \bar{c}_2'(2,0)(z,y) \\ \bar{g}_{12}^{(2,0)}(z,y) &= \frac{ik}{N} \{ \bar{c}_2''(2,0)(z,y) + N^2 \bar{c}_2^{(2,0)}(z,y) \} \\ \bar{p}^{(2,0)}(z,y) &= \bar{g}_{11}^{(2,0)}(z,y) + \frac{1}{iN} \bar{g}_{12}^{(2,0)}(z,y) \\ \bar{A}_{12}^{(2,0)}(z,y) &= \bar{g}_{12}^{(2,0)}(z,y) \\ \bar{A}_{11}^{(2,0)}(z,y) &= -\frac{1}{iN} \bar{g}_{12}^{(2,0)}(z,y) \\ \bar{A}_{22}^{(2,0)}(z,y) &= -2 \bar{g}_{11}^{(2,0)}(z,y) - \frac{1}{iN} \bar{g}_{12}^{(2,0)}(z,y)\end{aligned}$$

The free surface and interface shapes are (section XII. G.):

$$\begin{aligned}\eta^{(2,0)} &= \operatorname{Re} \left\{ \frac{1}{2i} (c_2^{(2,0)}(z,y) - i c_2^{(1,0)} \bar{c}_2'(1,0)) e^{2iz\phi} \right\} + \frac{\alpha\beta}{2} \quad \text{at } y=0 \\ \hat{\eta}^{(2,0)} &= \operatorname{Re} \left\{ \frac{1}{2i} (\bar{c}_2^{(2,0)}(z,y) - i \bar{c}_2^{(1,0)} \bar{c}_2'(1,0)) e^{2iz\phi} \right\} + \frac{\alpha\beta}{2} \quad \text{at } y=-h\end{aligned}$$

XIII. SOLUTION OF THE (0,1) SYSTEM

The main aim of this section is to obtain the velocity fields $u_i^{(0,1)}$ and $\bar{u}_i^{(0,1)}$ so that the effect of gravitational acceleration on the fluid material point trajectories and (especially) the mean drift can be calculated. Recall that this effect is negligible (section IX.B.) in "normal" mucous flow. Nevertheless, for a vertical trachea with pumping direction opposite to gravity, a "critical" value of the total fluid depth can be found for which the drift of a particle at the free surface is just zero. In some sense this defines a "pathological limit".

The (0,1) equations of section IX.F. are rewritten here for convenience.

$$A u_{i,t}^{(0,1)} = -P_{,i}^{(0,1)} + t_{ij,j}^{(0,1)} + g_i$$

$$A \bar{u}_{i,t}^{(0,1)} = -\bar{P}_{,i}^{(0,1)} + \bar{t}_{ij,j}^{(0,1)} + g_i$$

$$T t_{ij,t}^{(0,1)} = -t_{ij}^{(0,1)} + 2 d_{ij}^{(0,1)}$$

$$\bar{t}_{ij}^{(0,1)} = 2 k \sigma_{ij}^{(0,1)}$$

$$u_{x,\kappa}^{(0,1)} = \bar{u}_{x,\kappa}^{(0,1)} = 0$$

$$t_{12}^{(0,1)} = 0, \quad t_{22}^{(0,1)} = P_{,2}^{(0,1)} \quad \text{at } y=0, \quad u_i^{(0,1)} = \bar{u}_i^{(0,1)} \quad \text{at } y=-h$$

$$\Delta t_{12}^{(0,1)} = 0, \quad \Delta t_{22}^{(0,1)} = \Delta P_{,2}^{(0,1)} \quad \text{at } y=-h, \quad \bar{u}_i^{(0,1)} = 0 \quad \text{at } y=-l$$

XIII.A. Pressure terms can be eliminated from the equations and boundary conditions giving the vorticity equations, independent of gravity because it too has been suppressed by differentiation. Gravity does appear, however, in the second boundary condition, although only the \bar{e}_1 component enters. Dropping superscripts:

$$A\{u_{1,y} - u_{2,x}\} = t_{1j,jy} - t_{2j,jx}$$

$$\frac{A}{k}\{\bar{u}_{1,y} - \bar{u}_{2,x}\} = \nabla^2 \{\bar{u}_{1,y} - \bar{u}_{2,x}\}$$

$$u_{k,k} = \bar{u}_{k,k} = 0$$

$$Tt_{ij,t} = -t_{ij} + u_{i,j} + u_{j,i}$$

$$t_{12} = 0, \quad A u_{1,t} = t_{1j,j} - t_{22,x} + g_1 \quad \text{at } y=0$$

$$t_{12} = k\{\bar{u}_{1,y} + \bar{u}_{2,x}\} \quad \text{at } y=-h$$

$$A u_{1,t} + t_{22,x} - t_{1j,j} = A \bar{u}_{1,t} - k \nabla^2 \bar{u}_1 + 2k \bar{u}_{2,xy} \quad \text{at } y=-h$$

$$u_i = \bar{u}_i \quad \text{at } y=-h$$

$$\bar{u}_i = 0 \quad \text{at } y=-l$$

The omission of g_2 in the equations implies that only the streamwise component of gravity, g_1 , affects the flow to this approximation.

XIII.B. All unknown functions are expanded in Fourier series:

$$u_i^{(0,1)} = \sum_{n=0}^{\infty} \operatorname{Re} \{ c_i^{(0,1)} e^{in\phi} \}$$

$$\bar{u}_i^{(0,1)} = \sum_{n=0}^{\infty} \operatorname{Re} \{ \bar{c}_i^{(0,1)} e^{in\phi} \}$$

$$t_{ij}^{(0,1)} = \sum_{n=0}^{\infty} \operatorname{Re} \{ g_{ij}^{(0,1)} e^{in\phi} \}$$

Gravity is similarly expanded: $g_1 = \sum_{n=0}^{\infty} \operatorname{Re} \{ \lambda_j e^{in\phi} \}$

where

$$\lambda_j = \lambda_{jn} = g_1 \quad n=0$$

$$\lambda_j = 0 \quad n=1, 2, 3, 4, \dots$$

The equations for the Fourier coefficients are the same as that of the (1,0) system (section XI.A.) except for the second boundary condition, which now contains a gravitational term.

$$A u_{1,z} = t_{1j,j} - t_{2z,z} + g_1$$

$$A i n c_1 = 2iN g_u + g'_{1z} + \lambda_j$$

Using the relationships giving c_1 , g_{1j} in terms of c_2 , we obtain

$$c''_2 - \left\{ 3N^2 + \frac{2AiN}{Q} \right\} c'_2 = \frac{2iN}{Q} \lambda_j$$

The full set of equations in terms of c_2 and \bar{c}_2 alone are thus:

$$\begin{aligned} c''_2 - 2(N^2 + \frac{inA}{Q}) c'_2 + N^2(N^2 + \frac{2inA}{Q}) c_2 &= 0 \\ \bar{c}''_2 - 2(N^2 + \frac{inA}{2K}) \bar{c}'_2 + N^2(N^2 + \frac{inA}{K}) \bar{c}_2 &= 0 \end{aligned} \quad (\text{XIII.B.1})$$

$$c''_2 + N^2 c_2 = 0 \quad \text{at } y=0$$

$$c'''_2 - (3N^2 + 2\frac{A_{1n}}{Q}) c'_2 = \frac{2iN}{Q} \bar{y} = 0 \quad n=0,1,2,3,\dots \quad \text{at } y=0$$

$$c''_2 + N^2 c_2 - \frac{2K}{Q} (\bar{c}''_2 + N^2 \bar{c}_2) = 0 \quad \text{at } y=-h$$

$$c'''_2 - (3N^2 + 2\frac{A_{1n}}{Q}) c'_2 - \frac{2K}{Q} \{ \bar{c}'''_2 - (3N^2 + A_{1n}) \bar{c}'_2 \} = 0 \quad \text{at } y=-h$$

$$c'_2 - \bar{c}'_2 = 0, \quad c_2 - \bar{c}_2 = 0 \quad \text{at } y=-h$$

(XIII. B. 2)

$$\bar{c}'_2 = 0, \quad \bar{c}_2 = 0 \quad \text{at } y=-1$$

$$N \equiv n\omega, \quad Q \equiv \frac{1}{1+i\pi T}$$

As in all previous cases, these fourth order differential equations (XIII.B.1) have solutions of the form

$$c^{(0,1)}_2 = \sum_{k=1}^4 a_k e^{A_k y}, \quad \bar{c}^{(0,1)}_2 = \sum_{k=1}^4 \bar{a}_k e^{A_k y}$$

which give the matrix equation $\mathcal{M}_{ij} \xi_j = \xi_i \quad i=1,2,\dots,8$

In the present instance, however, $\xi_i = 0 \quad \forall n, i=1,2,\dots,8$

(recall that ξ_i was non-zero for $n=1$ in (1,0) and for $n=0,2$ in (2,0)). Since $\det \mathcal{M}_{ij} \neq 0$ then $\xi_j = 0$, so that

$$c_i^{(0,1)} = \bar{c}_i^{(0,1)} = q_{ij}^{(0,1)} = 0 \quad \text{for } n=1,2,3,\dots$$

XIII.C. To find the zero mode solution, the system in section XIII.A. is used, where all functions are dependent on y alone so that $f_{,x} = f_{,t} = 0$ for every f .

momentum $t_{12}'' = 0$, $\bar{u}_1''' = 0$

continuity $u_2' = 0$, $\bar{u}_2' = 0$

consitiutive $t_{12} = u_1'$

boundary conditions $t_{12}(0) = 0$, $t_{12}'(0) + g_1 = 0$

$t_{12}(-h) = k \bar{u}_1'(-h)$, $t_{12}'(-h) = k \bar{u}_1'''(-h)$

$u_1(-h) = \bar{u}_1(-h)$, $\bar{u}_1(-1) = 0$

It follows at once that $u_2 = \bar{u}_2 = 0$.

The equations for u_1 and \bar{u}_1 are $u_1''' = \bar{u}_1''' = 0$ having solutions of the form

$$u_1 = ay^2 + by + c, \quad \bar{u}_1 = \bar{a}y^2 + \bar{b}y + \bar{c}$$

The six remaining boundary conditions determine the six constants, giving the result:

$$u_1^{(0,1)} = -\frac{g_1}{2} \left\{ y^2 + \frac{1}{k} [h^2(1-k) - 1] \right\}$$

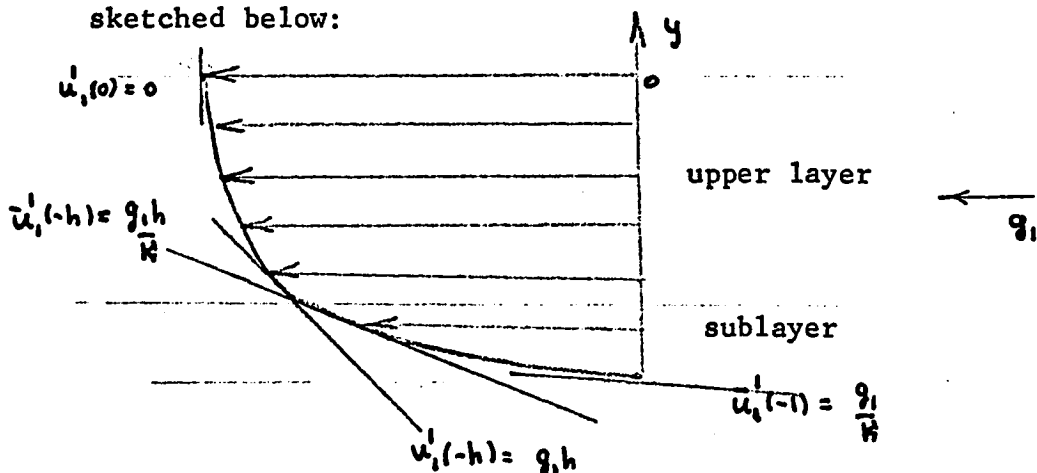
$$\bar{u}_1^{(0,1)} = -\frac{g_1}{2k} [y^2 - 1]$$

$$u_2^{(0,1)} = \bar{u}_2^{(0,1)} = 0$$

(XIII. C)

For negative g_1 , the diagram of the velocity profile is

sketched below:



Since the analytical solution of this system is rather simple, the following inferences can be made:

1. $u_1^{(0,1)}$ and $\bar{u}_1^{(0,1)}$ are directly proportional to g_1 , so that the maximum magnitude of the velocities occurs when the gravity vector is parallel to the direction of the travelling wave geometry.
2. The profiles are parabolic.
3. The bracketed quantities $\{ \}$ $\leq 0 \forall y$ so that u_1 and \bar{u}_1 are always directed along g_1 .

4. The velocity field is independent of relaxation time but dependent on the viscosity ratio (i.e. no elastic effect).
5. The maximum magnitude of velocity occurs at $y=0$ because $u_1'(0)=0$. Hence, the maximum mean material drift due to gravity occurs at the free surface.
6. The magnitude of the velocities (and drift) increases as the ratio of sublayer to mucous viscosities decreases. Thus,

$$\lim_{K \rightarrow 0} u_1^{(0,1)} \rightarrow \infty , \quad \lim_{K \rightarrow 0} \bar{u}_1^{(0,1)} \rightarrow \infty$$

XIII.D. The free surface and interface shapes can be determined by integration of the equations

$$u_2^{(0,1)} = \gamma_{,t}^{(0,1)} \text{ at } y=0 , \quad \bar{u}_2^{(0,1)} = \bar{\gamma}_{,t}^{(0,1)} \text{ at } y=-h$$

subject to condition (XI.F.3):

$$\int_0^{2\pi} \gamma^{(0,1)} d\phi = \int_0^{2\pi} \bar{\gamma}^{(0,1)} d\phi = 0$$

Since $u_2^{(0,1)} = \bar{u}_2^{(0,1)} = 0$, we find

$$\boxed{\begin{aligned} \gamma^{(0,1)} &= 0 \\ \bar{\gamma}^{(0,1)} &= 0 \end{aligned}}$$

XIII.E. As said previously (section IX.B.) in order to utilize gravitational effects, it is necessary to define a pathological flow situation. Suppose that the gravity vector acts parallel to the wall so that g_1 is a maximum. If $\beta > 0$ and $|\alpha\beta| \rightarrow 1$ the wall particle moves clockwise tending to induce a net positive material drift (see section VI.C.7.).

— — — — → Drift due to wall point path

(cilia)



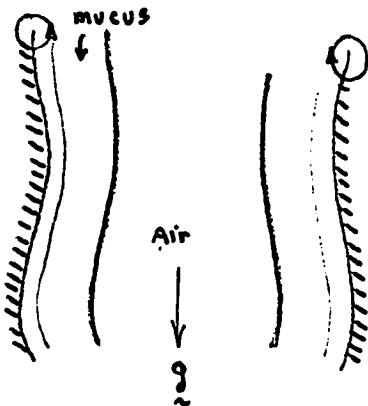
If $g = -1e_1$, then gravity tends to decrease the drift:

g ←

← — — — Drift due to gravity



In a real physiological situation, the above may correspond to the flow in the trachea of an upright human in which case a longitudinal cross section (not to scale) would look like the sketch:



Gravitational effects oppose ciliary effects.

The cyclic material drift of fluid (section XIV) turns out to be of the form

$$\text{drift} = 2\pi \{ A^{(2,0)} \epsilon^2 + A^{(0,1)} B \}$$

$$\text{where } A^{(0,1)}(y) = -\frac{g_1}{2} \left\{ y^2 + \frac{1}{k} [h^2(1-k) - 1] \right\}$$

and $A^{(2,0)}(y)$ is the drift coefficient due to wall motion.

We shall define a "pathological" muco-ciliary flow as one in which the cyclic drift of a material particle at the free surface is zero, with gravity and ciliary effects in opposition. The total depth of the fluids can be varied such that the following relationship holds:

$\text{net drift at the free surface} = A^{(2,0)}(0) \epsilon^2 + A^{(0,1)}(0) B = 0$

$$\text{where } A^{(2,0)} = A^{(2,0)}(\mu, \bar{\mu}, d, \omega, G, \lambda, \beta, h) ,$$

$$A^{(0,1)} = A^{(0,1)}(\mu, \bar{\mu}, h) , \quad B = \frac{\rho g d}{\mu \omega}$$

From this equation, it is clear that some of the factors tending to increase the influence of gravity may be

- a. increasing total depth, d ($B \uparrow$ and $\epsilon \downarrow$)
- b. decreasing mucous viscosity ($B \uparrow$).
- c. decreasing beating frequency ($B \uparrow$)
- d. decreasing sublayer viscosity ($A^{10} \downarrow$)

Since there are no quantitative physiological data from which to pick values of viscosity and elasticity of the mucus in diseases where gravity plays an important role, we are forced to choose arbitrary values based on the idea that when the mucus is "watery" and "plentiful," gravitational forces can be important (Ewert).

We shall suppose that the (metachronal) wavelength of the wall, the path of a wall material particle, and the frequency of the ciliary beating remain as in normal flow. An interesting question to ask is whether a realistic "critical" layer thickness will result if we make plausible guesses at rheological properties of "watery" mucus. For maximum simplicity consistent with the Ewert description, we assume that the mucus is also a Newtonian fluid, and that it has the same viscosity as the serous fluid. Therefore, we have a single Newtonian fluid, and we choose its viscosity to be 1 poise (a factor of 10^3 less

viscous than "normal" mucus, but 10^2 times more viscous than water). In this case, the constants are

$$\lambda = 30 \text{ micron}$$

$$\omega = 100 \text{ rad/sec}$$

$$\mu = 1 \text{ poise} = \bar{\mu}, \quad \gamma_R = 0 \quad (k=1, T=0)$$

$$\Theta = 1 \text{ microns}, \beta = 1.5$$

A critical depth for which the drift of a fluid particle on the free surface is zero turns out to be:

$$d_{\text{critical}} \approx 42 \text{ microns}$$

This is much smaller than the radius of the trachea, so it is at least physiologically possible. We conclude that in some pathological conditions gravity effects may be important.

XIV. PARTICLE TRAJECTORIES AND CYCLIC DRIFT

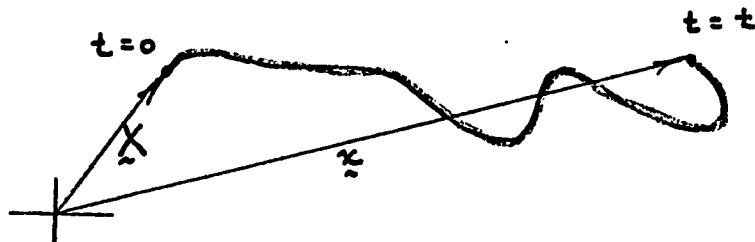
XIV.A. In this section, the trajectory and cyclic drift of fluid material points will be obtained. The point transformation connecting the material (Lagrangian) coordinate system $\{\underline{X}\}$ to the spatial (Eulerian) coordinate system $\{\underline{x}\}$ can be symbolized as

$$x_i = x_i(\underline{X}, t)$$

where the initial position of the particle (the material coordinate) is

$$X_i = x_i(\underline{X}_0)$$

This identifies that particle of fluid throughout the motion. Thus, a particle path or trajectory is obtained by the curve $x_i(\underline{X}, t)$, holding X_i fixed as t varies.



For small enough t , the motion can be written as the expansion

$$x_i = X_i + \epsilon x_i^{(1,0)} + \epsilon^2 x_i^{(2,0)} + \mathcal{B} x_i^{(0,1)} + \dots$$

and we shall assume the above is valid for times smaller than one period.

Velocity is defined in the Lagrangian frame as

$$u_{L_i}(x, t) = \frac{\partial x_i(x, t)}{\partial t}$$

and the transformation between Eulerian $u_i(x, t)$ and

Lagrangian $u_{L_i}(x, t)$ forms of velocity is

$$u_i(x, t) \xrightarrow{x(x, t)} u_{L_i}(x, t)$$

which gives the functions $x_i^{(k,m)} = x_i^{(k,m)}(x, t)$ via a Taylor expansion about $\epsilon = B = 0$. The resulting equations are valid in both fluids, with substitution of the appropriate velocity fields:

$$u_i = \epsilon u_i^{(1,0)}(x, t) + \epsilon^2 u_i^{(2,0)}(x, t) + B u_i^{(0,1)}(x, t) + \dots$$

$$x_i = X_i + \epsilon x_i^{(1,0)} + \epsilon^2 x_i^{(2,0)} + B x_i^{(0,1)} + \dots$$

$$F_i^{(k,m)} = A_i^{(k,m)} + \sum_{n=1}^{\infty} R_n \{ B_i^{(k,m)} e^{in\Phi'} \}$$

$$x_i^{(k,m)} = \int_0^t F_i^{(k,m)}(x, t') dt'$$

$$F_i^{(1,0)} \equiv u_i^{(1,0)}(x, t'), \quad F_i^{(0,1)} \equiv u_i^{(0,1)}(x, t')$$

$$F_i^{(2,0)} \equiv \int_0^{t'} u_k^{(1,0)}(x, t'') dt'' \frac{\partial u_i^{(1,0)}}{\partial x_k}(x, t') + u_i^{(2,0)}(x, t')$$

$$A_i^{(k,m)} = A_i^{(k,m)}(\gamma), \quad B_i^{(k,m)} = B_i^{(k,m)}(n, x)$$

$$\Phi' \equiv \omega x + t'$$

Thus from the Eulerian velocity field, we get $F_i^{(k,m)}$ which gives $x_i^{(k,m)}$ by direct integration. Note that the zero part of $F_i^{(k,m)}$ gives a linear dependence on t in the trajectory expansion, but that it is still valid for times less than one period.

XIV. B. The $x_i^{(1,0)}$ calculation:

Recall from section XI. H. that for the upper fluid

$$u_i^{(1,0)} = \operatorname{Re} \{ c_i^{(1,0)} e^{i\phi} \}$$

so that

$$F_i^{(1,0)} = u_i^{(1,0)} = A_i^{(1,0)} + \operatorname{Re} \{ B_i^{(1,0)} e^{i\Phi'} \}$$

$$B_i^{(1,0)} = 0 \quad k=2,3,4,\dots \quad , \quad A_i^{(1,0)} = 0$$

∴

$$x_j^{(1,0)} = \operatorname{Re} \{ i B_j^{(1,0)} e^{i\alpha X} (1 - e^{it}) \}$$

$$B_j^{(1,0)} = c_j^{(1,0)}$$

Similar equations hold for the sublayer.

XIV.C. The $\kappa_i^{(2,0)}$ calculation is more complicated. The functions of interest are

$$u_i^{(1,0)} = \operatorname{Re} \{ c_i^{(1,0)} e^{iz_i \phi} \}$$

$$u_i^{(2,0)} = \operatorname{Re} \{ c_i^{(2,0)} r_0(y) + c_i^{(2,0)} r_2(y) e^{z_i \phi} \}$$

$$F_i^{(2,0)} = \int_0^{t'} u_k^{(1,0)}(x, t'') dt'' \frac{\partial u_i^{(1,0)}}{\partial x_k}(x, t') + u_i^{(2,0)}(x, t')$$

Since the calculation of $F_i^{(2,0)}$ involves a time integral of $u_k^{(1,0)}$,

a time-independent term appears in the product of the $u_i^{(1,0)}$ quantities and we expect the modes $n=0, 1$ and 2 to be present.

This is due to the constant of integration. If the product is denoted by Π_i ,

$$\Pi_i = \Pi_i + \bar{\Pi}_i$$

$$\Pi_i = \int_0^{t'} u_1^{(1,0)} dt'' \frac{\partial u_i^{(1,0)}}{\partial x_1}(x, t')$$

$$\bar{\Pi}_i = \int_0^{t'} u_2^{(1,0)} dt'' \frac{\partial u_i^{(1,0)}}{\partial x_2}(x, t')$$

After much algebra (see Appendix C), $I_i^{(2,0)}$ is found, yielding $F_i^{(2,0)}$ according to the equation $F_i^{(2,0)} = I_i^{(2,0)} + u_i^{(2,0)}(x, t')$

$$F_i^{(2,0)} = \operatorname{Re} \left\{ c_1^{(2,0)}(0, y) - \frac{L}{2\alpha} + \frac{R}{2\alpha} e^{i\Phi'} + (c_1^{(2,0)}(z, y) - \frac{M}{2\alpha}) e^{iz\Phi'} \right\}$$

$$F_2^{(2,0)} = \operatorname{Re} \left\{ -\frac{K}{2} e^{i\Phi'} + c_2^{(2,0)}(z, y) e^{iz\Phi'} \right\}$$

where K , L , M , R are defined in section XIV. E.

Since

$$F_i^{(2,0)} = A_i^{(2,0)} + \sum_{n=1}^2 \operatorname{Re} \{ B_i^{(2,0)}(n, x) e^{in\Phi'} \}$$

we can calculate $A_i^{(2,0)}$ and $B_i^{(2,0)}$ which give the trajectory

$$x_i^{(2,0)}$$

XIV. D. The $x_i^{(0,1)}$ calculation:

Recall from equations (XIII. C.) that

$$u_1^{(0,1)} = -\frac{g_1}{2} \{ y^2 + \frac{1}{K} [h^2(1-K)-1] \}$$

$$\bar{u}_1^{(0,1)} = -\frac{g_1}{2K} \{ y^2 - 1 \}$$

$$u_2^{(0,1)} = \bar{u}_2^{(0,1)} = 0$$

$$f_i^{(0,1)} = u_i^{(0,1)}(x, t) = A_i^{(0,1)}$$

$$B_i^{(q,1)} = 0 \quad n=1, 2, 3, \dots$$

∴

$$x_i^{(0,1)} = A_i^{(0,1)} t$$

$$A_1^{(0,1)} = -\frac{g_1}{2} \left\{ Y^2 + \frac{1}{K} [h^2(1-\omega_r^2) - 1] \right\}$$

$$A_2^{(0,1)} = 0$$

For the sublayer, we have

$$\bar{x}_i^{(0,1)} = \bar{A}_i^{(0,1)} t$$

$$\bar{A}_1^{(0,1)} = -\frac{g_1}{2K} \{ Y^2 - 1 \}$$

$$\bar{A}_2^{(0,1)} = 0$$

XIV.E. The complete result for the upper fluid is given below.

y and X_2 are used interchangeably, as are x and X_1 .

$$x_i = X_i + \epsilon x_i^{(1,0)} + \epsilon^2 x_i^{(2,0)} + B x_i^{(0,1)} + \dots$$

$$x_j^{(1,0)} = \operatorname{Re} \{ i B_j e^{i \alpha x} (1 - e^{i t}) \}$$

cause a mean cyclic drift

$$x_j^{(0,1)} = A_j^{(0,1)} t$$

$$x_j^{(2,0)} = A_j^{(2,0)} t + \operatorname{Re} \{ i B_j^{(2,0)} (1, x) e^{i \alpha x} (1 - e^{i t}) \} + \\ + \operatorname{Re} \{ \frac{i}{2} B_j^{(2,0)} (2, x) e^{2i \alpha x} (1 - e^{i t}) \}$$

where

$$B_1(y) = - \frac{c_2^{(1,0)}}{i \alpha}, \quad B_2(y) = c_2^{(1,0)}$$

$$A_1^{(0,1)} = A_1^{(0,1)}(y) = - \frac{g_1}{2} \left\{ y^2 + \frac{1}{K} [h^2 (1 - K) - 1] \right\}$$

$$A_1^{(2,0)}(y) = \frac{1}{2} \alpha \operatorname{Re} \{ 2 \alpha c_1^{(2,0)}(0, y) - L \}$$

$$A_2^{(0,1)} = A_2^{(2,0)} = 0$$

$$B_1^{(2,0)}(1, \underline{x}) = \frac{R}{2\alpha}, \quad B_2^{(2,0)}(1, \underline{x}) = -\frac{K}{2}$$

$$B_1^{(2,0)}(2, \underline{x}) = \frac{1}{2\alpha} \left\{ i c_2'^{(2,0)}(2, y) - M \right\}$$

$$B_2^{(2,0)}(2, \underline{x}) = c_2'^{(2,0)}(2, y)$$

$$K = K(\underline{x}) = i \left\{ c_2^{(1,0)} c_2'^{(1,0)} + c_2''^{(1,0)} c_2'^{(1,0)} \right\} e^{-i\alpha X}$$

$$L = L(y) = c_2^{(1,0)} c_2'^{(1,0)} + c_2''^{(1,0)} c_2''^{(1,0)}$$

$$M = M(y) = c_2^{(1,0)} c_2'^{(1,0)} - c_2''^{(1,0)} c_2''^{(1,0)}$$

$$R = R(\underline{x}) = L e^{-i\alpha X} + M e^{i\alpha X}$$

For the Newtonian sublayer, all the above are valid except that
barred functions are used and

$$\bar{A}_1^{(0,1)} = -\frac{g_1}{2K} \{ y^2 - 1 \}$$

XIV.F. The cyclic drift of fluid material particles can be found easily from the trajectory as

$$\text{drift}_i \equiv x_i(\underline{x}, 2\pi) - x_i$$

where $t = 2\pi$ is the dimensionless period. Since the term

$$1 - e^{in2\pi} = 0 \quad n = 1, 2, 3, \dots$$

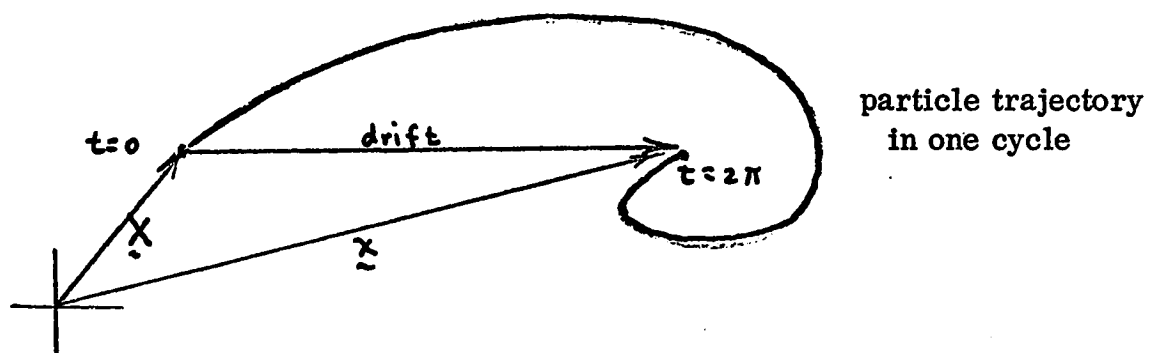
the only contribution to the drift comes from $A_i^{(0,1)}$ and $A_i^{(2,0)}$.

In fact, for both Newtonian and non-Newtonian fluids,

$$\text{drift}_1 = 2\pi \{ \epsilon^2 A_1^{(2,0)} + BA_1^{(0,1)} \}$$

$$\text{drift}_2 = 0$$

Thus, there is no y drift; on the average, and the particle travels in the $\pm \underline{e}_1$ direction. A possible trajectory may be like the following sketch:



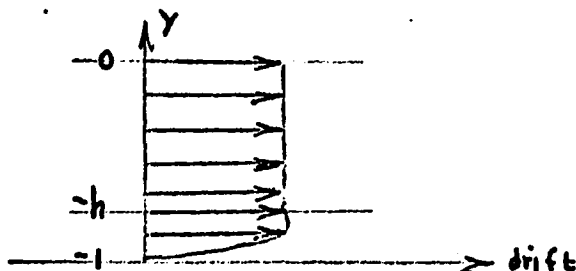
Note that the drift per cycle is a function of y and not of x , so that all particles along the x axis at a given height y will drift the same amount in one period regardless of their initial position x . We can set $x = 0$ without loss of generality.

The drift of fluid particles is plotted as a function of y for $-1 \leq y \leq 0$ (the undisturbed region) in section XVI. The drift of particles initially in regions outside of $[-1, 0]^*$ has not been plotted.

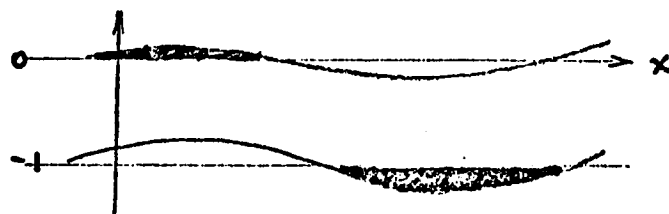
The volume flow rate can be calculated from the drift function by integration with respect to y over $[-1, 0]$. That is

$$\text{volume flux} = \frac{1}{\text{period}} \left\{ \int_{-1}^h \overline{\text{drift}}_1(y) dy + \int_{-h}^0 \overline{\text{drift}}_1(y) dy \right\}$$

where a typical drift curve may be



* Corresponding to a particular choice of x , the point (x, y) may not be in $[-1, 0]$, e.g:



Empirical data often consist of the average speed of a finite alien particle observed over a long period of time. We can obtain this average drift speed merely by dividing the cyclic drift by the period:

$$\text{avg. speed} = \frac{\text{drift}}{\text{period}}$$

XV. WORK RATE AND ENERGY DISSIPATION

From the stress tensor and velocity field, the rate of work of the wall and the rate of dissipation of mechanical energy within the fluid can be calculated. The rate of change of mechanical energy of a material volume can be written as follows:

1. 2. 3.

$$\frac{1}{2} \iint_R \frac{du^2}{dt} dv = \iint_R b_i u_i dv - \iint_R S_{ij} u_{;j} dv + \iint_{\partial R} u_i S_i da$$

- where 1. is the rate at which body forces do work
2. is the rate at which internal stresses do work
3. is the rate at which surface tractions do work

Neglecting inertial and gravitational forces (hence potential energy) relative to viscous forces for normal muco-ciliary flow gives

$$\iint_R S_{ij} u_{;j} dv = \iint_{\partial R} u_i S_i da$$

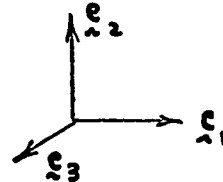
which means that the work rate done by the boundary tractions balances the kinetic energy dissipation.

Since our problem is two-dimensional,

$$da = dx$$

per unit length in the ξ_3 direction, where $d\alpha = \text{arc}$
length along a boundary curve. Similarly,

$$d\tau = d\alpha$$



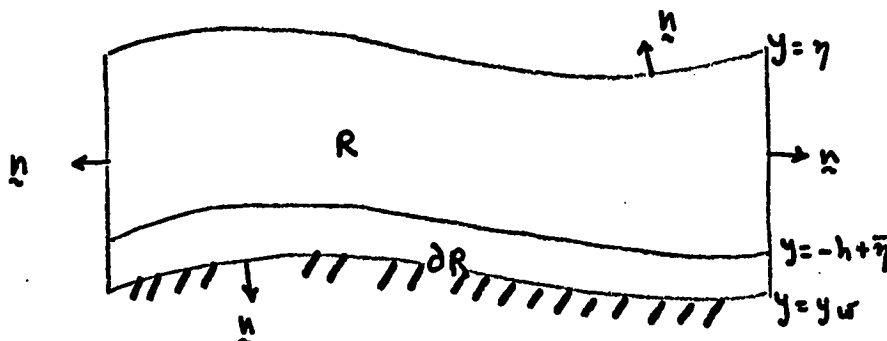
Thus the energy balance is roughly

$$\int_R S_{ij} u_{ij} d\alpha = \int_{\partial R} u_i S_i d\alpha \quad (\text{XV.1})$$

i.e. the rate of volumetric dissipation is equal to the rate at which work is done on the fluid by the boundary forces.

XV.A. Work Rate due to Boundary Forces.

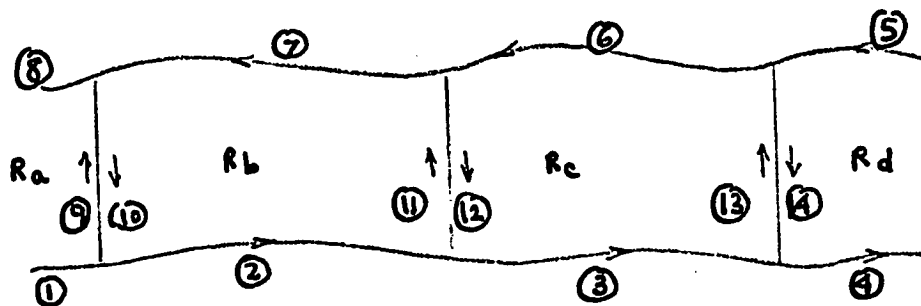
The region R covering one period is drawn below:



where n is the outward normal to R . The total traction on ∂R is S_t , whose relation to the stress tensor is

$$S_i = S_{ij} n_j$$

(i) The contribution to $\int_{\partial R}$ over the end surfaces $\lambda \approx 0$, does not affect the energy because it is equal and opposite at the two ends. For m wavelengths, we have



$$\begin{aligned} \int_{\partial R} &= \int_{\partial R_a} + \int_{\partial R_b} + \int_{\partial R_c} + \int_{\partial R_d} + \dots \\ &= \left\{ \int_{①}^{③} + \int_{③}^{⑤} \right\} + \left\{ \int_{②}^{⑦} + \int_{⑦}^{⑥} \right\} + \left\{ \int_{③}^{⑬} + \int_{⑬}^{⑭} \right\} + \left\{ \int_{④}^{⑭} + \int_{⑭}^{⑤} \right\} + \dots \end{aligned}$$

Due to periodicity, each of the brackets above has the same value so that

$$\int_{\partial R} = m \left\{ \int_{\text{wall}} + \int_{\text{free surface}} \right\}$$

m wavelengths

and the contribution to the work rate per wavelength is

$$\int_{\text{wall}} u_i S_i \, da + \int_{\text{free surface}} u_i S_i \, da$$

End effects are not involved.

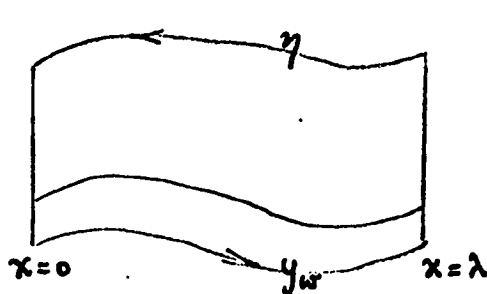
(ii) The work rates at the free surface and wall will be denoted by the symbols $\dot{W}_{f.s.}$ and \dot{W}_w so the mechanical energy balance is

$$\mathcal{D} = \dot{W}_{f.s.} + \dot{W}_w \quad (\text{XV.A.1})$$

where \mathcal{D} = dissipation $\equiv \int_R S_{ij} u_{i,j} \, da$

$$\dot{W}_{f.s.} \equiv \int_{x=0}^{x=\lambda} u_i S_i \Big|_{y=\eta} \, da$$

$$\dot{W}_w \equiv \int_{x=0}^{x=\lambda} \bar{u}_i \bar{S}_i \Big|_{y=y_w} \, da$$



Calculations for both free surface and wall work rates can be considered as follows:

$$\text{integrand: } u_i S_i = u_i S_j n_j \Big|_{y=y_0+f}$$

$$f = \epsilon f^{(1,0)} + \epsilon^2 f^{(2,0)} + \dots$$

normal: (n_i is the outer normal to the free surface but
the inner normal to the wall)

$$n_i = n_i^{(0,0)} + \epsilon n_i^{(1,0)} + \epsilon^2 n_i^{(2,0)} + \dots$$

$$n_i = -\epsilon f_{,x}^{(1,0)} - \epsilon^2 f_{,x}^{(2,0)} + \dots$$

$$n_2 = 1 - \frac{1}{2} \epsilon^2 f_{,x}^{(1,0)} + \dots$$

velocity: $u_i \Big|_{y_0+f} = \epsilon u_i^{(1,0)}(y_0) + \epsilon^2 \{ f u_{i,y}^{(1,0)}(y_0) + u_i^{(2,0)}(y_0) \} + \dots$

stress:

$$S_{ij} \Big|_{y_0+f} = S_{ij}^{(0,0)} + \epsilon \{ S_{ij}^{(1,0)}(y_0) \} + \epsilon^2 \{ f S_{ij,y}^{(1,0)}(y_0) + S_{ij}^{(2,0)}(y_0) \} + \dots$$

$\nwarrow -P_0 \delta_{ij}$

arc length: $ds = \frac{1}{2} \{ 1 + \frac{1}{2} \epsilon^2 f_{,x}^{(1,0)} + \dots \} d\phi$

traction: $S_{ij} n_j \Big|_{y_0+f} = S_i$

$$S_i = S_i^{(0,0)} + \epsilon S_i^{(1,0)} + \epsilon^2 S_i^{(2,0)} + \dots$$

$$S_i^{(0,0)} = -P_0 n_i^{(0,0)}$$

$$S_i^{(1,0)} = S_{ij}^{(1,0)} n_j^{(0,0)} - P_0 n_i^{(1,0)} \quad \text{at } y_0$$

$$S_i^{(2,0)} = \{ f^{(1,0)} S_{ij,y}^{(1,0)} + S_{ij}^{(2,0)} \} n_j^{(0,0)} + S_{ij}^{(1,0)} n_j^{(1,0)} - p_0 n_i^{(2,0)} \text{ at } y_0$$

$$u_i = \epsilon U_i^{(1,0)} + \epsilon^2 U_i^{(2,0)} + \dots$$

$$U_i^{(1,0)} = u_i^{(1,0)}, \quad U_i^{(2,0)} = f^{(1,0)} u_{i,y}^{(1,0)} + u_i^{(2,0)} \text{ at } y_0$$

$$u_i S_i \Big|_{y_0+f} = \epsilon U_i^{(1,0)} S_i^{(0,0)} + \epsilon^2 \{ U_i^{(2,0)} S_i^{(0,0)} + U_i^{(1,0)} S_i^{(1,0)} \} + \dots$$

$$u_i S_i \Big|_{y_0+f} = \epsilon^2 u_i^{(1,0)} \{ s_{12}^{(1,0)} + p_0 f_{,x}^{(1,0)} \} + \dots \text{ at } y_0$$

$$u_2 S_2 \Big|_{y_0+f} = -p_0 [\epsilon u_2^{(1,0)} + \epsilon^2 \{ u_2^{(2,0)} + f^{(1,0)} u_{2,y}^{(1,0)} \}] + \epsilon^2 u_2^{(1,0)} S_{22}^{(1,0)} + \dots \text{ at } y_0$$

$$d\phi = \frac{1}{2} d\phi + O(\epsilon^2)$$

$$\text{sum} = [u_i S_i + u_2 S_2] \Big|_{y_0+f}$$

$$\dot{N} = \frac{1}{2} \int_0^{2\pi} \text{sum} d\phi$$

(ii.a) Work rate at the free surface ($y = \eta$)

$$\frac{S_{ij}}{\eta} = -P_0 \delta_{ij}$$



$$S_i^{(K,m)} = -P_0 n_i^{(K,m)}, \quad f^{(1,0)} = \eta^{(1,0)}$$

$$\frac{u_i S_i}{\eta} = \epsilon^2 u_i^{(1,0)} P_0 \eta_{,x}^{(1,0)} \quad \text{at } y=0$$

$$\frac{u_2 S_2}{\eta} = -P_0 [\epsilon u_2^{(1,0)} + \epsilon^2 \{ u_2^{(2,0)} + \eta^{(1,0)} u_{2,y}^{(1,0)} \}] \quad \text{at } y=0$$

$$\text{Sum} = P_0 \{ -\epsilon u_2^{(1,0)} - \epsilon^2 u_2^{(2,0)} + \epsilon^2 (u_1^{(1,0)} \eta_{,x}^{(1,0)} - \eta^{(1,0)} u_{2,y}^{(1,0)}) \} \quad \text{at } y=0$$

$$\text{but } (u_1^{(1,0)} \eta_{,x}^{(1,0)} - \eta^{(1,0)} u_{2,y}^{(1,0)}) = \frac{R\theta}{2} \{ i c_2' c_2^* - i c_2^* c_2' + 2i c_2 c_2' e^{2i\phi_3} \}$$

$$= R\theta \{ i c_2^{(1,0)} c_2^{(1,0)*} e^{2i\phi_3} \}$$

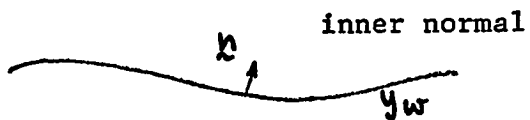
$$\therefore \dot{N}_{f.s.} = \int_0^{2\pi} \sum d\phi = 0$$

(XV.A.2)

because $u_2^{(1,0)}$ and $u_2^{(2,0)}$ and the parenthetical expression have no zero mode parts and the integral vanishes.

(ii.b) Work rate at the wall

$$f^{(1,0)} = y_w^{(1,0)} = \sin \phi$$



$$y_{w,x}^{(1,0)} = \alpha \cos \phi$$

Since we have used the inner normal in the above, and since the integral $\int_{\partial R}$ is based on the outer normal, the integrand is multiplied by -1 to obtain the correct result.

$$\bar{u}_1^{(1,0)} = u_{w_1}^{(1)} = \beta \sin \phi \quad , \quad \bar{u}_2^{(1,0)} = u_{w_2}^{(1)} = \cos \phi$$

$$\bar{u}_2^{(2,0)} = u_{w_2}^{(2)} - \sin \phi \bar{u}_{2,y}^{(1,0)} \quad \text{at } y=-1$$

$$u_{w_2}^{(2)} = -\frac{1}{2} \alpha \beta \sin 2\phi$$

$$\bar{u}_2^{(2,0)} + f^{(1,0)} \bar{u}_{2,y}^{(1,0)} \Big|_{y=-1} = u_{w_2}^{(2)} = -\frac{1}{2} \alpha \beta \sin 2\phi$$

$$\bar{u}_{,1}^{(1,0)} f_{,x}^{(1,0)} = \alpha \beta \sin \phi \cos \phi$$

$$\text{sum} = -P_0 \left[\epsilon \cos \phi + \epsilon^2 \left\{ -\frac{\alpha \beta}{2} \sin 2\phi - \alpha \beta \sin \phi \cos \phi \right\} + \right.$$

$$\left. + \epsilon^2 \left[u_{w_1}^{(1)} S_{12}^{(1,0)} + u_{w_2}^{(1)} S_{22}^{(1,0)} \right] \right]_{y=1}$$

The terms multiplying P_0 integrate out to zero and

$$\dot{W}_w = -\frac{1}{\alpha} \int_0^{2\pi} \text{sum} d\phi$$

$$\dot{W}_w = -\frac{\epsilon^2}{\alpha} \int_0^{2\pi} \left\{ u_{w_1}^{(1)} S_{12}^{(1,0)} + u_{w_2}^{(1)} S_{22}^{(1,0)} \right\} d\phi + \dots$$

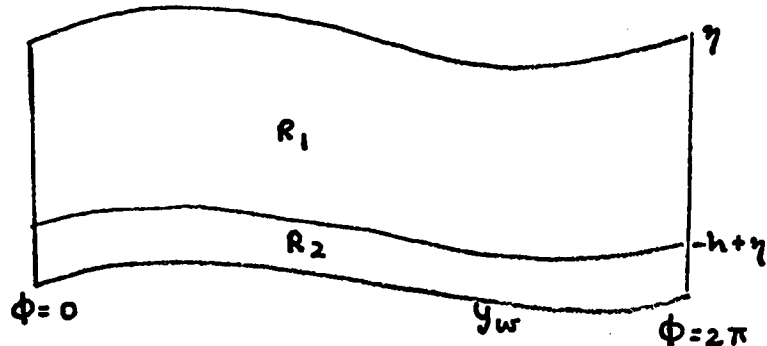
$$u_{w_1}^{(1)} = \beta \sin \phi$$

(XV.A.3)

$$u_{w_2}^{(1)} = \cos \phi$$

XV.B. Rate of Dissipation of Kinetic Energy.

$$\mathcal{D} \equiv \int_R S_{ij} u_{ij} da = \int_{R_1} S_{ij} u_{ij} da + \int_{R_2} S_{ij} u_{ij} da$$



$$da = dx dy = \frac{1}{2} d\phi dy$$

$$f \equiv S_{ij} u_{ij}, \quad \bar{f} \equiv \bar{S}_{ij} \bar{u}_{ij}$$

$$\int_{R_1} S_{ij} u_{ij} da = \frac{1}{2} \int_{-\bar{\eta}+h}^{\bar{\eta}} \int_0^{2\pi} f d\phi dy$$

$$\int_{R_2} \bar{S}_{ij} \bar{u}_{ij} da = \frac{1}{2} \int_{y_w}^{-h+\bar{\eta}} \int_0^{2\pi} \bar{f} d\phi dy$$

$$f = S_{ij} u_{i,j} = (S_{22} - S_{11}) u_{2,y} + S_{12} (u_{1,y} + u_{2,x})$$
$$\downarrow \qquad \qquad \qquad \downarrow$$
$$= (t_{22} - t_{11}) u_{2,y} + t_{12} (u_{1,y} + u_{2,x})$$

$$D = \int_0^{2\pi} F(\phi) d\phi + \int_0^{2\pi} \bar{F}(\phi) d\phi$$

$$F(\phi) \equiv \frac{1}{\alpha} \int_{-h+\hat{\eta}(\phi)}^{\eta(\phi)} f(y, \phi) dy$$

$$\bar{F}(\phi) \equiv \frac{1}{\alpha} \int_{y_m(\phi)}^{-h+\hat{\eta}(\phi)} \bar{f}(y, \phi) dy$$

$$\bar{f} = (t_{22} - t_{11}) \bar{u}_{2,y} + t_{12} (\bar{u}_{1,y} + \bar{u}_{2,x})$$

The integrals F and \bar{F} are both of the form:

$$I = \int_{a^{(0)} + \epsilon a^{(1)}(\phi) + \dots}^{b^{(0)} + \epsilon b^{(1)}(\phi) + \dots} f dy$$

where

$$a^{(0)} = \text{constant}$$

$$b^{(0)} = \text{constant}$$

$$f = \epsilon^2 f^{(2)}(y, \phi) + O(\epsilon^3)$$

$$I = \int_{a^{(0)}}^{b^{(0)}} f dy + \int_{a^{(0)} + \epsilon a^{(1)} + \dots}^{a^{(0)} + \epsilon a^{(1)} + \dots} f dy + \int_{b^{(0)}}^{b^{(0)} + \epsilon b^{(1)} + \dots} f dy$$

$\uparrow \qquad \uparrow \qquad \uparrow$

$I_1 \qquad I_2 \qquad I_3$

The Mean Value Theorem of integral calculus implies that

$$I_1 = O(\epsilon^3)$$

$$I_3 = O(\epsilon^3)$$

thus $I = \epsilon^2 \int_{a^{(0)}}^{b^{(0)}} f^{(2)}(y, \phi) dy + O(\epsilon^3)$

The energy dissipation correct to second order is then:

$$\mathcal{D} = \int_0^{2\pi} F(\phi) d\phi + \int_0^{2\pi} \bar{F}(\phi) d\phi$$

$$F(\phi) = \frac{\epsilon^2}{\alpha} \int_{-h}^0 f^{(2)}(y, \phi) dy + O(\epsilon^3)$$

(XV. B)

$$\bar{F}(\phi) = \frac{\epsilon^2}{\alpha} \int_{-l}^{-h} \bar{f}^{(2)}(y, \phi) dy + O(\epsilon^3)$$

$$f^{(2)} = (t_{22}^{(1,0)} - t_{11}^{(1,0)}) u_{2,y}^{(1,0)} + t_{12}^{(1,0)} (u_{1,y}^{(1,0)} + u_{2,x}^{(1,0)})$$

$$\bar{f}^{(2)} = (\bar{t}_{22}^{(1,0)} - \bar{t}_{11}^{(1,0)}) \bar{u}_{2,y}^{(1,0)} + \bar{t}_{12}^{(1,0)} (\bar{u}_{1,y}^{(1,0)} + \bar{u}_{2,x}^{(1,0)})$$

XVI. GRAPHS AND RESULTS

XVI.A. General discussion

In this section, we discuss the behavior of this mathematical model, both for "normal" muco-ciliary flow, and for cases in which some parameters have been changed moderately from the "normal" values (sections XVI.B.,C.). As a matter of intrinsic fluid mechanical interest, the fully Newtonian case and some variations from it have also been worked out (section XVI.D.). The analytical solutions found in sections XI through XV are computed in a straightforward manner using the IBM 7094.

Since the primary function of the mammalian respiratory muco-ciliary system is thought to be that of cleansing the body of foreign particulate matter, the principal physiological interest is in the material drift* of the fluid layers. Therefore, most of the graphs presented are numerically computed results for the cyclic material drift as a function of distance from the free surface (or wall) for different values of the parameters. Other graphs include particle trajectories, and

*

The cyclic material drift divided by one period is the mucous flow rate or average drift speed of fluid particles.

the shapes of free surfaces and interfaces. Values of the average volume flux of fluid through any line $-1 \leq y \leq 0$, and the work rate at the wall are found for "normal" flow. All of these solutions are correct to second order in the wall amplitude, i.e. to $O(\epsilon^2)$.

The basic state is taken to be the "normal muco-ciliary flow" previously defined in section VIII.D. Additional cases in which key parameters are changed from this standard give some insight into what might happen in slightly pathological cases, e.g. with changes in serous viscosity, mucous viscosity, mucous rigidity, frequency, wavelength, etc. (sections XVI.B. and C.).

Dimensional values of net cyclic material displacement ("drift"), average drift speed, volume flux and work rate are computed for normal flow. Comparisons of the average drift speed of the model mucus with data on real muco-ciliary flow rates in mammals show at least a reasonable order of magnitude for the model. This suggests that this mathematical model of the muco-ciliary system may be reasonable.

In addition to the average speed, a rough biological estimate of the time rate of working of the cilia can be compared to the theoretically obtained value. Due to lack of published

experimental results on other quantitative aspects of mucociliary flow, quantitative comparisons between experiment and theory necessarily end with the aforementioned two, and only qualitative agreement can be discussed beyond that.

A table presenting the model's predictions on the tendencies of mucous drift to increase or decrease with changes in the values of the parameters is given in section XVI.C.8.

XVI.B. Normal Flow

XVI.B.1. Discussion of Figures XVI.B.1,2,3.

The values of the dimensionless numbers for "normal" mucociliary flow (section VIII.D.9) are $\alpha = 1.$, $\beta = 1.5$, $T = 1.5 (10^3)$, $K = .67 (10^{-4})$, $h = .8$.

The displacement profile, the cyclic drift of fluid particles (Fig. XVI.B.1) shows that all of the mucus tends to move the same amount in one period (nearly like a viscoelastic solid) but that the serous fluid drift is a strongly dependent function of distance from the wall. Note that the drift is in the $+ \xi$ direction, opposite to that of the travelling wave wall geometry. A serous particle at the wall ($y = -1$) of course has zero net displacement per cycle because of the

no-slip condition and the fact that a wall point path is closed (Fig. XVI.B.3). It seems plausible (and is consistent with biologists interpretations; e.g. Lucas and Douglas, 1934) that the clockwise wall point motion tends to push the fluid in the ξ direction because then the wall points intrude farther into the fluid when moving in the ξ direction.* It is also plausible that the visco-elasticity causes a segment of the mucus to spring back after it is deformed. This tendency presumably retards serous fluid particles near the interface, so the serous fluid displacement has a local maximum in drift. It may be "dragging" the mucus along. The velocity gradients near the interface are probably governed primarily by the product $K\Gamma$ in the case of normal flow. This differs from a case in which the upper layer is Newtonian ($\Gamma=0$) since K alone then determines the difference in the rate of strains of the two layers. For example, consider a balance of "extra" stresses at the interface:

$$\tau_{ij} \doteq \dot{\tau}_{ij}$$

*

We shall see, however (section XVI.D.1.), that this is not the dominant driving mechanism!

where the constitutive equations are of the form (section IX.D.):

$$T \frac{\partial}{\partial t} t_{ij} = -t_{ij} + d_{ij}$$

$$\dot{t}_{ij} = 2 \kappa \ddot{d}_{ij}$$

Supposing that the stress $t_{ij} = O\{\sin(\alpha x + t)\}$, we see that $O\{T \frac{\partial}{\partial t} t_{ij}\} \gg O\{t_{ij}\}$ because $T \gg 1$ and so $\dot{t}_{ij} = O\{\frac{1}{T} d_{ij}\}$. The balance of stresses is then

$$\frac{1}{T} d_{ij} \doteq 2 \kappa \ddot{d}_{ij}$$

or $\ddot{d}_{ij} \doteq \frac{1}{2 \kappa T} d_{ij}$ (XVI. B. 1. a)

Hence, $\kappa T = \frac{\bar{\mu} \omega}{G}$ influences the velocity gradients to a large extent.* Note that the gradients in the serous layer are larger than those in the mucous layer because $\kappa T \ll 1$.

Figure XVI.B.2 shows a small phase shift between the wall and the free surface. Since the wall geometry moves in the $-\xi$ direction, the free surface may be considered to lag the wall by about 30° . This shift if also affected by the serous viscosity according to the product κT .

*

We shall consider the dependence of the solution on κT in more detail in section XVI.C.

XVI.B.2. Comparison of computed model values with experimental data on biological systems.

The majority of the biological experiments performed on muco-ciliary systems use microscopy to observe the mucosa and to measure ciliary beat frequency, the average drift speed (usually called the "mucous flow rate" by physiologists) and large scale dye streak patterns (a consequence of "ciliary streaming"). Both in vivo and in vitro* studies have been undertaken, with the latter subject to criticism since "...prerequisites for a normal mucous flow are an intact blood and nerve supply to the mucosa" (Ewert, 1965). Sensitivity to variations in air temperature and humidity, and to chemical and ionic changes have been studied.

By and large, the measurements of "mucous flow rates" (drift speed) have been measurements of the average speed of a foreign particle placed "upon" the mucous layer surface. These results are the ones available for judging the applicability of the present continuous wall model. Unfortunately there seem to be no data on particles within the mucous and serous layers

*

In vitro here denotes a removed section of ciliated epithelium in which the cilia continue to beat.

although dye may have diffused appreciably toward the cell surface. If in a normal mucous flow most of the fluid particles in the upper layer drift the same amount, the surface speed is an accurate measure of the whole mucous transport, even though it says nothing about the serous sublayer. It also suggests that little error would be caused by sinkage of a small enough alien particle into the mucus. For the normal case the computed dimensionless drift of a particle on the free surface is

$$\text{drift}^* = 0.331$$

$$\text{drift} = d \times \text{drift}^*$$

where $d = 5$ microns. The dimensional value of the drift in one cycle is therefore

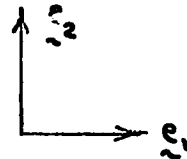
$$\text{drift} = 0.165 (10^{-2}) \text{ mm}$$

The ratio of this drift per cycle to the wavelength is 0.055.

XVI.B.2.a. The average drift speed or mucous flow rate is simply

$$u_{avg} = \frac{\text{drift in one period}}{\text{period}}$$

$$\text{period} = \frac{1}{15} \text{ sec.}$$



$$u_{avg} = 4.5 \text{ drift}^* \frac{\text{mm}}{\text{min}} \quad \text{e}_1$$

Thus, for a particle in the mucous layer under the normal flow conditions, the average speed is

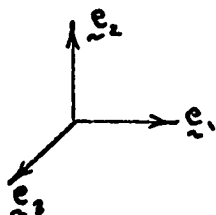
$$u_{avg} \doteq 1.5 \frac{\text{mm}}{\text{min.}} \quad \text{e}_1$$

This may be compared to the observed data which range from a low of $2.5 \frac{\text{mm}}{\text{min}}$ to a high of $15 \frac{\text{mm}}{\text{min}}$, depending on the mammal studied, the particular organ considered and the conditions of the experiment. The theoretical model result thus falls near the lower bound of the biological data, so that the theory predicts a mucous flow rate of the correct order of magnitude.

XVI.B.2.b. The volume flux of fluid transported through $\text{e}_1 \leq y \leq 0$ per unit length in e_3 can be found by integration of the cyclic drift.

$$\begin{aligned}\text{flux} &= \frac{1}{\text{period}} \int_{-d}^0 \text{drift}(y) dy \\ &= \frac{d^2}{\text{period}} \int_{-1}^0 \text{drift}^*(y^*) dy^* \\ &= 3.75 (10^{-6}) \text{ flux}^* \frac{\text{cm}^2}{\text{sec}}\end{aligned}$$

$$\text{flux}^* \equiv \int_{-1}^0 \text{drift}^* dy^*$$



For "normal" mucous flow, $\text{flux}^* \doteq .32$ so that

$$\boxed{\text{flux} \doteq 1.2 (10^{-6}) \frac{\text{cm}^2}{\text{sec}}} \quad \text{or} \quad \frac{\text{cm}^3/\text{sec}}{\text{cm} \text{ in } e_3}$$

Comparing this with experimental data is difficult since most physiologists have collected the fluid volume by large scale drainage out of a set of tubes of various cross sections.

XVI.B.2.c. The work rate (power) at the wall (over one wavelength, per unit length in ξ_3) is determined by integration of the scalar product of the wall velocity and traction (section XV.A.2.)

$$\dot{W} = \int_{x=0}^{x=\lambda} \underline{u}_w \cdot \bar{\underline{s}} \, da(x) \quad \text{at } y = y_w$$

where \underline{u}_w is the wall velocity and $\bar{\underline{s}}_i$ is the stress traction $\bar{s}_{ij} = s_{ij} n_j$.

$$\underline{u}_w = d\omega \underline{u}_w^*$$

$$\bar{\underline{s}}_i = \mu \omega \bar{s}_i^*$$

$$da = d \, ds^*$$

$$\dot{W} = \mu \omega^2 d^2 \dot{W}^*$$

$$\dot{W} = 3.75 \dot{W}^* \frac{\text{dyne}}{\text{sec}}$$

From the numerical results for "normal" muco-ciliary flow,

$\dot{W}^* = .214(10^{-4})$ so that the power per unit length is

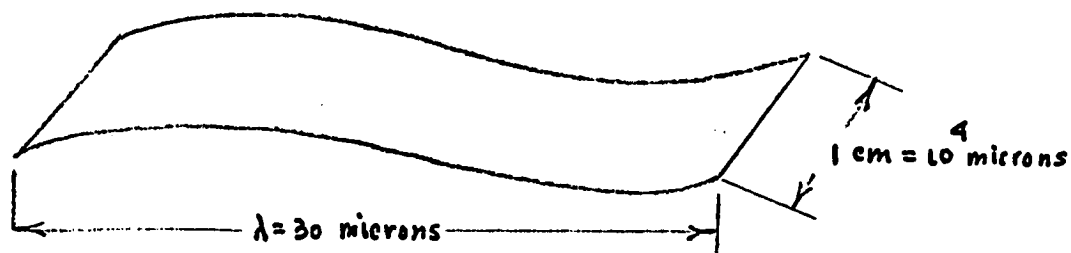
$$\boxed{\dot{W} \doteq 8.05(10^{-5}) \frac{\text{dyne}}{\text{sec}}} \quad \text{or} \quad \frac{\text{erg/sec}}{\text{cm in } \xi_3}$$

The numerical value of the energy dissipation \mathfrak{D}^* (section XV.B.) differs from \dot{W}^* by $O(10^6)$. That is,

$|\dot{W}^* - \mathfrak{D}^*| = O(10^6)$ so that the relative difference is

$$O\left(\frac{10^6}{10^{-4}}\right) = 1\%$$

Consider the power expended by the waving wall for an area one wavelength by one centimeter.



In the normal case, the power expended in the area above

(\dot{W}_{Area}) is

$$\dot{W}_{\text{Area}} = 8.05(10^{-5}) \frac{\text{erg}}{\text{sec}}$$

This result should be compared to the actual power produced by a wall of waving cilia. Multiplying the number of cilia in the area by the power each expends (biochemically)

during one beat would give an upper bound on the allowable ciliary work rate. In this model, however, the tips of the cilia have been replaced by a continuous wall so that the hydrodynamic interactions of the cilia are not included. The work rate obtained from this theory, then, corresponds primarily to that of the tip region and should thus be much smaller than the actual power expended by a real ciliated epithelium, which includes that of the viscous interaction between cilia and the actual inefficiency of the cilia themselves in converting chemical to mechanical energy, which would show as heat lost to the air.

XVI.C. Departures from the "normal" state

Internal and external influences (e.g. hormonal changes, noxious gases, viral agents) can affect mucous flow in several ways. Increased viscosity of mucus and serous fluid may occur in diseases like cystic fibrosis and in instances in which the mucosa is dehydrated, for example: excessive fever or alcohol intake and extreme dry atmosphere (Proctor). An excess of "watery" mucus may occur in individuals due to emotional stress, common colds, and respiratory diseases like bronchial asthma. The thickness of the mucous layer seems to increase after

exposure to irritant gases like SO_2 (Dalhamn, 1956). It would be informative to predict (from our model) the effects of changing serous viscosity, mucous viscosity, depth, and other quantities from their normal values.

In this subsection, we shall discuss the results of changing the values of the parameters in a neighborhood of the normal state. These changes are small enough so that gravitational and inertial forces can still be neglected, i.e. $A \ll 1$ and $B \ll 1$, and so the amplitude to depth ratio remains small ($\epsilon^2 \ll 1$). Curves of cyclic drift and particle trajectory are presented for different values of the sublayer viscosity, modulus of rigidity, frequency, etc.

As noted previously (section XVI.B.1), the product kT seems to be the primary influence on the velocity gradient ratio at the interface. In addition, according to the matrix equation giving the Fourier coefficients $C_2^{(1,0)}$ and $C_2^{(2,0)}$ (section XI.C.) the viscosity ratio and relaxation time enter in the combination

$$\Theta = k + ikT$$

The imaginary part exerts the stronger influence because

$kT \gg k$. This product is

$$KT = \left(\frac{\bar{\mu}}{\mu}\right) \left(\frac{\mu\omega}{G}\right) = \frac{\bar{\mu}\omega}{G}$$

Note that it is independent of mucous viscosity. The above indicates that, in a neighborhood of the normal state, the flow is not very sensitive to changes in mucous viscosity, but changes in serous viscosity and mucous elasticity are important.* The form of this dependence will be considered in section XVI.C.7.

XVI.C.1. Figures XVI.C.1.a,b: Serous viscosity $\bar{\mu}$

If all other dimensional parameters are fixed at their normal values, changes in the serous viscosity affect only the dimensionless viscosity ratio (K).** Figure XVI.C.1.a shows that increasing $\bar{\mu}$ decreases the drift and vice-versa. This can be traced to changes in KT which occur when $\bar{\mu}$ changes. For decreasing KT , larger velocity gradients may

*

Numerical results showed no change in the mucous drift and the power expended by the wall upon doubling or halving the normal mucous viscosity.

**

This is not the same as varying the mucous viscosity because μ enters in the dimensionless relaxation time $T = \frac{\mu\omega}{G}$ as well as the viscosity ratio.

exist in the serous layer, possibly allowing an increased material drift of fluid.

The wall work rate (power) increases as $\bar{\mu}$ increases according to the computed results:

$\bar{\mu}$	$\dot{W}^* (10^{-4})$
$2\bar{\mu}_N$.340
$\bar{\mu}_N$.214
$.5\bar{\mu}_N$.115

Since the dissipation of mechanical energy approximately equals the power applied at the boundaries in flows where inertia is negligible (section XV.), then the energy dissipation increases as the sublayer viscosity increases. Therefore, an increase in drift and a decrease in wall work rate result from a decrease in $\bar{\mu}$.

XVI.C.2. Figures XVI.C.2.a,b: Modulus of rigidity G and frequency ω for fixed λ

Changes in the modulus of rigidity, the elastic property of the mucus, affect the flow. Increasing G makes the "spring" more rigid, so that it will deform less under some fixed load. Also the ratio of viscosity μ to modulus G

(relaxation time) decreases; the material is less "elastic" and more "viscous". This effect can be seen from the trajectory curves (Fig. XVI.C.2.b) in which decreasing G allows for a larger "recoil", resulting in a reduction of the net cyclic drift.

The frequency of the ciliary beat enters this case by virtue of the dimensionless time T which is defined as $T = \omega \tau_g = \frac{\omega \mu}{G}$. If the wavelength is fixed, then variations in ω cause changes in T alone (this differs from a situation in which ω changes but wave speed is constant).

Thus, increasing frequency and decreasing modulus of rigidity both cause an increasing T . In other words, changes in G or ω (when λ is fixed) can be treated the same way since they affect the parameter T alone. One graph will suffice for both.

These curves (Figs. XVI.C.2.a,b) look the same as Figs. XVI.C.1.a,b). Indeed, they are equivalent because the solution depends on κT so that doubling κ with T fixed is the same as doubling T with κ fixed. Hence, increasing μ is equivalent to decreasing G by the same factor.

Since the power is dimensionalized by $\mu \omega^2 d^2$

(section XVI.B.2.c) then changes in ω and G which alter the relaxation time in the same way will affect \dot{W} differently because $\mu \omega^2 d^2$ changes in one case. Consider the 2 tables below (let $a = \mu_N \omega_N^2 d_N^2$).

(i) fixed ω :

G	T	$\dot{W}^*(10^{-4})$	$\dot{W} = \mu \omega^2 d^2 \dot{W}^*$	drift \dagger
$\frac{1}{2} G_N$	$2 T_N$.17	.17 a	.27
G_N	T_N	.214	.214 a	.33
$2 G_N$	$\frac{1}{2} T_N$.23	.23 a	.352

(ii) fixed G :

ω	T	$\dot{W}^*(10^{-4})$	$\dot{W} = \mu \omega^2 d^2 \dot{W}^*$	drift
$2 \omega_N$	$2 T_N$.17	$4(.17) a$.27
ω_N	T_N	.214	.214 a	.33
$\frac{1}{2} \omega_N$	$\frac{1}{2} T_N$.23	$\frac{1}{4} (.23) a$.352

$$\omega \downarrow \sim \text{drift} \uparrow \sim \dot{W} \downarrow$$

$$G \uparrow \sim \text{drift} \uparrow \sim \dot{W} \uparrow$$

Thus, although the drift increases the same amount in both instances, more work has to be done by the cilia when G increases (ω fixed) than when ω decreases (G fixed).

XVI.C.3. Figure XVI.C.3: Frequency ω for fixed wave speed c

If the frequency of the ciliary beat changes but the wave speed remains the same, then the wavelength also varies according to the equation $\lambda = \frac{2\pi c}{\omega}$. Two dimensionless parameters are changed: the time ratio T and the wave number α . Clearly, this differs from the situation in which ω varies but λ is fixed. Here increasing ω causes T to increase which loosely means more "elasticity", but the dimensionless wave number α also increases, which changes the kinematics of the problem.*

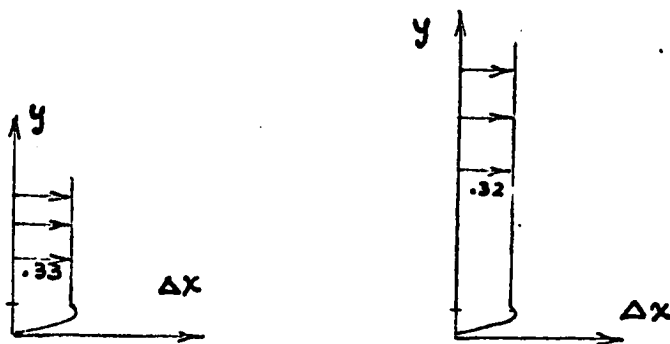
Only small changes in ω are considered (Fig. XVI.C.3) so as not to invalidate the condition that $(\alpha \beta \epsilon)^2 \ll 1$ (equation VI.C.4.b). The curves show that increasing the beating frequency while keeping the wave speed fixed will increase the net drift.

XVI.C.4. Depth, d

The effect of increasing the total depth of the two

* In a sense, we can consider this as two opposing effects: the tendency of T to decrease the drift and the tendency of α to increase the drift.

fluids while keeping the depth of the serous fluid fixed* at 1 micron (i.e. increasing the depth of the mucus alone) is that the cyclic drift of mucous particles stay nearly the same. At first glance, this may seem unusual because when the depth increases, some of the mucus is farther from the ciliary wall driving the flow and so it would appear likely to drift less. But this is not the result; apparently the unchanged serous fluid layer is able to drag along a thicker slab of mucus without much effort. The thicker mucous layer may act as a "stiffer beam" than the thinner one. In particular,



Thus, the volume flux (i.e. flow rate) of mucus increases when the mucous layer depth increases moderately, providing the depth of the serous fluid sublayer and all other constants remain fixed.

*

The effect of gravity, which may be important for large enough total depths, has been neglected.

XVI.C.5. Figure XVI.C.5: Ratio of depth of the mucus layer h to the total depth d .

As the depth of the mucus layer increases while the total depth remains constant, the serous-mucus interface approaches the wall. The drift of particles may be retarded because the no-slip condition causes the material to return almost to its original position after one cycle and because the serous layer would have to be sheared more strongly to keep up the speed of the mucus. In the limit as $h \rightarrow d$ (no serous fluid between the tips of the cilia and the mucus), there is almost no material drift at all; the mucus behaves like a spring subject to a periodic displacement.

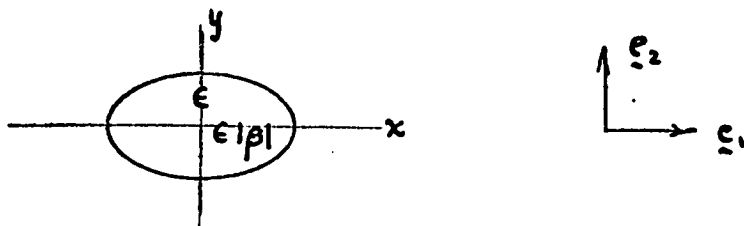
Experiments hinting at agreement with this result have been performed on simulated cilia by C. E. Miller (1968). According to him, "...motion of particles is initiated only if the visco-elastic material (Nuogel-in-Varsol) is a small portion of the total fluid or if it occupies the region above the tips of the vibrating ribbons". That is, if the visco-elastic fluid touches the tips of the ribbons, there is no fluid drift. In addition, many physiologists believe that the transport of mucus is retarded if there is a deficiency in the amount of serous fluid. This too is in accord with the

theoretical model.

A more detailed examination of the dependence of the drift on β will be given in section XVI.C.7.

XVI.C.6. Figure XVI.C.6: Axis ratio, β

The trajectory of a cilium tip may correspond to that of a wall particle in this continuous wall model. Recall that $|\beta|$ is the ratio of the x to y elliptical axes



where positive β indicates a clockwise direction. Since the wall particles drive the fluid motion, the flow must be sensitive to changes in β ; increasing positive β draws out the ellipse and causes a larger fluid drift in ξ_1 . As β decreases from its normal value, the ellipse approaches a circle of radius ϵ ($\beta \rightarrow 1$) and the drift of mucus decreases. Larger departures in β are probably not biologically realistic

for muco-ciliary flow, but they are intrinsically interesting fluid mechanically, and will be considered in part D of this section for a purely Newtonian case.

XVI.C.7. Dependence of drift on dimensionless parameters near the normal state.

We may gain some insight into the solution by trying "empirically" to discover simple, approximate dependencies of the drift on some of the dimensionless parameters. For a particle of mucus at the free surface, the cyclic drift is of the form

$$D = \epsilon^2 \mathfrak{F}(\alpha, \beta, h, \kappa, \tau) \quad (\text{XVI.C.7.a})$$

where the dependence on ϵ^2 is known from the analytical solution.*

For the sake of simplicity, we assume that $\mathfrak{F}(\alpha, \beta, h, \kappa, \tau)$ can be factored, viz.

$$\mathfrak{F} = \mathfrak{F}_\alpha(\alpha) \mathfrak{F}_\beta(\beta) \mathfrak{F}_h(h) \mathfrak{F}_\kappa(\kappa) \mathfrak{F}_\tau(\tau)$$

* The drift = $2\pi A_1^{(2,0)} \epsilon^2$ neglecting gravity terms (section XIV.F.).
Thus

$$\mathfrak{F} = 2\pi A_1^{(2,0)} \Big|_{Y=0}$$

But we know from the analytical results that the k, T factor-ing won't work, so we try another form:

$$\mathcal{F} = \mathcal{F}_\alpha(\alpha) \mathcal{F}_\beta(\beta) \mathcal{F}_h(h) \mathcal{F}_{kT}(kT) \quad (\text{XVI.C.7.b})$$

Figures XVI.C.7.a,b,c,d give the dependence of the (dimensionless) drift on some of the parameters. ($D \equiv$ drift)

(i) \mathcal{F}_{kT} (Fig. XVI.C.7.a)

$$D \sim e^{m_1 kT}$$

$$m_1 = \frac{\Delta \ln D}{\Delta kT} \doteq -1.8$$

$$\mathcal{F}_{kT} = e^{-1.8 kT}$$

(ii) \mathcal{F}_h (Fig. XVI.C.7.b)

$$D \sim h - a e^{m_2 h}$$

$$\ln(h-D) = m_2 h + \ln a$$

$$m_2 = \frac{\Delta \ln(h-D)}{\Delta h} \doteq 3.4$$

$$a = (h-D)e^{-3.4 h} \doteq .03 \quad \text{when } h=.8$$

$$\mathcal{F}_h = h - .03 e^{3.4 h}$$

(iii) \mathfrak{F}_β (Fig. XVI.C.7.c)

$$D \sim \beta^{m_3}$$

$$m_3 = \frac{\Delta \ln D}{\Delta \ln \beta} \doteq 2.3$$

$$\mathfrak{F}_\beta = \beta^{2.3}$$

(iv) \mathfrak{F}_α

We can find \mathfrak{F}_α by considering the dependence of the drift on the frequency at constant c (Fig. XVI.C.7.d).

$$D \sim \omega^{m_4}$$

$$m_4 = \frac{\Delta \ln D}{\Delta \ln \omega} \doteq .94$$

$$D \sim \omega^{.94}$$

Changes in ω for fixed c cause the dimensionless quantities α and T to vary according to*

$$T \equiv \frac{M\omega}{G} \quad \alpha \equiv \frac{\omega d}{c}$$

The change in T in terms of α is then

*

Also see section XVI.C.3.

$$T = \frac{\mu \omega}{G} = \frac{\mu c}{G d} \alpha \quad (\text{XVI.C.7.c})$$

For normal values of μ, c, G, d (section VIII.D.8.) we have $T = 1.5(10^3) \alpha$. Thus in order to find β_α , we must take β_{KT} into account by using $T = 1.5(10^3) \alpha$.

Considering α and T to change for changing ω , we get

$$D \sim \beta_\alpha(\alpha) e^{-1.8 K (1.5)(10^3) \alpha}$$

Since $K = K_N = .67(10^{-4})$, then $K (1.5)(10^3) = .1$ and

$$D \sim \beta_\alpha(\alpha) e^{-1.18 \alpha} \quad (\text{XVI.C.7.d})$$

But $D \sim \omega^{.94} = C \alpha^{.94}$ so that (XVI.C.7.d) gives:

$$C \alpha^{.94} = \beta_\alpha(\alpha) e^{-1.18 \alpha}$$

or $\beta_\alpha(\alpha) = C e^{1.18 \alpha} \alpha^{-.94}$

The complete form of the dependence of the cyclic drift of a mucous particle valid near the normal* state is

*

This equation may not be valid at other limiting states.

$$D = C \epsilon^2 \underbrace{\alpha^{.94}}_{\beta_\alpha} e^{.18 \alpha^{2.3}} \left(h - .03 e^{3.4 h} \right) \underbrace{e^{-1.8 kT}}_{\beta_{kT}}$$

(XVI. C. 7. e)

Note that the drift depends on $kT = \frac{\bar{\mu}\omega}{G}$ so that the mucous layer acts like an elastic slab near the normal state.

DRIFT AS A FUNCTION OF kT

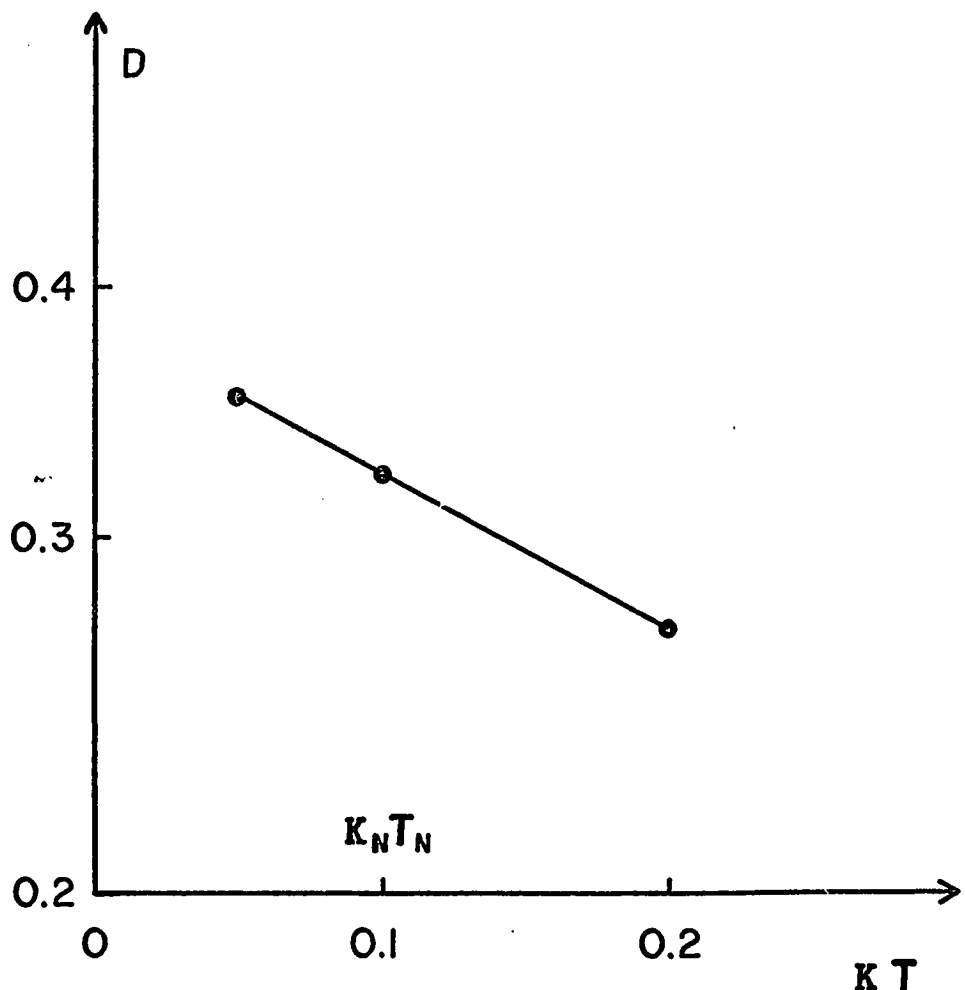


Fig. XVI.C.7.a

DRIFT AS A FUNCTION OF h

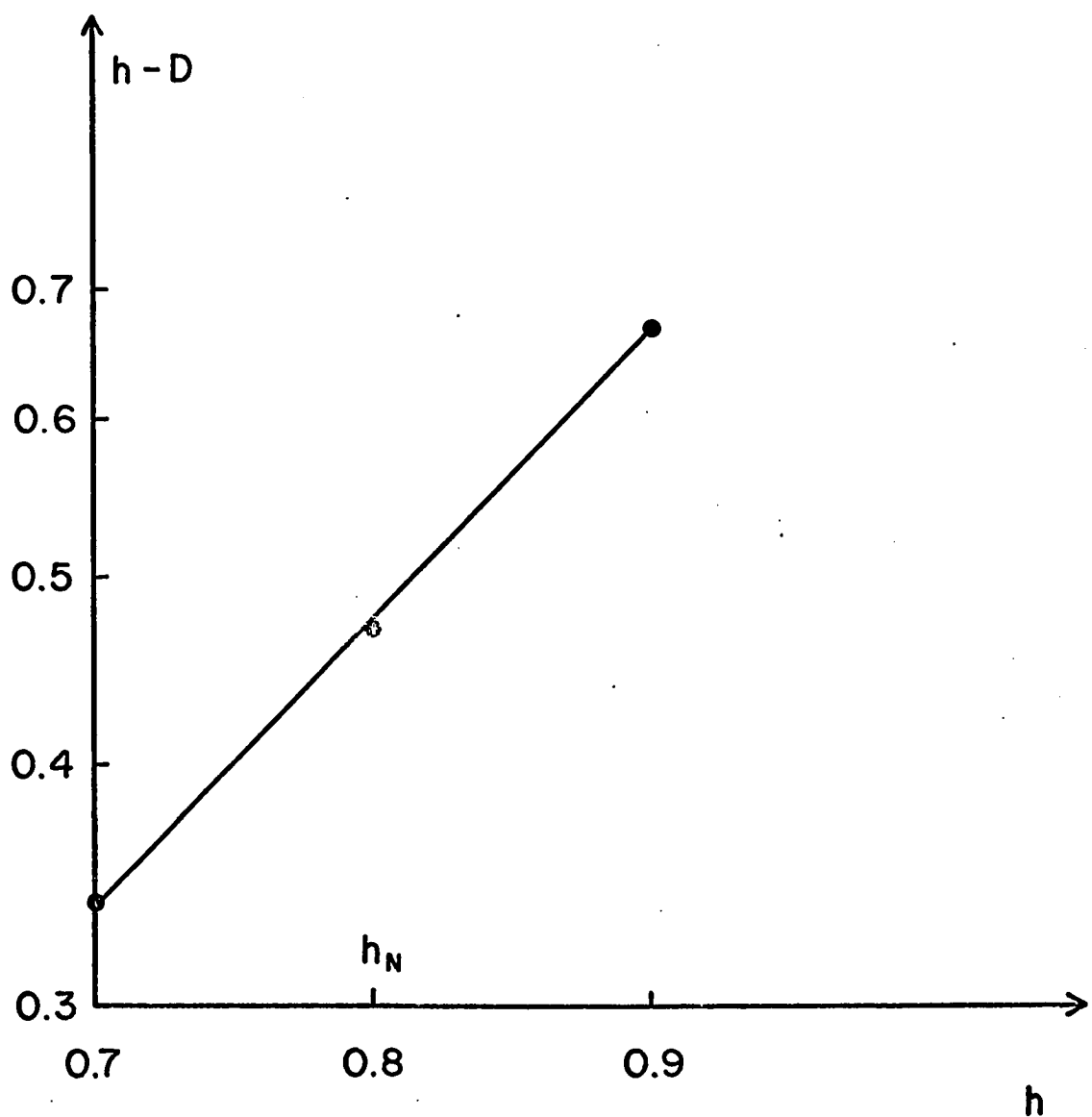


Fig. XVI.C.7.b

DRIFT AS A FUNCTION OF β

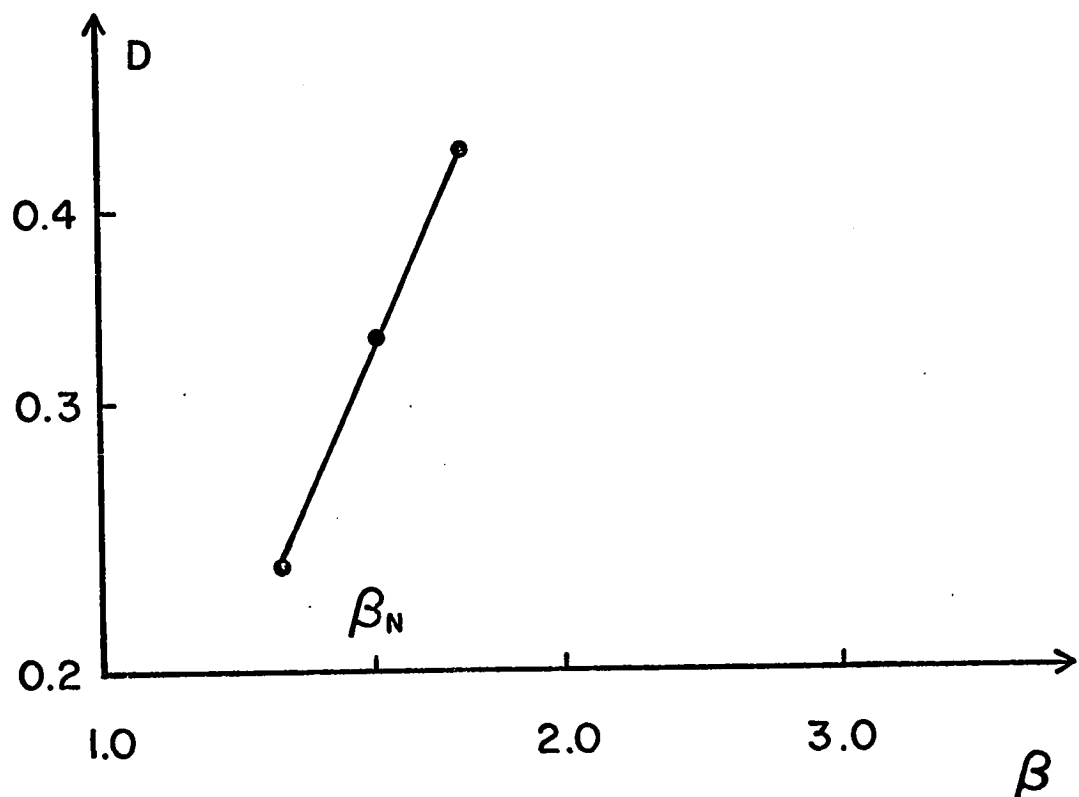


Fig. XVI.C.7.c

DRIFT AS A FUNCTION OF ω
AT CONSTANT WAVE SPEED

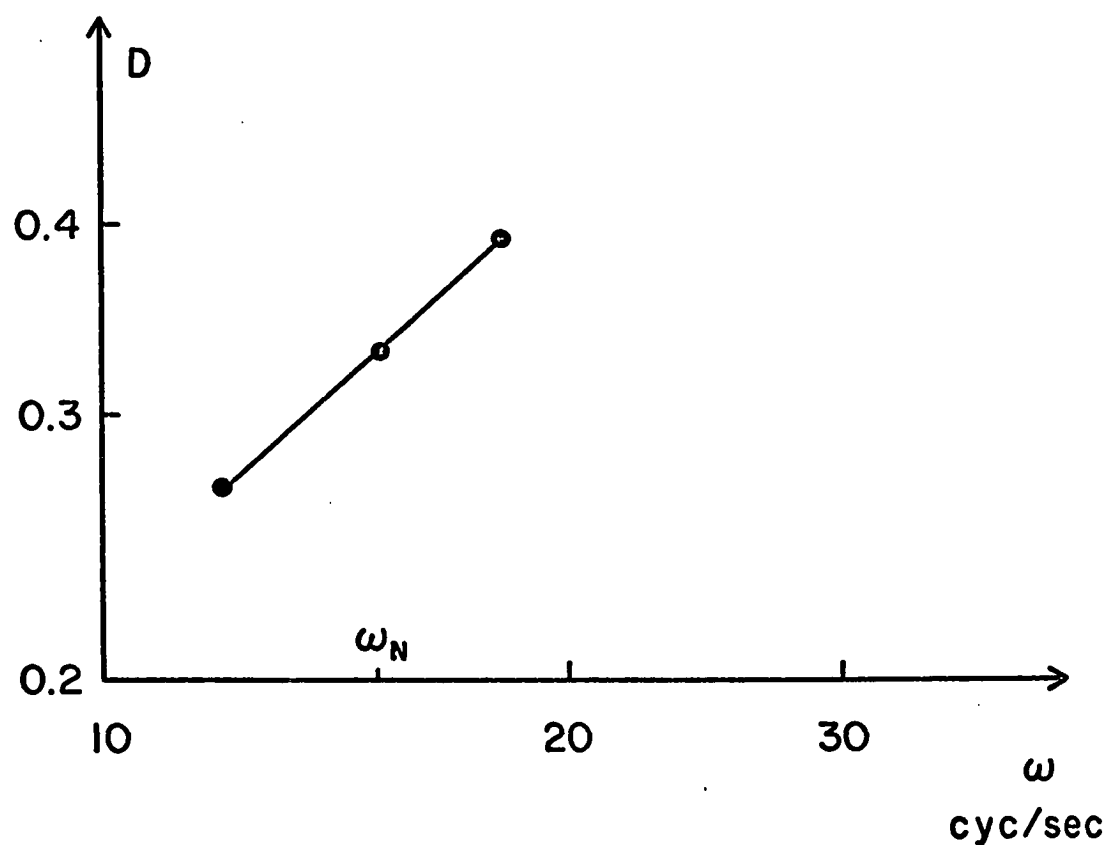


Fig. XVI.C.7.d

XVI.C.8. Tables of drifting tendencies and power expended.

From the computed results, the qualitative effect on the cyclic material drift of varying the eight dimensional constants and the dimensionless constant β can be listed in table form.

↑ denotes increasing in value

↓ denotes decreasing in value

Some of the factors tending to increase the fluid material drift are:

1. increasing the horizontal and/or vertical axes of the wall particle ellipse (β and Θ) that corresponds to the cilium tip.
2. increasing the modulus of rigidity (G) of the mucus so that it behaves more like a Newtonian fluid. In other words, decreasing the compliance (thus relaxation time) of the mucus while its viscosity is held constant should tend to increase the drift.
3. decreasing the viscosity of the serous fluid sublayer.
4. decreasing the wavelength of the metachronal wave or the wave speed while keeping the frequency fixed.
5. increasing the frequency of the ciliary beat while keeping wave speed fixed.

Change in dimensional constant	Change in dimensionless constant	Change in material drift
1. sublayer viscosity $\bar{\mu} \downarrow$	$K \downarrow$	\uparrow
2. mucous viscosity $\mu \uparrow$	$K \downarrow$ $T \uparrow$	$\uparrow \doteq 0$ \downarrow
3. modulus of rigidity $G \uparrow$	$T \downarrow$	\uparrow
4. frequency of beat $\omega \uparrow$ fixed c	$T \uparrow$ $\alpha \uparrow$	$\downarrow = \uparrow$ \uparrow
fixed λ	$T \uparrow$	\downarrow
5. total depth $d \uparrow$	$\alpha \uparrow$ $\epsilon \downarrow$	$\uparrow \doteq 0$ \downarrow
6. wavelength and wave speed (ω fixed), $\lambda \uparrow$, $c \uparrow$	$\alpha \downarrow$	\downarrow
7. vertical wall particle amplitude $\theta \uparrow$	$\epsilon \uparrow$	\uparrow
8. depth of mucus $h \uparrow$	$h' \uparrow$	\downarrow
9. horizontal to vertical wall particle amplitude ratio	$\beta \uparrow$	\uparrow

Table XVI.C.8.a

It is also informative to consider how the work rate at the wall (power expended by the cilia tips) varies with changes in some of the parameters.

change in dimensional constant	power expended at the wall
$\bar{\mu} \uparrow$	\uparrow
$G \uparrow$	\uparrow
$\omega \uparrow$ (fixed λ)	\uparrow

Table XVI.C.8.b

XVI.D. The Full Newtonian Fluid Case

The flow of a purely Newtonian fluid induced by a waving wall with a free surface is fundamentally different from a peristaltic pump (see section III.) in which there is no free surface and the fluid is squeezed between two waving walls. It is of general intrinsic interest to consider the flow of a single Newtonian fluid under various changes in some of the parameters.

Small departures from a reference fluid will be considered

by separately increasing both the relaxation time (from zero) and viscosity of the upper fluid so that $\frac{1}{K}$ is greater than unity and T is greater than zero thereby making the fluid slightly visco-elastic.

The case of a Newtonian upper fluid of nearly the same viscosity as the sublayer is not at all close to that of the normal muco-ciliary flow, but may apply in some extreme pathological situations. As noted before (section XVI.C.), the solution to the general flow problem depends on $\Theta = K + iKT$. For a single Newtonian fluid, $K=1$ and $T=0$ but for normal muco-ciliary flow, $K=O(10^{-4})$ and $T=O(10^3)$. Thus in one case, the complex number Θ is primarily real and in the other, it is primarily imaginary. The solutions are different in character.

XVI.D.1. Figures XVI.D.1.a,b,c,d,e: Effect of axis ratio (β) on single Newtonian fluid

Figures XVI.D.1.a and b show the drift and the particle trajectories at three distances from the wall for the cases with circular clockwise ($\beta=1$) and counterclockwise ($\beta=-1$) wall particle paths. Figure XVI.D.1.c indicates that the drift is positive when $\beta=-1$ and that for small $|\beta| < 1$,

there is a "back flow" near the wall (i.e. the drift is negative). In particular, there is a net negative drift for the case of $\beta = 0$ (vertical wall particle path); this case corresponds to that of an inextensible wall to first order in ϵ . * The above phenomenon can be explained by the importance of the longer and shorter regions of the wall curve in the limiting cases where $|\alpha\beta| \rightarrow 0$ and $|\alpha\beta| \rightarrow 1$ as discussed in section VI.C.7.

The vertical amplitude of a fluid particle trajectory (Fig. XVI.D.1.d), hence the free surface amplitude (Fig. XVI.D.1.e), increases as β decreases. This may be due to the fact that as β decreases, the length of the crest of the wall curve decreases ** so that the net effect may be likened to that of a steepening bump:



This might induce a larger amplitude in the free surface.

*

See section VI.C.6.

**

See section XVI.C.7.

XVI.D.2. Figures XVI.D.2.a,b,c: Relaxation time ($\tau = \omega \zeta_R$), nearly Newtonian fluid (two layers)

Non-zero values of the relaxation time of the upper fluid introduce a non-zero imaginary part for the complex quantity $\Theta = k + i\kappa\tau$ on which the solution depends. Specifically, the Fourier coefficient $c_2^{(1,0)}$ is real when $\tau=0$ but it is complex when $\tau \neq 0$. This can be seen directly from the matrix (section XI.D.) of the coefficients*, or it can be determined simply from the computer output.

For a Newtonian flow ($\tau=0$), $c_2^{(1,0)}$ is real, and from the equation, $\eta^{(1,0)} = -\text{Re} \{ i c_2^{(1,0)} e^{i\phi} \}$, we obtain a pure sine curve for the free surface to order ϵ . Hence, there is no phase shift between the wall and the free surface for a Newtonian flow, at least to first order (Figs. XVI.D.4,5). However, a visco-elastic case (complex $c_2^{(1,0)}$) gives both sine and cosine terms; there is a phase shift when $\tau \neq 0$ (Fig. XVI.D.2.c).

Figure XVI.D.2.b indicates that the elasticity of the upper layer gives a fluid point a large displacement and recoil; a "spring-like" behavior. This decreases net drift

*

All components of ζ_i and \mathbf{x}_{ij} are real if $\tau=0$ so that the solution vector ζ_i is also real thus implying that $c_2^{(1,0)}$ is real.

per cycle and flattens the drift profile as relaxation time increases.

Notably there is no maximum in the drift profile in the sublayer region for these slightly visco-elastic cases (Fig. XVI.D.2.a). We may infer that the upper layer here is "pumped along", rather than being primarily "dragged along" by the sublayer.

Figure (XVI.D.3.a) shows that when the upper layer is Newtonian but much more viscous than the sublayer, it must be dragged along.

XVI.D.3. Figures XVI.D.3.a,b,c: Viscosity ratio ($\kappa = \frac{\bar{\mu}}{\mu}$)

In the Newtonian case ($G=\infty$ or $T=0$) changes in either the sublayer or upper layer viscosity cause corresponding changes only in the parameter κ ; unlike the case for a visco-elastic upper layer ($G < \infty$) in which changes in $\bar{\mu}$ and μ must be considered separately.* Increasing the upper layer viscosity (decreasing κ) causes the cyclic drift to decrease (Fig. XVI.D.3.a) and the trajectory of a fluid particle to become less elongated (Fig. XVI.D.3.b). Decreasing κ

* If $\bar{\mu} \uparrow$, $\kappa \downarrow$ but if $\mu \downarrow$ then $\kappa \uparrow$ and $T \downarrow$.

also gives a maximum in the drift curve for small enough values (Fig. XVI.D.3.a). Although the drift curves flatten out in the upper fluid region for both increasing relaxation time and decreasing viscosity ratio, their effects on the solution in the sublayer region must be different because there is no bump evident in Figure XVI.D.2.a.

The free surface is in phase with the wall for different values of κ (Fig. XVI.D.3.c), in agreement with our previous discussion (section XVI.D.2).

For a fixed outer fluid layer viscosity, decreasing sublayer viscosity results in a smaller energy dissipation (or wall power) which could allow larger free surface amplitudes.*

*

The computed values of energy dissipation are (dimensionless):

$$\kappa = .95 \quad \mathfrak{D}^* \doteq .4$$

$$\kappa = .50 \quad \mathfrak{D}^* \doteq .3$$

$$\kappa = .10 \quad \mathfrak{D}^* \doteq .12$$

where $\mathfrak{D} = \mu \omega^2 d^2 \mathfrak{D}^*$.

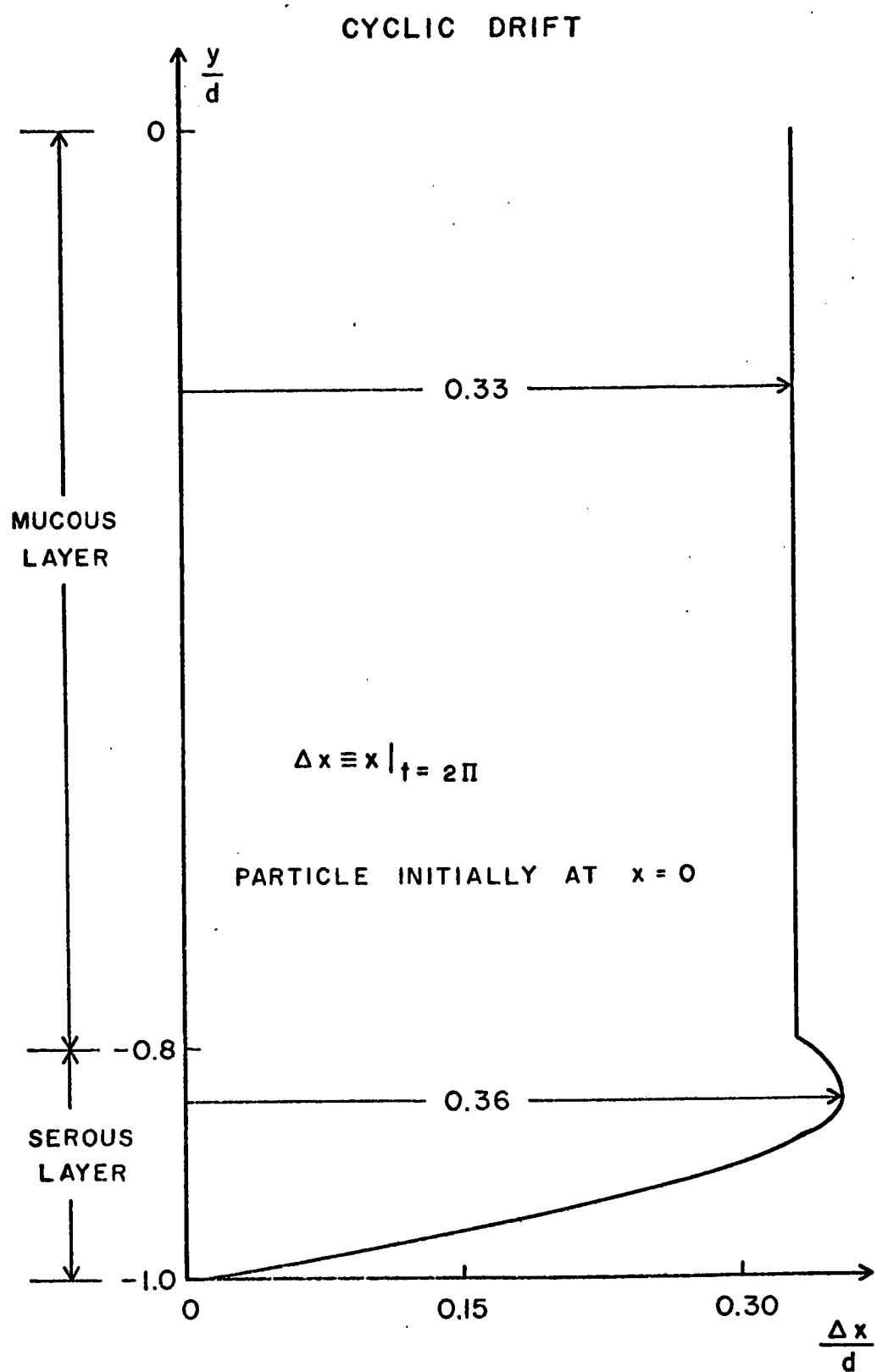


Fig. XVI. B.1

FREE SURFACE AND INTERFACE

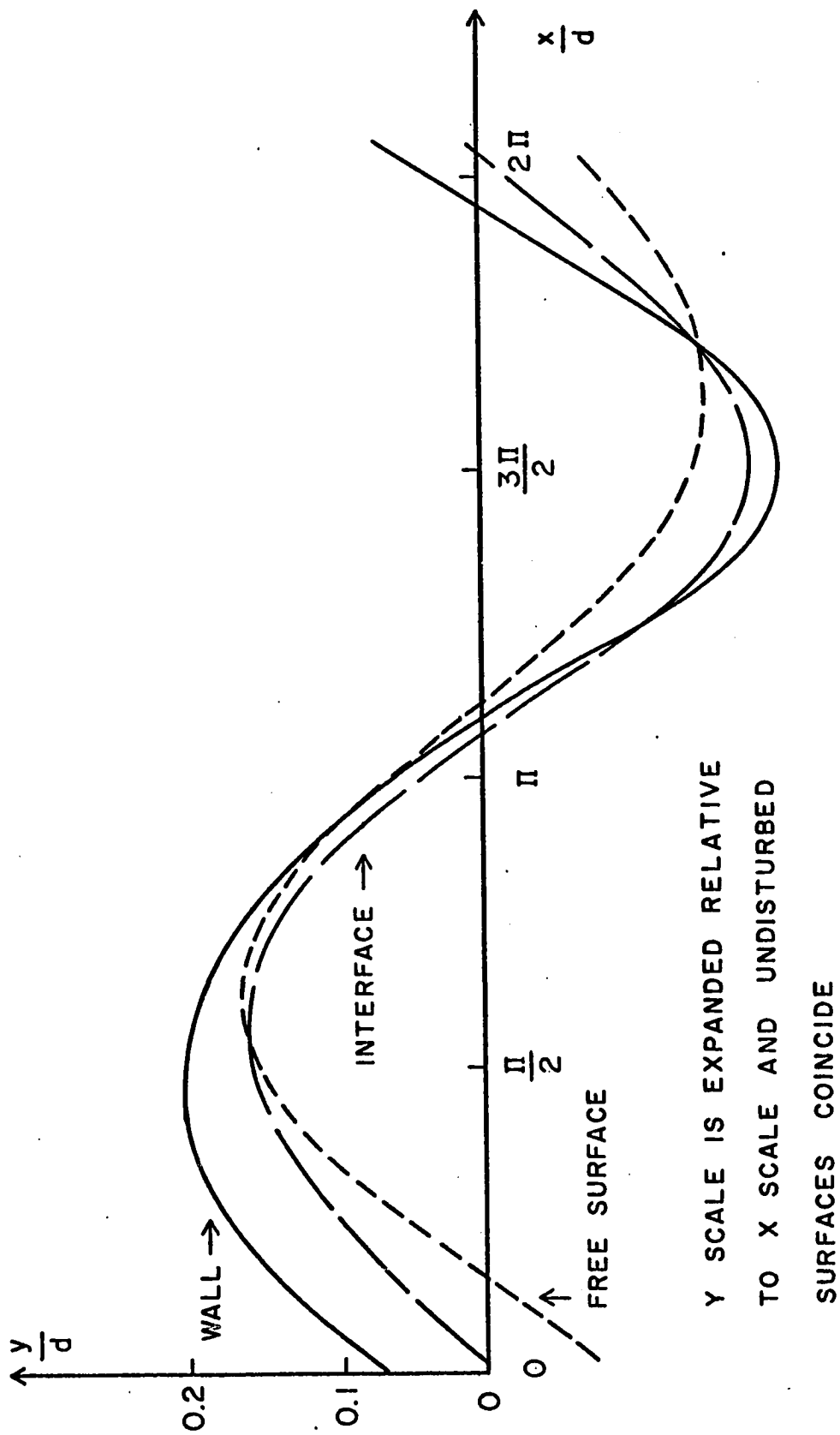


Fig. XVI. B. 2

Y SCALE IS EXPANDED RELATIVE
TO X SCALE AND UNDISTURBED
SURFACES COINCIDE

CYCLIC TRAJECTORIES

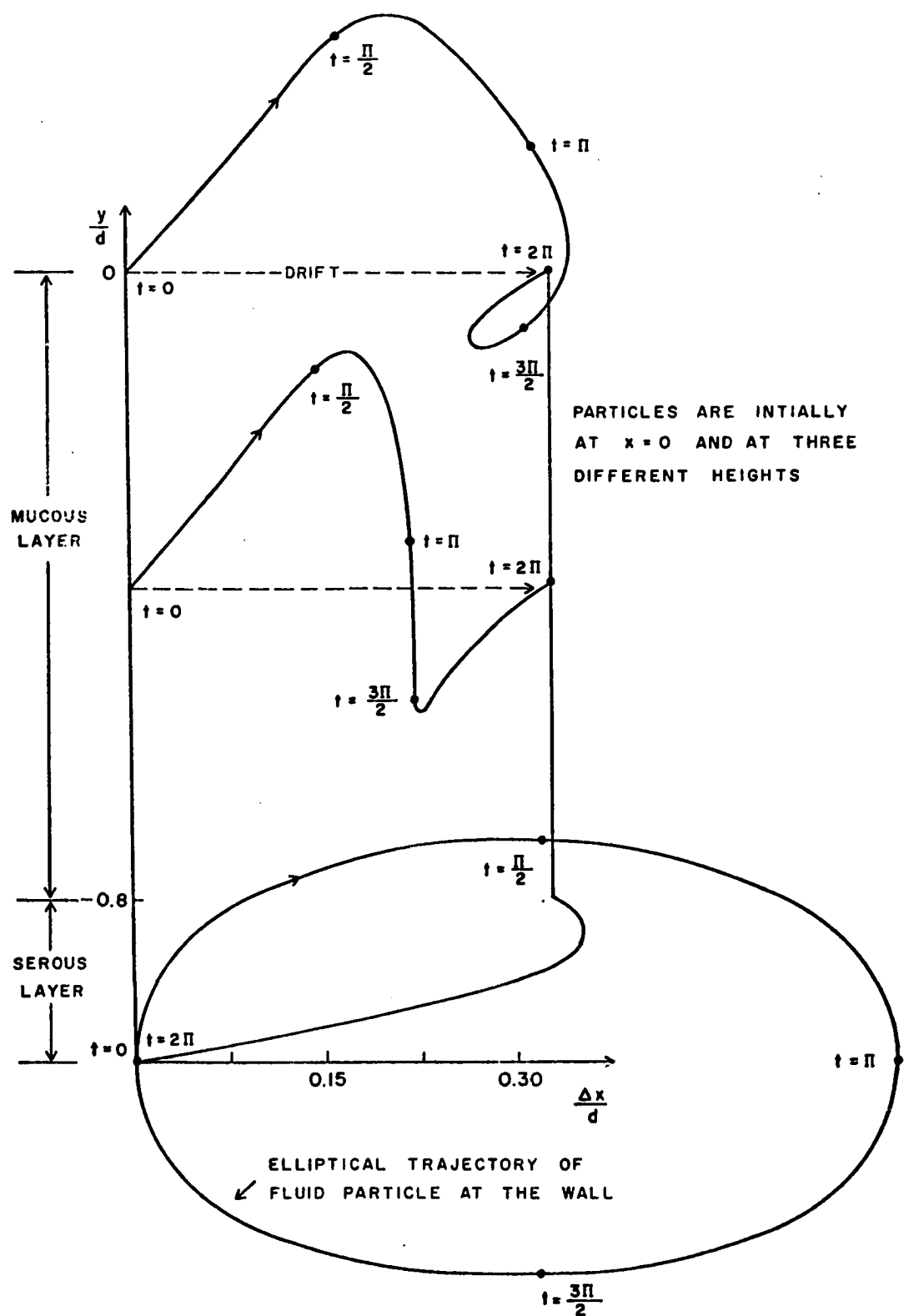


Fig. XVI. B. 3

CYCLIC DRIFT FOR DIFFERENT
SUBLAYER VISCOSITIES

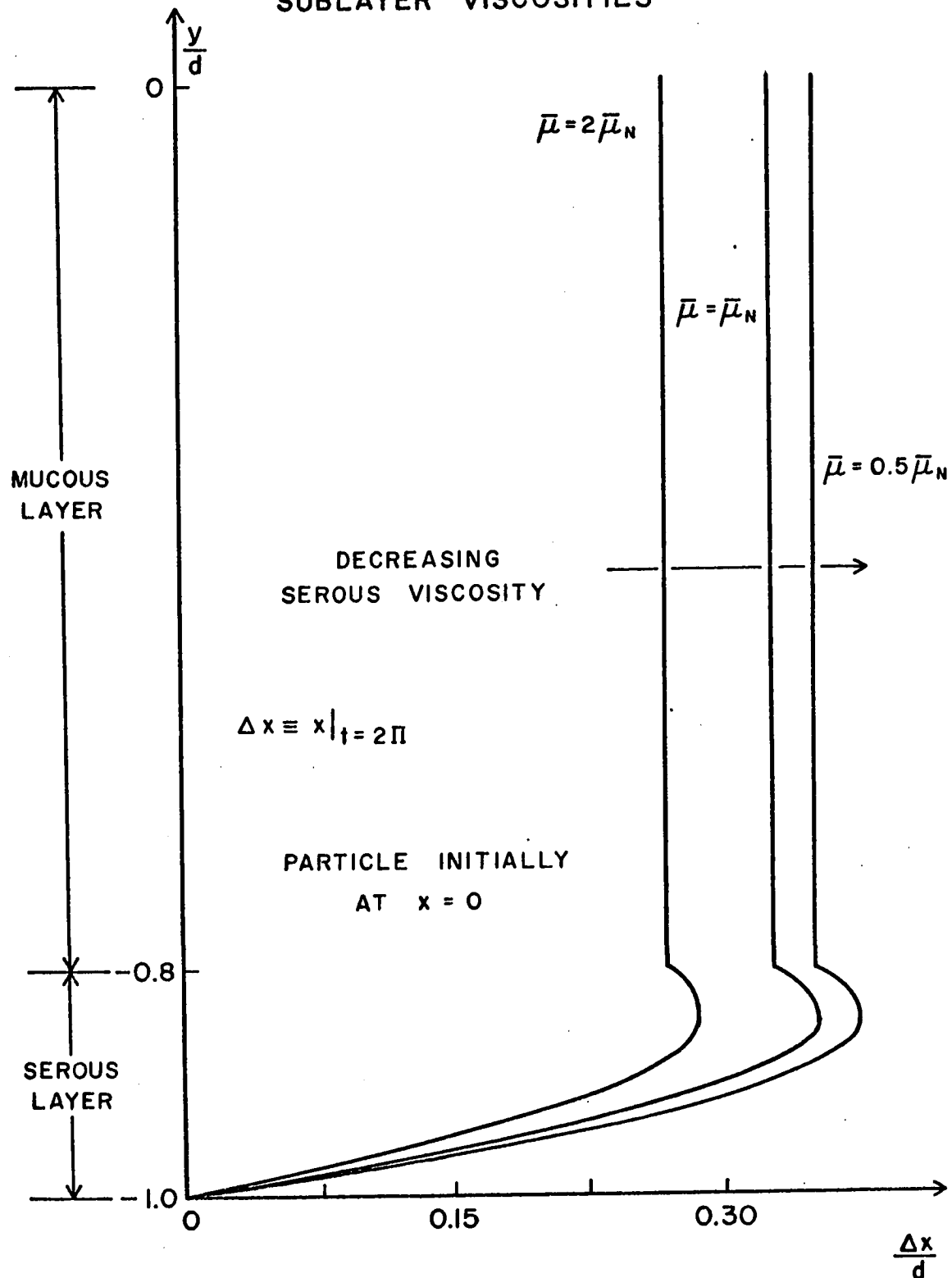


Fig. XVI. C.1.a

CYCLIC PARTICLE TRAJECTORIES FOR
DIFFERENT SUBLAYER VISCOSITIES

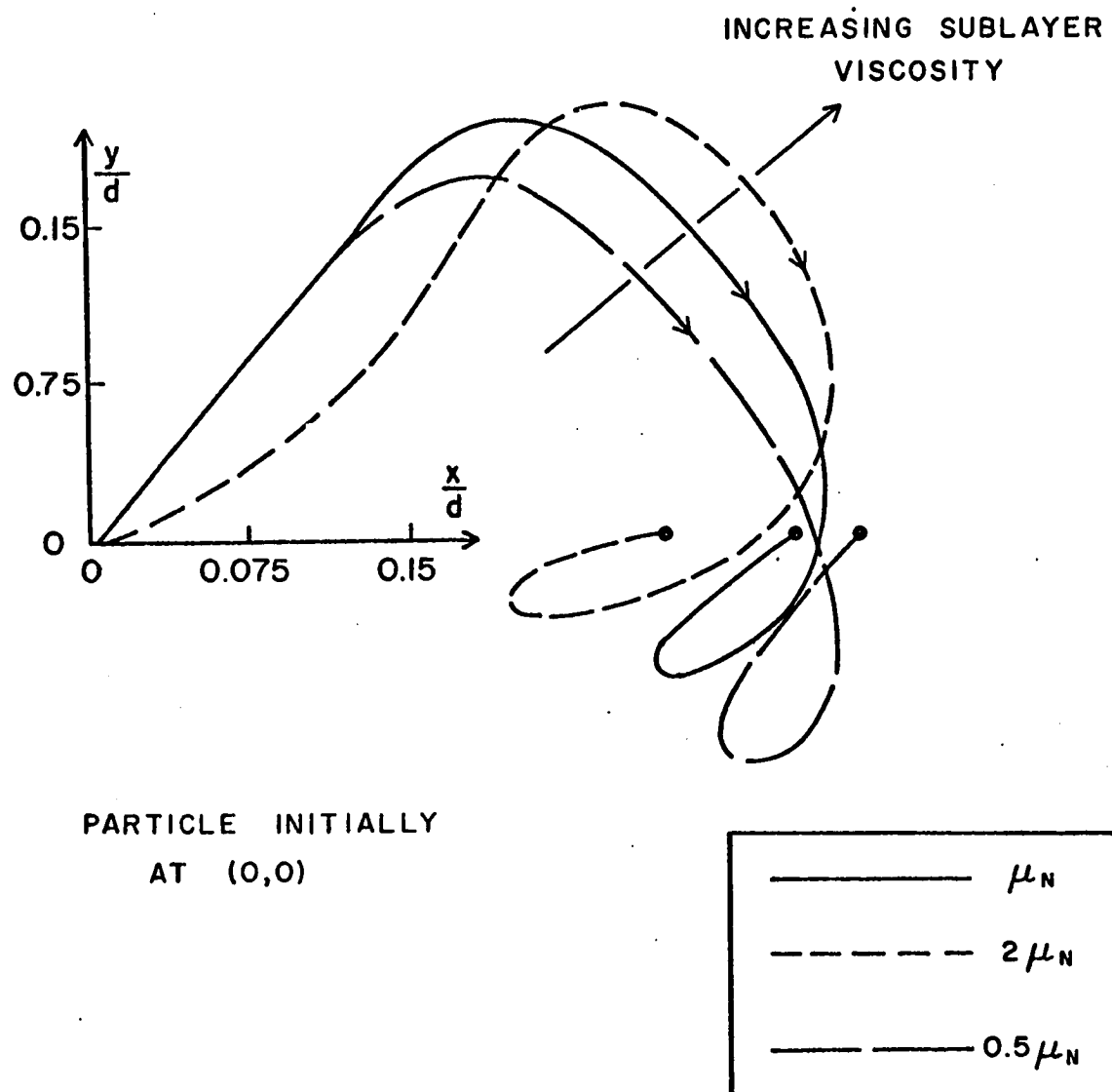


Fig. XVI.C.1.b

CYCLIC DRIFT FOR DIFFERENT MODULI
OF RIGIDITY OR FREQUENCIES
AT CONSTANT WAVELENGTH

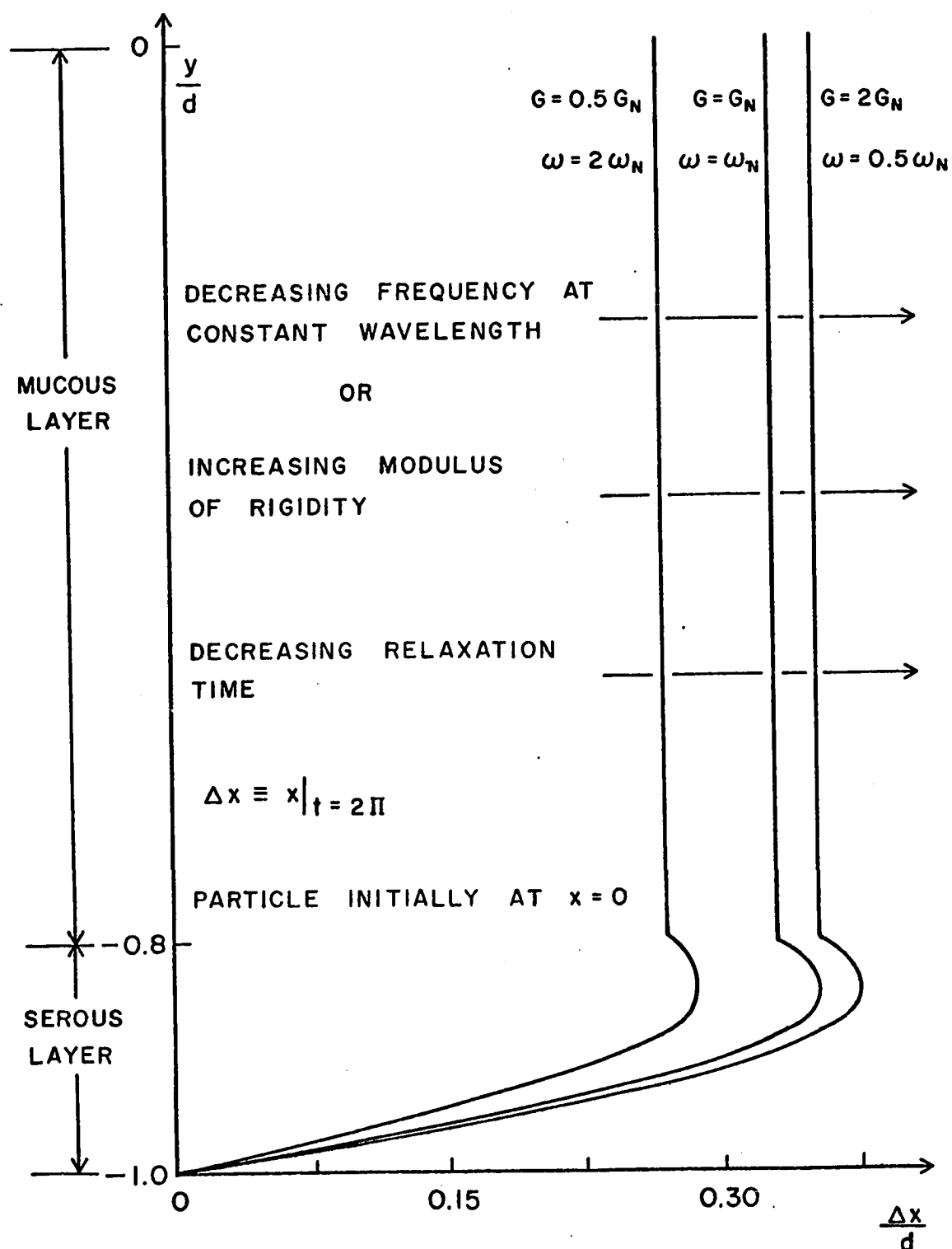


Fig. XVI.C.2.a

CYCLIC PARTICLE TRAJECTORIES FOR
 DIFFERENT MODULI OF RIGIDITY OR
 FREQUENCY AT CONSTANT WAVELENGTH

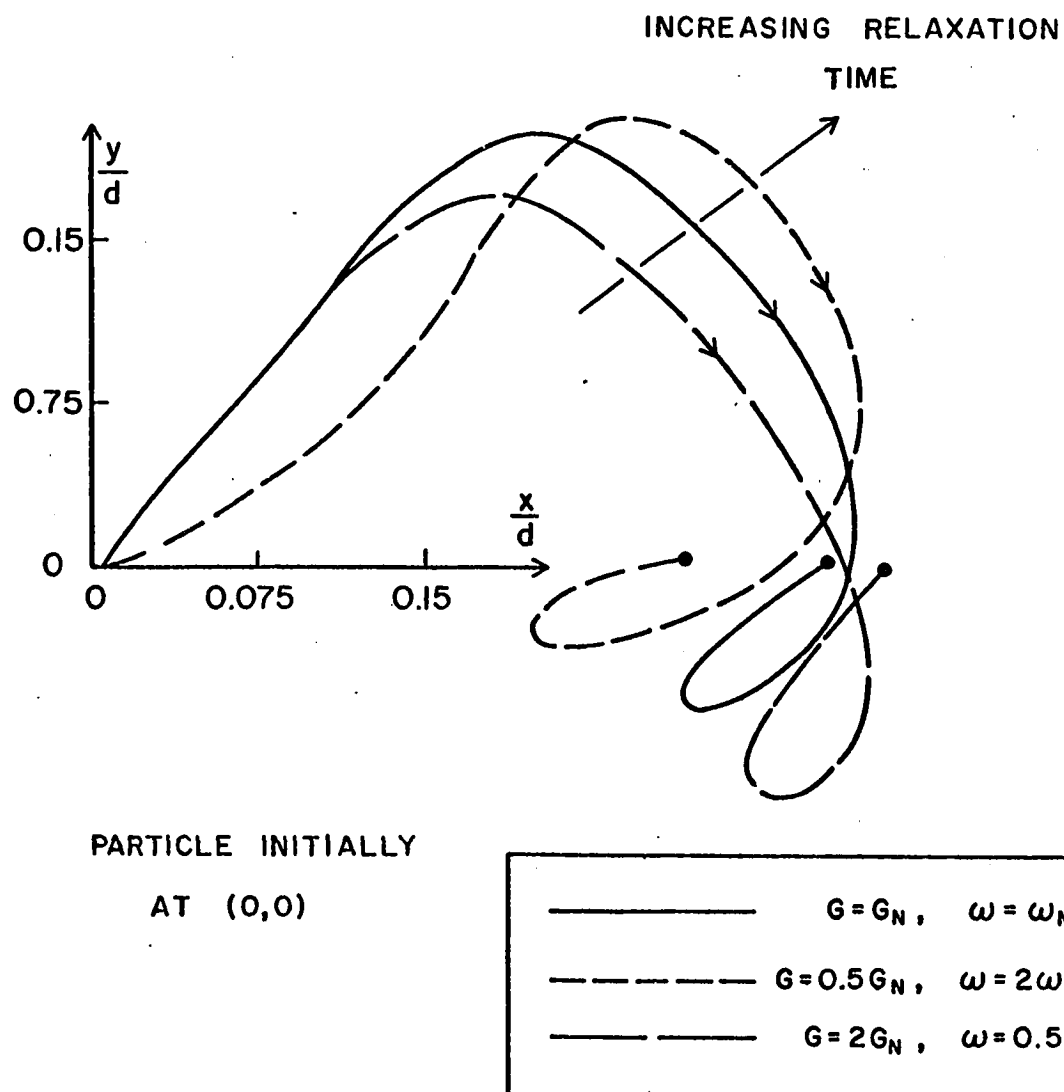


Fig. XVI.C.2.b

CYCLIC DRIFT FOR DIFFERENT FREQUENCIES
AT CONSTANT WAVE SPEED

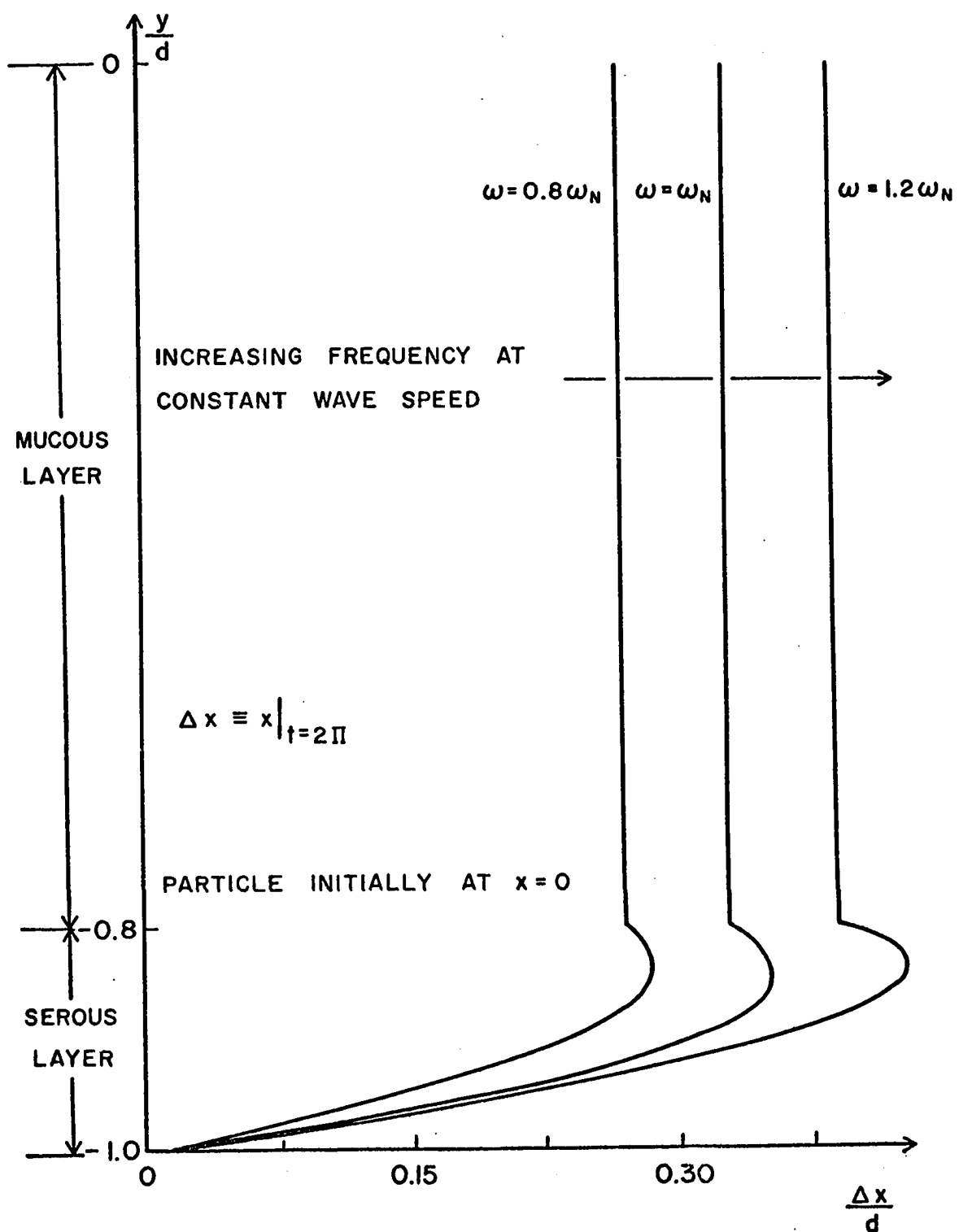


Fig. XVI.C.3

CYCLIC DRIFT FOR DIFFERENT
RELATIVE DEPTHS OF MUCUS

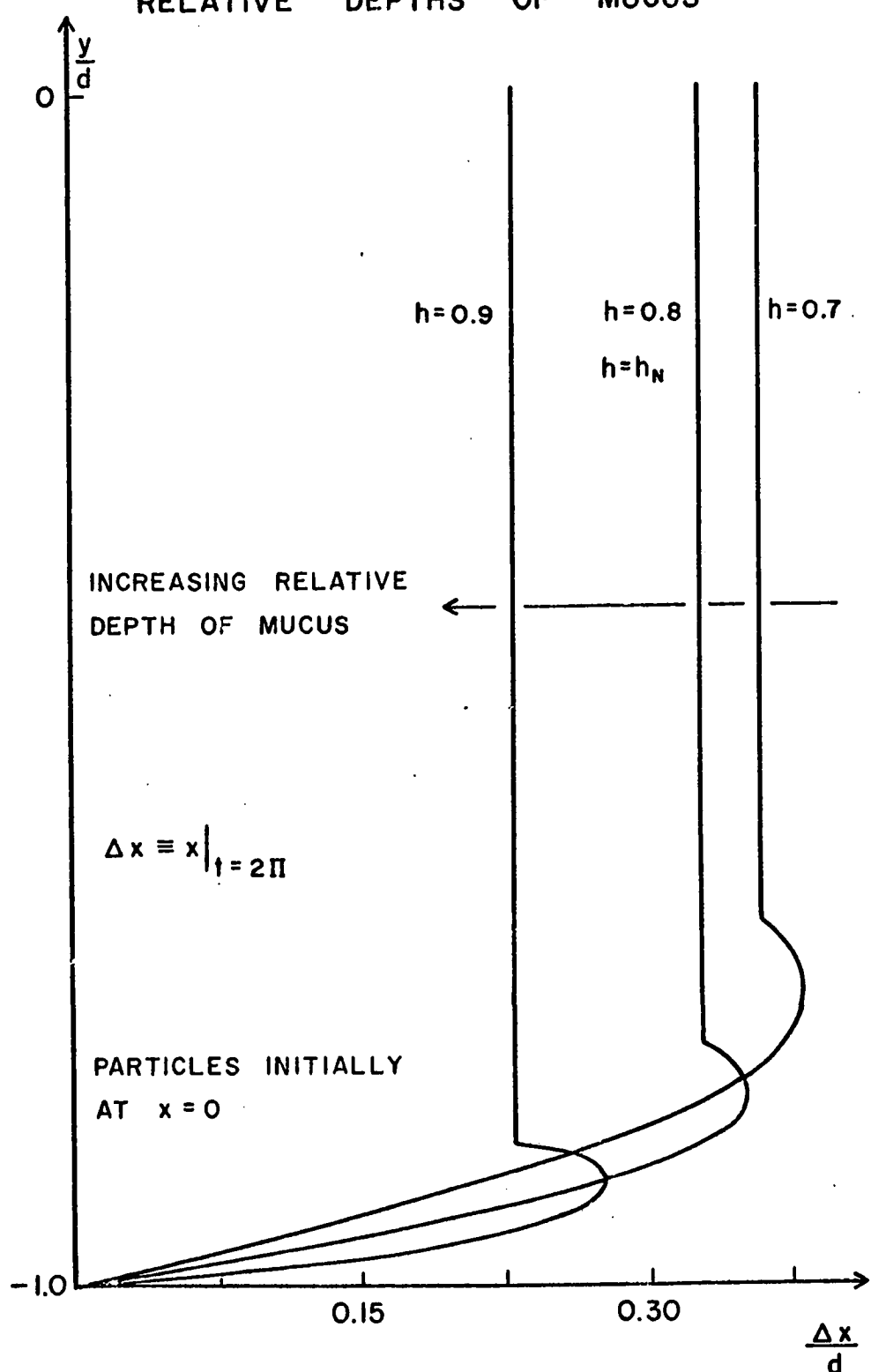


Fig. XVI.C.5

CYCLIC DRIFT FOR DIFFERENT AXIS
RATIOS OF WALL PARTICLE PATH

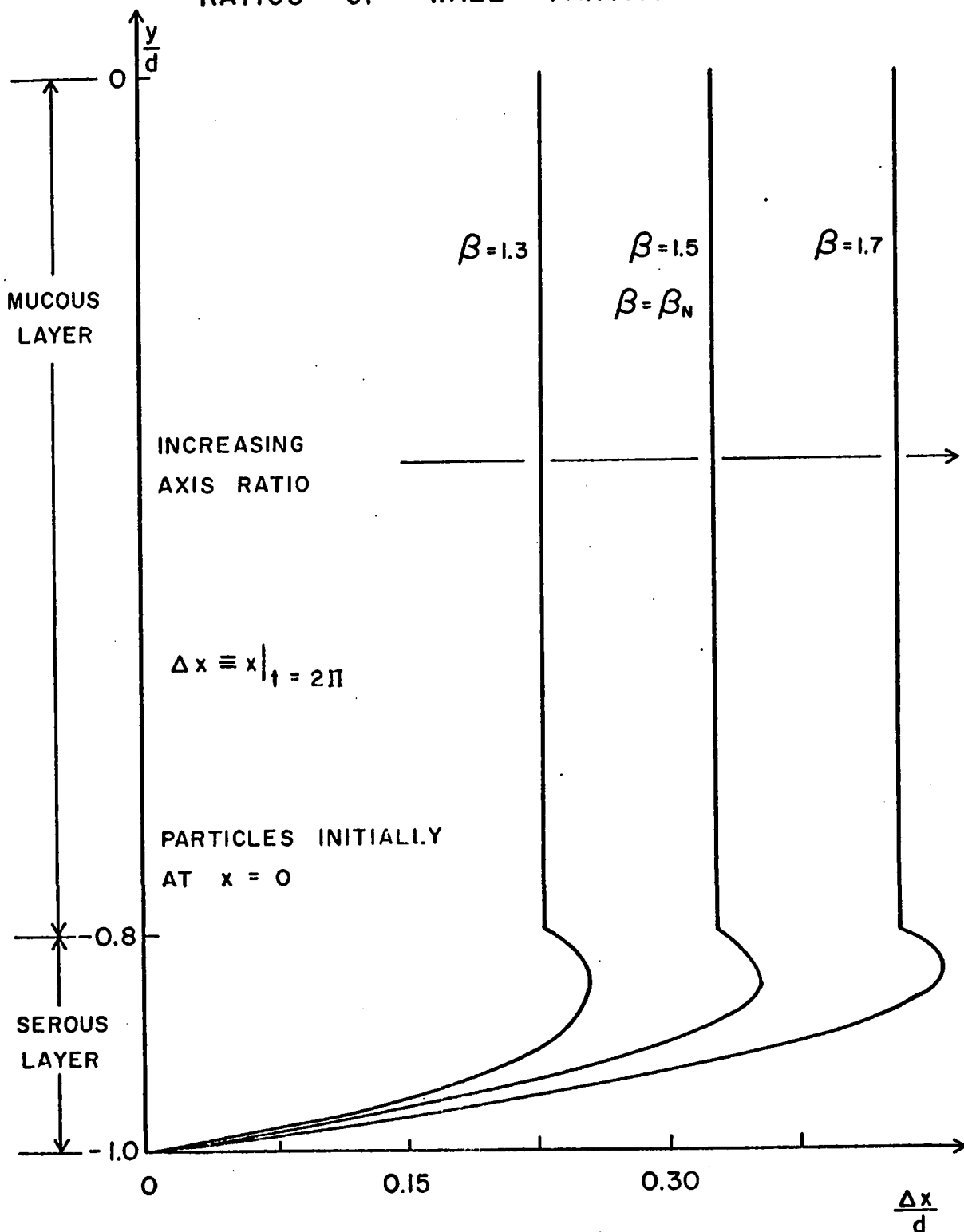


Fig. XVI.C.6

CYCLIC TRAJECTORIES AND DRIFT FOR
CIRCULAR CLOCKWISE WALL PARTICLE PATH
(SINGLE NEWTONIAN FLUID)

PARTICLES
INITIALLY
AT $x = 0$

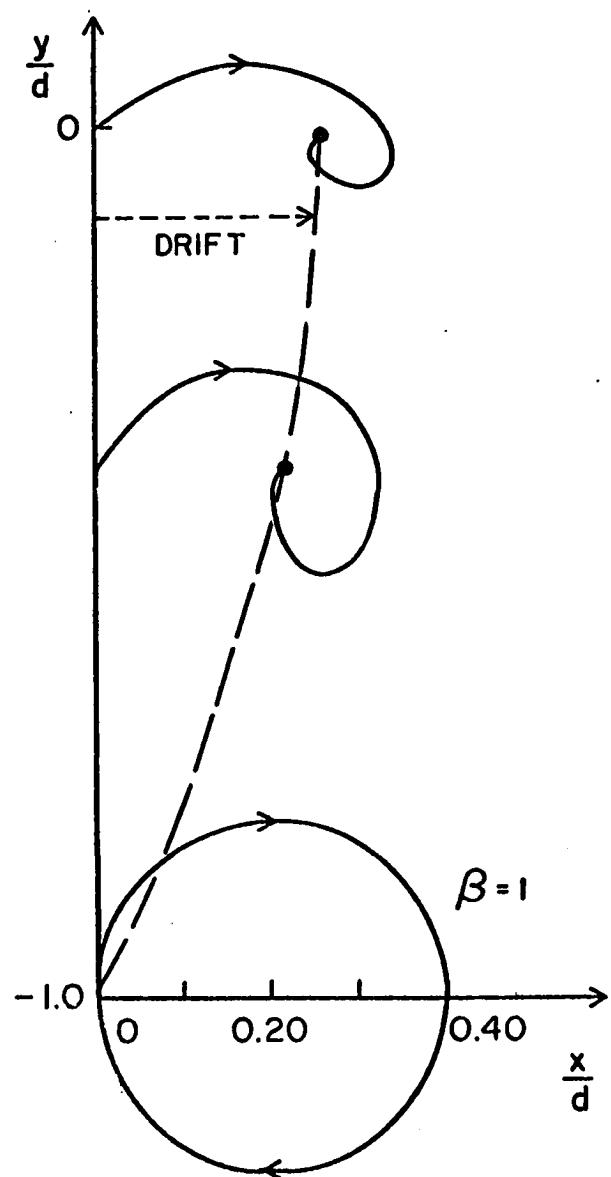


Fig. XVI.D.1.a

CYCLIC TRAJECTORIES AND DRIFT FOR CIRCULAR
COUNTER CLOCKWISE WALL PARTICLE PATH
(SINGLE NEWTONIAN FLUID)

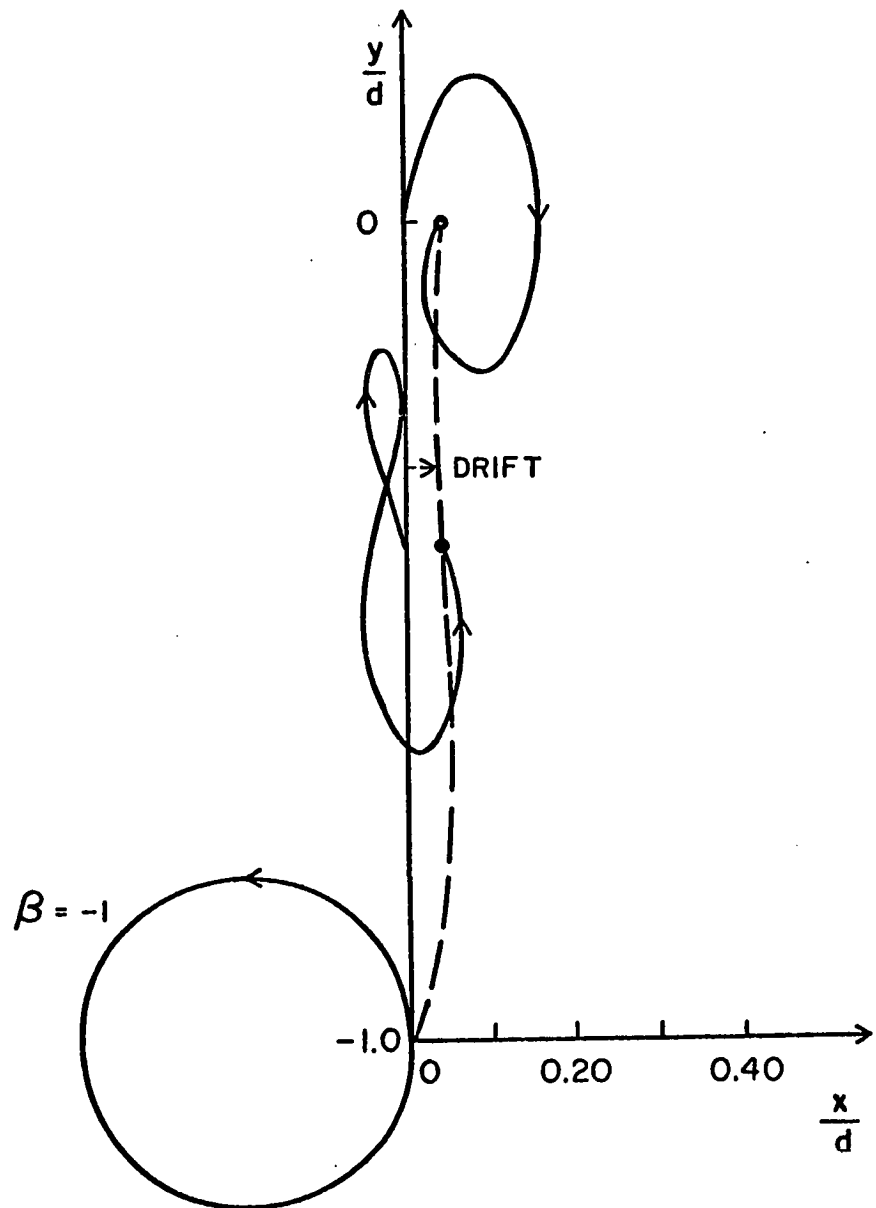


Fig. XVI. D. 1. b

CYCLIC DRIFT FOR DIFFERENT AXIS
RATIOS OF WALL PARTICLE PATH

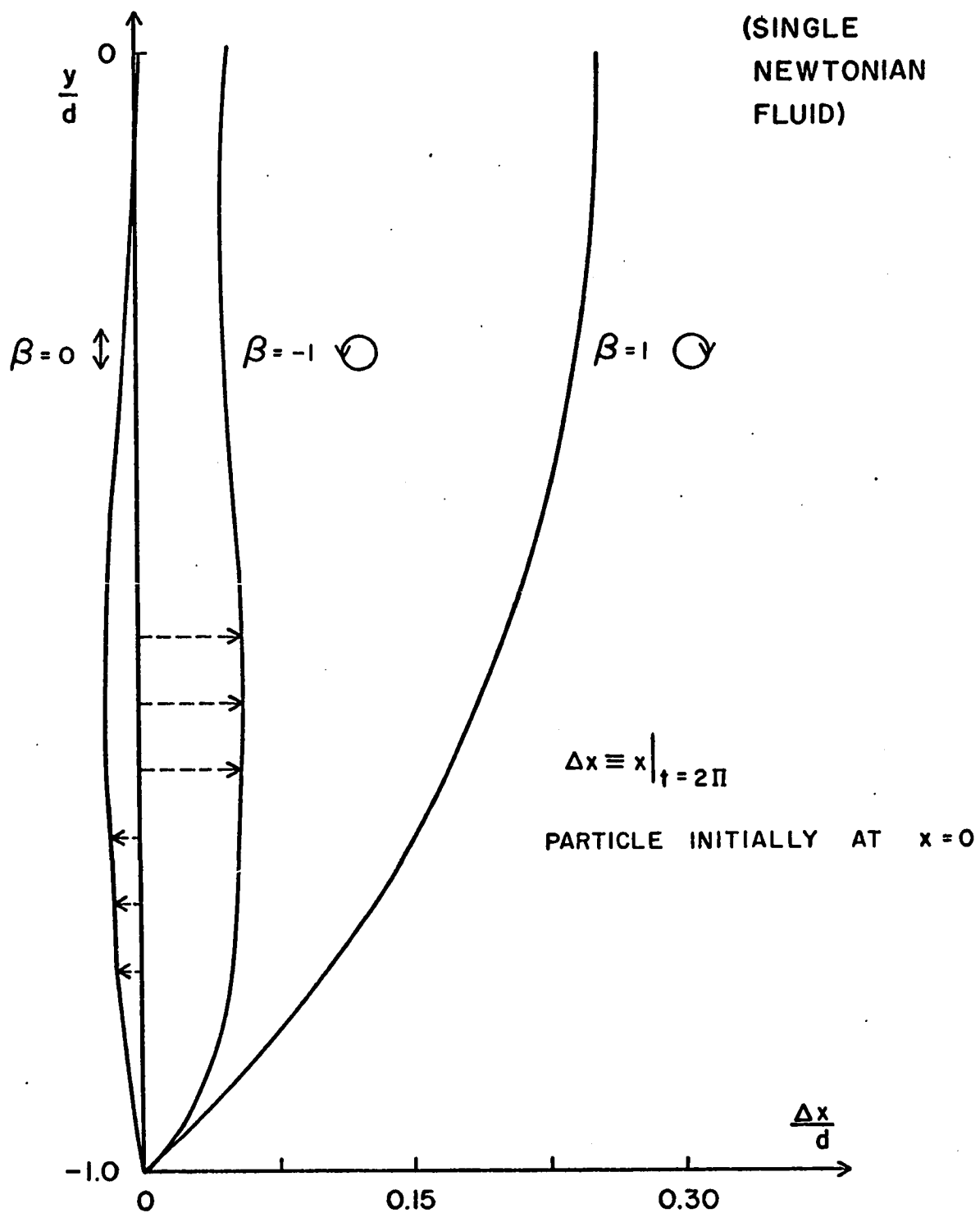


Fig. XVI. D.1.c

CYCLIC PARTICLE TRAJECTORIES FOR
 DIFFERENT AXIS RATIOS OF WALL
 PARTICLE PATH

(SINGLE NEWTONIAN FLUID)

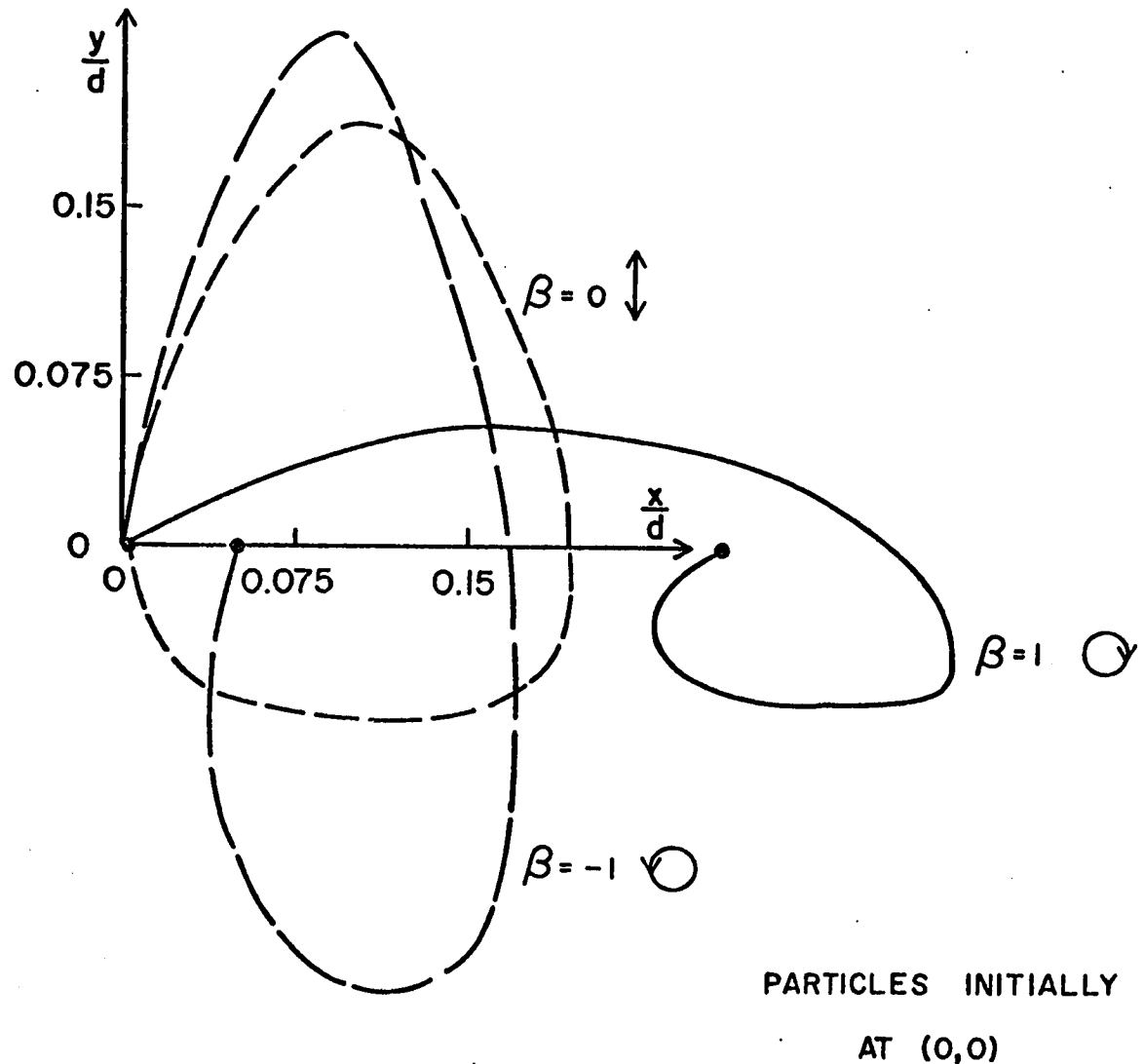


Fig. XVI.D.1.d

FREE SURFACE FOR DIFFERENT AXIS RATIOS OF
 WALL PARTICLE PATH (SINGLE NEWTONIAN FLUID)

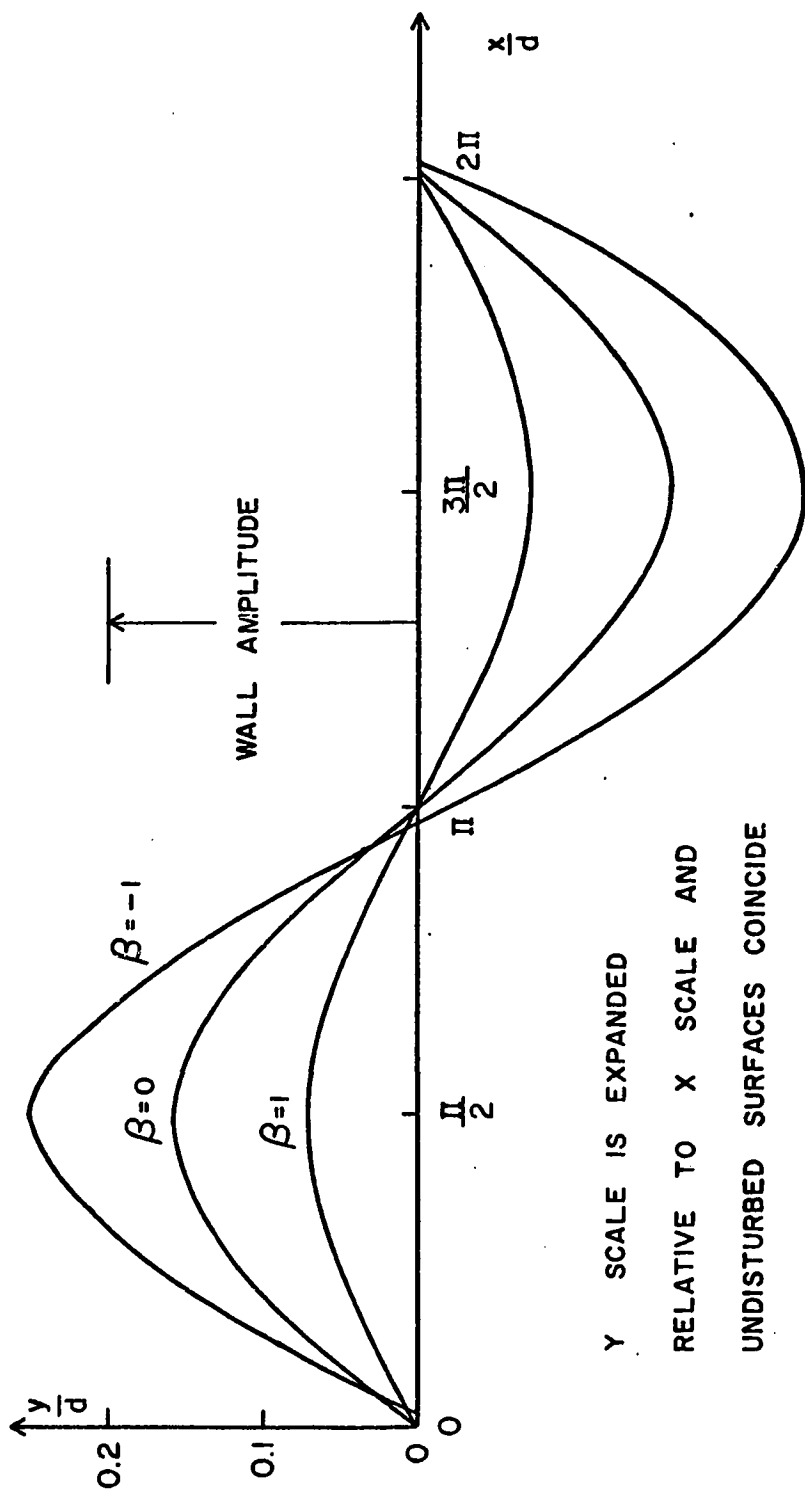


Fig. XVI.D.1.e

CYCLIC DRIFT FOR
DIFFERENT RELAXATION TIMES

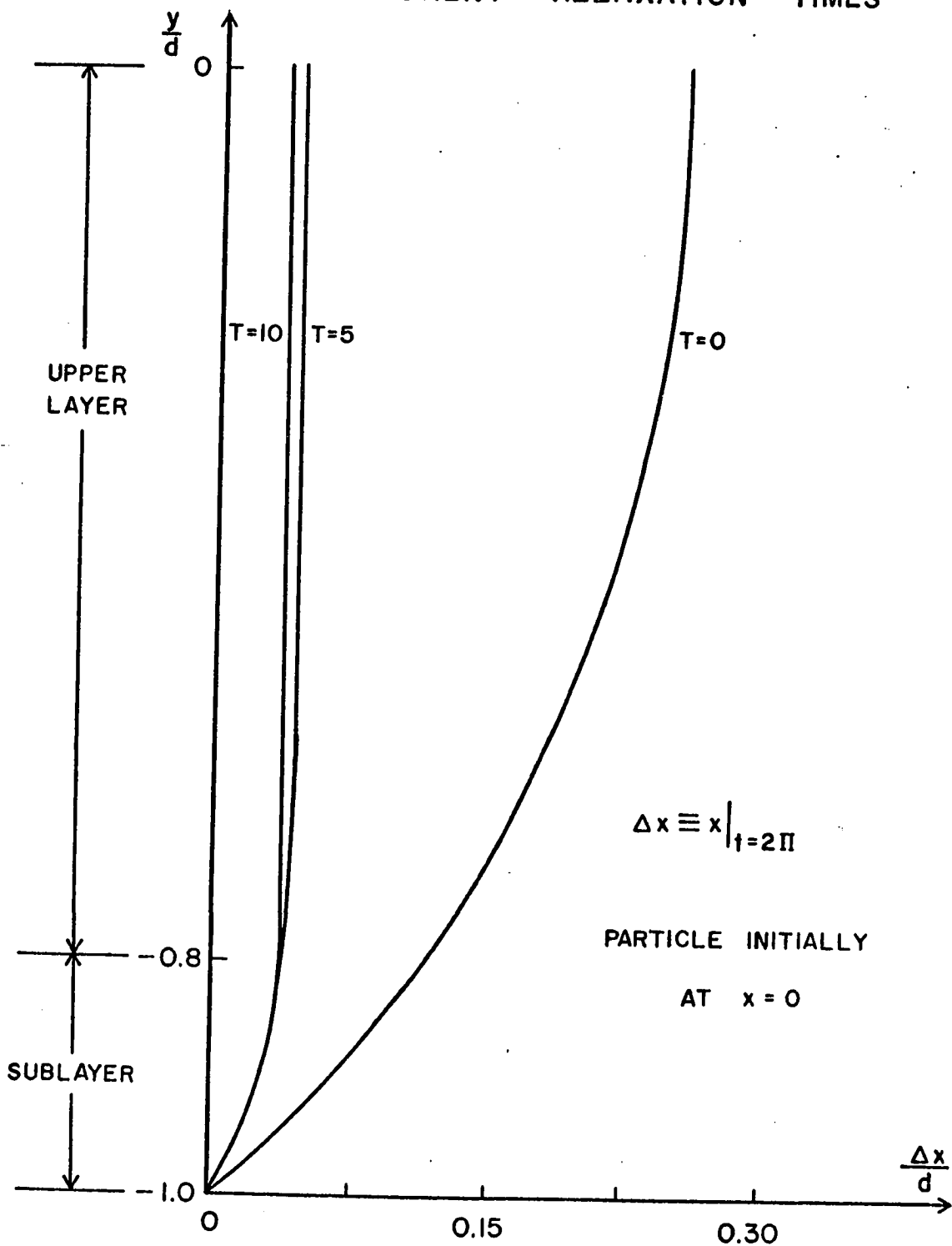
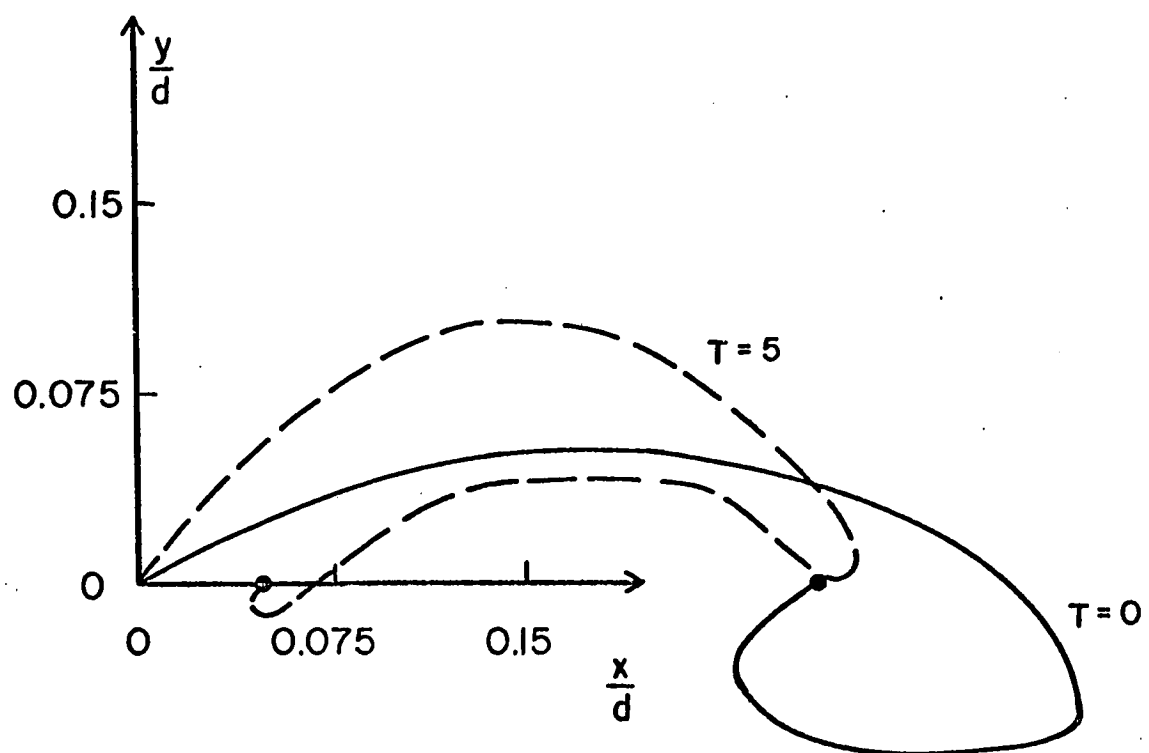


Fig. XVI. D. 2.a

CYCLIC PARTICLE TRAJECTORIES
FOR DIFFERENT RELAXATION TIMES



PARTICLE INITIALLY AT $(0,0)$

Fig. XVI.D.2.b

FREE SURFACE FOR A VISCO-ELASTIC UPPER LAYER

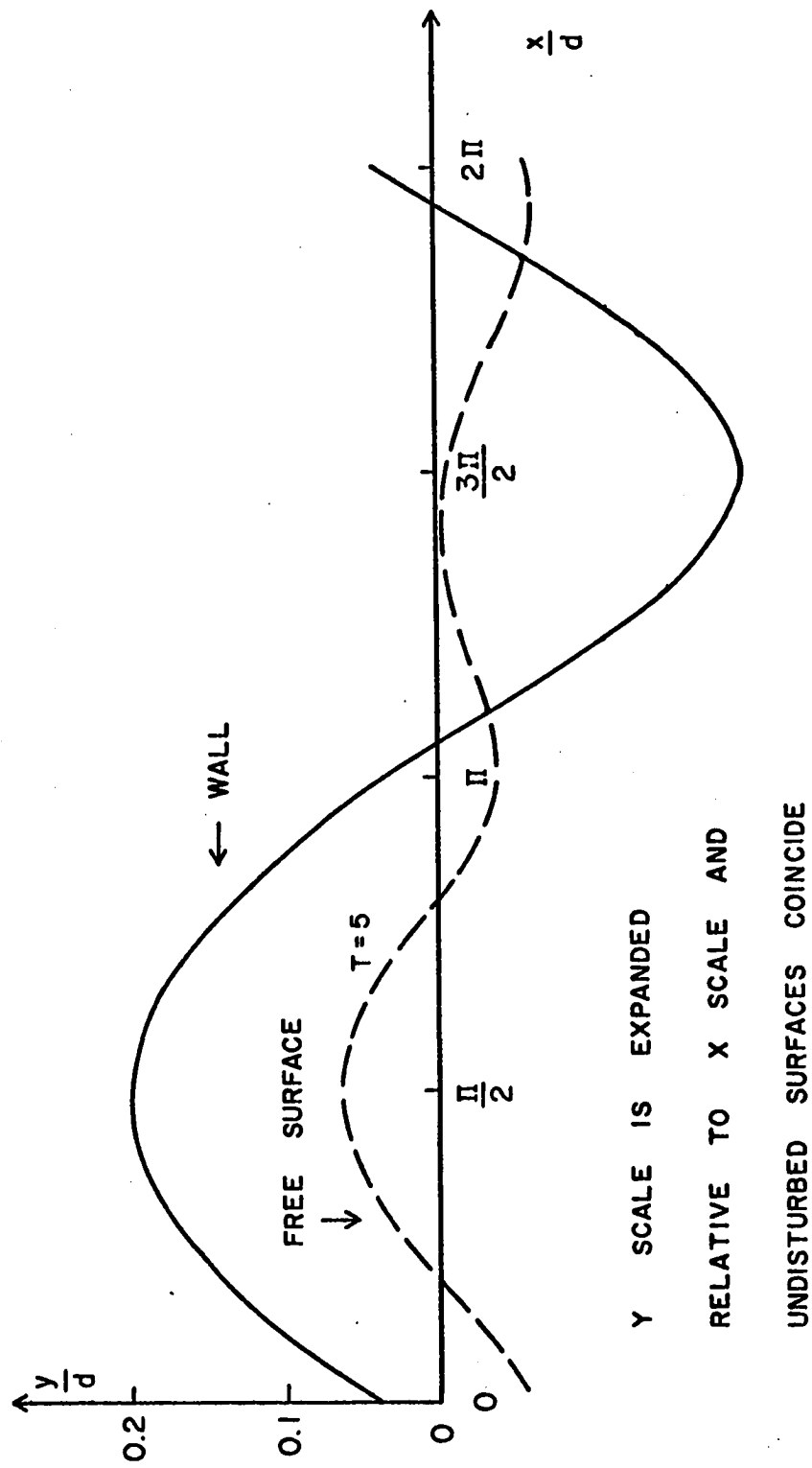


Fig. XVI. D. 2. c

CYCLIC DRIFT FOR
DIFFERENT VISCOSITY RATIOS

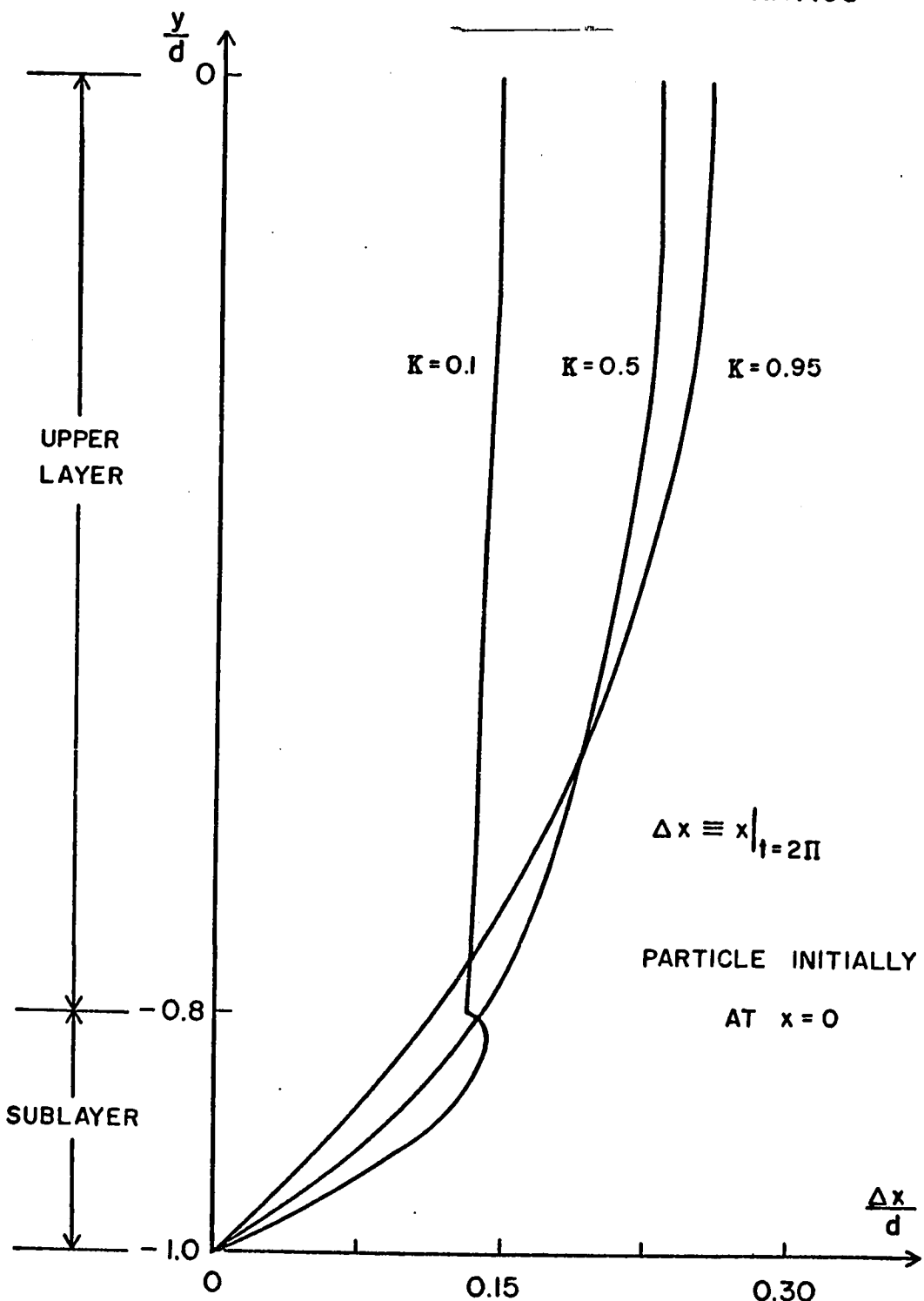


Fig. XVI.D.3.a

CYCLIC PARTICLE TRAJECTORIES
FOR DIFFERENT VISCOSITY RATIOS

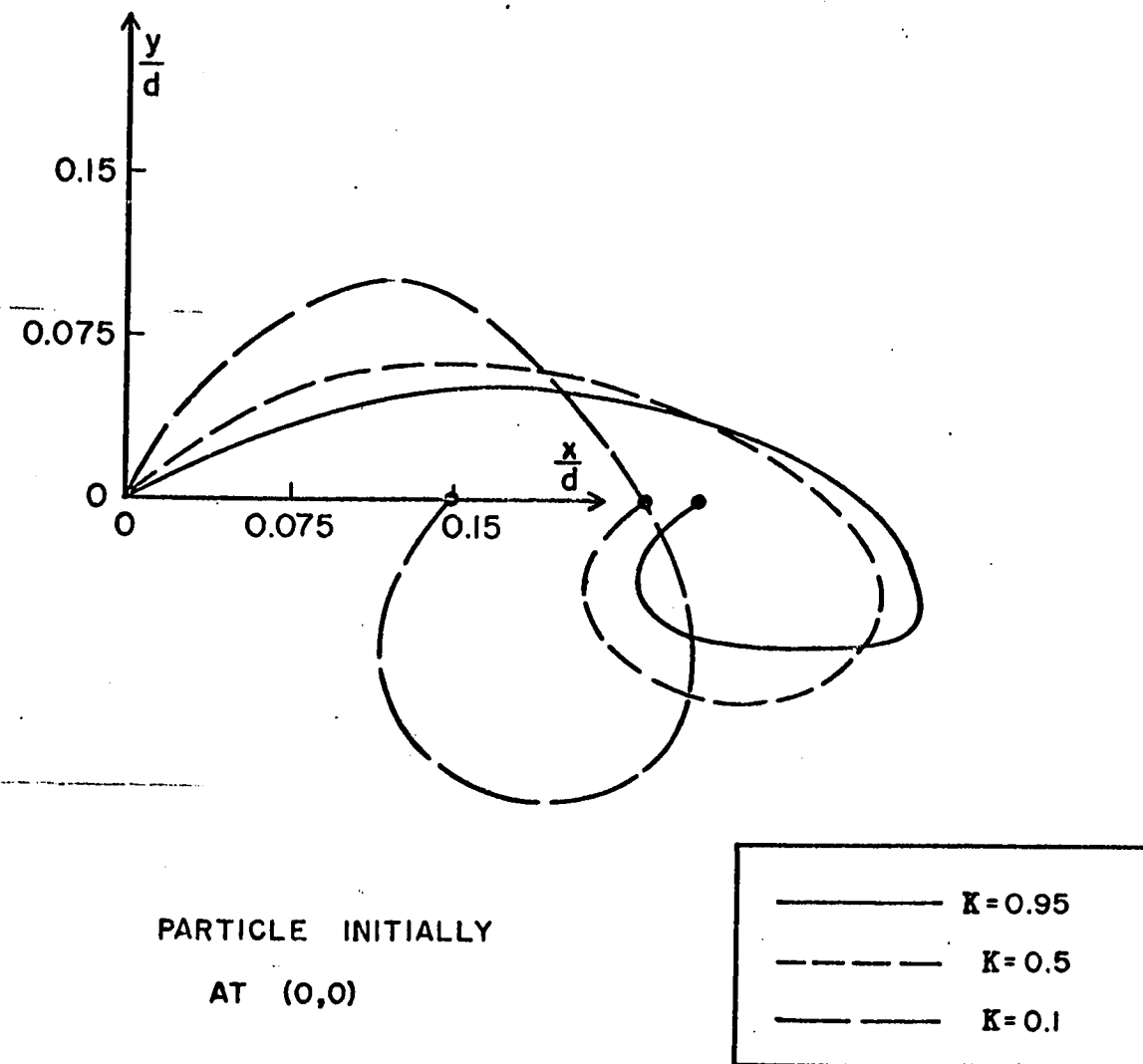


Fig. XVI.D.3.b

FREE SURFACE FOR DIFFERENT VISCOSITY RATIOS

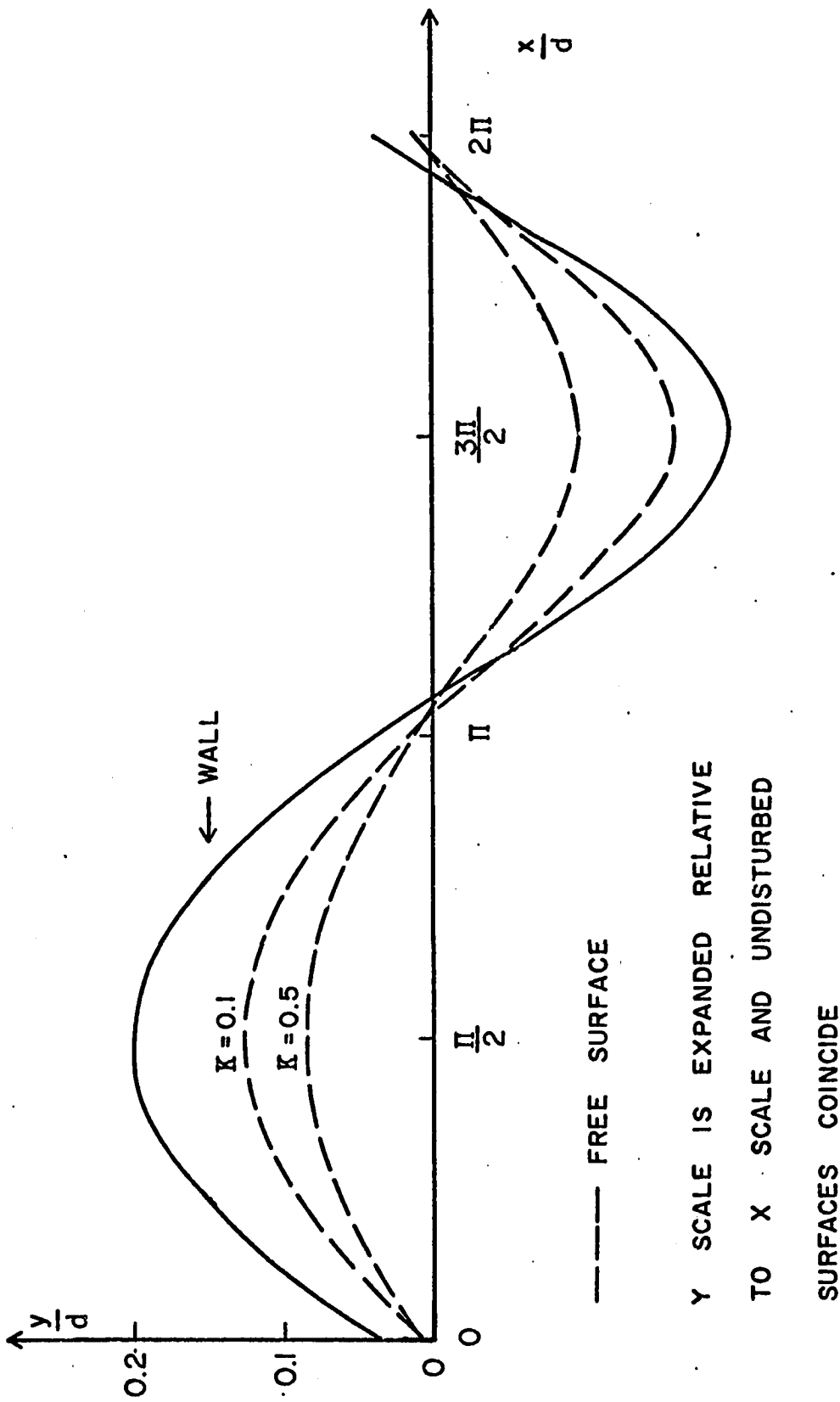


Fig. XVI. D. 3. c

FREE SURFACE AND WALL (SINGLE NEWTONIAN FLUID)

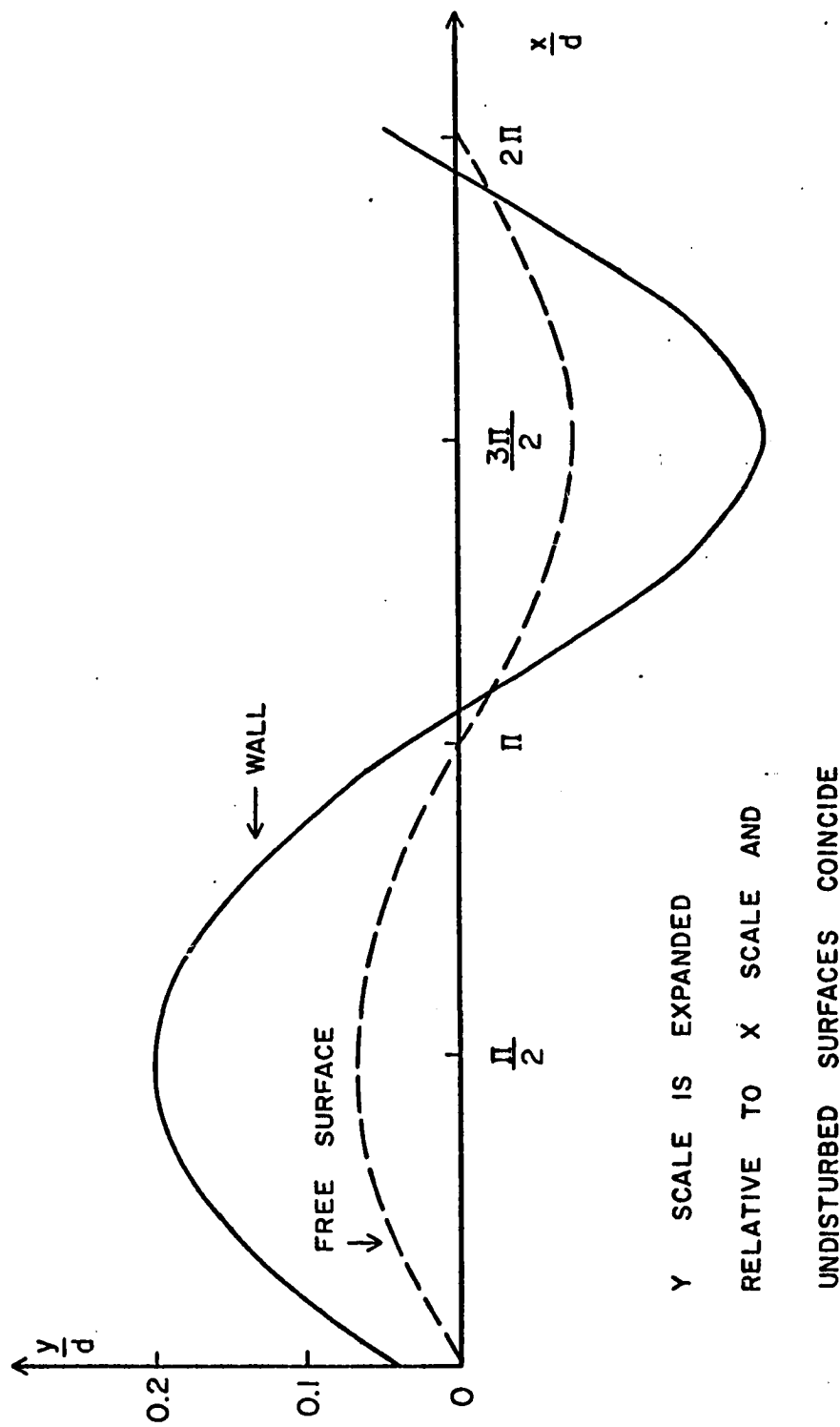


Fig. XVI.D.4

HORIZONTAL VELOCITY PROFILES (SINGLE NEWTONIAN FLUID)

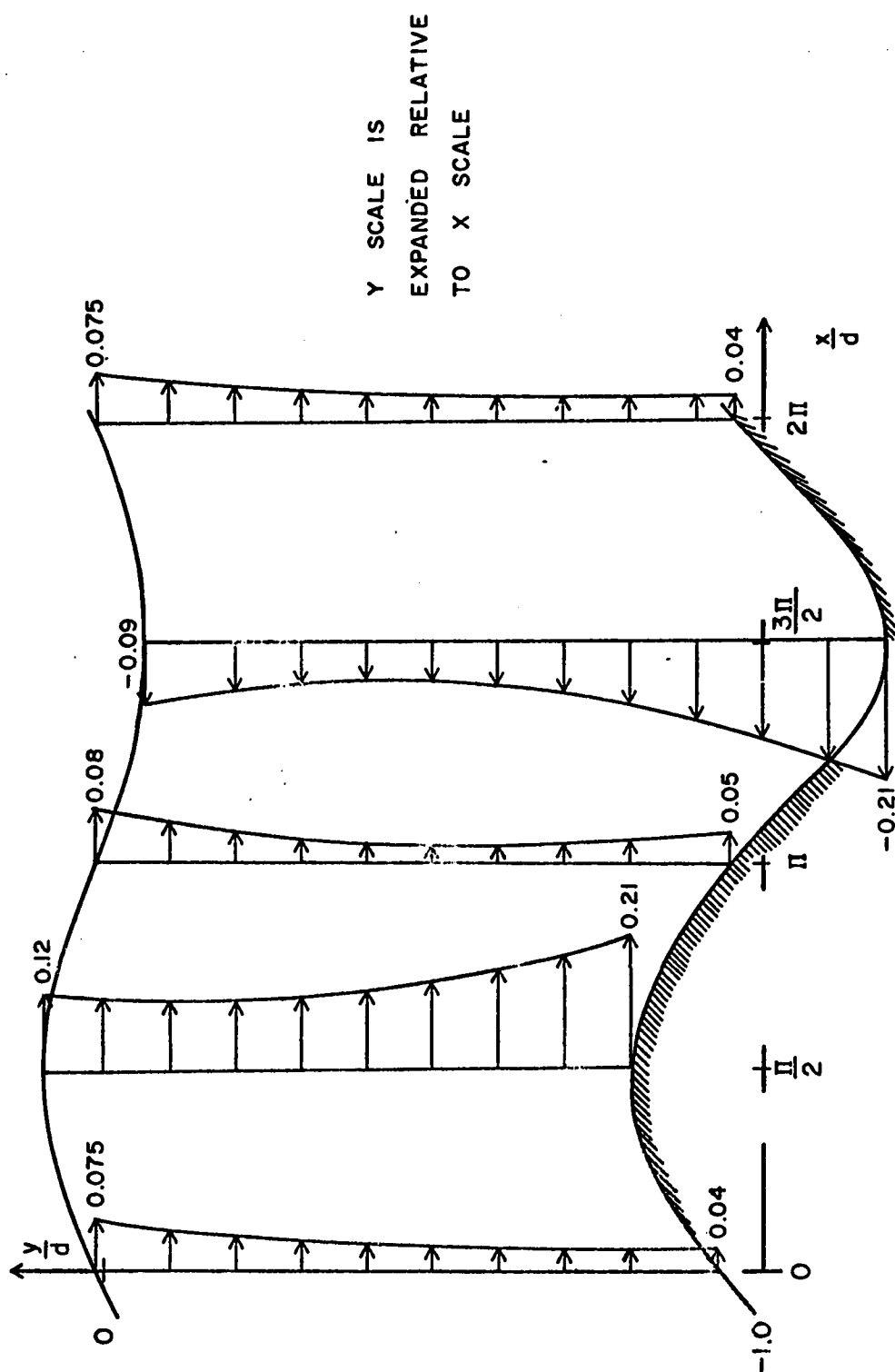


Fig. XVI.D.5

CAPTAIN MUCUS

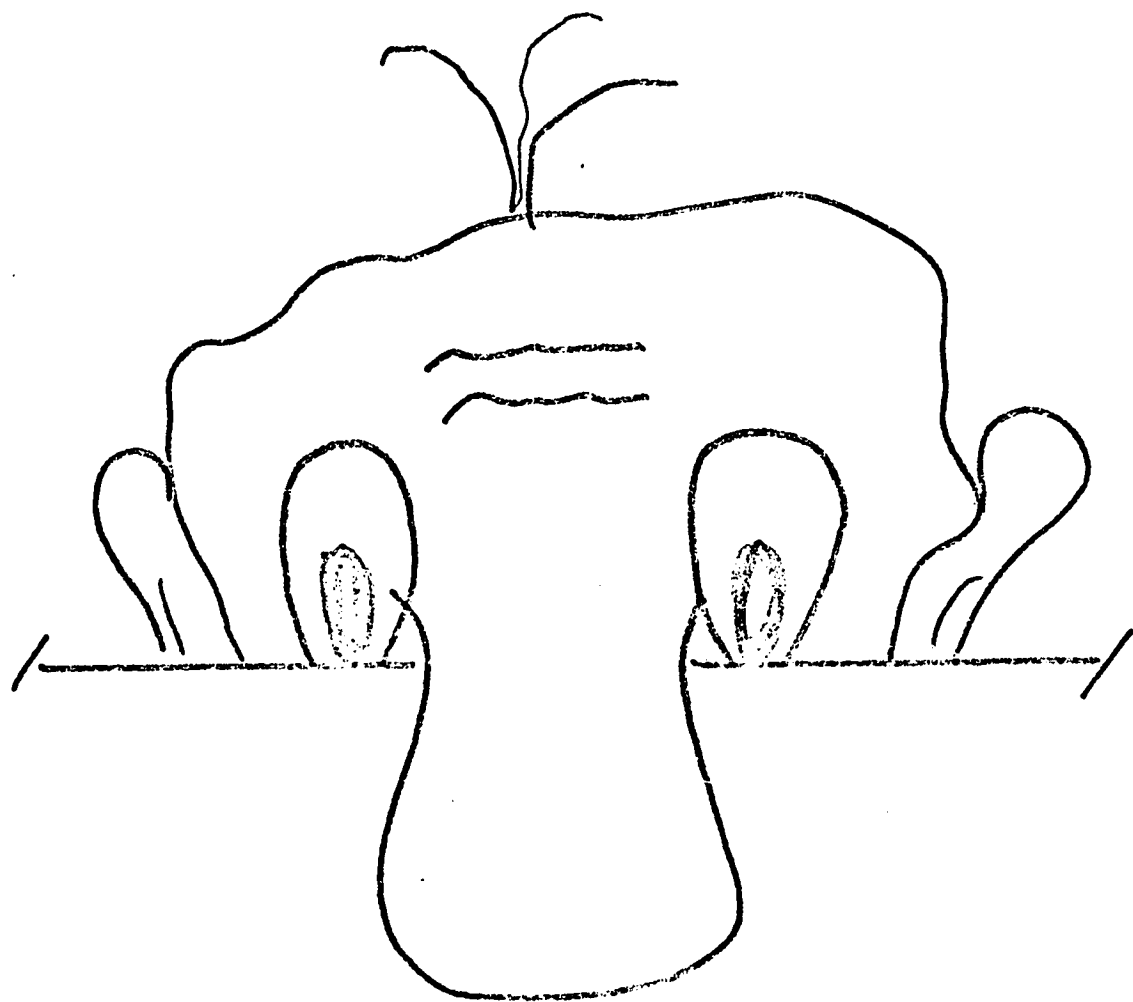


FIG. IV.A.2

APPENDIX A.

The Fourier coefficients γ_{ij} , b_i , Ψ_i , b_{3i} , b_{1i} of the inhomogeneous functions (section XII.D.) are worked out in this section, in terms of the Fourier coefficients of the $(l, 0)$ stem, using the product formula

$$ab = \frac{1}{2} \operatorname{Re} \{ AB^* \} + \frac{1}{2} \operatorname{Re} \{ AB e^{2i\phi} \}$$

$$a = \operatorname{Re} \{ Ae^{i\phi} \}, \quad b = \operatorname{Re} \{ Be^{i\phi} \}$$

Recall the first order solutions (section XI.H.):

$$\begin{aligned} u_i^{(1,0)} &= \operatorname{Re} \{ c_i^{(1,0)} e^{i\phi} \}, & s_{ij}^{(1,0)} &= \operatorname{Re} \{ A_{ij}^{(1,0)} e^{i\phi} \} \\ \bar{u}_i^{(1,0)} &= \operatorname{Re} \{ \bar{c}_i^{(1,0)} e^{i\phi} \}, & \bar{s}_{ij}^{(1,0)} &= \operatorname{Re} \{ \bar{A}_{ij}^{(1,0)} e^{i\phi} \} \\ t_{ij}^{(1,0)} &= \operatorname{Re} \{ g_{ij}^{(1,0)} e^{i\phi} \} \end{aligned}$$

1. the coefficient γ_{ij} :

$$\begin{aligned} G_{ij} &= \sum_{n=1}^{\infty} \operatorname{Re} \{ \gamma_{ij} e^{in\phi} \} = u_k t_{ij,k}^{(1,0)} + t_{ik}^{(1,0)} \omega_{kj}^{(1,0)} - t_{kj}^{(1,0)} \omega_{ik}^{(1,0)} \\ \omega_{ij}^{(1,0)} &\equiv \frac{1}{2} (u_{ij}^{(1,0)} - u_{ji}^{(1,0)}) , \quad \omega_{11}^{(1,0)} = \omega_{22}^{(1,0)} = 0 \\ \omega_{12}^{(1,0)} &= \operatorname{Re} \{ w^{(1,0)} e^{i\phi} \} = -\omega_{21}^{(1,0)} \end{aligned}$$

where

$$\omega^{(1,0)} = \frac{i}{2\alpha} (c_2^{(1,0)} - \omega^2 c_{\frac{1}{2}}^{(1,0)})$$

The extra stresses obey the relations

$$t_{12}^{(1,0)} = t_{21}^{(1,0)}, \quad t_{11}^{(1,0)} = -t_{22}^{(1,0)}$$

After algebraic manipulation, we obtain $\gamma_{ij} = 0$ for $n \neq 0, 2$

and for the modes $n = 0, 2$:

$$\gamma_{11} \Big|_{n=0} = \frac{1}{2} \left\{ c_2^{(1,0)} g_{11}^{(1,0)} + c_2^{(1,0)} g_{11}^{(1,0)} - 2 g_{12}^{(1,0)} w^{(1,0)} \right\} = -\gamma_{22} \Big|_{n=0}$$

$$\gamma_{12} \Big|_{n=0} = \frac{1}{2} \left\{ c_2^{(1,0)} g_{12}^{(1,0)} + c_2^{(1,0)} g_{12}^{(1,0)} + 2 g_{11}^{(1,0)} w^{(1,0)} \right\}$$

$$\gamma_{11} \Big|_{n=2} = \frac{1}{2} \left\{ -c_2^{(1,0)} g_{11}^{(1,0)} + c_2^{(1,0)} g_{11}^{(1,0)} - 2 g_{12}^{(1,0)} w^{(1,0)} \right\} = -\gamma_{22} \Big|_{n=2}$$

$$\gamma_{12} \Big|_{n=2} = \frac{1}{2} \left\{ -c_2^{(1,0)} g_{12}^{(1,0)} + c_2^{(1,0)} g_{12}^{(1,0)} + 2 g_{11}^{(1,0)} w^{(1,0)} \right\}$$

Some needed derivatives are

$$\gamma_{11}' \Big|_{n=2} = \frac{1}{2} \left\{ -c_2^{(1,0)} g_{11}^{(1,0)} + c_2^{(1,0)} g_{11}^{(1,0)} - 2 g_{12}^{(1,0)} w^{(1,0)} - 2 g_{12}^{(1,0)} w^{(1,0)} \right\}$$

$$\gamma_{12}' \Big|_{n=2} = \frac{1}{2} \left\{ -c_2^{(1,0)} g_{12}^{(1,0)} + c_2^{(1,0)} g_{12}^{(1,0)} + 2 g_{11}^{(1,0)} w^{(1,0)} + 2 g_{11}^{(1,0)} w^{(1,0)} \right\}$$

$$\begin{aligned} \gamma_{12}'' \Big|_{n=2} = & \frac{1}{2} \left\{ -c_2^{(1,0)} g_{12}^{(1,0)} - c_2^{(1,0)} g_{12}^{(1,0)} + c_2^{(1,0)} g_{12}^{(1,0)} + c_2^{(1,0)} g_{22}^{(1,0)} + \right. \\ & \left. + 2 g_{11}^{(1,0)} w^{(1,0)} + 4 g_{11}^{(1,0)} w^{(1,0)} + 2 g_{11}^{(1,0)} w^{(1,0)} \right\} \end{aligned}$$

2. the coefficient b_1 :

$$B_1 = \sum_{n=1}^{\infty} \operatorname{Re} \{ b_n e^{in\phi} \} = \bar{\gamma}_{1,x}^{(1,0)} S_{11}^{(1,0)} - \bar{\gamma}_{12,y}^{(1,0)} T_{12,y}^{(1,0)} \quad \text{at } y=0$$

Using the $(1,0)$ solutions and the product formula, we get

$$b_1 = 0 \quad n = 0, 1, 3, 4, 5, \dots$$

$$b_1 = i c_2^{(1,0)} g_{12}^{(1,0)} \quad n = 2 \quad \text{at } y=0$$

3. the coefficient b_2 :

$$B_2 = \sum_{n=0}^{\infty} \operatorname{Re} \{ b_n e^{in\phi} \} = \bar{\gamma}_{1,x}^{(1,0)} \Delta S_{11}^{(1,0)} - \bar{\gamma}_{12,y}^{(1,0)} \Delta T_{12,y}^{(1,0)} \quad \text{at } y=-h$$

$$S_{11}^{(1,0)} = \operatorname{Re} \left\{ -\frac{i}{2\alpha^2} \left(c_2^{(1,0)} + \alpha^2 c_2^{(1,0)} \right) e^{i\phi} \right\}$$

$$\bar{S}_{11}^{(1,0)} = \operatorname{Re} \left\{ -\frac{i}{2\alpha^2} \left(\bar{c}_2^{(1,0)} + \alpha^2 \bar{c}_2^{(1,0)} \right) e^{i\phi} \right\}$$

$$\bar{\gamma}_{12,y}^{(1,0)} = -\operatorname{Re} \left\{ i \bar{c}_2^{(1,0)} e^{i\phi} \right\}$$

$$\therefore b_2 = 0 \quad n = 0, 1, 3, 4, 5, \dots$$

$$b_2 = i \bar{c}_2^{(1,0)} \left\{ g_{12}^{(1,0)} - \bar{g}_{12}^{(1,0)} \right\} \quad \text{at } y=-h, \quad n=2$$

The other coefficients are obtained in the same way:

$$\Psi_1 = \Psi_2 = 0 \quad n = 0, 1, 2, 3, \dots$$

$$b_{3_1} \Big|_{n=0} = \frac{1}{2\alpha} \bar{c}_2^{(1,0)} \left\{ \bar{c}_2^{(1,0)} - c_2^{(1,0)} \right\} \quad \text{at } y=-h$$

$$b_{3_1} \Big|_{n=2} = \frac{1}{2\alpha} \bar{c}_2^{(1,0)} \left\{ \bar{c}_2^{(1,0)} - c_2^{(1,0)} \right\} \quad \text{at } y=-h$$

$$b_{3_1} = 0 \quad n = 1, 3, 4, 5, \dots$$

$$b_{3_2} = 0 \quad n = 0, 1, 2, 3, \dots$$

$$b_{4_1} \Big|_{n=0} = \frac{1}{2\alpha} \left\{ \alpha^2 \rho^2 + \bar{c}_2^{(1,0)} \right\} \quad \text{at } y=-1$$

$$b_{4_1} \Big|_{n=2} = \frac{1}{2\alpha} \left\{ \alpha^2 \rho^2 - \bar{c}_2^{(1,0)} \right\} \quad \text{at } y=-1$$

$$b_{4_1} = 0 \quad n = 1, 3, 4, 5, \dots$$

$$b_{4_2} = 0 \quad n = 0, 1, 2, 3, 4, \dots$$

APPENDIX B.

In the following few pages, we shall show that the inhomogeneous part of the fourth order differential equation, $g^{(2)}(y)$, is zero (section XII. E.). This implies that the non-trivial solutions exist for only the homogeneous equation, and that the particular solution is zero for the mode $n=2$. Superscripts are dropped here for convenience.

$$g(n, y) = 2N^2 T \gamma_{11}' - iNT (\gamma_{12}'' + N^2 \gamma_{12})$$

$$\gamma_{11}' = \frac{1}{2} \{ -c'' g_{11} + c g_{11}'' - 2g_{12} w - 2g_{12} w' \}$$

$$\gamma_{12} = \frac{1}{2} \{ -c' g_{12} + c g_{12}' + 2g_{11} w \}$$

$$\begin{aligned} \gamma_{12}'' = \frac{1}{2} \{ & -c''' g_{12} - c'' g_{12}' + c' g_{12}'' + c g_{12}''' + 2g_{11} w + \\ & + 4g_{11} w' + 2g_{11} w'' \} \end{aligned}$$

$$g_{11} = -Q c' , \quad g_{12} = \frac{iQ}{N} (c'' + \omega^2 c)$$

$$w = \frac{i}{N} (c'' - \omega^2 c)$$

where

$$c = c_2^{(1,0)}, \quad g_{ij} = g_{ij}^{(1,0)}, \quad w = w^{(1,0)}$$

$$Q = \frac{1}{1+iT}, \quad N = 2\omega$$

We shall use the fourth order differential equation,

$$c'''' - 2\alpha^2 c'' + \alpha^4 c = 0 \quad , \quad c'''' = 2\alpha^2 c'' - \alpha^4 c ,$$

$$c'' = 2\alpha^2 c''' - \alpha^4 c'$$

$$(i) \gamma_{12}'' = \frac{1}{2} \{ -c''' g_{12} - c'' g_{12}' + c' g_{12}'' + c g_{12}''' + 2g_{11} w + 4g_{11}' w' + 2g_{11} w'' \}$$

$$-c'' g_{12}' + 4g_{11} w' = \frac{iQ}{N} \{ -5c''' c''' + 3\alpha^2 c' c'' \}$$

$$c' g_{12}'' + 2g_{11} w'' = \frac{iQ}{N} \{ -c' c'' + 3\alpha^2 c' c'' \} = \frac{iQ}{N} \{ \alpha^2 c' c'' + \alpha^4 c c' \}$$

$$-c''' g_{12} + 2g_{11} w = \frac{iQ}{N} \{ -3c''' c''' + \alpha^2 c c'' \}$$

$$c g_{12}''' = \frac{iQ}{N} c \{ c'' + \alpha^2 c''' \} = \frac{iQ}{N} \{ 3\alpha^2 c c''' - \alpha^4 c c' \}$$

$$\text{Addition gives } \gamma_{12}'' = \frac{iQ}{2N} \{ -8c''' c''' + 4\alpha^2 c' c'' + 4\alpha^2 c c'' \}$$

$$(ii) \gamma_{12} = \frac{1}{2} \{ -c' g_{12} + c g_{12}' + 2g_{11} w \}$$

$$-c' g_{12}' + c g_{12}' = \frac{iQ}{N} \{ c c''' - c' c'' \}$$

$$2g_{11} w = \frac{Qi}{N} \{ -2c' c'' + 2\alpha^2 c c' \}$$

$$\therefore \gamma_{12} = \frac{Qi}{2N} \{ c c''' - 3c' c'' + 2\alpha^2 c c' \}$$

$$(iii) \gamma'_{11} = \frac{1}{2} \{ -c''g_{11} + c g''_{11} - 2g'_{12}w - 2g_{12}w' \}$$

$$-c''g_{11} + c g''_{11} = Q \{ c''c' - cc'' \}$$

$$-2g'_{12}w - 2g_{12}w' = \frac{Q}{N^2} \{ 4c''c''' - 4\alpha^2cc' \}$$

Addition gives

$$2N^2\gamma'_{11} = Q \{ 4\alpha^2(c'c'' - cc''') + 4c''c''' - 4\alpha^2cc' \}$$

$$(iv) \gamma''_{12} + N^2\gamma_{12} = \frac{i}{2N} Q \{ -8c''c''' - 8\alpha^2c'c'' + 8\alpha^2cc''' + 8\alpha^4cc' \}$$

$$-iN(\gamma''_{12} + N^2\gamma_{12}) = Q \{ -4c''c''' - 4\alpha^2c'c'' + 4\alpha^2cc''' + 4\alpha^2cc' \}$$

The function g can now be formed:

$$\begin{aligned} (v) \frac{1}{T} g(2,y) &= 2N^2\gamma'_{11} - iN(\gamma''_{12} + N^2\gamma_{12}) \\ &= Q \{ 4\alpha^2c'c'' - 4\alpha^2cc''' + 4c''c''' - 4\alpha^2cc' - \\ &\quad - 4c''c''' - 4\alpha^2c'c'' + 4\alpha^2cc''' + 4\alpha^2cc' \} \end{aligned}$$

$$= 0$$

$$\therefore \boxed{g(2,y) = 0 \quad \forall y}$$

APPENDIX C. Calculation of I_i and $F_i^{(2,0)}$ (section XIV.C.)

Recall that $F_i^{(2,0)} = I_i(x, t') + u_i^{(2,0)}(x, t')$ and $I_i = \Pi_i + \text{III}_i$

where $\Pi_i = \int_0^{t'} u_i^{(1,0)}(x, t'') dt'' \frac{\partial u_i^{(1,0)}}{\partial x_1}(x, t')$

$$\text{III}_i = \int_0^{t'} u_i^{(1,0)}(x, t'') dt'' \frac{\partial u_i^{(1,0)}}{\partial x_2}(x, t')$$

$$u_i^{(1,0)}(x, t') = \operatorname{Re} \{ c_i^{(1,0)}(y) e^{i\Phi} \} = u_i$$

$$u_i^{(2,0)} = u_i^{(1,0)}(x, t') = \operatorname{Re} \{ c_i^{(2,0)}(0, y) + c_i^{(2,0)}(z, y) e^{2i\Phi} \}$$

$$c_i^{(1,0)} = \frac{i}{\omega} c_2^{(1,0)}, \quad c_2^{(1,0)}(0, y) = 0$$

$$\Phi = \alpha x + t, \quad \Phi' = \alpha x + t'$$

The product formula is $a = \operatorname{Re} \{ A e^{i\Phi} \}, \quad b = \operatorname{Re} \{ B e^{i\Phi} \}$

$$ab = \frac{1}{2} \operatorname{Re} \{ A^* B + A B e^{2i\Phi} \}$$

The time integral of u_K is obtained first: (dropping superscripts)

$$\begin{aligned} \int_0^{t'} u_K(x, t'') dt'' &= \operatorname{Re} \int_0^{t'} c_K^{(1,0)}(y) e^{i\Phi''} dt'' \\ &= \operatorname{Re} \{ c_K e^{i\alpha x} i(1 - e^{-it'}) \} \\ &= \operatorname{Re} \{ i c_K e^{i\alpha x} \} - \operatorname{Re} \{ i c_K e^{i\Phi'} \} \end{aligned}$$

The partial derivatives of u_j are

$$\frac{\partial u_j}{\partial x_1} = \operatorname{Re} \{ i \alpha c_j e^{i\Phi'} \}, \quad \frac{\partial u_j}{\partial x_2} = \operatorname{Re} \{ c_j' e^{i\Phi'} \}$$

1. calculation of \bar{I}_j

$$\begin{aligned} \bar{I}_j = \int_0^{t'} u_j dt'' \frac{\partial u_j}{\partial x_1} &= \operatorname{Re} \{ i c_i e^{ixX} \} \operatorname{Re} \{ i \alpha c_j e^{i \Phi'} \} - \\ &\quad - \operatorname{Re} \{ i c_i e^{i \Phi'} \} \operatorname{Re} \{ i \alpha c_j e^{i \Phi'} \} \\ \operatorname{Re} \{ i c_i e^{ixX} \} &\equiv \operatorname{Re} \{ i c_i e^{-it'} e^{i \Phi'} \} \end{aligned}$$

Using the product formula and the above identity,

$$\bar{I}_j = \frac{1}{2} \operatorname{Re} \{ c_j c_i^* (e^{-it'}) + c_j c_i (1 - e^{-it'}) e^{2i\Phi'} \}$$

2. calculation of \bar{III}_j

$$\begin{aligned} \bar{III}_j = \int_0^{t'} u_2 dt'' \frac{\partial u_j}{\partial x_2} &= \operatorname{Re} \{ i c_2 e^{-it'} e^{i \Phi'} \} \operatorname{Re} \{ c_j' e^{i \Phi'} \} - \\ &\quad - \operatorname{Re} \{ i c_2 e^{i \Phi'} \} \operatorname{Re} \{ c_j' e^{i \Phi'} \} \\ &= \frac{1}{2} \operatorname{Re} \{ -i c_2^* c_j' (e^{-it'}) + i c_2 c_j' e^{2i\Phi'} (e^{-it'}) \} \end{aligned}$$

3. calculation of I_j

$$\begin{aligned} I_j &= \bar{I}_j + \bar{III}_j \\ &= \frac{1}{2} \operatorname{Re} \{ (e^{-it'}) (\alpha c_j c_i^* - i c_2^* c_j') + (e^{-it'}) (\alpha c_2 c_j' - \alpha c_j c_i) e^{2i\Phi'} \} \end{aligned}$$

$$j=2 : (\alpha c_2 c_i^* - i c_2^* c_j') = -i (c_2 c_2' + c_2 c_2')$$

$$(i c_2 c_2' - \alpha c_2 c_1) = i c_2 c_2' - i c_2 c_2' = 0$$

$$\therefore I_2 = -\frac{1}{2} \operatorname{Re} \{ K e^{i\bar{\Phi}'} \}$$

$$K \equiv i(c_2' c_2'' + c_2'' c_2') e^{-i\alpha X}$$

$$j=1: (\alpha c_1 c_1^* - i c_2'' c_1') = \frac{1}{\alpha} (c_2' c_2'' + c_2'' c_2'')$$

$$(ic_2 c_1' - \alpha c_1 c_1) = \frac{1}{\alpha} (c_2' c_2' - c_2 c_2'')$$

$$I_1 = -\frac{1}{2\alpha} \operatorname{Re} \{ L - R e^{i\bar{\Phi}'} + M e^{2i\bar{\Phi}'} \}$$

$$L \equiv c_2' c_2'' + c_2'' c_2''$$

$$M \equiv c_2' c_2' - c_2 c_2''$$

$$R \equiv L e^{-i\alpha X} + M e^{i\alpha X}$$

4. calculation of $F_j^{(2,0)}$

$$F_j^{(2,0)} = I_j + u_j^{(2,0)}(x, t')$$

$$F_1^{(2,0)} = I_1 + u_1^{(2,0)} = \operatorname{Re} \{ (c_1^{(2,0)}, y) - \frac{L}{2\alpha} \} + \frac{R}{2\alpha} e^{i\bar{\Phi}'} + (c_1^{(2,0)}, y) - \frac{M}{2\alpha} \} e^{2i\bar{\Phi}'} \}$$

$$F_2^{(2,0)} = I_2 + u_2^{(2,0)} = \operatorname{Re} \{ -\frac{K}{\alpha} e^{i\bar{\Phi}'} + (c_2^{(2,0)}, y) e^{2i\bar{\Phi}'} \}$$

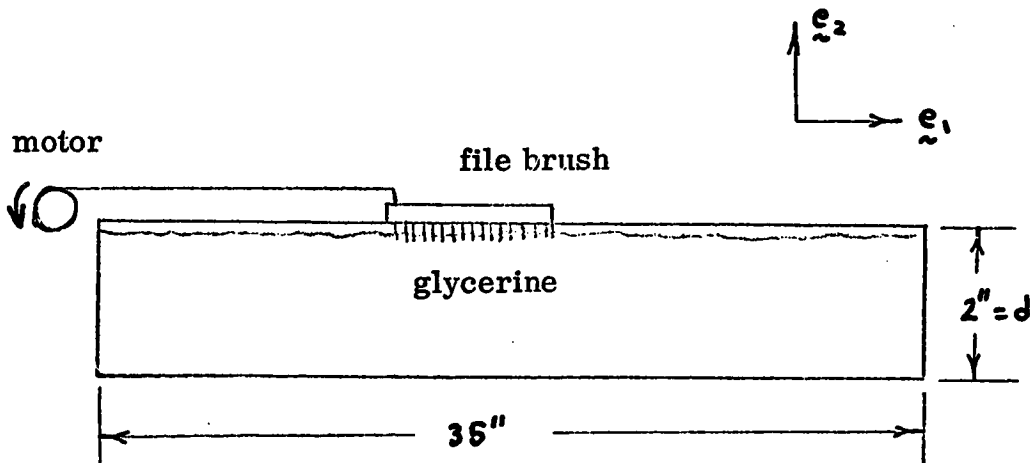
APPENDIX D. Experiment

A simple experiment has been performed in order to show that the replacement of the discrete cilia carpet on the epithelium by a smooth wall may be a valid assumption. * Since inertial and gravitational forces can be neglected in normal muco-ciliary flow, and since the cilia are immersed in a Newtonian serous fluid, we looked at the related problem of the "Stokes flow" induced by a brush moving slowly through pure glycerine. This experiment is, of course, not strictly analogous to the physiological problem because the individual bristles do not move in any coordinated wavy pattern and because the ratio of bristle diameter to bristle spacing may be different from that on the mammalian tracheal epithelium.

*

This smooth wall approach has also been taken in a recent paper on ciliary propulsion of micro-organisms by Blake (J. Fluid Mech., 46, 1971), published after this work was completed.

The experiment consisted of towing a wire-bristle brush through a tank of glycerine at a constant slow speed ($U = 3.14 \text{ in./min.}$). A sketch of the experiment appears below. The depth of the tank d is 2 in., the width is $2\frac{1}{2}$ in., and the length is 35 in.



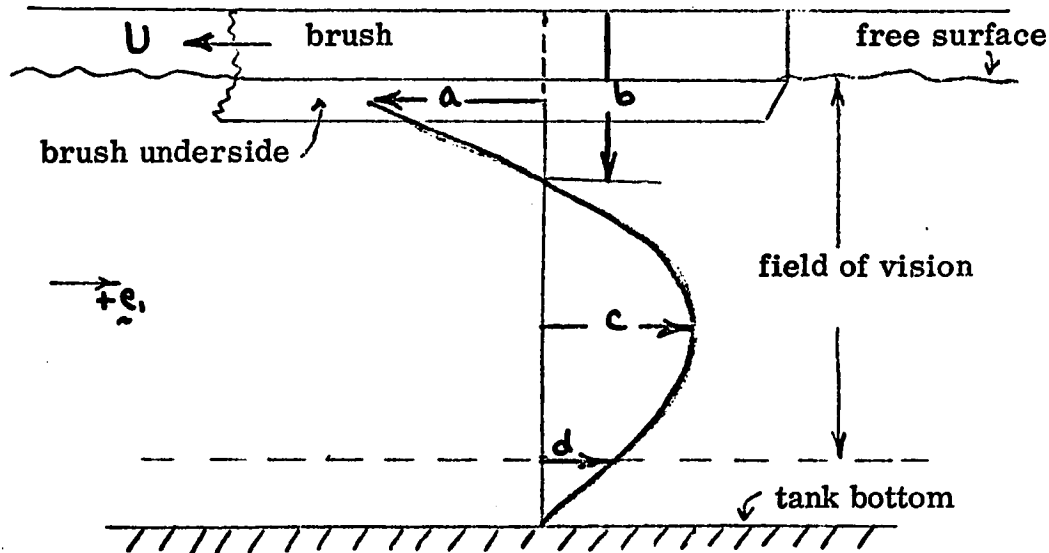
A Reynolds number based on the depth d , the velocity U , and the viscosity and density of glycerine is calculated to be*

$$Re \equiv \frac{\rho U d}{\mu} = .057$$

* From the Handbook of Chemistry and Physics, 39th Ed., (Chem. Rubber Publishing Co.), the values of viscosity and density of glycerine are $\mu = 1490 \text{ cP}$ (20°C) and $\rho = 1.26 \text{ g/cm}^3$ (60°F).

The level of the glycerine was about halfway up the bristle length. No attempt was made to analyze the boundary condition in greater detail by varying the depth of the fluid or its viscosity. The bristles are spaced approximately four diameters apart while the cilia are presumably one diameter apart (Dalhamn and Rhodin, 1956) so that the file brush is not as densely packed as the ciliated epithelium.

A dye line vertical at $t = 0$ is deformed due to the motion of the brush as seen in the sequential photographs of the plate and brush cases (Figures D.1 - D.6). The brush drags the fluid near the surface along with it ($-e$, direction) and mass conservation explains the displacement near the tank bottom. At $t > 0$, the dye line looks typically as follows:



Two trial runs, one with a plate attached to the brush underside and one with the brush alone, are listed in Table XVII. D. 1. Pictures of the location of the brush and the displacement of the dye line were taken at $t = 0$, $t_1 = 15 \text{ sec}$, $t_2 = 30 \text{ sec}$.

t	Fig.	$a (\text{mm})$	$b (\text{mm})$	$c (\text{mm})$	$d (\text{mm})$
0	1	1.0	1.0	1.0	1.0
t_1	2	-20.	-11.	11.	7.
t_2	3	-38.	-10.	16.	10.
///	///	///	///	///	///
0	4	0	0	0	0
t_1	5	-20.	-12.	10.	6.
t_2	6	-42.	-10.	15.	10.

Table XVII. D. 1

If the initial position of run number 1 is standardized to 0. by subtracting 1. from each measurement, we get

t	Fig.	a (mm)	b (mm)	c (mm)	d (mm)
0	1	0.	0.	0.	0.
t_1	2	-21.	-12.	10.	6.
t_2	3	-39.	-11.	15.	9.

Table XVII. D. 2

Comparison of Tables XVII. D. 1 and 2 shows that the maximum difference in displacement between runs 1 and 2 is about 10%.

The streak lines for the two separate experiments with and without a flat plate attached onto the brush underside show that the two cases are nearly the same (i. e. 10% difference). This difference is due primarily to the fact that the flat plate overrides the constant pressure free surface boundary condition present in the case without

the plate. The difference is small enough compared to the overall deformation so that the conclusion that the flow with and without the flat plate is nearly the same is qualitatively valid.

Thus, a smooth wall boundary condition may be a good "engineering approximation" to the metachronal waving of cilia. Naturally it would be interesting to generalize the analytical model to the case of a porous wall.

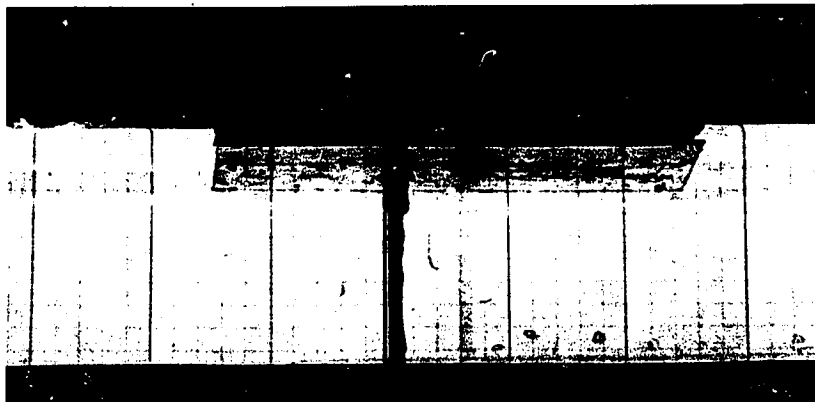


Fig. D.1

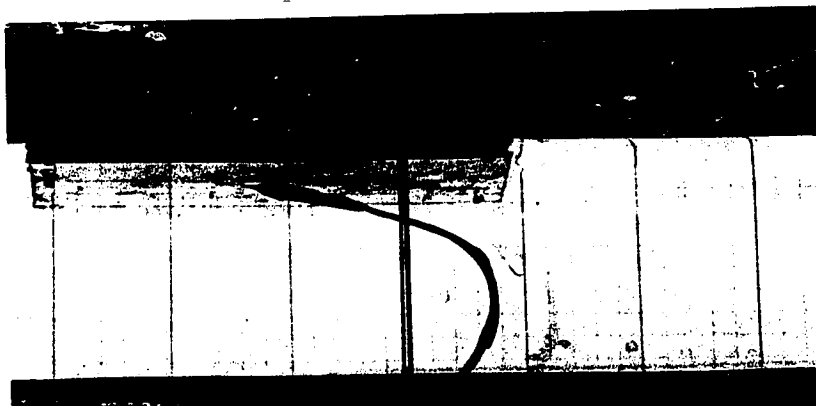


Fig. D.2



Fig. D.3

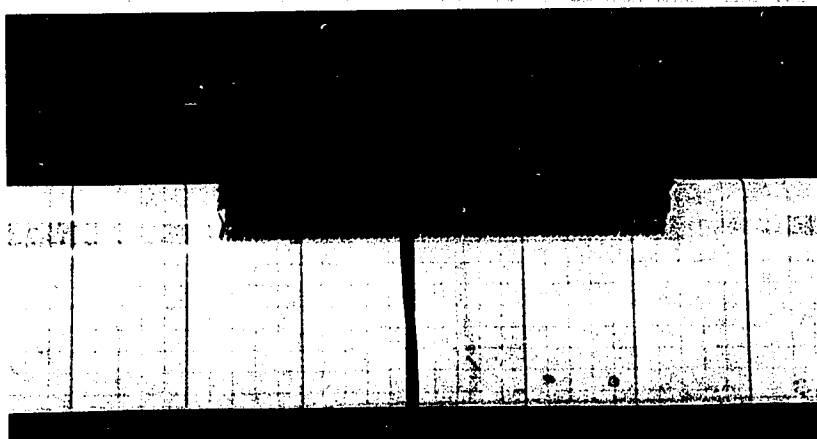


Fig. D.4

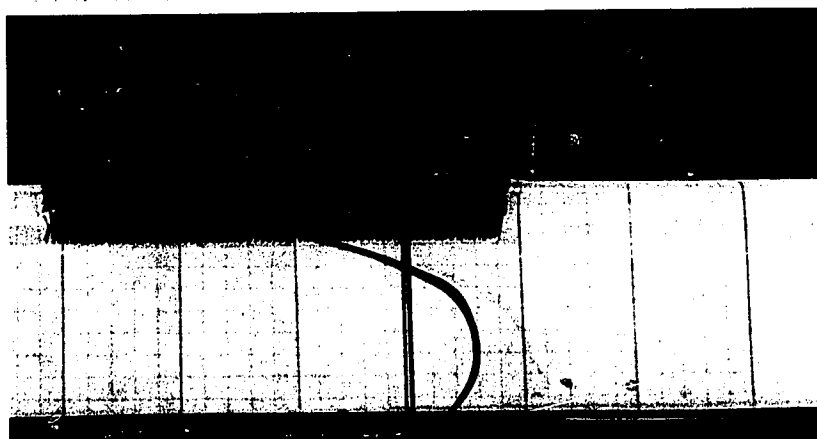


Fig. D.5

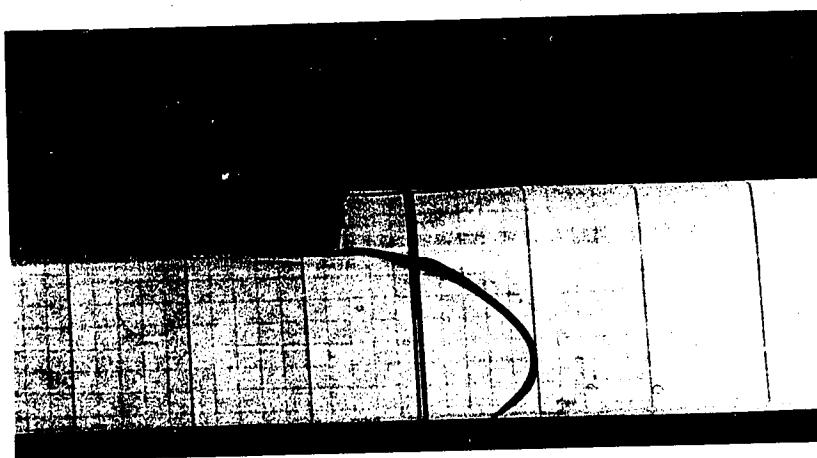


Fig. D.6

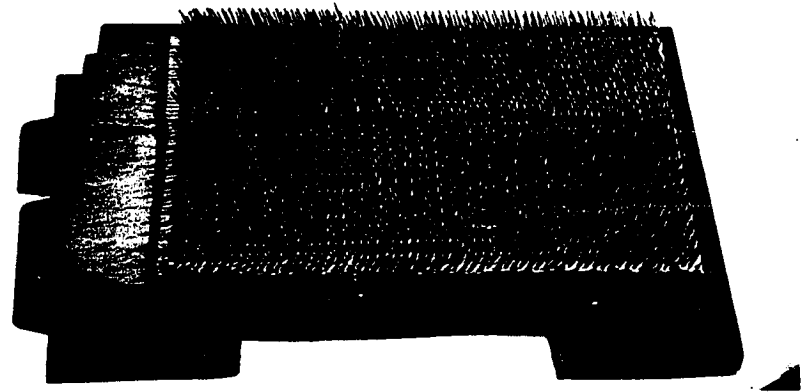


Fig. D.7

BIBLIOGRAPHY

I. Medical

- Afzelius, B. (1966). Anatomy of the Cell. Chicago Univ. Press.
- Bang, B. G. (1961). The surface pattern of the nasal mucosa and its relation to mucous flow. J. Morph., 109, 57-72.
- Bang, B. G. and Bang, F. B. (1961). Effect of water deprivation on nasal mucous flow. Proc. Soc. Exper. Bio. and Mec., 106, 516-521.
- Breuninger. H. (1964). Über das physikalisch-chemische Verhalten des Nasenschleims. Archiv Ohren, Nasen und Kehlkopfheilk., 184, 133-138.
- Dalhamn, T. (1956). Mucous flow and ciliary activity in the trachea of healthy rats and rats exposed to respiratory irritant gases. Acta Physiologica Scandinavica, 36, Supp. 123.
- Dalhamn, T. and Rhodin, J. (1956). Electron Microscopy of the tracheal ciliated mucosa in rat. Zeitschrift fur Zellforschung, Bd. 44, 345-412.
- Ewert, G. (1965). On mucous flow rate in the human nose. Acta Otolaryng. Supp. 200, 1-54.
- Gray, J. (1928). Ciliary Movement. Cambridge Univ. Press.
- Hilding, A. C. (1943). The role of ciliary action in production of pulmonary atelectasis, vacuum in the paranasal sinuses and in otitis media. Ann. Otol., Rhinol., and Laryng., 52, 816-833.
- Hilding, A. C. (1956). On cigarette smoking, bronchial carcinoma, and ciliary action. I, II, III, IV. New Eng. J. Med., 254, 775-781, 1155-1160 and Ann. Otol., Rhinol. and Laryng., 65, 116-130, 736-746.

Hilding, A. C. (1959). Ciliary streaming through the larynx and trachea. J. Thoracic Surg., 37, 108-117.

Horridge, G. A. and Tamm, S. L. (1969). Critical point drying for scanning electron microscopic study of ciliary motion. Science, 163, 817-818.

Jakowska, S. (1966). Interdisciplinary investigation of mucus production and transport. Annals New York Acad. of Sci., 130, Art. 3, 869-973.

Keiser-Nielsen, H. (1953). Mucin. Dansk Videnskabs Forlag A/S.

Lucas, A. M. (1932). Ciliated Epithelium. Cowdry's Special Cytology I. New York: Hoeber.

Lucas, A. M. and Douglas, L. C. (1934). Principles underlying ciliary activity in the respiratory tract. Arch. Otolaryng., 20, 528-541.

Proctor, D. (1964). Physiology of the upper airway. Handbook of Physiology, Respiration I. 309-345, Baltimore: Waverly Press.

Proetz, A. W. (1941). Applied Physiology of the Nose. 1st ed. St. Louis: Annals.

Rivera, J. A. (1962). Cilia, Ciliated Epithelium, and Ciliary Activity. Oxford: Pergamon Press.

Sleigh, M. A. (1962). The Biology of Cilia and Flagella. New York: Macmillan.

Tremble, G. E. (1948). Clinical observations on the movement of nasal cilia. Laryngoscope, 58, 206.

Whitmore, R. L. (1968). Rheology of the Circulation. Oxford: Permagon Press.

II. Mechanics

- Barton, C. and Raynor, S. (1967). Analytical investigation of cilia induced mucous flow. Bull. Math. Physics, 29, 419-427.
- Denton, R., Forsman, W., Hwang, S. H., Litt, M., and Miller, C. E. (1968). Viscoelasticity of mucus. Am. Rev. Resp. Dis., 98, 380-391.
- Eirich, F. R. (1956). Rheology, I. New York: Academic Press.
- Eringen, A. C. (1962). Non-linear Theory of Continuous Media. New York: McGraw-Hill.
- Fredrickson, A. G. (1962). On stress-relaxing solids, I. Chem. Eng. Sci., 17, 155-166.
- Fredrickson, A. G. (1964). Principles and Applications of Rheology. Englewood Cliffs: Prentice-Hall.
- Hwang, S. H. (1967). Viscoelastic behavior of biological fluids. Ph.D. Dissertation. Ann Arbor University Microfilms.
- Hwang, S., Litt, M. and Forsman, W. (1969). Rheological properties of mucus. Rheo. Acta, Band 8, Heft 4, 438-448.
- Litt, M. (1970). Mucus rheology. Arch. Intern. Med., 126, 417-423.
- Miller, C. E. (1968). The kinematics and dynamics of ciliary fluid systems. J. Exp. Biol., 49, 617-629.
- Miller, C. E. and Goldfarb, H. (1965). An in-vitro investigation of ciliated activity. Trans. Soc. Rheo., 9, 135-144.
- Miller, C. E. and Barnett, B. (1966). Flow induced by biological mucociliary systems. Annals New York Acad. Sci., 130, 890-901.
- Oldroyd, J. G. (1950). On the formulation of the rheological equations of state. Proc. Roy. Soc., A200, 520-541.

Prager, W. (1961). Introduction to Mechanics of Continua. Boston:
Ginn and Co.

Ross, S. and Corrsin, S. (1970). A wavy-wall analytical model of
muco-ciliary pumping. Bulletin of the Am. Physical Soc.,
Series II, 15, 1539.

Shapiro, A., Jaffrin, M. and Weinberg, S. (1969). Peristaltic
pumping with long wavelengths at low Reynolds number. J. Fluid
Mech. 37, 799-825.

Taylor, G. I. (1951). Analysis of the swimming of microscopic
organisms. Proc. Roy. Soc., A209, 417-460.

Truesdell, C. and Toupin, R. A. (1960). The classical field
theories. Handbuch der Physik, III/1. Berlin: Springer-Verlag.

Truesdell, C. (1965). The Elements of Continuum Mechanics.
New York: Springer-Verlag.

White, J. C. and Elmes, P. C. (1960). Some rheological properties
of bronchial mucus and mucoprotein. Flow Properties of Blood
and other Biological Systems. Copley and Stainsby, ed. Oxford:
Pergamon Press.

VITA

Name: Stephen Mark Ross

Date of Birth: June 20, 1945

Place of Birth: New York, New York

Marital Status: Married

Education:

1966-1971 The Johns Hopkins University, Ph. D. in
Fluid Mechanics, 1971

1962-1966 New York University, Bachelor of Engineering in
Mechanical Engineering

1959-1962 Linton High School, Schenectady, New York

Scholarships, Fellowships and Honors:

1969-1970 National Institute of Health Pre-Doctoral Fellowship

1966-1969 National Defense Education Act Title IV Fellowship

1962-1966 New York State Regents Scholarship

1966 Graduation with honors

1966 Award from American Society of Heating, Refrigeration
and Air Conditioning Engineers

Professional Organizations:

Tau Beta Pi honor society

Pi Tau Sigma honor society (mechanical engineering)

Publications:

1970: (with S. Corrsin). A wavy-wall analytical model of muco-ciliary pumping. Bull. of the Am. Physical Soc., Series II, 15, 1539.

1966: Advanced monitor gimbal positioning study. Report No. C6-2537/201
Section III. North Am. Aviation.

1966: Hamlin bubble level. Report No. IID 444-0428-001. North Am.
Aviation.